QUANTIFYING THE PERFORMANCE OF NATURAL VENTILATION WINDCATCHERS

A thesis submitted for the degree of Doctor of Environmental Technology

by

BENJAMIN MICHAEL JONES

School of Engineering and Design

Brunel University

July 2010

Abstract

The significant energy consumption of non-domestic buildings has led to renewed interest in natural ventilation strategies that utilise the action of the wind, and the buoyancy of hot air. One natural ventilation element is the Windcatcher, a roof mounted device that works by channelling air into a room under the action of wind pressure, whilst simultaneously drawing air out of the room by virtue of a low pressure region created downstream of the element. A significant number of Windcatchers are fitted in UK schools where good indoor air quality is essential for the health and performance of children. The performance of a ventilation system in a school classroom is determined by its ability to provide ventilation in accordance with UK government ventilation, air quality, and acoustic requirements. However, there is only limited performance data available for a Windcatcher, particularly when operating *in–situ*. Accordingly, this thesis investigates the performance of a Windcatcher in three ways: First, a semi-empirical model is developed that combines an envelope flow model with existing experimental data. Second, measurements of air temperature, relative humidity, carbon dioxide, and noise levels in school classrooms are assessed over summer and winter months and the results compared against UK Government requirements. Finally, air flow rates are measured in twenty four classrooms and compared against the semi-empirical predictions. The monitoring reveals that air quality in classrooms ventilated by a Windcatcher has the potential to be better than that reported for conventional natural ventilation strategies such as windows. Furthermore, an autonomous Windcatcher is shown to deliver the minimum ventilation rates specified by the UK Government, and when combined with open windows a Windcatcher is also capable of providing the required mean and purge ventilation rates. These findings are then used to develop an algorithm that will size a Windcatcher for a particular application, as well as helping to improve the ventilation strategy for a building that employs a Windcatcher.

Contents

List of Figures

List of Tables

Nomenclature

α	Kinetic energy coefficient
α_{rm}	Running mean constant
$\bar{\rho}$	Average density over length of Windcatcher quadrant (kg/m^3)
$\bar{T}_E$	Daily mean external temperature (°C)
$\bar{T}_{rm}$	Exponentially weighted running mean of daily mean external temperature (°C)
$\Delta\rho$	Change in air density between supplied room and surroundings (kg/m^2)
Δp_{in}	Pressure drop over supply Windcatcher quadrant (Pa)
Δp_{out}	Pressure drop over extract Windcatcher quadrant (Pa)
ΔT	Difference between internal and external temperatures (°C)
$\dot{Q}$	Volume flow rate through Windcatcher duct (m^3/s)
$\dot{Q}_I$	Air exchange between supplied room and surroundings (m^3/s)
$\dot{Q}_T$	Total extracted volume flow rate through the Windcatcher and façade opening (m^3/s)
$\dot{Q}_{Tmax}$	Maximum possible ventilation rate (m^3/s)
γ	Angle of volume control dampers (°)

$[\mathbf{J}]$	Jacobian matrix of first order partial derivatives
μ	Dynamic viscosity of air (kg/(m·s))
ρ_E	External density (kg/m^2)
ρ_I	Internal density (kg/m^2)
θ	Angle of incidence of wind to Windcatcher (°)
$\tilde{C}_p$	Corrected average coefficient of pressure over building façade
A	Cross sectional area of Windcatcher duct (m^2)
a	Topographical constant
A_d	Percentage free area of volume control dampers (%)
A_T	Total cross sectional area of the Windcatcher (m^2)
$C(0)$	Initial concentration of a tracer gas (ppm)
$C(t)$	Concentration of a tracer gas at time t (ppm)
C_p	Average coefficient of pressure
c_p	Specific heat capacity of air at constant pressure (J/kg K)
C_E	External concentration of a tracer gas (ppm)
C_{ss}	Steady state concentration (ppm)
d_1	Length of Windcatcher side 1 (m)
d_2	Length of Windcatcher side 2 (m)
d_H	Hydraulic diameter (m)
d_O	Opening depth of a window (m)
G	Rate of CO_2 production (cm^3/s)
g	Gravitational acceleration (m/s^2)

H	Total heat dissipated by ventilation (W)
h_O	Height of a window (m)
K	Loss factor
k	Topographical constant (m^{-a})
K_{in}	Losses inside Windcatcher supply quadrant
K_{out}	Losses inside Windcatcher extract quadrant
L	Duct length (m)
L_T	Length of louvred section (m)
p_E	External pressure (Pa)
p_I	Internal pressure (Pa)
p_w	Wind pressure (Pa)
R	Specific gas constant for air (J/kgK)
R^2	Coefficient of determination
t	Time (seconds)
T_E	External temperature (K)
T_I	Internal temperature (K)
T_O	Operative temperature (°C)
T_R	Radiant temperature (°C)
T_{Omax}	Upper operative temperature limit (°C)
T_{Omin}	Lower operative temperature limit (°C)
u	Velocity inside Windcatcher duct (m/s)
u_I	Room air speed (m/s)

u_w Wind velocity (m/s)

u_{10} Wind velocity measured in open country at a height of 10 m (m/s)

V Room volume (m^3)

w_O Width of a window (m)

X Temperature variable set according to building category (°C)

z_E Height of Windcatcher entry from floor (m)

z_I Height of Windcatcher entry to supplied room from floor (m)

z_O Height of façade opening from floor (m)

ACH Air Changes per Hour

ACU Air Conditioning Unit

AIDA Air Infiltration Development Algorithm

ASHRAE American Society of Heating, Refrigerating, and Air–Conditioning Engineers

BB Building Bulletin

BRE Buildings Research Establishment

BREEAM Buildings Research Establishment Environmental Assessment Method

BRI Building Related Illness

CABE Commission for Architecture and the Built Environment

CEC Commission for the European Communities

CFD Computational Fluid Dynamics

CIBSE Chartered Institute of Building Services Engineers

CO Carbon Monoxide

CO_2 Carbon Dioxide

CSA Cross Sectional Area

DoH Department of health

DSY Design Summer Year

DTI Department of Trade and Industry

EngD Engineering Doctorate

EPSRC Engineering and Physical Sciences Research Council

ETM Empirical Tightness Method

HVAC Heating, Ventilation, and Air Conditioning

IAQ Indoor Air Quality

ICT Information and Communication Technology

IEQ Indoor Environment Quality

IES Integrated Environmental Solutions

l/s Litres per second

MV Mechanically Ventilated

NHS National health service

NHSSDU NHS Sustainable Development Unit

NO_2 Nitrogen Dioxide

NV Naturally Ventilated

PhD Doctor of Philosophy

PM_{10} Micro Particulate Matter

RH Relative Humidity

SBS Sick Building Syndrome

SF_6	Sulphur Hexafluoride
STM	Simplified Theoretical Method
TAS	Thermal Analysis Software
TRY	Test Reference Year
VOC	Volatile Organic Compound

Acknowledgments

This research was completed with the help and support of a number of significant individuals and organisation to whom I am very grateful.

I would like to thank my academic supervisor, Dr. Ray Kirby, who during the many discussions we had in his study showed me the benefits of consistent attention to detail, good writing, and a straight forward approach; his patience, scientific insight, and guidance has been greatly appreciated. At Monodraught, grateful thanks go to my industrial supervisor, Tony Cull, for his positive support, diplomatic manner, and precious time. Thank you to my EngD and Monodraught colleagues who read my work and proffered advice.

Personal support and encouragement were always given by my wife, Jik, who suffered more than anyone else from this work; I can't thank her enough. Thank you to my parents and brother for listening in my many hours of doubt and to my Father for proof reading this dissertation.

Several great friends have shown a consistent interest in my studies and cheered me to the finishing line. They are Adrian Baty, Nigel Coatsworth, and Dr. Philip Dale.

Finally, this research was funded by the Engineering and Physical Sciences Research Council and Monodraught Ltd., and without their support it would not have been possible.

For Jik, Mum, Dad, and Daniel.

Author's Declaration

I hereby declare that I am the sole author of this thesis.

I authorise Brunel University to lend this thesis to other institutions or individuals for the purpose of scholarly research.

Signature: 

Date: 31st July 2010

I further authorise Brunel University to reproduce this thesis by photocopying or by other means, in total or in part, at the request of other institutions or individuals for the purpose of scholarly research.

Signature: 

Date: 31st July 2010

Executive Summary

Background

An Engineering Doctorate (EngD) is a four year research degree, awarded for industrially relevant research, based in industry and supported by a programme of professional development courses. It provides at least the intellectual challenge of a Doctorate of Philosophy (PhD) in a framework of experience and courses that prepare Engineering Doctors for industrial careers. The EngD was conceived in response to a belief held in industry, and supported by Government, that the traditional PhD research degree did not adequately prepare researchers for careers in industry.

This EngD programme is jointly managed by the Brunel University and the University of Surrey, and follows the theme of Environmental Technology. The overall thesis of the programme is that the traditional practices of Industry are unsustainable. For Sustainable Development (the concurrent preservation of a quality environment and sustained living standards) to be viable, future technologies must be developed to consider economic, social, and environmental factors. The EngD provides a graduate Research Engineer with the necessary skills to balance environmental risk along with all of the traditional variables of cost, quality, productivity, shareholder value, and legislative compliance.

This EngD is sponsored by the Engineering and Physical Sciences Research Council (EPSRC) and additional funding is provided by the industrial partner, Monodraught Ltd. Monodraught explore, develop, and create innovative low–energy building services solutions that use naturally available energy from the wind and the sun.

The Research Engineer must reconcile the competing demands of academia and industry while also considering environmental issues, see Figure 0.

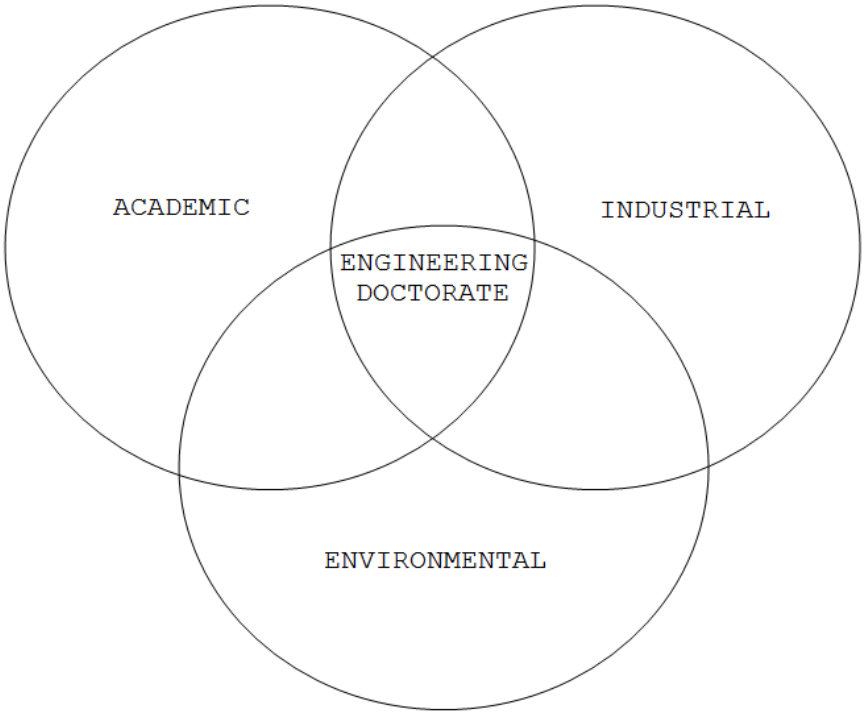

Figure 0: Competing concerns for the Research Engineer.

The EngD programme includes core and elective courses that must be completed by Research Engineers, which have the following aims:

- To provide a state of the art view of the relationship between Engineering and Sustainable Development, which can be applied in the research projects;
- To provide professional development in key business skills and competencies;
- To close any gaps in the knowledge required to undertake the research project.

The following courses have been successfully completed during the course of this research programme:

1. Advanced Leadership
2. Communications Management
3. Corporate Social and Environmental Responsibility

4. Energy Efficient Ventilation for Buildings
5. Entrepreneurship Masterclass for Research Students
6. Environmental Auditing and Management Systems
7. Environmental Economics
8. Environmental Risk Analysis
9. Environmental Law
10. Environmental Science and Society
11. Finance
12. Integrated Assessment
13. Life Cycle Approaches
14. Project Management
15. Research Methods
16. Social Research Methods for Environmental Strategy
17. Sustainable Development
18. Writing (a series of courses designed to help with the writing of academic literature)

Introduction To Research

The 160 million buildings within the European Union consume around 40% of its energy and produce over 40% of its total carbon dioxide (CO_2) emissions. In the UK, attitudes towards the use of energy within buildings are a cause for concern; for example, the Department for Energy and Climate Change reports that energy is often wasted because of poorly insulated buildings or where heating, ventilation, air conditioning, and lighting are poorly controlled. UK temperatures are expected to rise by 4–6°C over the next 50 years and so alternative

methods of providing cost effective, reliable, and energy efficient ventilation within buildings are of paramount importance.

The provision of good indoor environment quality in a building is important for the well–being of its occupants, but is a function of many different factors. However, symptoms of occupant discomfort are often shown to be related to the volume of air supplied to a building, and the type of ventilation provided. When surveys of occupants' perceptions of the indoor environment in mechanically ventilated buildings are compared against those that are naturally ventilated—buildings that are ventilated using naturally occurring forces and no mechanical ventilation—occupants often perceive the indoor environment to be better in the naturally ventilated buildings and report fewer symptoms of sick building syndrome, a set of adverse health symptoms that an occupant experiences indoors, but lessen when away from the building.

Children are particularly susceptible to the indoor air quality (IAQ) yet the IAQ and ventilation rates in many UK schools are often shown to be inadequate. Similarly, children are also negatively affected by noise which is often found to be above acceptable levels in UK schools. The UK Government has attempted to address this problem by issuing a series of guidelines that are specific to school buildings. Of particular relevance are Building Bulletins (BB) 101 and 93 that cover ventilation and air quality, and noise respectively. These documents set strict guidelines for levels of carbon dioxide, relative humidity (RH), temperature, and noise for all types of school and classroom.

The Windcatcher

The main differences between mechanical and natural ventilation are the characteristics and variability of the driving forces, which in naturally ventilated buildings are buoyancy and wind driven. The buoyancy forces are determined by the difference between the internal and external densities and thus temperatures. However, when the wind blows the resulting flows of air around a building are complex and unsteady, and are affected by two main factors: the prevailing outdoor conditions and the building itself. The principals of natural ventilation have been used for millennia to ventilate human shelters such as tents, houses, and public buildings such as places of religious worship. Therefore, effective natural ventilation

strategies can be found in vernacular architecture because they have evolved over the centuries to provide adequate ventilation for comfort, health, and heat dissipation. It follows that these traditional solutions to modern problems should be evaluated before investing in or proposing new mechanical solutions. One vernacular solution is the wind–catcher natural ventilation element that can be found in various guises throughout the middle east, which simultaneously supplies fresh air to, and extracts stale air from, a room at roof level whatever the wind's direction, and without mechanical assistance.

A modern equivalent is the Monodraught Windcatcher[1], which is made from glass reinforced plastic, and contains weatherproof louvres and an anti–bird mesh. Ducts channel air to and from the room where, at its base, a series of flow control dampers are protected by a grill. At the present time, only limited scientific performance data exists, and it is not possible to fully quantify its performance, particularly *in–situ*. Over 5500 Windcatcher elements have been delivered since 2002, with 5% to hospitals, 12% to offices, and 70% to UK schools. To date, Windcatchers have been fitted to over 1100 UK schools, thus making school buildings a special case, and the ventilation performance of Windcatchers in a school classrooms worthy of further investigation.

Aims and Objectives

The aim of this thesis is to quantify the performance of Monodraught Windcatchers used to ventilate UK school classrooms by comparing their performance against UK government guidelines for schools. To help meet this aim, the following objectives are set:

1. Quantify and understand the performance of a Windcatcher.

An understanding of the physics of a Windcatcher system—defined as the Windcatcher element, ducting, dampers, and grill—will help to develop an understanding of the complex interaction between the two driving forces, flow types through the ducts, and the energy losses through the whole system. Additional factors that may affect performance, such as the position of the Windcatcher element relative to architectural, topographical, and meteorological conditions will also be considered using the limited amount of theoretical and empirical

[1]The WINDCATCHER® is a proprietary product of Monodraught Ltd.

Windcatcher data that is already published.

2. Develop a detailed model that can accurately predict flow rates through a Windcatcher system.

A key performance indicator of a Windcatcher is the rate at which it delivers air into a room and stale air is extracted, and so it is important to be able to predict ventilation rates before choosing an appropriate size of Windcatcher for a particular building. The semi–empirical model is similar to the envelope flow model described by others and explicitly uses experimental data published in the literature for square Windcatchers in order to provide a fast but accurate estimate of Windcatcher performance. Included in the model are buoyancy effects, the effect of changes in wind speed and direction, as well as the treatment of sealed and unsealed rooms. Although this type of model relatively common it has never been applied to predict Windcatcher performance before.

3. Address the limited quantity of data for a Windcatcher functioning *in–situ* through a series of case–studies that measure key Windcatcher performance indicators and compare the findings against government guidelines.

Barometers of performance that require measurement include the ventilation rate, CO_2 concentration, temperature, and RH. Over 70% of Windcatcher elements are installed in more than 1100 UK schools, and so all of the case studies are of UK school classrooms. The measurements made in each classroom are compared against the relevant government guidelines for a school classroom.

4. Compare the ventilation performance of Windcatchers measured *in–situ* against those predicted by the model.

The information gathered here will feedback into the predictive model (objective 2) and augment the understanding of Windcatcher functionality and performance (objective 1).

Contributions to Knowledge

Semi–Empirical Model

A semi–empirical model has been developed that combines a simple analytic model with experimental data reported in the literature. The model uses data measured in the laboratory for the coefficient of pressure on each face of a 500 mm square Windcatcher, and then calculates the losses in each Windcatcher quadrant using further laboratory measurements of ventilation rates. However, this approach means that any errors present in the experimental measurements will also appear in the model and so the model can only be as good as the experimental data available. Moreover, the experimental data utilised here was obtained under laboratory conditions for a 500 mm square Windcatcher in a sealed room and so an assumption inherent in this approach is that this data may be extrapolated to real, *in situ*, applications in which air transfer between the room and the surroundings is permitted and different Windcatcher geometries are present. Included in the model are buoyancy effects, the consequences of changes in wind speed and direction, as well as the treatment of sealed and unsealed rooms.

The semi–empirical model has been shown to perform well against a range of experimental data and CFD predictions, and so offers the potential for use as a quick iterative design tool. With this in mind, a very simple expression for extract ventilation rates is proposed that neglects buoyancy effects, and so provides a very quick estimate of Windcatcher performance requiring no computational effort. This is very useful for industrial applications because it avoids the need for lengthy CFD calculations.

The semi–empirical model also predicts ventilation rates through a room ventilated by a Windcatcher in coordination with open windows, and estimates that this configuration is capable of significantly improving ventilation rates over and above those provided by an autonomous Windcatcher, and delivering those rates typically required by building regulations in the UK.

Indoor Environment Quality in Classrooms Ventilated by a Windcatcher

A set of seven case study buildings were chosen to demonstrate Windcatcher performance *in–situ* in a variety of environments and for a number of configurations. Measurements of

IAQ, ventilation, and noise were made in twenty four classrooms of seven UK schools, and the results demonstrate that a Windcatcher is generally capable of meeting the UK BB101 and BB93 standards for IAQ and noise.

RH does not appear to be a significant cause for concern in any of the classrooms measured. The measurements of summer temperatures show that none of the classrooms exceeded the maximum limit of 32°C set by BB101, and only one classroom exceeded 28°C, which indicates that none of the classrooms would exceed 28°C for more than 120 hours during the summer time. However, it should be noted that the monitoring was only conducted over a representative working week and not for the whole summer season and so this remains only an indicator of compliance. Six classrooms were found to have a mean internal temperature that was greater than the mean external temperature by $\Delta T \geq 5$°C, and this could be attributed to the comparatively large glazing areas and orientations of these room. These results suggest that all twenty four classrooms are compliant with the BB101 temperature requirements.

For the summer months all classrooms were able to meet the CO_2 requirements indicating sufficient per capita ventilation. Measurements of the ventilation rate in each classroom with a Windcatcher operating autonomously show that 40% of measured classrooms meet the minimum 3 l/s – person requirement and 23% meet the 5 l/s – person requirement. If the Windcatcher is used in coordination with open windows, then all classrooms meet the 3 l/s – person requirement, 94% meet 5 l/s – person, and 77% meet 8 l/s – person under this arrangement. Furthermore, for the classrooms studied here, it is evident that a Windcatcher can aid in the delivery of ventilation rates that meet the UK standards during the summer time and this also extends to meeting European and US standards.

However, the Windcatcher is rarely open during the winter months and although the maximum CO_2 limit of 5000 ppm is never reached, only 62% of classrooms meet the required mean CO_2 level of 1500 ppm and so the control strategy requires careful revision.

An increase in the rate of cooling at night that can be attributed to a Windcatcher is shown in two classrooms where the median cooling rate was found to be 0.64°C/hour and 0.43°C/hour. It is reasonable to expect other Windcatcher systems to deliver night cooling if they are also capable of functioning autonomously, the incoming air mixes well, and the external air temperature is less than the room air temperature.

Measurements of ambient noise in twenty three classrooms with the Windcatcher dampers

open suggest that the classrooms generally conform to BB93, although the sample size is relatively small and so there is probably insufficient data to conclude that Windcatchers do not represent a problem when meeting noise targets in schools.

Finally, a Windcatcher is shown to offer the potential to significantly improve natural ventilation rates in school classrooms and to help comply with IAQ standards for schools.

Comparison Between Predicted and Measured Ventilation Rates

The theoretical predictions and experimental measurements demonstrate that a Windcatcher is capable of delivering ventilation to a room when acting autonomously.

The predictions of ventilation rate by the semi–empirical model generally agree with those measured *in–situ*, but with three notable exceptions for a room ventilated by an autonomous Windcatcher. (i) Ventilation rates are sometimes over–predicted. (ii) The measured volume flow rates do not exceed $0.23\,\mathrm{m}^3/\mathrm{s}$, and appear to plateau when $u_w \geq 2\,\mathrm{m/s}$. This is not predicted by the model and its cause is unclear. (iii) Windcatchers with long duct sections exhibit relatively poor performance and this was also not predicted by the model.

Both the theoretical and experimental analysis of the Windcatcher demonstrate that Windcatcher performance can be significantly improved by the addition of open windows to a room. This aspect is likely to help rooms ventilated by a Windcatcher meet ventilation standards for buildings, such as BB101, in the UK. Generally, the predictions of ventilation rate made by the semi–empirical model for this configuration tend to under–predict those measured *in–situ*.

Design Methodology

Typical wind conditions were applied to the semi–empirical model using the CIBSE test reference year (TRY) database to predict the ventilation through a room ventilated by a Windcatcher every month, and was shown to be a useful design tool. These steps identified situations where the wind speed was very low, and here the Windcatcher system must rely on buoyancy forces to generate ventilation through a room. When the semi–empirical model was used to investigate this situation, the unsealed scenario is found to be unsuitable for situations where $u_w < 2\,\mathrm{m/s}$ and $|\Delta T| > 0^{\circ}\mathrm{C}$. Then, the sealed scenario should be used

to estimate ventilation rates under these circumstances and although the predictions seem plausible, they remain uncorroborated by empirical measurement.

The predictions suggest that an autonomous Windcatcher is capable of providing minimum ventilation rates specified by BB101 for a class of 30 occupants, and a Windcatcher in coordination with open windows can provide minimum, mean, and purge ventilation rates.

Finally, the investigation of the capabilities of the semi–empirical model produced a series of steps that a designer may use to correctly size a Windcatcher for a particular application.

Industrial Applications and Benefits

Monodraught Ltd. has always sought to stay ahead of the competition by commissioning small pieces of academic work from a number of British Universities to investigate the performance of the Windcatcher system. The research given here is part of a long term company strategy that puts research at its core. This includes the way that Windcatcher strategies are designed and tendered. With increased market place competition and a desire by customers to be given more information, this strategy makes complete sense. For example, the semi–empirical model is now central to the Monodraught design strategy, and has been incorporated into bespoke software (not discussed here) that is used by Monodraught Windcatcher design engineers to choose the correct size of Windcatcher for a particular application.

It is predicted that the knowledge given in this document, which has been derived independently from Monodraught and with academic rigor, will have a positive impact by

- Giving context to Windcatcher systems and their performance;
- Quantifying the performance of a Windcatcher system *in–situ*;
- Predicting the performance of a Windcatcher system and corroborating the predictions using measurements made *in–situ*;
- Presenting a simple, straight forward design process;
- Showing how the Windcatcher system can be used effectively and efficiently according to the season, which will lead to improved performance;
- Identifying future development work and research projects;

- Invoking confidence in stakeholders when specific claims about the Windcatcher system are made;
- Producing marketing material;
- Contributing to increased sales.

Publications

Jones, BM, Kirby, R, Kolokotroni, M, & Payne, T. 2007. Air Quality Measured in a Classroom Serviced by Natural Ventilation Windcatchers. *In: 2nd PALENC and 28th AIVC Conference: Building Low Energy Cooling and Advanced Ventilation Technologies in the 21st Century.*

Jones, BM, Kirby, R, & Kolokotroni, M. 2008. Quantifying the Performance of a Top–Down Natural Ventilation Windcatcher. *In: The 29th AIVC Conference: Advanced Building Ventilation and Environmental Technology for Addressing Climate Change Issues.*

Jones, BM, Kirby, R, Kolokotroni, M, & Payne, T. 2008. Air Quality Measured in a Classroom Served by Roof Mounted Natural Ventilation Windcatchers. *In: Proceedings of the 2008 Brunel/Surrey University EngD Conference.*

Jones, BM, & Kirby, R. 2009. Quantifying the Performance of a Top–Down Natural Ventilation Windcatcher^{TM}. *Building and Environment*, 44(9), 1925–1934.

Jones, BM, & Kirby, R. 2010. The Performance of Natural Ventilation Windcatchers in Schools: A Comparison between Prediction and Measurement. *International Journal of Ventilation*, 9(3), 273–286.

Chapter 1

Introduction

1.1 The Environment

The consumption of energy and the production of so called greenhouse gases are at the heart of the causes of anthropogenic climate change. Consumer demand outstrips the available supply of clean energy and so the emissions of carbon dioxide (a greenhouse gas) continue to increase. Buildings are at the hub of this problem. There are approximately 160 million buildings within the European Union that consume 40% of its energy and produce over 40% of its total carbon dioxide (CO_2) emissions (CIBSE, 2003).

In the short term, the United Kingdom is committed in law to reduce CO_2 emissions to 12.5% below 1990 levels by 2010 (which will almost certainly not be met) and have initially pledged to extend the cut to 20% by 2020 (CIBSE, 2004) and may be increased to 34% by commitments made in the budget of April 2009. These commitments are enforced throughout the national building stock by an amendment to the Buildings Act (2000) which enforces conservation of fuel and power, and the protection of the environment. European law, through the Energy Performance of Buildings directive (2002), has also forced environmental changes to the UK Buildings Regulations.

In the UK, attitudes towards the use of energy within buildings are a cause for concern. The Department for Trade and Industry (DTI) states that "energy is often wasted because of poorly insulated buildings or where heating, ventilation, air conditioning, and lighting are poorly controlled" (DTI, 2003). In the UK the climate is comparatively clement yet 41% of

all of energy consumed by non–domestic buildings is used for heating and 5% for cooling and ventilation (CIBSE, 2004). The latter figure may seem relatively small, but worldwide, refrigeration and air conditioning is estimated to account for 15% of global electricity consumption (IIF, 2002). UK temperatures are expected to rise by 4–6°C over the next 50 years and temperatures could regularly exceed 30–35°C during the summer (CIBSE, 2005c). Consequently, air conditioning use within the UK is also likely to increase with an associated increase in energy consumption. To combat this, and to conform to ever more stringent government energy and CO_2 emissions targets, alternative methods of providing cost effective, reliable, and energy efficient ventilation within buildings is of paramount importance.

1.2 The Indoor Environment

The dissipation of heat and the maintenance of positive internal thermal conditions are only two of the many components of the Indoor Environment Quality (IEQ) of a building. Other factors include indoor pollutants, noise, light, and odour, and they may have a direct or indirect effect on occupants (Mendell & Heath, 2005). Further examination of these constituents shows that indoor pollutants are made up of chemical, biological, and particulate contaminants such as formaldehyde from furniture, dust mites, and micro particulates from non–stoichiometric combustion, respectively.

Thermal conditions are governed by the temperature and humidity. Heat gains arise from the sun, electronic equipment, and the occupants themselves, while humidity is generally a function of the temperature, and human respiration and perspiration. Internal noise and light are controlled by the fabric of a building, and openings in its skin. Artificial lighting can be used to supplement and replace natural daylight when required. Odours arise from the concentration of occupant bio–effluents, catering, waste facilities, furniture and upholstery, and mould growth (CEC, 1992). The rates at which specific chemical and odour pollutants are emitted are often a function of other factors of IEQ. For example, the rate at which formaldehyde is released is a function of humidity (CEC, 1992) which in turn is governed by the temperature. Therefore, the components of IEQ are often intertwined and related.

If the pollution sources cannot be removed from a building, they must be controlled. This must be done collectively as the relative importance of each of the components of IEQ is

difficult to quantify, although broad trends have emerged. For example, surveys of occupants of many European non–domestic buildings have identified warmth and air quality as more important than the level of lighting and humidity (Humphreys, 2005). The same study also shows that the relative importance of IEQ factors is highly subjective, differing from country to country, and even building to building, because each set of occupants has different requirements of their building.

The occupants' perception of Indoor Air Quality (IAQ) is also identified as being important (Seppänen *et al.*, 2002), because the effects of poor IAQ can manifest themselves as one or more of a variety of negative symptoms that are traditionally grouped either under the title of Building Related Illness (BRI) or Sick Building Syndrome (SBS). The clear distinction between the two conditions is that the symptoms of a BRI can be clinically diagnosed, such as Legionnaires' disease or allergic asthma, while the causes of SBS have no clear etiology (Bakó-Biró, 2004). The lack of specific causative affects of SBS does not mean that it cannot be cured. By addressing key indoor environmental factors, most notably by increasing the ventilation rate (Seppänen & Fisk, 2002), significant reductions in its prevalence can be made. If this is not done, or if ventilation rates are too low, occupants will experience discomfort, and their general performance and productivity will reduce (Seppänen & Fisk, 2004).

Consequently, minimum ventilation rates are specified according to the type and task of a room by Part F of the Building Regulations (ODPM, 2006). In many modern non–domestic buildings, heating, ventilation, and air conditioning (HVAC) systems are seen as the solution because they offer total control of ventilation rates, temperature, and humidity, while filtration systems purify the supplied air. Centrally located HVAC systems duct air to wherever it is needed but require large volumes of space and infrastructure. Independent systems require no central input and may be installed quickly and easily to meet local needs. However, the Carbon Trust, a quango designed to accelerate the move towards a low carbon economy, states that:

> *A typical air–conditioned building has double the energy costs and associated CO_2 emissions of a naturally ventilated building. It is also more likely to have increased capital and maintenance costs.* (Carbon Trust, 2007)

The volume of air conditioning units (ACU) systems sold in each country within the EU

is a function of the gross national product (GNP) of each member state (Santamouris & Asimakopoulos, 1996). In the early 1990s, an explosion in demand for ACUs coincided with the first global surges in electricity consumption during summer months. Therefore, as sales of mechanical air conditioning systems and summer temperatures increase, incidences of peak electricity demand in the summer months are also likely to be more frequent. In the UK, electricity is primarily generated from carbon based fuels (DUKES, 2006) and so a summer increase in electricity demand would increase CO_2 output and a reduce air quality.

The argument for prudence when considering such systems may seem straightforward, but in some parts of the world mechanical air conditioning systems are associated with efficiency, prosperity, and status, and are used to convey these attributes, and not because they are necessary for the comfort and well–being of a building's occupants (Ackermann, 2002). Although there are many proponents of the air conditioned indoor environment who cite their contribution to personal freedom and increased productivity in hot regions of the world (Ackermann, 2002), mechanical systems do not always contribute to an indoor environment that is satisfactory for its occupants. In fact, when compared against buildings that are naturally ventilated (buildings that use no mechanical ventilation) occupants often perceive the indoor environment to be better in the naturally ventilated buildings (Hummelgaard *et al.*, 2007) and report fewer SBS symptoms (Fisk, 2000). Psychologically, this makes sense because naturally ventilated buildings have been the norm in vernacular architecture (Rudofsky, 1977a,b) for millennia, ever since Homo sapiens needed a shelter for comfort and security.

1.3 Naturally Ventilated Buildings

The outer skin of a building that separates the inside from the outside is known as its envelope. A building can be ventilated by natural forces if it has one or more openings in its envelope that allow air to flow in and out. The main differences between mechanical and natural ventilation are the characteristics and variability of the driving forces, which in naturally ventilated buildings are buoyancy and wind driven (Li & Heiselberg, 2002). Buoyancy forces are determined by the difference between the internal and external densities and thus temperatures. When the wind blows, the resulting flows of air around a building are complex and unsteady, and are affected by two main factors: the prevailing outdoor

conditions and the building itself (Santamouris & Asimakopoulos, 1996). The micro climate surrounding a building has unique wind velocity, temperature, humidity, and topographical properties while the effectiveness of a building to provide natural ventilation is governed by its architecture. Here, geometry, orientation, openings (number, size, and location), and internal flow paths are all of paramount importance.

These factors make naturally generated flows more complex than their mechanical counterparts and are, therefore, more difficult to predict. To help make natural ventilation easier to understand, Heiselberg (2004) characterises it into five aspects, each with corresponding parameters, see Table 1.1. A natural ventilation element uses some or all of the ventilation principals to exploit the natural driving forces by using the height of the building and one or

Table 1.1: The characteristics of natural ventilation (adapted from Heiselberg, 2004)

Characteristic Aspect	Characteristic Parameter
Natural Driving Force	Buoyancy
	Wind
Ventilation Principal	Single–Sided
	Cross
	Stack
Ventilation Element	Façade Opening
	Wind–Scoop
	Wind–Tower
	Wind–Catcher
	Oast or Cowl
	Atrium
	Chimney
	Embedded Ducts
Building Height	Low–Rise
	Medium–Rise
Supply and Exhaust Paths	Local
	Central

more supply and exhaust paths.

Buildings all over the world are naturally ventilated by relying on the porosity of the envelope and windows or other openings. Here, two types of flow path through the envelope are identified: those that are purpose provided and those that are unintentional or adventitious. Use of arbitrary openings can result in uncontrolled ventilation that has negative side effects such as occupant discomfort and high energy losses. However, it is possible to exercise control over the flow rates through a building by ensuring high levels of air tightness. In modern buildings these are normally below 0.5 air changes per hour (ACH) (Santamouris & Asimakopoulos, 1996). Therefore, when considering natural ventilation in this thesis, it is assumed that adventitious openings are kept to a minimum, and flow paths through the building envelope are intentional and predefined.

If the architecture and micro climate of a building are favourable, natural ventilation strategies can be employed cheaply with lower capital and running costs than mechanical systems. Such systems need no plant room and require minimal maintenance. High flow rates for cooling and purging are possible if enough openings are provided and there is no fan or system noise. During periods of exceptionally warm weather, discomfort is normally tolerated by occupants who adapt to the conditions by opening windows (or other purpose provided openings) and changing clothing (Humphreys & Nicol, 1998).

Even in temperate climates buildings are often found to be too hot (Linden, 1999). In these circumstances, natural ventilation can provide good indoor air quality levels, appropriate thermal comfort levels, and a reduction in the cooling loads of the buildings. The latter may be achieved through the use of night or nocturnal cooling techniques. At night, the external temperature drops below the internal temperature. This fact is exploited during the summer months by drawing cooler air inside to increase the dissipation of heat stored in the fabric of the building. The warmer air is then exhausted leaving the air and fabric temperatures lower than they might otherwise have been. Natural ventilation also helps occupants to relate to external conditions over their internal environment and exercise control, which can increase tolerance to a range of thermal conditions (Nicol & Humphreys, 2002; Hummelgaard *et al.*, 2007). Occupant performance and attendance may also be improved by a naturally ventilated indoor environment (Mendell & Heath, 2005; Shendell *et al.*, 2004).

Natural ventilation is not suited to every type of building or every environment, and so its

drawbacks are now discussed. Buildings with a deep plan or many individual rooms face air distribution problems that are difficult to solve without mechanical assistance. Furthermore, those that suffer from large heat gains may find that the lower mean flow rates provided by a natural ventilation strategy are not sufficient to dissipate them, and so mechanical ventilation may be more suitable. If a building is located in a noisy and polluted area, their ingress may be a health risk to occupants (Stansfeld & Matheson, 2003; Laxen & Noordally, 1987). Some designs may unwittingly incorporate security risks, such as large openings situated at ground level.

Even if a building is perfectly designed for natural ventilation and in a relatively open location, its biggest drawback is that it is subject to the whims of the weather. UK wind speeds fluctuate throughout the year, changing with the seasons. They may be estimated for a particular region with the help of annual average tables produced by the Meteorological (Met) Office and the Chartered Institute for Building Services Engineers (CIBSE). For example, these tables suggest that at Heathrow Airport near London, wind speeds and are greater than 2 m/s for 70% of the year (CIBSE, 2006a, Table 2.42). CIBSE (2005a) suggests that "the wind speed coincident with the temperature that is not exceeded for 99.6% of the time is in excess of 3.5 m/s for all UK locations." In some parts of the UK wind speeds are much higher, particularly in the winter, and so natural ventilation may not be suitable where the ingress of cold air causes discomfort, condensation, or high energy loss. At other times, particularly in mid summer, hot windless days are experienced. Here it can be argued that these days are infrequent and discomfort may be felt whatever the ventilation strategy. Furthermore, some public buildings, such as schools, are unoccupied when these conditions are most likely to occur. Nevertheless, the point is that the fluctuation of wind speeds makes the control of flow rates difficult to manage and can lead either to high energy losses or air quality problems.

Despite the drawbacks, a natural ventilation strategy remains a viable method of ventilating a building, satisfying the needs of its occupants without excessive energy consumption or harmful bi–products. Therefore, it can be said that natural ventilation is a sustainable technology, meeting the three pillars of sustainable development: the social, the environmental, and the economic (Porritt, 2005). It is important and warrants study. Why? It has already been said that natural ventilation flow paths are complex, and so if such strategies are to be

designed well, the physics must be understood. To do this the effects of each of the driving forces, the micro climate, the characteristics of air flow in and around the building, and the effect of varying the opening type, size, and location, must all be determined. There are a variety of strategies that have individual advantages and challenges, but a designer must be able to specify a natural ventilation scheme that meets the guidelines of the time.

Heiselberg's classification (see Table 1.1, p. 16) shows that natural ventilation is achieved using three main principals. The single–sided principal uses one or more openings on a single façade and relies on wind or buoyancy to drive air flow. The net value of these forces is often small and so flow rates are low. Consequently, the penetration of the flow is restricted. Cross ventilation uses air entering through a façade on one side of a building and exiting on the other. The flow rates are more reliable than single–sided ventilation and it is easier to achieve good penetration, subject to a clear flow path free from internal obstacles. This can also be a constraint, as the internal space relies on an open–plan interior for the best results. Finally, stack ventilation uses flow generated by the difference between internal and external temperatures and is so called because of the analogy with flows through a chimney stack (Etheridge & Sandberg, 1996). The pressure difference between the two zones is augmented by a long duct that terminates at roof level. Air enters the building through low level openings and is drawn through the room before entering the duct. Greater flow rates are achieved in the winter, while the flow direction can reverse in summer when the external temperature is greater than the internal temperature. A back–draught can occur when the stack pressure cannot overcome the static pressure of the cold air above it.

These ventilation principles may be achieved using one or more ventilation elements. The most important types are listed in Table 1.1 and each has its own specific technical and architectural possibilities and consequences (Heiselberg, 2004). A wide variety of natural ventilation elements can be seen in vernacular architecture all over the world. A wind–tower is a chimney that rises above roof level so that it is incident to the wind whatever its direction. An area of negative pressure forms at the top of the chimney providing suction. This device and can be seen in the Pantheon in Rome, built by Agrippa in 27 AD (McCarthy, 1999). A derivative is the oast–house, used to dry hops in the Kent countryside. However, in order to provide protection from the weather, its opening is turned away from the wind. To be most effective it must be omni–directional and rotate according to the direction of the wind, thus

adding cost and maintenance implications. Wind–scoops turn their opening directly into the wind and are traditionally common in areas where the wind blows from a predominant direction. In the Sind district of Western Pakistan, wind–scoops have been a prominent feature of the skyline for the past 500 years, where despite the multi–storey architecture of the buildings, air is channeled into every recess of the interior (Rudofsky, 1977a,b). The history of the wind–scoop is now known to date back to at least 1500 BC because drawings of houses with roof mounted wind–scoops, known colloquially as a *Malqaf*, have been found in Egyptian tombs (Roaf, 1982).

An amalgamation of these principals is found in the wind–catcher, which consists of a tower subdivided to contain several shafts, each connected to a vertical face. The wind–catcher is known in Iran as a *Badgir* where their use has been reliably traced to the 14^{th} century, although a hypothesis of pre–Christian construction is, to date, uncorroborated (Roaf, 1982). In Iran, the brick structure of the wind–catcher heats up during the day and so it acts like a chimney, expelling hot air from the building (Roaf, 1982). When the wind blows, a positive pressure difference is created across the windward shafts, channelling air into a building. Conversely, a negative pressure difference across the leeward shafts draws stale air out of the building. A draw–back of this element is that the wind and buoyancy forces can act against each other reducing its efficiency.

Natural ventilation principles and vernacular elements can be seen incorporated into modern architecture. The Queens Building at De Montfort University, the Coventry University Library (Simons & Maloney, 2003), Portcullis House in the City of Westminster, and Swiss Re (also known as *The Gherkin*) in the City of London are four high profile examples. There are an increasing number of recently devised natural ventilation elements available to a designer today, such as the Wing Jetter, in addition to modern–day versions of traditional elements such as the wind–catcher (see Khan *et al.*, 2008).

When used in areas where the wind is consistent and strong, modern wind–catchers have several key advantages that make them attractive to building services engineers. Firstly, a wind–catcher can function autonomously or with additional low level envelope openings. By locating them on the top of a building, the pollution content of the supplied air is lower than at street level (Laxen & Noordally, 1987). They can also be used to supply air into a building with a deep plan and multiple storeys. When compared to other modern elements (see Khan

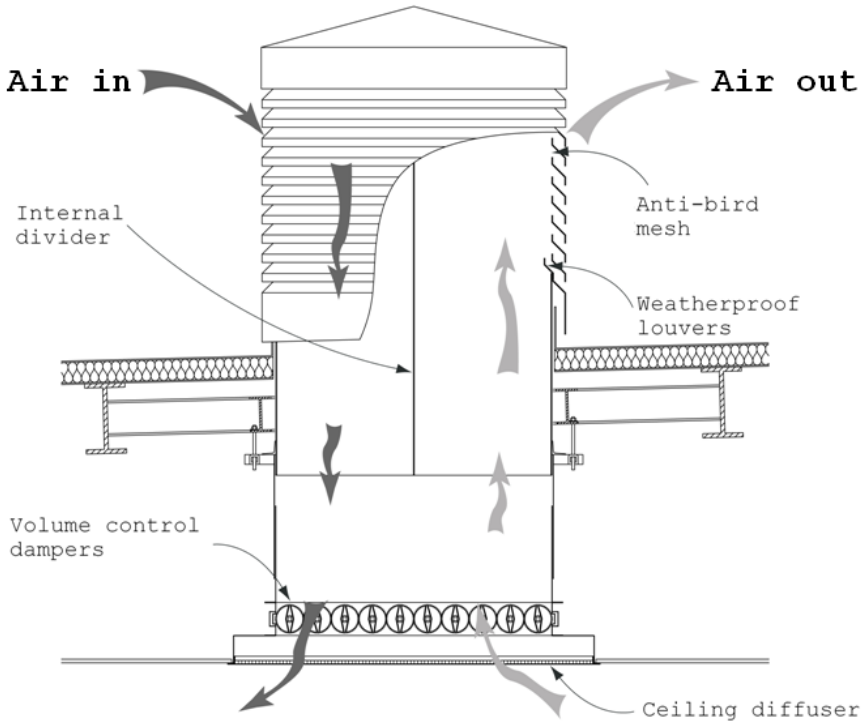

Figure 1.1: The Monodraught Windcatcher.

et al. (2008) for a full explanation of many modern ventilation elements) the wind–catcher has few moving parts, and therefore less to go wrong. This makes them relatively easy to retrofit onto a variety of roof types, and much cheaper to install, run, and maintain than many equivalent systems. Their main disadvantages are that a reliable wind force is required for consistent performance and although modern wind–catchers do not contain any thermal mass, (unlike their vernacular counterparts) there is the possibility of conflict between the wind and buoyancy driving forces, which could adversely affect performance. Finally, in winter when external temperatures are comparatively lower than internal temperatures, draughts through the element may cause discomfort to occupants.

The Monodraught Windcatcher[1], see Figure 1.1, is the most widely sold modern wind–catcher and is the subject of this thesis. From this point forward the term Windcatcher

[1]The WINDCATCHER® is a proprietary product of Monodraught Ltd.

refers to the Monodraught product whereas the term wind–catcher will refer to the vernacular generic element. The Windcatcher is made from glass reinforced plastic, and contains weatherproof louvres and an anti–bird mesh. Ducts channel air to and from the room where at its base a series of flow control dampers are protected by a grill. At the present time, only limited scientific performance data exists, and it is not possible to fully quantify their performance, particularly *in–situ*.

Over 5500 Windcatcher elements have been delivered since 2002, with 5% to hospitals, 12% to offices, and 70% to UK schools (Monodraught, 2009). To date, Windcatchers have been fitted to over 1100 UK schools, thus making school buildings a special case, and the reasons for choosing a Windcatcher to ventilate a school worthy of further investigation.

1.4 School Buildings

Children are particularly susceptible to poor IAQ (Mendell & Heath, 2005) yet the quality of indoor air and ventilation rates in many UK schools are often shown to be inadequate (Mumovic *et al.*, 2009). Similarly, children are also negatively affected by noise (Shield & Dockrell, 2003) which is often found to be above acceptable levels in UK schools (Shield & Dockrell, 2004). The UK Government has attempted to address this problem by issuing a series of guidelines that are specific to school buildings. Of particular relevance to Windcatchers are Building Bulletins (BB) 101 and 93 (DfES, 2006, 2003) that cover ventilation and air quality, and noise, respectively. These documents set strict guidelines for levels of carbon dioxide, relative humidity (RH), temperature, and noise for all types of school and classroom.

In 2006, the UK Government started a new wave of school construction and refurbishment with a budget of 45 billion that is expected to continue until 2020 (Mumovic *et al.*, 2009). Traditionally, schools have always had a narrow plan architecture and been naturally ventilated, but today schools are more air tight, use deeper plans, maximise use of floor space, and have an increased quantity of information and communication technology (ICT) equipment (DfES, 2006). Until recently, mechanical ventilation systems were being considered to dissipate increasing heat gains and provide sufficient ventilation for a positive learning environment. However, schools are found to consume 10% of all energy used in

the commercial and public buildings sector and expenditure on building infrastructure is 7% of the total education budget per student, which is more than the relative operating costs of an office building (see Pegg, 2008). Buildings that are naturally ventilated cost between 10—15% less than those that are mechanically ventilated (DfES, 2006) and so natural ventilation strategies are actively encouraged in school design. Section 4 of BB101 advocates the use of purpose–designed natural ventilation strategies, as opposed to mechanical or window–opening strategies, because they have (amongst other things) cheaper capital, running, and maintenance costs, and greater sound insulation that reduces traffic noise. This argument is also made by guidance on Schools for the Future (BB95) (DfES, 2002), which states that designers should "aim for natural ventilation where possible." *ClassVent* (DfES, 2005) is a simple spreadsheet based design tool available to download from several stakeholder websites, such as www.TeacherNet.gov.org, and can be used to choose a ventilation strategy and size a ventilation opening. Included among its ventilation elements is a roof terminal that is similar to a Windcatcher. In many schools Windcatchers are used to meet ventilation, IAQ, and noise guidelines because they allow for wide plan architecture, are a low–energy technology, and have the advantage that they can be retrofitted to a classroom.

Therefore, when considering a building type that would make an ideal case–study to evaluate the performance of a Windcatcher, schools are an excellent choice because they have a number of desirable properties. All schools are designed to perform the same task, the education of children, and so they have similar occupancy densities and patterns, long vacation periods allowing for more detailed analysis using specialist techniques, and clearly defined IAQ benchmarks against which performance may be measured. It is for these reasons that school classrooms are the focus of this thesis.

Finally, the evolution of a new type of school means that some of the already limited ventilation, IAQ, and noise data collected from the UK school stock are out of date. Although some research into new–build schools has already begun (Pegg, 2008), there is a clear need to monitor them and the purpose–provided ventilation strategies that they employ in order to check that they function as they have been designed to, and their performance conforms to government standards, before establishing design and implementation best practice where possible.

1.5 Research Aim and Objectives

The aim of this thesis is to quantify the performance of Monodraught Windcatchers used to ventilate UK school classrooms by comparing their performance against UK government guidelines for schools.

If a prima facie of this thesis is an acceptance that a Windcatcher can deliver air into a building—the longevity, heavy weight construction, and beautification of vernacular wind–catchers suggest that this is so—this project aspires to meet the following objectives in order to quantify the performance of a Windcatcher.

The first objective is to quantify and understand the performance of a Windcatcher. An understanding of the physics of a Windcatcher system—defined as the Windcatcher element, ducting, dampers, and grill—will help to develop an understanding of the complex interaction between the two driving forces, flow types through the ducts, and the energy losses through the whole system. Additional factors that may affect performance, such as the position of the Windcatcher element relative to architectural, topographical, and meteorological conditions will also be considered using the limited amount of theoretical and empirical Windcatcher data that is already published.

The second objective is to develop a detailed model that can accurately predict flow rates through a Windcatcher system. A key performance indicator of a Windcatcher is the rate at which it delivers air into a room and stale air is extracted, and so it is important to be able to predict ventilation rates before choosing an appropriate size of Windcatcher for a particular building. The semi–empirical model is similar to the envelope flow model described by others and explicitly uses experimental data published in the literature for square Windcatchers in order to provide a fast but accurate estimate of Windcatcher performance. Included in the model are buoyancy effects, the effect of changes in wind speed and direction, as well as the treatment of sealed and unsealed rooms. Although this type of model relatively common it has never been applied to predict Windcatcher performance before.

The literature review (Chapter 2) will show that there is limited data for a Windcatcher functioning *in–situ*. The third objective will address this lack through a series of case–studies that measure key Windcatcher performance indicators such as ventilation rate, CO_2 concentration, temperature, and RH. Over 70% of Windcatcher elements are installed in

more than 1100 UK schools, and so all of the case studies are of UK school classrooms. The measurements made in each classroom are compared against the relevant government guidelines for a school classroom.

The fourth and final objective is to compare the ventilation performance of Windcatchers measured *in–situ* against those estimated by the model. The information gathered here will feedback into the predictive model (objective 2) and augment the understanding of Windcatcher functionality and performance (objective 1).

1.6 Thesis Outline

It is intended that this thesis will make a detailed contribution to the understanding of Windcatcher performance. The techniques for predicting flow through Windcatcher systems will be useful as design tools and the case studies will serve as valuable examples of the performance of Windcatchers in practice. The collection of chapters that make up this thesis will guide the reader through the journey of research that leads to the conclusions in Chapter 8.

Chapter 2 provides a detailed review of the drivers for research and other peer–reviewed literature that has influenced this work. The review considers IEQ parameters with a focus on schools and the effects of poor air quality on their occupants. Consideration is given to the constituents of good IAQ and the methods for achieving it. Natural ventilation methods are acknowledged as a method for providing good IAQ in school classrooms and the Windcatcher is considered as a natural ventilation element that could be used to meet current government requirements.

Chapter 3 considers the need for a designer to quickly, accurately, and easily predict flow rates through a Windcatcher system in order to correctly size the system for a particular application. Estimating the performance of the Windcatcher is complicated by complex flow patterns and the interaction between the two driving forces. Therefore, in order to realise a more accurate understanding of the energy losses inside a Windcatcher it is necessary to study the air flow in detail. This is done by developing an analytic model for a variety of situations, based upon conservation of energy and mass. By explicitly using existing experimental data to quantify the energy losses, a semi–empirical model is formulated whose predictions are

compared against experimental data given in the literature.

Chapter 4 introduces each of the case–study school buildings that have been chosen to show how Windcatchers perform *in–situ* and in a variety of environments. Because over 70% of Windcatcher systems are installed into school buildings, all of the case study buildings are schools. Therefore, the case–studies also have a secondary function as data collected from them will contribute to the limited number of published reviews of air quality and ventilation rates in UK school buildings. The parameters of each building are also compared against similar case studies in the literature.

Chapter 5 presents the data recorded in each case–study buildings so that it can easily be compared to government benchmarks and the performance of the Windcatcher systems can quickly be identified. The Chapter will also detail the methodologies employed to measure the IAQ, ventilation, and noise, highlighting merits and faults, and determining the reliability of each of the data sets, which are then compared against similar sets in the literature.

Chapter 6 seeks to corroborate the semi–empirical model by comparing its estimations of flow rates through a Windcatcher system with those measured in the case study buildings and in literature.

Chapter 7 draws together the themes from the previous chapters to discuss general recommendations for the use and application of Windcatchers, the ability of Windcatcher systems to meet current guidelines, and the transferability of these observations to other building types.

Chapter 8 makes conclusions based upon the observations of the preceding chapters.

Chapter 9 discusses further work that could be carried out to enhance the current knowledge of the Windcatcher system.

Finally, the proceeding chapters contain a list of all references and appendices.

Chapter 2

Literature Review

2.1 Indoor Environment Quality and Ventilation

Most people spend 80–90% of their lives inside some type of building, yet there is a strong belief that the indoor environment may pose more of a risk to human health than the outside (Bakó-Biró, 2004). But what exactly is health? The World Health Organisation (WHO) has a longstanding and wide definition:

> *Health is a state of complete physical, mental, and social well–being and not merely the absence of disease or infirmity.* (WHO, 1946)

Providing good health to each occupant of a building is not straightforward if each of these five human factors must be considered. There are many stimuli such as the thermal conditions, air quality, noise, and light that effect each occupant differently. The effects may be direct, impairing concentration for example, or indirect, affecting productivity (Mendell & Heath, 2005). If these stimuli are not addressed they can be the cause of ill–health that manifests itself in one of two forms. The first is through a set of symptoms that have a clear etiology, and are known as a Building Related Illness (BRI) (Bakó-Biró, 2004). Bakó-Biró classifies them into three groups:

1. Airborne infectious diseases (Legionnaires' disease, Pontiac fever, airway infections);
2. Hypersensitivity diseases (allergic asthma, rhinitis, and pneumonitis);

3. Toxic reactions (carbon monoxide, pesticides).

When there is a clear link between cause and effect, it is relatively simple to address the source of the BRI. However, associations are not always clear and although symptoms may be recognisable, the causes are less certain. Therefore, a second group is identified where the symptoms are known as Sick Building Syndrome (SBS), described by Apte *et al.* as:

> *A set of adverse health or discomfort symptoms that individuals experience when they spend time indoors, particularly in office buildings, and that lessen while away from the building.* (Apte *et al.*, 2000)

Apte *et al.* go on to classify symptoms into four groups based upon the area of the body where they occur:

1. Upper respiratory and mucosal (dry, itchy, and sore eyes, nose, sinus, or throat);
2. Lower respiratory (cough, tight chest, breathing problems);
3. Neuro–physiological (headache, mental fatigue, dizziness etc.);
4. Skin irritation (itching, stinging, dryness, or reddening).

The lack of specific causative effects does not mean that SBS cannot be cured. By addressing key indoor environment quality (IEQ) factors, most notably by increasing the ventilation rate, the frequency and prevalence of symptoms can be reduced (Seppänen *et al.*, 1999).

A relationship between ventilation and positive aspects of IEQ is established by many studies in the literature because ventilation is a means of regulating the thermal comfort of the occupants and atmospheric pollutants that determine the overall indoor air quality (IAQ). The results of a survey of occupants in 26 offices across Europe show that the "approval of levels of warmth and air quality are more important than levels of lighting or humidity" (Humphreys, 2005). Now the reasons why good ventilation can be effective in the provision of good IEQ are considered. The relative warmth of occupants is governed by the science of thermal comfort while air quality is related to the ventilation rate. Because ventilation systems either generate noise or allow noise ingress, its contribution to IEQ is also evaluated.

2.1.1 Thermal Comfort and Ventilation

Early studies into the thermal comfort of the occupants of buildings are directly related to temperature (see Nicol, 1974, for example) while more recent literature suggests a psychological approach that considers parameters of past cultural and climatic experiences, and expectations (see Auliciems, 2001). Two distinct approaches to thermal comfort are discussed within the literature: the Heat Balance model; and the model of Conceptual Thermal Adaptation. The first approach suggests that comfort is a "universally definable state of affairs, the other that it is a social–cultural achievement" (Chappells & Shove, 2005). However, although each approach to the achievement of thermal comfort may differ, the definition remains consistent.

> *Thermal comfort is that condition of mind which expresses satisfaction with the thermal environment.* (Fanger, 1970)

The temperature that a person neither feels too hot nor too cold is known as Thermal Neutrality. Thermal comfort is said to be achieved in a building when the highest possible percentage of all occupants are thermally comfortable (Fanger, 1970), and acknowledges that it is improbable to achieve complete satisfaction .

Heat balance models (also known as *static* or *constancy* models), view the "person as a passive recipient of thermal stimuli and are premised on the assumption that the effects of a given thermal environment are mediated exclusively by the physics of heat and mass exchanges between the body and the environment" (Brager & De Dear, 1998) thus seeming to ignore Fanger's *condition of mind*. They are widely used by international standards (see ISO, 2005, for example) and professional design guidelines in the UK (see CIBSE, 2006a).

The models assume that when thermal comfort is attained, heat production is equal to the heat lost by a person and so key variables are (Fanger, 1970):

- Activity level and metabolism (heat production by the body);
- Thermal resistance of clothing;
- Air temperature;
- Mean radiant temperature;

- Relative air velocity;
- Water vapour pressure in ambient air (humidity).

The findings are based upon laboratory experiments in climate chambers that yield consistent and replicable results (Brager & De Dear, 1998). The average clothing insulation (expressed as a *clo* unit) and the metabolic rate (expressed as a *met* unit) of each occupant are applied to the model to determine an optimum comfort temperature for a specific activity in a particular indoor environment. Brager & De Dear (1998) point out that the calculated results of comfort can be widely different to the actual comfort of occupants determined by a survey. This is perhaps the obvious problem of using a model defined in a laboratory to determine a subjective quantity, and then attempting to apply it to dynamic, real life, conditions where factors such as demographics (gender, age, culture, economic status), context (season, climate, buildings design, and function), environmental interactions (indoor air quality, acoustics, and lighting), and cognition (attitude, preference, and expectation) are unaccounted for (Brager & De Dear, 1998; Humphreys & Nicol, 1998).

The thermal adaption approach has been conceived more recently and hypothesises that "if a change occurs such as to produce discomfort, people react in a way which tends to restore their comfort" (Nicol & Humphreys, 2002), thus implying that occupants adapt to their indoor environment. Brager & De Dear (1998) suggest that three conscious modifications, or processes of adjustment, can be carried out by an occupant to reach thermal comfort:

1. Personal adjustment (clothing, posture, moving to a different location, consumption of hot/cold food or beverages);
2. Technological or environmental adjustment (fans, blinds, heating);
3. Cultural adjustments (scheduling of activities, dress codes, siestas).

It is also suggested that the ability of each occupant to control their environment, be it perceived or real, is of primary importance and so the efficiency of adaptation to an indoor environment may be expressed in terms of available control versus exercised control versus perceived control (Brager & De Dear, 1998).

This is shown in practice by comfort surveys and indoor temperature data collected from offices in Pakistan in the 1970s by Nicol *et al.* (1999). The Pakistani climate delivers a wide variety of outdoor temperatures and so a range of corresponding indoor temperatures are also experienced. Because the only control available to the surveyed occupants were desk fans and the ability to change clothes, clear correlation between the use of these processes and thermal comfort is seen in the results. Thermal comfort is deemed to be better in the buildings with the greatest temperature variation (in some cases 13°C to 36°C), where the occupants had to be adapting to their environment to remain comfortable. Here, Nicol & Humphreys (2002) argue that it is the temperature expected in a particular circumstance rather than an attitude to the available building services that is important, which has to be the case in the Pakistan study. In the UK, Raja (Raja *et al.*, 2001) reports that occupants with access to controls such as windows, blinds, and curtains report fewer cases of thermal discomfort. This correlates with other literature that shows the cooling effect of internal air flow; for example, Aynsley (2008) shows that when the air temperature is above 23°C the body needs to lose heat in order to maintain a constant internal temperature. Then, the percentage of the optimum cooling effect achieved by an air flow is approximately 72% at 1.27 m/s, 82% at 2.54 m/s , 90% at 3.81 m/s, and 100% at 7.62 m/s. After this peak the cooling effect decreases to zero at around 10.16 m/s. However, it should be noted that the data does not indicate other environmental conditions that could also affect the comfort of occupants. However, De Dear & Brager (2002) say that the question engineers should be asking is not "should we provide more controls?" but "how do we do it?"

The heat balance models are derived using climate chambers where the air is delivered mechanically and is, by default, pre–conditioned. Brager & De Dear (1998) compare thermal comfort data from buildings ventilated using HVAC systems with those ventilated by natural principals and find a clear distinction in the responses of occupants that cannot be accounted for by an adjustment to clothing or activity. Consequently, they hypothesise that the most plausible explanation is that the previous experiences of occupants governs their expectations, which is strongly affected by a sense of whether or not conditions are under their control. Another advantage of a naturally ventilated (NV) building is that the internal conditions are a function of external conditions. Therefore, occupants are able to relate to their indoor environment visually, thermally by wearing seasonal clothing, and by making

use of environmental adjustments such opening or closing windows.

Although the adaptive approach addresses Fanger's *condition of mind*, a criticism of the adaptive approach to thermal comfort is that its very complexity makes its application to building design impossible (McCartney & Nicol, 2002). However, Brager and De Dear's hypothesis has been applied to develop simple control strategies that use a rolling mean of external temperature (see here McCartney & Nicol, 2002; Nicol & Humphreys, 2002; CIBSE, 2006a; BSI, 2007).

In mechanically ventilated (MV) buildings the relationships between its occupants and thermal comfort are also complex. Here, Brager & De Dear (2000) have shown that occupants of MV buildings expect a very narrow bandwidth of temperature variability, and so in effect by increasing the complexity of control systems and building services, the expectations of the occupant is also increased.

When considering the future of thermal comfort, Chappells & Shove (2005) suggest that rather than considering a more efficient way to maintain a standard temperature, which is energy intensive, the meaning of comfort and the way of life associated with it should be explored, and so existing diversity and the wide variety of occupant expectations can be exploited, and the commitment to an unsustainable future avoided. Brager & De Dear (2000) recommend a completely separate set of standards for NV buildings that consider the adaptive approach.

National and international standards have been slow to consider the adaptive approach; for example ISO Standard 7730 (ergonomics of the thermal environment) uses Fanger's comfort equation that requires inputs of *clo* and *met* units (ISO, 2005). It took the American Society of Heating, Refrigerating and Air–Conditioning Engineers (ASHRAE) until 1992 to add an "Adaptive Comfort for NV buildings in Warm Climates" section to its standard for Thermal Environmental Conditions for Human Occupancy (Standard 55) (see De Dear & Brager, 2002). In the UK, CIBSE Guide A for Environmental Design (CIBSE, 2006a) details the heat balance method employed by ISO 7730, but later considers further factors such as age, gender, and the state of an occupant's health.

This section has shown that thermal comfort is a highly subjective quantity, that may be achieved by the consideration of personal, technological or environmental, and cultural factors, and not just the internal temperature. The type of ventilation strategy has been

identified as being an important factor in the delivery of thermal comfort, with occupants of NV buildings showing a greater tolerance to differing thermal conditions when they are given control over their environment. Moreover, by getting the internal thermal conditions right, the direct benefits to occupants upholds their right to health, while the indirect benefits can be considerable in terms of financial cost (see Fisk, 2000, for a full breakdown). Nicol & Humphreys (2002) hopes that it may be possible in the future to produce thermal standards for a building that do not "resort to specification of the indoor climate".

Thermal comfort is normally assessed by survey; however, performing surveys can be fraught with difficulty and dependent upon the prevailing conditions in a building. For example, a survey carried out in extreme psychological and/or environmental conditions may produce equally extreme responses from the surveyed occupants of a building (Nicol & Roaf, 2005). Fascinatingly, Thörn (2000) cites a survey which determined that SBS symptoms occurred even after all measurable causative elements had been removed, with the real problem being an impasse between the owner of the building, the employer, and the employees. Nicol & Roaf (2005) feel that "surveys are therefore measuring a moving target". The achievement of thermal comfort among occupants of a room ventilated by a Windcatcher does not necessarily prove the functionality of a Windcatcher, but instead shows that a wide range of desirable factors are agreeable to the majority of occupants of a room, which may be unrelated to a Windcatcher. However, it is recognised that control of the internal room temperature is highly important and is related to the rate of ventilation. Consequently, the measurement of internal room temperature and external ambient temperature data are of vital importance for achieving the aim and objectives of this research because ventilation is a key moderator of the thermal environment, and therefore important for achieving thermal comfort among the occupants of a classroom. Finally, no matter how intriguing the psychosocial relationships between the occupants, the classrooms, and a Windcatcher may be, they are not of interest here, for it is the functionality of the Windcatcher that is under test. For these reasons, and because of the many confounding factors, the difficulties involved in surveying school children, and because their findings will not help meet the aim of this research, surveys have not been used in the context of this thesis.

2.1.2 Indoor Air Quality and Ventilation

Ventilation is defined by the Commission for the European Communities (CEC) as "the supply to and removal of air from a space to improve the air quality" (CEC, 1992). Because of the amount of time people spend inside buildings, the content of indoor air has become a dominant medium of exposure to an array of harmful pollutants. Even after 150 years of study (see Sundell, 2004, for a full history) it is not possible to show which pollutants are causative, only those that are important. Mølhave (2003) shows that all pollutants may be split into two groups: gases and vapours, and viable and non–viable particulate matter.

The first group contains compounds such as nitrogen dioxide (NO_2), carbon monoxide (CO), bio–effluents [such as carbon dioxide (CO_2)], volatile organic compounds (VOCs) that include formaldehyde and paint, and reactive compounds such as ozone (O_3). The second group contains fine respirable particulate matter such as PM_{10}s (defined as particles less than $10\,\mu$m) that are a product of combustion, building materials such as asbestos, man–made fibres, and organic matter that includes, mould, spores (pollen), and microbes (bacteria, fungi). These pollutant are emitted from, or are contained in, the building fabric, textile surfaces [furniture, carpets, blinds, curtains, see Seppänen *et al.* (1999)], consumer products [PCs, printers, photocopiers, see Bakó-Biró *et al.* (2004)], or in the ventilation source (ducting). For specific target concentrations of selected pollutants see Liddament (1996, Chapter 2, Table 2.1).

The concentration of a pollutant in the air of a room is a function of its rate of emission, the rate at which unpolluted air is brought into the room, and any other factors that effects its production. Pollutants are are controlled best at their source, but if this is not possible, isolation, the use of sorbents, and ventilation are secondary solutions.

The WHO states under articles 25 and 29 of the Universal Declaration of Human Rights, that all people have a right to breath healthy indoor air (WHO, 2000). Fanger (2006) says that the quality of indoor air should be defined by its effect on humans, and so one method determining IAQ is by determining the perception of the IAQ by the occupants based upon bioeffluent odour (the perceived IAQ). However, the sensory responses to an indoor pollutant are not always proportional to their toxicity and so perceived IAQ is not always a universal measure of overall IAQ (Seppänen & Fisk, 2004). For example, the ventilation strategy

can affect the perception of IAQ, and here natural ventilation has been shown to impact favourably because fewer symptoms of SBS are reported (Fisk, 2000). Furthermore, occupants of NV buildings are shown to be more tolerant of variations in carbon dioxide levels and temperatures than in MV buildings (Hummelgaard *et al.*, 2007). In many studies, CO_2 and RH levels are continuously monitored over a period of time to determine their effect on occupants; for example Bakó–Biró used these parameters when looking at the effects of ventilation on the learning performance of children in school classrooms (Bakó-Biró *et al.*, 2008) and when determining the effects of emissions from personal computers on occupants (Bakó-Biró *et al.*, 2004).

The chemical composition of outdoor air (by volume) consists of three dominant elements: nitrogen (78%); oxygen (21%); and argon (1%). Other constituents make up only 0.04%, and carbon dioxide (CO_2) is now present at a mean ambient concentration of 0.0386% or 386 parts per million (ppm) (NOAA, 2009). Inside a building, Persily (1997) shows that the measurement of CO_2 over time is a very useful indication of IAQ and ventilation in a building because it is produced as a bi–product of either human respiration or combustion. If internal CO_2 only occurs from human respiration, its rate of production is related to the number, size (age, gender, mass), and physical activity of the occupants (see BSI, 1991; Roulet & Foradini, 2002). When the internal CO_2 concentration rises above the ambient level, it can be used as a tracer gas with which to study building ventilation (see Etheridge & Sandberg, 1996, Chapter 12, for a number of well–established techniques). Persily is very clear that CO_2 is not considered to be directly hazardous to people in the concentrations generally found in buildings, and can only be used to indicate specific and limited aspects of IAQ, not the overall level of IAQ. Emission of pollutants from building materials or textile surfaces may be goverened by other factors—for example formaldehyde release is a function of RH (CEC, 1992)—and so their concentration is not generally related to the number of occupants in a room or, therefore, CO_2. Consequently some studies that choose to use CO_2 as an indicator of ventilation when studying the association between ventilation and health do not always find a link as consistently as studies that measure ventilation directly (see here Daisey *et al.*, 2003; Persily, 1997).

Attempts are often made to use CO_2 as an indicator of SBS (see Erdmann & Apte, 2004, for example), although SBS itself does "not indicate either a particular exposure or a specific

disease" (Apte *et al.*, 2000). Furthermore, some studies have attempted to link the internal CO_2 concentration with health, performance, and attendance issues. An early example is reported by Myhrvold *et al.* (1996) who show [with limited data, see Mendell & Heath (2005)] correlations between SBS symptoms and CO_2 concentrations above 1500 ppm, while lower ventilation levels correspond to increased CO_2 concentrations that they associate with reduced work performance. High CO_2 concentration has also consistently been found to be associated with increased sick leave when used as an indicator of ventilation in offices (Milton *et al.*, 2000) and school classrooms (Shendell *et al.*, 2004). When reviewing over twenty studies that measured CO_2 concentrations and SBS symptoms in non–domestic buildings, Seppänen *et al.* (1999) found that the majority showed an increase in SBS symptoms with higher CO_2 concentrations, while in a similar study Apte *et al.* (2000) found a similar relation ship between CO_2 concentration and health. A threshold value, below which reductions in CO_2 concentrations would not be associated with further decreases in health symptoms was not ascertained by Seppänen, but Apte suggests a maximum acceptable concentration of 1000 ppm. Furthermore, Seppänen's analysis shows that SBS symptoms continue to decrease even as CO_2 concentrations drop below 800 ppm. Other large scale studies (see Smedje *et al.*, 1997, who measured IAQ in school classrooms) found "no significant relationships between complaints about IAQ and air exchange rate or concentration of carbon dioxide". Apte *et al.* (2000) states that negative associations should not be interpreted as evidence that ventilation plays no part in the prediction of the prevalence of SBS symptoms in buildings, because we already know that there is evidence of a link between the two (see Seppänen *et al.*, 1999, for example). The reason why CO_2 is often used as indicator of some occupant response to their indoor environment such as IAQ, SBS, or performance, is because it is easy to measure over a long period of time, whereas long term measurement of ventilation is more problematic, intrusive, and expensive. There is no direct link between CO_2 and poor IAQ or SBS health symptoms, and so inaccuracies in the data can occur, but the literature does generally agree that high levels of carbon dioxide (above 1000 ppm) will increase the statistical probability of SBS symptoms (Apte *et al.*, 2000).

The pressure of air is related to the amount of moisture contained within it; the more water molecules present in a sample, the higher its pressure will be. Relative humidity (RH) is a ratio of the vapour pressure of a sample of air and the saturated vapour pressure of

air at the same temperature expressed as a percentage (McMullan, 2002). Like CO_2, it is difficult to be specific about the levels required for thermal comfort and good IAQ, although levels between 30–70% are thought to be acceptable (CEC, 1992). However, unlike CO_2, RH is a direct cause of poor IAQ through the release of formaldehyde (CEC, 1992) and can be directly related to the number of occupants because, in a sedentary environment, up to 25% of the body's excess heat is lost through transpiration; the evaporation of moisture through perspiration and breathing (Liddament, 1996). Furthermore, this can rise to between 50–80% when activity and temperature increase. The rate of human tranpiration is reduced by high RH and so leads to discomfort, and is increased by a low RH that leads to dehydration.

By using a climate chamber to introduced pollutants (such as floor varnish) to occupants, Fang *et al.* (1998) report that with a constant level of pollution, temperature and RH have a strong and significant impact on the perception of IAQ and that perceived IAQ decreases with increasing air temperature and RH. But, if pollution levels increase, the impact of temperature and RH on the perception of IAQ decreases. Finally, the influence of pollution on perceived IAQ decreases with increased air temperature and humidity. So, for higher levels of temperature and RH, additional pollutants are less important than they are at lower humidity.

It is also known that the propagation of dust mites increases when RH levels are in the region of 70–80% and that RH levels correlate directly with the production of fungal spores (Jones, 1999). This is important because at higher levels of RH, concentrations of alternaria (a mold allergen) in the air and dust mite antigens in floor dust are increased. Note here that both are associated with a higher prevalence of respiratory symptoms (Fisk, 2000). Mold has also been linked with high RH in some American schools (Daisey *et al.*, 2003). Consequently, it is recommended during the winter that RH levels are reduced below 45% for a period of time to reduce dust mite numbers (CEC, 1992), but this can lead to other problems because tests in offices find that RH levels below 25% in winter cause symptoms such as the dryness of the nose and throat (Jaakkola & Miettinen, 1995). Mechanical systems have an advantage in these circumstances because they can modify the humidity of incoming air. When studying workers in 41 offices in Helsinki, Jaakkola & Miettinen (1995) found that workers in MV and air–conditioned office buildings (with and without humidification and air recirculation) experience more work–related symptoms of SBS when compared with those in NV buildings.

Steam, evaporative humidification, and air recirculation are considered as determinants of the symptoms. In places where the winters are warm and humid, allergies to dust mites are more common (Daisey *et al.*, 2003), and so the importance of monitoring RH in such climates during the winter season are obvious.

When the ventilation rate through a room is compared against direct and indirect occupant responses to IAQ there are a greater number of statistically significant relationships than for CO_2. For example, direct occupant responses are demonstrated by considering the relationship between health symptoms, here categorised as SBS symptoms, and ventilation rate using the responses of nearly 30,000 occupants of non–domestic buildings. Seppänen *et al.* (1999) developed an indication of *relative risk* to show that the probability of SBS symptoms occurring at low ventilation rates, rather than high, are 1.1–6 times more likely. Here, high and low ventilation rates are defined as up to 20 litres per second per person (l/s – person) and below 10 l/s – person, respectively. The results are not definitive and Seppänen & Fisk (2004) point out that there is no threshold ventilation rate above which the relative risk of SBS symptoms reduces to unity, and that the direct benefits to occupants decrease in magnitude per additional unit of ventilation. However, they also show a statistical increase in the worsening in a least one health outcome when the ventilation rate is below 10 l/s – person; similar results are also obtained by Wargocki *et al.* (2000) and Apte *et al.* (2000). Wargocki *et al.* (2002) show that the perceived IAQ of occupants, and their comfort, increases with the per capita ventilation rate, and that outdoor supply rates should exceed 25 l/s – person to reduce the risk of SBS symptoms and short–term sick leave, and to increase productivity. This ventilation rate is significantly higher than those specified by all national standards for an office space or a classroom, would be highly energy intensive, and would only deliver a small relative benefit to the occupants (see Seppänen & Fisk, 2004).

The majority of studies are carried out in MV offices with HVAC systems, although some exist for NV buildings. When the two types of ventilation method are considered as confounding factors, Seppänen & Fisk (2004) reports that "relative to NV buildings there is a statistically significant increase in the prevalence of one or more SBS symptoms in HVAC buildings." In fact, a lower prevalence of SBS symptoms among occupants of NV buildings was found despite lower ventilation rates (Seppänen *et al.*, 1999).

There are also a number of significant studies that consider the indirect responses of

occupants to IAQ. In a closed laboratory test, Wargocki *et al.* (2000) show an increase in the productivity of subjects who completed simple tests. Here, only a 1.7% increase was found when the ventilation rate was increased two–fold at various rates of between 3 l/s – person and 30 l/s – person. Seppänen & Fisk (2004) also reviewed this study and points out that the results are for a single pollutant source, here a dirty carpet located behind a screen, and so the results are only applicable to this type of pollutant source. Seppänen *et al.* (2006) show a quantiative relationship himself between the ventilation rate and improved work performance, but with a high level of uncertainty.

Several key studies examine the effects of ventilation rate on more vulnerable occupants, such as children, who are more susceptible to pollutants than adults because they breath greater volumes of air relative to their body mass, and their potential to sustain long lasting damage is higher because their tissue and organs are still growing (Mendell & Heath, 2005). For example, the literature review of Mendell & Heath (2005) shows evidence of links between low ventilation rates and adverse health effects in children and adults in school buildings, manifested as poor academic performance and absenteeism, while Shaughnessy *et al.* (2006) demonstrate a significant association between the ventilation rate and the achievement of school children in mathematical tests. Furthermore, by using similar intervention tests in school classrooms, Wargocki & Wyon (2007b,a) show that as per capita ventilation rates increase, the speed and accuracy of student performance also increases, and in a study of over 200 children in the UK, Bakó-Biró *et al.* (2008) show that poorly ventilated classrooms significantly impair the attention and vigilance of children.

The benefits of providing good IAQ are clear in the literature:

> *It pays to provide indoor air quality.* (Fanger, 2006)

In order to provide good IAQ, most national standards for buildings have, historically, specified the rate of outdoor air that must be brought into a room per occupant. Persily (2006) notes that relying on outdoor ventilation is inherently limited given the wide range of internal pollutant emission sources and rates, and the variation in susceptibility of different occupants to exposure. However, he concludes that we appear to have no choice but to use ventilation criteria that may not meet our desire for a good IAQ.

In 2006 the ventilation rate for a UK office space was increased from 8 to 10 l/s – person

by a re–issue of the Buildings Regulations (ODPM, 2006), whereas in the USA ASHRAE Standard 62 specifies 8.5 l/s – person. It is no coincidence that early work exploring perceived IAQ by Yaglou in 1936 (see Persily, 2006), which shows that a ventilation rate of between 7.5 to 9 l/s – person reduces bioeffluent odour to an *acceptable* level for anyone who enters an occupied room from clean surroundings, forms the basis of the ASHRAE Standard and the UK Building Regulations. This highlights the uncertainty surrounding the measurement of IAQ and its effects on occupants. Persily (2006) suggests that we should "acknowledge the limitations of what we do know, and perhaps will ever know, about how much outdoor air is needed in buildings."

This section has identified and highlighted three key parameters in the provision of IAQ: the ventilation rate, and the internal CO_2 and RH levels—showing that their measurement gives a limited, yet important indication of the IAQ. Furthermore, links between perceived IAQ and performance, and good IAQ and health, attendance, and cognition have been established. When considering ventilation strategies to provide good IAQ, occupants of NV buildings are more tolerant to their conditions than those in a MV building. Finally, the affects of poor IAQ are far greater on the most vulnerable occupants, particularly children. Given these facts, the indoor air quality found in school classrooms is now explored.

2.1.3 Indoor Air Quality and Ventilation in Schools

The occupancy density of an average UK school classroom is 0.42—0.56 persons/m^2, which is extremely high at when compared to a density of 0.10 persons/m^2 found in an average UK office (Clements-Croome *et al.*, 2008). Consequently, the demand placed upon the ventilation strategy to provide good IAQ is greater and so IAQ and ventilation provision is tightly regulated.

In North America, the ASHRAE Standard 62.1 (ASHRAE, 2007) recommends a default minimum ventilation rate for acceptable indoor air quality in school classrooms of 6.7 to 7.4 l/s – person, depending upon the age of the children, but is generally cited in the literature as a blanket rate of 8 l/s – person (see Daisey *et al.*, 2003; Clements-Croome *et al.*, 2008). It also shows that the maintenance of a steady state CO_2 concentration of 700 ppm above ambient levels will ensure the provision of 7.5 l/s – person, and will constrain body odour. In the USA, the standard is voluntary until adopted by a local code or other regulation, and its

pros and cons are discussed by Persily *et al.* (2007).

In Europe, several standards present guidelines for good indoor air quality, see CEC (1992), EN13779 (BSI, 2004), and EN15251 (BSI, 2007). EN15251 classifies IAQ into four bands of performance from 1 to 4 (or I to IV as appropriate), that correspond the proportion of occupants that are dissatisfied with the indoor air quality (10%, 20%, 30%, and >30% respectively) and ventilation rates of 10, 7, 4, and <4 l/s – person respectively, see Olesen (2007) for further guidance. EN13779 also classifies IAQ into high, medium, moderate, and low quality bands (defined as bands 1 to 4), that correspond to values of 250 ppm, 500 ppm, 800 ppm, and 1200 ppm respectively for the indoor CO_2 concentration above the ambient, and a per capita rate of ventilation for non–smoking rooms of 20, 12.5, 8, and 5 l/s – person, respectively. Various national guidelines specify other ventilation rates for classrooms; for example, Conceição & Lucio (2006) report that the Portuguese standard is 8.3 l/s – person, Geelen *et al.* (2008) show that The Netherlands Standard 1089 stipulates 5.5 l/s – person and a guideline peak value of CO_2 at 1200 ppm, and Smedje & Norback (2000) record that Swedish standards require 8 l/s – person and an internal CO_2 concentration below 1000 ppm.

In the UK, Building Bulletin 101 (BB101) (DfES, 2006) provides the regulatory framework for the adequate provision of ventilation in schools and is supplementary to part F of the Building Regulations (ODPM, 2006). It gives clear guidelines for ventilation rates per capita and internal temperature during occupied hours. However, it refers to the buildings regulations (ODPM, 2006) for RH guidelines. BB101 defines occupied hours to be between 0900 hrs and 1530 hrs (see DfES, 2006, Section 1.7) and for the purposes of this document, these times are inferred when the terms *teaching day* and *occupied hours* are used.

BB101 uses CO_2 as the key performance indicator, prescribing the following criteria when it is measured at head height during the continuous period between the start and finish of a teaching day:

- A maximum concentration of 5000 parts per million (ppm);
- A mean concentration below 1500 ppm;
- The ability to lower the concentration to 1000 ppm.

Of course, in the absence of a combustion source, the rate at which CO_2 is produced

within a space depends on its volume, the number of occupants, as well as their size, activity, and metabolic rate (Persily 1997). Thus, one can link desired CO_2 levels to ventilation rates and here BB101 states that a natural ventilation system should be capable of providing:

- A minimum of 3 l/s – person;
- A minimum daily average of 5 l/s – person;
- A purge ventilation rate of 8 l/s – person.

Regulations for the internal temperature and RH are set according to the use of internal space heating, with the heating season defined by BB101 (see DfES, 2006, Section 1.7) as 1st October to 30st April. BB101 only specifies temperatures outside of the heating season and in order to show that a school will not suffer overheating, two of three following criteria must be met:

1. There should be no more than 120 hours when the air temperature in the classroom rises above 28°C;
2. The average internal to external temperature difference should not exceed 5°C (i.e. the internal air temperature should be no more than 5°C above the external air temperature on average);
3. The internal air temperature when the space is occupied should not exceed 32°C.

CIBSE (2006a) recommend operative temperatures between 19–21°C in the heating season and a minimum air temperature of 16°C is set by the Health and Safety Executive (HSE, 1996) for office type accommodation. Building Bulletin 87 (BB87) (DfEE, 2003) also advises maintaining an air temperature of 18°C at a height of 0.5 m above the floor in areas where there is the normal level of physical activity associated with teaching, private study or examinations.

The mean RH in a classroom is set in accordance with part F of the building regulations for office–type accommodations [see DfES (2006) section 3.2 and ODPM (2006) appendix A] and must not exceed 70% for more than 2 hours in any 12 hour period, and 90% for more than 1 hour in any 12 hour period, during the heating season.

The adverse effect of poor indoor air quality (IAQ) on the health and productivity of building occupants is well known, see for example Mendell & Heath (2005). Poor IAQ can be particularly detrimental to children in schools who spend approximately 12% of their time inside school buildings, which is more than in any other building type other than their homes (Mendell & Heath, 2005; Grimsrud *et al.*, 2006). A range of dangerous gases such as NO_2 (Stranger *et al.*, 2008), CO (Chaloulakou & Mavroidis, 2002), and particulate matter (see Chen *et al.*, 2000) are known to be present in the air of school classrooms.

Most investigations of IAQ and ventilation rates in school classrooms in the literature are for MV classrooms. Reports of internal RH and temperature are less common and are normally considered to be of peripheral interest. For example, in North America, Godwin & Batterman (2007) report on ventilation rates in 64 MV lower and middle school classrooms in Michigan, USA, during the spring. The ventilation rates were found to be inadequate in most cases with only 27% of classrooms meeting the required standard of 8 l/s – person, and although some of the classrooms had manually opening windows, it was felt that the weather conditions may have restricted their use, and so the results may be a function of the season. Mean temperatures and RH are deemed to be within acceptable ranges set by the ASHRAE handbook (see Godwin & Batterman, 2007) at 23 ± 3°C and 38 ± 9% respectively. This suggests that mechanical systems do not always provide adequate ventilation to meet national standards, a finding echoed by other studies of ventilation rates in MV classrooms in the USA and Canada. For example Grimsrud *et al.* (2006) report substandard ventilation in 5 of the 8 schools they studied and very low RH of 10–20% in winter (a function of air heating units) that is known to significantly affect comfort, and high temperatures that were a function of poorly located or inoperable thermostats. Bartlett *et al.* (2004) analysed 11 portable classrooms in a single school district of British Columbia, Canada, finding that ventilation rates and CO_2 concentrations are below those required by ASHRAE Standard 62. When making one–off spot checks of CO_2 in 3801 classrooms in Washington State, Prill *et al.* (2002) find that internal concentrations are over 1000 ppm in 43% of the classrooms, with 67% having a malfunctioning extract fan. Later, Shendell *et al.* (2004) use the same data to show that in 50% of the classrooms, ventilation rates are less than the ASHRAE standard rate of 7.5 l/s – person. Furthermore, they show that a rise of internal CO_2 concentration 1000 ppm above external levels results in a 10–20% relative increase in student absence.

Shaughnessy *et al.* (2006) measured a mean ventilation rate of 3.9 l/s – person in 50 US classrooms, equivalent to half of the ASHRAE Standard 62 requirement. In addition, the effect of reduced ventilation upon performance was measured using mathematical tests, and showed a significant association between the two parameters.

In Hong Kong, Lee & Chang (1999, 2000) find that CO_2 levels in five mechanically and naturally ventilated Hong Kong school classrooms fail to meet the ASHRAE standard because of overcrowding and inadequate ventilation provision. Perhaps unexpectedly, the internal CO_2 concentrations are better in the NV classrooms.

In Europe, where far fewer classrooms are MV, natural ventilation strategies using manually opening windows are common. In Germany, windows are generally used to regulate the indoor air quality and Hellwig *et al.* (2009a,b) report that CO_2 concentrations are greater than 1500 ppm in 7 of 15 classroom monitored in the summer and in 32 of 36 classroom measured in the winter. Classroom temperatures are also found to be too hot in the summer and too cold in the winter, which is thought to be a function of insufficient ventilation provision and the number of open windows. Smedje *et al.* (1997) reviews perceived and measured IAQ, and the ventilation rate in classrooms from 38 schools (27% are NV) located in mid Sweden. Ventilation rates range from 0.1 to 22.4 l/s – person with the lowest ventilation rates found in NV classrooms. Here, the IAQ is perceived to be worse in schools with a mechanical extract and best in schools with a mechanical supply and extract. Furthermore, at an equivalent level of exposure to airborne pollutants, fewer complains arise from the occupants of NV classrooms, but it is noted that the complaints are not related to the classroom ventilation rate. Therefore, they suggest that since subjective IAQ is related to the measured exposure levels of airborne compounds, the emission of pollutants must be higher in MV schools. In a further study, Smedje & Norback (2000) study the links between improved ventilation with the health and exposure of children in 39 schools in Sweden. They report that the ventilation rates in schools are often below the specified Swedish ventilation standard of 8 l/s – person and above the CO_2 standard of 1000 ppm. For example, they report that in 1993, 77% of investigated schools failed to meet the Swedish standard in a mixture of NV and MV classrooms. Furthermore, the installation of new ventilation systems increased the ventilation rate and reduced exposure to pollutants such as pollen, thus having a positive affect on the frequency of asthma symptoms among the students. In Norway, Myhrvold *et al.* (1996)

measured CO_2 concentration in 35 MV classrooms finding that CO_2 concentration is below 1000 ppm in 49% of classrooms, below 1500 ppm in 74% of classrooms, and above 1500 ppm in only 26% of classrooms, indicating that 49% of classrooms would meet ASHRAE Standard 62.1 and 74% would meet the UK BB101 Standard. In the Netherlands, two sources report the internal CO_2 concentrations in a number of primary schools. Firstly, from a study of seven primary schools in the Rotterdam, van Dijken *et al.* (2006) show CO_2 concentrations to be in excess of 1000 ppm for a median average of 80% of the time between April and May, while another study of sixteen classrooms from 8 schools in Groningen shows that CO_2 exceeds 1000 ppm for a median average of 77% of teaching hours in February and March. In a study of 11 classrooms in 11 primary schools, of which three have mechanical extract systems while the rest are NV, mean CO_2 concentrations are found to be between 888 ppm and 2112 ppm when measured between January and March, although it is not clear how the ventilation strategy affects the internal CO_2 concentration. Secondly, Geelen *et al.* (2008) report that the median CO_2 concentration exceeded 1000 ppm during teaching hours in 81 classes from 20 NV primary schools.

In the warmer southern European climate, Conceição & Lucio (2006) measured the ventilation rate in a Portuguese school classroom, cross ventilated using sash windows, and show the ventilation rate to be equivalent to 2.4 l/s – person. In Greece, Santamouris *et al.* (2008) measured ventilation and internal CO_2 concentrations in 62 NV classrooms in Athens finding that 29% of classrooms have a mean CO_2 concentration above 1500 ppm during teaching hours, and approximately 38%, 55%, and 77% of classroom have a mean ventilation rate during teaching hours of less than 3, 5, and 8 l/s – person, respectively. Both of the southern European studies show that majority of the classrooms fail to meet ASHRAE standard 62.1.

Santamouris *et al.* (2008) has also extensively reviewed the literature collating measurements of ventilation rate and internal CO_2 concentration during occupied hours from 1187 classrooms, of which 287 are NV and 900 are MV, to form a database. The database shows that 25% and 53% of NV classrooms have a mean CO_2 concentration of less than 1000 ppm and 1500 ppm, respectively, while in MV classrooms 55% and 85% have a mean CO_2 concentration of less that 1000 ppm and 1500 ppm, respectively. Furthermore, the database also shows that 50%, 30%, and 5% of NV classrooms have a mean ventilation rate during teaching hours greater than 3, 5 and 8 l/s – person, respectively, while 99%, 61%, and 50% of MV

classrooms have a ventilation rate greater than 3, 5 and 8 l/s – person, respectively. All of this data shows that school classrooms worldwide are chronically under–ventilated. Furthermore, if geographical, architectural, and seasonal considerations are ignored, the ventilation rate in an NV classroom is, on average, much lower than in a MV classroom, and only half of NV classrooms would meet the UK BB101 Standard for CO_2 and 30% would meet the ventilation rate requirements.

Only a limited number of studies of ventilation and air quality in UK classrooms and their conformity with the standards of the time have been conducted and reported in the academic literature in recent years. Traditionally, UK schools have been designed to be NV and to exploit natural daylight using a narrow plan architecture and manually opening windows located in a single façade. Cross ventilation is sometimes employed using passive stacks or clerestory (upper level) windows, but a criticism of this strategy is that the occupants often have to choose between draughts or poor IAQ (DfES, 2006).

Although some UK school classrooms are MV, the majority employ one of the following natural ventilation strategies:

(a) Single–sided ventilation with a single opening;

(b) Single–sided ventilation with high and low–level openings;

(c) Cross ventilation and cross ventilation with a height difference;

(d) Stack ventilation;

(e) Multiple classrooms with stack ventilation served by a corridor or atrium;

(f) Top down split duct roof–mounted ventilation (a wind–catcher).

See also Figures 2.1—2.8, beginning p. 48.

The mean ventilation rates specified by BB101 can be addressed using mechanical ventilation; for example, in a study of 5 MV classrooms, Mumovic *et al.* (2009) show that a mean ventilation rate of 5 l/s – person is achieved in 4 of them. However, the UK Government suggests that to minimise environmental impact and to reduce running and maintenance costs, school designs should "aim for natural ventilation where possible" (DfES, 2002). This aim is in addition to the potential of natural ventilation systems to improve IAQ and, hence, the

performance of children in schools. Accordingly, in order to deliver the IAQ levels prescribed by BB101, any natural ventilation strategy must meet the challenges presented by modern classrooms, such increased air tightness, deeper plans, and the increased presence of ICT equipment.

In order to investigate appropriate strategies, Coley & Beisteiner (2002) measured CO_2 concentrations and ventilation rates in seven classrooms from four schools for a week during the heating season. The ventilation strategy was based on opening windows located either in a single façade, or on opposite sides of the classroom. Coley and Beisteiner report a mean CO_2 concentration in the classrooms of 1957 ppm during occupied hours, which is above the limit set by BB101, and show that only one classroom was below the 1500 ppm limit. Furthermore, five of the classrooms failed to meet the required purge ventilation rate of 8 l/s – person. This report shows that during the heating season, CO_2 is too high and ventilation rates are too low, which is thought to be a function of the number of window that were open. Here, it is noted by Coley and Beisteiner that the windows were not generally opened in the heating season for several reasons: they are difficult to open, and children seated near to them experience draughts. In a related study, Beisteiner & Coley (2002) measured CO_2 concentrations and ventilation rates in four NV classrooms, from two schools, for a week during the summer season using the same methodology employed in the winter study. This time, two classrooms achieved a mean CO_2 concentration below the BB101 limit of 1500 ppm, and only two met the required purge ventilation rate. Although these results are better than the winter results, the provision of ventilation remains inadequate during the summer despite greater reported use of the windows. Similarly, Griffiths & Eftekhari (2008) show that a school classroom, NV using windows and trickle vents, can meet the current mean CO_2 concentrations during the teaching day providing the windows are open, but the purge requirement of 8 l/s – person cannot be met.

Most recently Mumovic *et al.* (2009) monitored eighteen classrooms in nine schools over five days during the winter time. The classrooms have natural, mechanical, and mixed–mode ventilation strategies; results show that six of the classrooms exceeded the required mean CO_2 concentration during the teaching day and all were NV. Furthermore, two–thirds of the NV classrooms failed to meet the required purge rates, and only two of the fourteen NV classrooms met the mean ventilation rate of 5 l/s – person. Conversely, the MV classrooms

were all able to meet the required mean CO_2 concentration and the purge ventilation rate.

If a natural ventilation strategy is to be used in a school classroom, it is likely that an alternative strategy to openable windows is required to meet BB101 ventilation requirements. Kolokotroni *et al.* (2002a) monitored IAQ parameters and ventilation rates during the summer in four classrooms which use a natural ventilation strategy that combines manually opening windows with a passive stack. Internal RH was found to acceptable between 45–65% in all classrooms, and in one classroom the internal temperature was more than 5°C above the external temperature indicating over heating. However, mean CO_2 concentrations in all classrooms were less than 800 ppm and so are within the mean CO_2 criteria during the teaching day, showing that a stack system using manually opening windows can meet the ventialtion rates (indicated by mean CO_2) during the summer.

This review shows a world–wide trend of inadequately ventilated school classrooms, which will have negative consequences for their vulnerable occupants. In the UK there is very limited data on the IAQ and ventilation rates one may expect to find in a classroom. The information that has been gathered shows that, although there is a real need to use a natural ventilation strategy where possible for sustainable (environmental, social, and economic) reasons, they are currently not functioning as they should. Therefore, an alternative to the natural ventilation strategies discussed here is required, such as the Windcatcher, if the requirements of BB101 are to be met consistently.

Most UK schools are ventilated using windows located in a single façade. Here, rule–of–thumb guidelines (see CIBSE, 2005a) for the effective penetration of air to the back of

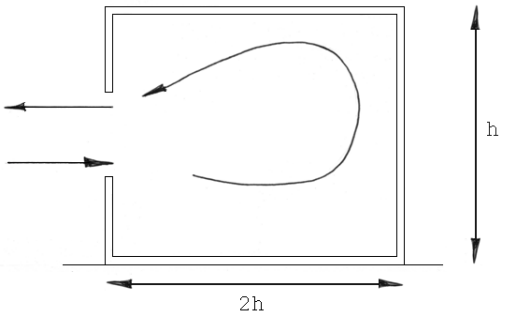

Figure 2.1: Single sided ventilation, single opening.

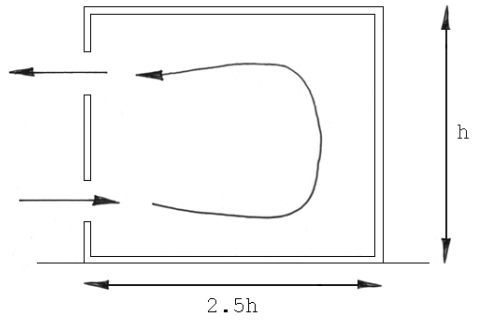

Figure 2.2: Single sided ventilation, double opening.

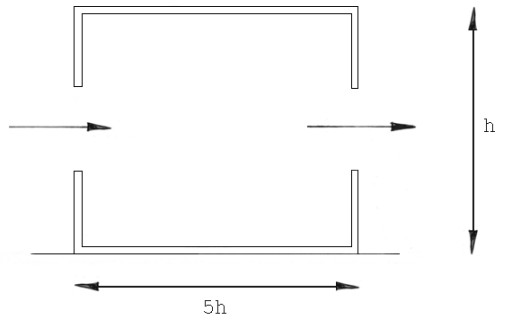

Figure 2.3: Cross ventilation, façade opening.

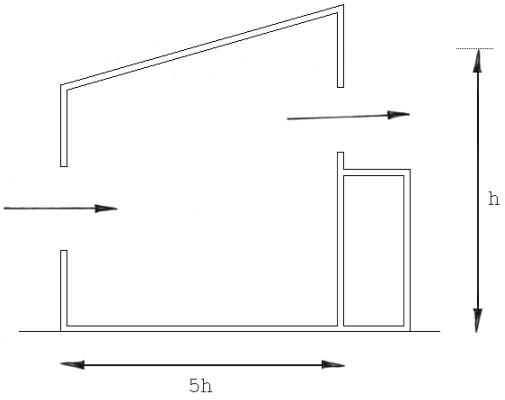

Figure 2.4: Cross ventilation, façade opening and clerestory windows.

a room ventilated using single–sided single–opening ventilation suggest that the ratio of the depth of the room to its hight should be no greater than 2, see Figure 2.1. If two rows of windows are vertically separated by approximately 1.5 m to provide single–sided double–opening ventilation, the depth can be increased by up to 25%, and here the rule–of–thumb guidelines (CIBSE, 2005a) suggest that the depth to height ratio must be less than 2.5, see Figure 2.2. BB101 (DfES, 2006) has identified a modern trend for building classrooms with a deep–plan architectire that renders the single–sided approach to natural ventilation inappropriate. Consequently, the penetration of air into a room must be increased and here cross ventilation can be used where rule–of–thumb guidelines (CIBSE, 2005a) suggest that the

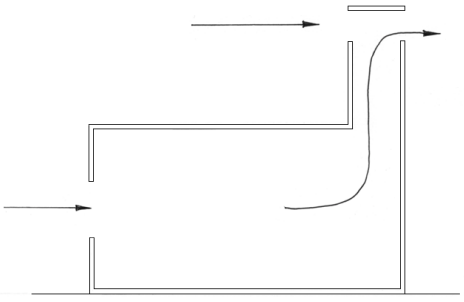

Figure 2.5: Stack ventilation.

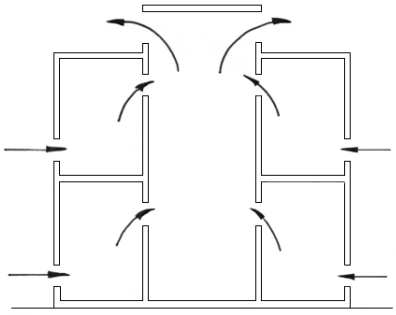

Figure 2.6: Stack ventilation, corridor and/or atrium.

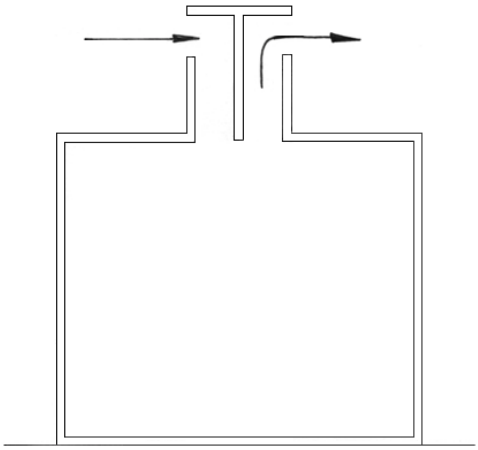

Figure 2.7: Top down ventilation, wind–catcher.

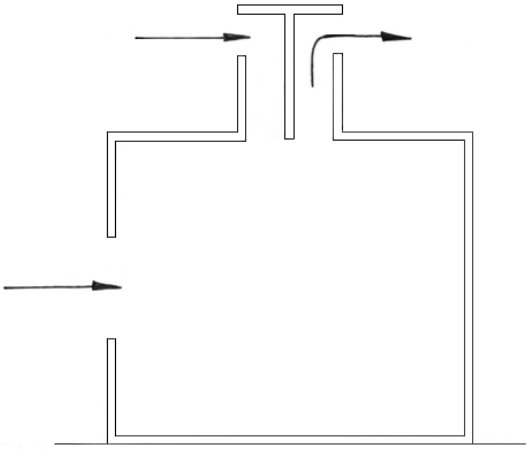

Figure 2.8: Top down ventilation, wind–catcher with façade opening.

depth to height ratio can be increased to 5. Cross ventilation strategies require openings on opposite façades, using windows (see Figure 2.3), clerestory windows (see Figure 2.4), or where this is not possible, perhaps because a corridor is in the way, a passive stack (see Figure 2.5) or a central atrium (see Figure 2.6) to carry stale air out of the building. However, the cross ventilation approaches that use a specialist outlet element, such as a stack or atrium, require them to be in an area of negative pressure. Although the orientation of a building can be determined by referencing local weather data, the wind direction will vary, which could disrupt the flow strategy and render the system in–operable in some circumstances. One further approach is to use top–down wind driven natural ventilation, either on its own (see Figure 2.7), or in combination with open windows (see Figure 2.8). By entraining air into a room from roof level, the incoming air contains fewer pollutants; for example Laxen & Noordally (1987) show that the concentration of NO_2 declines with height, reverting to background levels at approximately 20 m above ground level (see also Gage *et al.*, 2001). Omni–directional elements such as the Windcatcher allow wind energy to be captured whatever its direction, and so offer the potential to provide more consistent natural ventilation flow rates in schools whatever the prevailing weather conditions. To date, the Windcatcher has been installed in over 1100 UK schools by Monodraught Ltd. Accordingly, the physics of a Windcatcher and existing research that attempts to quantify their performance is explored in Section 2.2.

2.1.4 Indoor Environmental Noise and Ventilation

The human ear is capable of responding to sound frequencies from approximately 20Hz to 20kHz, but is much more responsive to broadband noise rather than a single tone of sound (Kinsler *et al.*, 1982). In a building, broadband noise is the combination of direct sound from a source and the reverberation of that sound. Ling (2001) shows that noise comes from three sources:

1. External noise (entering a building through ventilation openings or envelope. defects)
2. Internal noise (from ventilation systems or electronic equipment).
3. Path effects (sound transported through a building via a ventilation system or building voids).

Noise within a building is generally below 85–90 dBA and will not cause auditory damage to the ears, however the non–auditory effects are far more dangerous to health (Stansfeld & Matheson, 2003). Here, Stansfeld and Matheson link occupational and environmental noise with hypertension, and aircraft and traffic noise with psychological symptoms. Aircraft and traffic noise is associated with raised blood pressure and is also shown to impair the reading comprehension and the long term memory of children. Furthermore, it is generally accepted that noise has a detrimental effect upon the learning and attainment of primary school children, who are more susceptible than adults (Shield & Dockrell, 2003).

Therefore, the investigation of noise in schools and its affect on children is of great interest. Different types of noise (conversational babble and environmental noises for example) are shown to produce different effects on children when performing different tasks (Dockrell & Shield, 2006), while road traffic noise has a negative effect on the attention span of school children (Sanz *et al.*, 1993). More sudden noises, such as sirens, trains, or aircraft, may affect children and teachers "disproportionately to their contribution to the overall noise environment of a school." (Shield & Dockrell, 2003) Other noise related quantities such as the reverberation time and sound absorption of a classroom are a function of design and cannot be linked directly to the ventilation system. These effects are not discussed here, but they are discussed in a in review of literature by Shield & Dockrell (2003).

The World Health Organisation (WHO, 1999) and the American Standards Institute (ANSI, 2002) both specify background levels of noise for classrooms of 35dB L_{Aeq} during teaching hours. In the UK, Building Bulletin 93 (BB93) (DfES, 2003) provides the regulatory framework for noise levels in schools. Upper limits are specified as $L_{Aeq,30min}$, an average uninterrupted measurement of A weighted sound pressure level over 30 minutes in an unoccupied and unfurnished classroom. Here, BB93 (DfES, 2003, Table 1.1) sets the upper limit at 35 dBA in a conventional classroom and 40 dBA in a science and technology laboratory. BB101 (DfES, 2006) allows an additional 5 dB $L_{Aeq,30min}$ when the purge ventilation rate of 8 l/s – person is provided by natural ventilation. For all all other ventilation rates the BB93 limits apply.

Shield & Dockrell (2004) measured noise levels outside 142 urban schools in London, where 86% of the them were exposed to road traffic noise; the average external sound pressure level was calculated to be 57 dB $L_{Aeq,5min}$. Ling (2001) reports that measurements of road traffic noise should be measured over an 18 hour period from 0600–2400 hours, so these results should only be considered a snapshot, but were chosen by Shield and Dockrell to be "typical of the school day" and so avioded rush hour, arrival, departure, and play time periods.

As part of the same study, internal measurements were made inside 30 empty classrooms where the mean background levels was found to be 47 dB $L_{Aeq,2min}$, which is 12 dBA above those specified by BB93. Although the measurements were only made over periods of 2 minutes, continuous monitoring over a number of hours revealed that the fluctuation of noise was minimal, and so was considered to be approximately constant. Seven of the classrooms are reported as having audible heating/ventilation noise where mean background levels were highest, although specific ventilation strategies are not reported. Shield and Dockrell note that the noise levels measured in Victorian classrooms were, on average, 3.2 dBA lower than those measured in modern classrooms and that the glazing type appeared to make no difference to classroom noise levels in this study, although it is acknowledged that the sample size is deemed to be too small for definitive conclusions to be made. However, Shield and Dockrell point out that background traffic noise is predominantly made up of low frequencies that are difficult to attenuate using glazing. Most NV school classrooms must open windows to provide fresh air, thus increasing the ingress of noise (Ling, 2001). Andersen & Hopkins (2005) show that some types of windows, here those manufactured by Velux, only need to open 2 cm

(a distance determined in the laboratory and not in the field) to provide sufficient ventilation while maintaining adequate sound insulation. However, the fact remains that background levels in UK classrooms are already too high and opening windows increases them. A recent study of noise levels in 12 UK school classrooms built since 2003 (see Mumovic *et al.*, 2009) shows that 50% of measured classrooms fail to meet government requirements, with all mechanically ventilated classrooms failing to meet the internal ambient noise criteria. Most interesting of all, the report concludes that more noise is generated internally than externally.

Noise generated by mechanical ventilation systems arises from aerodynamic turbulence caused by fans, and contractions and expansions in its duct work that may consists of branching elements, diffusers, grills, and turning vanes (Ling, 2001). Natural ventilation systems have comparably large openings that offer low resistance to the ingress of external noise. In fact, the need to provide low–resistance ducts for the free–flow of air and to reduce noise ingress is a paradox. This was found to be a problem in the Coventry University Library where occupants applied their own acoustic lining to an exposed concrete natural ventilation duct (Simons & Maloney, 2003).

The average broadband traffic noise found in urban areas is approximately 70 dBA (Shield & Dockrell, 2003) and so an attenuation of 35–30 dBA must be made by the façade of the building and any ventilation elements. One cost effective response is to line ducts with an absorbent material. Here, a non–peer reviewed assessment of a square Monodraught Windcatcher, of cross sectional area 0.64 m^2, by the Building Research Establishment (BRE, 2005) shows that when it was tested in accordance with ISO 717–1 (ISO, 1997) and ISO 140–10 (ISO, 1991) to produce a standard acoustic difference from one room to another, the addition of a 25 mm open cell polyurethane foam acoustic lining to a duct (of length 1.1 m) and its partition, increases the airborne sound insulation by 11 dB. However, Oldham *et al.* (2004) show that duct lining is designed to attenuate mid and high frequencies and has mixed effects on low frequency traffic noise. A more expensive solution is to use active noise control which Oldham *et al.* show can attenuate lower frequencies by around 22 dBA. De Salis *et al.* (2002) offer a note of caution because badly designed active control systems can themselves be the cause of problems. De Salis *et al.* suggest the use of external architectural features such as fences or earth mounds. Dockrell & Shield (2006) advocates internal measures and suggests using ceiling tiles, carpeting and curtains, and wall covering to absorb sound.

The literature shows the negative effects of noise on the occupants of buildings, with children affected more than adults. Most studies of noise in schools are for NV classrooms, however there are no *in–situ* measurements of noise in classrooms or any other type of room ventilated by a Windcatcher. Clearly, the need to attenuate noise through a natural ventilation system is at odds with the requirement to allow air to flow with as little resistance as possible. The consideration of both factors may lead to a compromise that could negatively affect the occupants of a room ventilated by a Windcatcher, thus making the measurement of noise *in–situ* highly important.

2.2 The Measurement and Prediction of Natural Ventilation

The principals of natural ventilation have been used for millenia to ventilate human shelters such as Bedouin tents (Roaf, 1982), houses (Rudofsky, 1977a,b; Chaichongrak *et al.*, 2002), and places of religious worship (McCarthy, 1999) for example. The earliest example of a specific natural ventilation element, a wind–scoop, has been found on papyrus scrolls stored in Egyptian tombs and dated to around 1500 B.C. The fundamentals of natural ventilation theory, (see Etheridge & Sandberg, 1996; Linden, 1999, for example), and a series of techniques for making empirical measurements in the laboratory (Cook, 1998; Cook *et al.*, 2003), and in the field (Liddament, 1996) have been established. However, natural ventilation, which may be defined as the flow of air between a building and its surroundings driven using naturally occurring forces, is fraught with uncertainty. This section will show that there are still a great many unknowns, but also that there are a number of methods that may be employed to measure and estimate natural ventilation flow rates. Those that are relevant to the investigation of a Windcatcher are now explored.

2.2.1 Predicting Natural Ventilation Performance

Etheridge & Sandberg (1996) state that there are two basic ventilation processes (i) flow through the skin of a building, defined as the *envelope*, and (ii) internal air motion.

A pressure difference across an opening in a building's envelope creates a flow of air through it, and the flow rate is governed by the difference between the internal and external pressure, the geometry of the opening, and the properties of the air (Etheridge & Sandberg,

1996). Air flow through a number of openings are not mutually exclusive because the total flow must obey the principal of conservation of mass. However, these simple fundamental principals are sometimes omitted in the literature, see Elmualim (2006a) or Li & Mak (2007) for example.

The variability of the driving forces, and the complex flow patterns make natural ventilation hard to predict. Furthermore, several studies (Hunt & Linden, 2000; Li *et al.*, 2001; Chenvidyakarn & Woods, 2005, for example) show that air flow in a building can, under certain circumstances, exhibit non–linear dynamics and so more than one steady–state solution may exist for a single set of conditions. Consequently, the choice of methodology for predicting natural ventilation flow rates is important and defined by the required outcome. Methodologies used to predict the performance of natural ventilation strategies have been categorised by Chen (2009) into the following groups:

- Analytic models.
- Empirical models
- Small–scale experimental models.
- Full–scale experimental models.
- Multi–zone models.
- Zonal models.
- Computational Fluid Dynamics (CFD) models.

Analytic models are often derived from the fundamental equations of fluid dynamics and heat transfer, such as mass, momentum, and energy conservation (Chen, 2009), and can be solved using methods as simple as a graph (see Etheridge, 2002, for example) or a spread sheet (Li & Heiselberg, 2002). Analytic methods have been widely used to estimate flow behaviour in a single zone box with high and low openings in opposite walls when the wind acts with the buoyancy forces to form displacement ventilation, a stratified layer will form whose height can be estimated (Linden, 1999). When the wind and buoyancy forces are in opposition, the flow direction depends upon their relative strengths, but if flow enters from the upper opening,

the internal and incoming air mix together (known as mixing ventilation) (Heiselberg *et al.*, 2004) and the type and patterns formed by the internal flow has consequences for the pre–heating of incoming air in winter (Fitzgerald & Woods, 2007), or the transport of airbourne pathogens in hospitals (Li *et al.*, 2007) for example.

Simple envelope flow models used for the estimation of single sided ventilation through one or more openings in a single zone, and cross ventilation through two or more openings in a single zone when wind or buoyancy driven, have been incorporated into national standards, see BS 5925 (BSI, 1991). Furthermore, methods for predicting the air flow through atria and passive stacks are presented in professional literature, see (CIBSE, 2005a), and calculation software is detailed by Liddament (1996).

One method of increasing the accuracy of analytic models is to incorporate data from experimental measurement or advanced computer simulation to form an empirical model that Chen (2009) describes as the "*bread and butter* tools for ventilation design". These models are used by most design handbooks, design guidelines and product catalogues for ventilation design, see Karava *et al.* (2003) for example, who derive an empirical model of flow through trickle vents.

The advantage of using a small scale model is its cost. Here, measurement or visualisation techniques are used to establish flow paths and ventilation performance once dynamic similarity has been achieved. For example, Etheridge (2004) and Costola & Etheridge (2008) used a wind tunnel and anemometry to measure flow through a model stack. In addition, models placed in wind tunnels have been used to establish the characteristics of flow through a series of simple sharp edged openings, and to derive discharge coefficients (Karava *et al.*, 2004). Furthermore, Sawachi *et al.* (2006) derived wind pressure coefficients for buildings of different shapes and surrounding topographies, which can be applied easily to analytic models. Tables of similarly derived coefficients are also widely available, see Liddament (1996), Orme & Leksmono (2002), and Santamouris & Asimakopoulos (1996).

In addition to the wind tunnel testing of scale models, water baths are also commonly used to investigate the effects of buoyancy through the injection of a dyed and/or saline solution. Because brine is more dense than water, the model is inverted and the solution injected through the top of the model, and observations of flow paths and velocity and density are made using shadow graphs and digital imaging techniques. For example, Gage

et al. (2001) investigated the entrainment of cold air into a single zone through an inverted chimney mounted in the ceiling model showing that "the experiments clearly demonstrate that it is possible to use stack forces to draw ambient air down into a space from roof level via an inverted chimney using a displacement mode of passive ventilation", which has direct application to the physics of a Windcatcher. Furthermore, water tank models have been used to establish the non–linear dynamics predicted by Hunt & Linden (2000) and others, and such experimentation is normally accompanied by a theoretical analysis and/or a CFD study, see Heiselberg *et al.* (2004) for example.

Full–scale modelling can be conducted both in the laboratory and *in–situ*. Here, the line between *in–situ* modelling and the evaluation of the ventilation performance of an existing building blurs. Chen (2009) describes *in–situ* modelling as the use of an existing building to estimate ventilation rates through a similar, hypothetical building.

In the laboratory, the performance of ventilation elements can be assessed in a wind tunnel. Khan *et al.* (2008) review several full size natural ventilation elements, such as the rotational chimney cowl, whose performance has been determined by wind tunnel analysis. The performance of a Windcatcher has been assessed using a wind tunnel, see Elmualim *et al.* (2001) and Awbi & Elmualim (2002), and these studies are discussed in Section 2.3.2.

Laboratory based climate chambers can be used to simulate a room or zone, and when the effects of outdoor conditions are examined, a wind tunnel is used to replicate conditions. Here, Etheridge & Sandberg (1996, Chapter 12) detail a *test house* used to determine the effectiveness of the three main tracer gas techniques: the decay method, the constant injection method, and the constant concentration method. Note that these key methods of determining ventilation rates through a room both in the laboratory and *in–situ* are discussed in detail in Section 2.2.2.

Zonal and multi–zone models are also known as Network models. Liddament (1996) suggest considering a building as a number of *zones* or *cells* connected by flow pathways. A multi–zone model, where each room is considered to be a zone, assumes that the air in each room is well mixed and so is used to estimate ventilation rates, energy, and pollutant transfer. Conversely, Chen (2009) shows that a zonal model avoids the assumption of full mixing by dividing a single room into a finite number of cells (<1000) so that it can determine ventilation inside a large space or deal with the effects of stratification. Chen concludes that

they are difficult to develop and could be superseded by CFD models.

The use of computational fluid dynamics (CFD) models is increasing; in an overview of the tools used to predict ventilation performance in buildings, Chen (2009) finds that over 70% of the literature in his review used CFD. Etheridge & Sandberg (1996) state that CFD provides a numerical solution to the partial differential equations that govern a flow field. Furthermore, to model ventilation in a confined space where density differences caused by heating occur, turbulence and buoyancy must also be accounted for. When the boundary conditions are fixed and the flow is steady, the results are time averaged, but when the boundary conditions change with time and the flow is unsteady, the calcuations are ensemble averages (Etheridge & Sandberg, 1996). In theory, CFD brings the real world to one's desk, yet, as with any model, a series of assumptions have to be made about that modelled environment which means that one can only expect qualitative information to be obtained. Consequently CFD is often used to validate an analytic model (see Heiselberg *et al.*, 2004; Evola & Popov, 2006), data obtained from full scale wind tunnel testing (Elmualim, 2006a; Etheridge, 2009), or flow rates measured in an actual building (Horan & Finn, 2005), although there are a significant number of studies that do not compare the predictions made by a CFD model against empirically or theoretically determined flow rates, see Hughes & Ghani (2008, 2009) for example.

2.2.2 Measuring Natural Ventilation Performance

The energy consumption and IAQ of a building are closely related to the air flow through its envelope, thus the *in–situ* measurement of total air flow rates through a single zone or series of zones will give a good indication of these parameters. The most accurate and commonly used techniques involve the injection of a tracer gas into the atmosphere of a room and the subsequent measurement of its concentration over time. The rate at which air free from the tracer gas is brought into the room is determined from the concentration history. Etheridge & Sandberg (1996) and Liddament (1996) detail three techniques. (i) The Decay Method injects of a small amount of tracer gas into a single zone that is thoroughly mixed to establish a uniform concentration and its exponential decay is monitored over a period of time. (ii) The Constant Concentration method modifies the continuous rate of injection of a tracer gas into a single zone so that a near constant concentration of a tracer gas in maintained. The volume

flow rate of the tracer gas is proportional to the overall ventilation rate through the zone. (iii) Finally, the Constant Emissions or Injection method releases a tracer gas at a steady injection rate and mixes it into the local atmosphere so that an equilibrium concentration is reached. This concentration is also proportional to the overall ventilation rate through the zone.

An ideal tracer gas is one that is uncommonly found in the atmosphere; here, Niemelä *et al.* (1991) review three different tracer compounds determining that the completeness of mixing through the room is the key to their performance and not their relative properties. Most studies use sulphur hexafluoride (SF_6) as a tracer gas, and determine the ventilation rates by plotting the natural log of the concentration against time and obtaining the gradient of the resulting straight line of negative slope by linear data regression, see Kolokotroni *et al.* (2002b); Kirk (2004a); Kirk & Kolokotroni (2004b) for example. Then, the coefficient of determination (R^2) can be used as an indication of the extent of exponential decay and thus the accuracy of mixing. Others have used CO_2 because it is cheaper and more readily available as a bi–product of respiration, see Bartlett *et al.* (2004); Coley & Beisteiner (2002). Furthermore, if the number of occupants and the rate at which they emit CO_2 are known, the total ventilation rate can be estimated using the constant emission method (Roulet & Foradini, 2002). However, because CO_2 is readily found in the atmosphere, the accuracy of this method can be low unless great care is taken to eliminate compounded equipment errors, see Persily (1996, 1997). It is generally uncommon for errors made in the measurement of ventilation rates using the tracer gas techniques to be discussed in the literature—an exception is Bartlett *et al.* (2004)—however, Sherman (1990) estimates that overall errors are $\pm 10\%$ and Persily (2006) states that they are no better than $\pm 20\%$.

Cook (1998) details two further methods: the empirical tightness method (ETM) and simplified theoretical method (STM). The ETM calculates the average air tightness by estimating infiltration rates when the building is pressurised to 50 Pa, which is undertaken as standard on all new buildings. The overall ventilation rate through the building is determined as a function of the surrounding topography and meteorological conditions, giving an estimation that is approximate at best. Similarly, the STM uses a single equation that incorporates an estimation of the effective leakage area, and factors that affect the air flow into and out of a zone, to estimate the total air flow rate through a building. The effective leakage area

is a measure of the air tightness at a reference pressure difference of 4 Pa, but can also be extrapolated from a similar measurement made at 50 Pa. Neither of these methods are in common use and have been superseded by the tracer gas techniques.

So, by using the tracer gas techniques, it is possible to determine the overall ventilation rate through a room. However, it must be remembered that this is a measurement of the total ventilation rate through a single zone and not the specific flow rate through an element such as a Windcatcher. Because of the likelihood of a turbulent flow regime, and the non–circular cross section of their ducts—they are triangular—this type of measurement requires highly sensitive equipment such as an omni–directional hot–wire anemometer (see Liddament, 1996, for details of duel wire and ultrasonic anemometers) and a series of measurements across a section of the duct using a grid pattern to determine the average flow rate, see Douglas *et al.* (1995, Chapter 6).

2.3 Measurement and Prediction of Air Flow Through a Windcatcher

The term wind–catcher often incorporates any element that naturally ventilates a room from roof level. However, not all devices are omni–directional, nor can they supply and extract air simultaneously, see Montazeri & Azizian (2008) for example, and so it is argued here that these should retain the terms wind–scoop, oast or cowl, wind–tower, chimney, or their vernacular equivalents as appropriate. Therefore, a wind–catcher is defined as a device that can simultaneously supply fresh air to, and extract stale air from a room at roof level whatever the wind's direction, and without mechanical assistance.

There are several examples reported in the literature of the measurement and prediction of flow rates through a modern commercially produced Windcatcher, although these are not as prevalent as those for other elements such as windows or passive stacks. Measurements of the Windcatcher have generally been restricted to the laboratory where several methodologies have been employed to determine flow rates through the Windcatcher with changing conditions. Very few studies have examined Windcatcher performance *in–situ*, but one study carefully details the performance of vernacular wind–catchers.

2.3.1 Quantifying the Performance of Vernacular Wind–Catchers

The wind–catcher originates from the hot arid climate of the middle–east. Over 100 examples may still be found in the city of Yazd on the Iranian Plateau, where the prevailing winds blow reliably at around 9 m/s. Here, Roaf (1982) has made an extensive study of the Yazdi wind–catchers, detailing construction methods, dimensions, components, and everyday use. The wind–catchers are a status symbol and so they are built of brick, stone, and plaster, with most having have a rectangular cross section, although other planforms such as hexagonal are used. They protrude, on average, 5 m above the buildings they are mounted upon, and can be as tall as 22 m to take advantage of the higher wind speeds found at increased elevation, see Liddament (1996). Their cross sectional areas (CSA) vary from as little as $0.32\,\mathrm{m}^2$ to a huge $77\,\mathrm{m}^2$, and are partitioned to form up to 12 individual shafts that run from the face of the wind–catcher all the way to the room below. Here, Roaf suggests that the relationship between the CSA of each duct and the wind–catcher face is critical because there comes a point when, by increasing the duct CSA, the air flowing down the shaft is slowed down enough so that the wind–catcher become inefficient. Furthermore, it is reported that air flowing through windward shafts often fails to enter the room because it is returned up through the leeward shafts. This phenomena is known as *short circuiting*. In strong wind conditions short circuiting is thought to represent only a small proportion of the total flow through the wind–catcher, however, when the velocity of incoming air at the base of the windward shaft is less than 0.3 m/s, it represents a considerable proportion of the total air in circulation.

Karakatsanis *et al.* (1986) use a wind tunnel and scale model of a wind–catcher connected to a house to estimate the total ventilation rate through the house. The wind–catcher has a rectangular planform (ratio of 0.85:1) and is located adjacent to a single façade of the house. Generally, air flows into the house through the wind–catcher and is extracted through three open windows located on the three remaining façades. When the wind is incident to a single smaller wind–catcher quadrant the flow rate of air through the wind–catcher and the house is at its maximum. Here, the ventilation rate is $0.093\,\mathrm{m}^3/\mathrm{s}$ per unit area of wind–catcher cross sectional area and per unit value of wind velocity. Therefore, for a wind speed of 9 m/s a wind–catcher with cross sectional area $1\,\mathrm{m}^2$ will supply the house at a rate of $0.72\,\mathrm{m}^3/\mathrm{s}$.

Karakatsanis *et al.* also show that the ventilation rate can be increased by adding a courtyard to the house which increases the magnitude of the faade pressure coefficients. Yaghoubi *et al.* (1991) measured air velocity inside a mosque ventilated by a wind–catcher finding that it varies between 0 m/s and 2 m/s over a full day and is always above 0.5 m/s between 0900 and 2000 hours. Here, Aynsley (2008) suggests that an air velocity of 0.5 m/s will provide 20% of the maximum possible cooling effect and at 2 m/s it will provide 80%. Although these figures don't take into account other factors discussed in Section 2.1.1, they are an indication of how occupants achieve thermal comfort in a naturally ventilated building located in hot and arid conditions (Bahadori, 1994).

A wind–catcher is an integral part of the ventilation strategy employed in a Yazdi house that exploits its orientation to the sun to avoid significant solar heat gains, the prevailing wind, and the cooling effect of its local micro–climate provided by vegetation and pools of standing water. The wind–catcher extends from the roof to the ground floor where air enters the room through a door in the shaft that is 1.5–1.8 m high, and is extracted through the leeward wind–catcher quadrants and via windows and doors positioned on the opposite side of the room. Although the temperature of the incoming air is often higher than room temperature, it is the physiological cooling and the psychological effect of sitting in a stream of moving air that provides comfort to the occupants, see Aynsley (2008) for example.

Clearly, the architecture and construction materials of the buildings also play a significant part in the success of a wind–catcher based ventilation strategy in Yazd, but the very longevity of the wind–catcher combined with the time, money, and energy put into their construction, and the artistry of their subsequent beautification, must represent a successful ventilation strategy that could have a role to play in modern building services. The noted Egyptian architect Hassan Fathy is quoted as saying:

> *Before investing or proposing new mechanical solutions, traditional solutions in vernacular architecture should be evaluated and then adopted or modified and developed to make them compatible with modern requirements.* (from McCarthy, 1999)

2.3.2 Theoretical and Experimental Investigations of a Windcatcher

A Windcatcher channels air into a room through a series of louvres under the action of wind pressure and draws air from a room by virtue of a low pressure area created down stream of the element. It can be of any shape although it is desirable to maximise the pressure drop on the leeward side of the element to increase flow rates. Accordingly, a Windcatcher of rectangular cross–section is shown to outperform those of other geometries, such as hexagonal (Gage & Graham, 2000) and circular (Elmualim & Awbi, 2002a). The rectangular Windcatcher model tested by Gage & Graham (2000) is orthogonally divided, although this has also been shown to have a performance that is $2\frac{1}{2}$ times less than one that is diagonally divided (see Shea *et al.*, 2003) to form four triangular quadrants, so that one or more act as a supply duct to a room, while the remaining ducts extract air from a room. The diagonal division of rectangular elements is also shown by Montazeri & Azizian (2008) to be common in vernacular wind–catchers.

Elmualim & Awbi (2002a), Parker & Teekeram (2004b) and Elmualim (2006a) have all used a wind tunnel with an open working section to measure the performance of a square Windcatcher connected to a sealed room. The Windcatcher was located centrally in the section and upstream static and total pressures were measured using a pitot–static tube. Pressure tappings were located in each Windcatcher face. The velocity of the air flow in each quadrant was measured centrally, which enabled measurements to be made of the change of flow rate through a Windcatcher with corresponding changes in wind speed and of the average coefficient of pressure over each face of a Windcatcher. In addition, Parker (2004a), Elmualim & Awbi (2002a), and Su *et al.* (2008) have also performed similar tests for a circular Windcatcher. Here, Parker & Teekeram (2004b) concentrated on the measurement of the average coefficient of pressure (C_p) over the face of a square Windcatcher for wind of normal incidence, but Elmualim (2006a) has extended this study to measure the C_p for different angles of incidence in order to generate an overall indication of a Windcatcher's performance. However, there is a distinction between the methodologies applied by Parker & Teekeram (2004b) and Elmualim (2006a); the experimental data reported by Elmualim used six pressure tappings arranged in rows of three at the top and bottom of the windward face, while only two pressure tappings were located on the vertical centre line of the side and

leeward Windcatcher faces. This methodology may introduce errors because the tappings do not fully cover the Windcatcher faces and so they will not adequately measure the effects of flow separation. Parker and Teekeram used fifteen pressure tapping positioned in a grid pattern over the Windcatcher face which is likely to provide a more accurate average of C_p by virtue of their better coverage. The measurements of C_p demonstrate the action of each Windcatcher quadrant; those with a positive value act as supply ducts, while those with a negative value act as extract ducts. This is confirmed by Elmualim & Awbi (2002a) who used smoke visualisation tests. Elmualim & Awbi (2002a) and Elmualim (2006a) also used a CFD model to corroborate the laboratory measurements of C_p for the windward quadrant at normal incidence, and find good agreement (1% error). However, the comparison for the leeward face is less sucessful and a difference of 77% is found, although given the highly turbulent nature of the air flow around a square Windcatcher, this is unsurprising. As the angle of incidence of the wind is varied, the error between predicted and measured values of C_p for the leeward face increases. This may be explained by the limited number of pressure tappings that were used and the turbulence around the Windcatcher element.

Similar measurements of mean C_p have been made by Parker (2004a) and Elmualim *et al.* (2001) for a circular Windcatcher divided into four quadrants. Here, Parker used a grid of fifteen pressure tappings, while Elmualim used two located on the vertical centre line at the top and bottom of the element. However, there is a 94% disagreement between the measurements made by Parker and Elmualim for the windward quadrant; Parker's mean value is just positive by virtue of the large pressure variation across the face of the windward quadrant, while the value determined by Elmualim *et al.* is greater than that found on the windward quadrant of a square Windcatcher. The lack of symmetry in the data provided by Parker suggests that his central pressure tappings were not at normal incidence to the wind, and the exclusively central location of the pressure tappings of Elmualim *et al.* which fail to measure the pressure variation shown by Parker may explain the large difference between the two measured values. An estimation of the mean C_p made using a CFD model (see Elmualim & Awbi, 2002a) finds good agreement with the measured value for the windward quadrant, but a comparison between the predicted and measured values for the side and leeward quadrants are less sucessful.

Whilst the values of C_p are important for indicating the direction of the flow and the

magnitude of the velocity, they do not quantify the overall performance of the Windcatcher on their own. The key performance parameter of a Windcatcher is the rate at which it supplies fresh air to a room and simultaneously extracts stale air extracted from a room. In order to determine the ventilation rate through a Windcatcher, a measure of the losses within the element must be evaluated under controlled conditions. Accordingly, the ventilation rates through a 500 mm square Windcatcher supplying a sealed room were measured by Elmualim & Teekaram (2002) and Awbi & Elmualim (2002) in a wind tunnel. Elmualim & Teekaram (2002) and Awbi & Elmualim (2002) are unsure whether they have found a linear relationship between the duct flow rate and the wind speed, but Kirk & Kolokotroni (2004b), who also measured the net flow rates for multiple Windcatchers operating in an open plan office using the tracer gas decay method, observed a linear relationship between the extracted flow rate and the wind velocity. A linear relationship was also observed by Shea *et al.* (2003) who measured Windcatcher performance *in–situ*.

Awbi & Elmualim (2002) shows that the greatest net flow rates through the Windcatcher are achieved when the wind is normal to a single quadrant, but as the wind rotates from the normal to 45°, so that it is incident to two Windcatcher quadrants and air is supplied and extracted through two quadrants each, the net flow rate decreases. Therefore, limiting cases of performance are established with the wind incident to one and two Windcatcher faces.

Measurements of flow rates through a circular Windcatcher of diameter 500 mm have been made by Elmualim *et al.* (2001) and Elmualim & Awbi (2002a) in a wind tunnel. They show that the net flow rates are always less than those achieved through a square Windcatcher for an equivalent wind speed. When the wind was incident to two circular Windcatcher ducts, establishing which supplied and which extracted air was difficult because the flow through the ducts was thought to be bi–directional. The net flow rate through a 550 mm circular Windcatcher was measured by Su *et al.* (2008) in a wind tunnel who found that the net flow rate is relatively unaffected by wind direction; a difference of only 20% is reported between the same limiting cases established by Awbi & Elmualim (2002) for a square Windcatcher. A significant problem with the circular Windcatcher is its aerodynamic efficiency, an undesirable property for a Windcatcher. Accordingly, Parker (2004a) suggests that the addition of external fins positioned at the quadrant boundaries will increases the net flow rate through the Windcatcher, although his investigation only revises the mean

values of C_p on each Windcatcher quadrant and he did not measure flow rates through the Windcatcher ducts. Another method of increasing the flow rate through a room ventilated by a Windcatcher is to add façade openings such as windows. Su *et al.* (2008) used a CFD model to show that the net flow rates through a room ventilated by a circular Windcatcher and a window could be increased by up to four times.

The results have all been obtained for a Windcatcher in a wind tunnel supplying a sealed room, yet those from Elmualim & Teekaram (2002), and Awbi & Elmualim (2002) show that more air enters the room than leaves it when the wind is incident to a single Windcatcher quadrant, and when the wind is incident to two Windcatcher quadrants, the reverse is true. Consequently, there must be some mass transfer between the supplied room and its surrounding, or perhaps more likely, errors in the experimental measurements. In a later analysis of the same data, Elmualim (2006a) highlights key errors made during the wind tunnel study; measurements of air flow through each Windcatcher duct were not taken simultaneously and so the conditions may have varied from one measurement to another. Furthermore, a single uni–directional hand–held anemometer (see TSI, 1995, for specifications) was used to measure the velocity in each duct and was positioned centrally. Here, the turbulent nature of the air flow found in a triangular duct (see Hurst & Rapley, 1991, for example) requires a series of velocity measurement to be made across a section of the duct using a grid pattern, so that an average can be calculated, but this procedure was not followed.

A mass imbalance was also highlighted by Shea *et al.* (2003) who measured a net flow out of a square Windcatcher located on a building in open country, indicating that there was infiltration into the supplied room to compensate for the mass shortfall. Mass imbalance through a circular Windcatcher was also noted by Elmualim *et al.* (2001) and Elmualim & Awbi (2002a) especially when the wind was incident to a single Windcatcher quadrant; here, the extracted volume of air was found to be double that of the supplied air. Furthermore, short–circuiting was also observed between supply and extract ducts, and similar observations have been made by Hughes & Ghani (2008) using a CFD model of a square Windcatcher.

The wind tunnel allows the natural driving forces to be varied in a controlled way. Accordingly, Elmualim (2005a,b) used the wind tunnel to evaluate the effects a difference between internal and external density by generating a 10°C temperature difference between the supplied room and its surrounding. Here, the buoyancy forces are shown to affect measured flow

rates when the wind speed is less than approximately 1.5 m/s. A comparison against predictions made by a CFD model yield very poor agreement at low wind speeds (see Elmualim, 2005b). Su *et al.* (2008) simulated the effect of a difference between the internal and external air temperature on a circular Windcatcher by varying the pressure of the supplied room. They show that a pressure difference only affects the net flow rate when the wind speed is less than 2 m/s which is consistent with the findings of a CFD model and those of Elmualim (2005a) for a square Windcatcher. Furthermore, Kirk & Kolokotroni (2004b) measured net ventilation rates through a circular Windcatcher located *in–situ* with the wind speed less than 1.5 m/s finding a linear relationship between the temperature difference and the net flow rate.

The performance of a 500 mm square Windcatcher measured in a wind tunnel under controlled conditions has been modelled by Elmualim (2006a) using CFD, although only a limited agreement between the predicted and measured ventilation rates was made. Li & Mak (2007) also used CFD to predict the net ventilation rates in and out of a 500 mm Windcatcher with the wind incident to a single quadrant, and although they demonstrate good agreement with the wind tunnel measurements of Elmualim & Teekaram (2002) and Awbi & Elmualim (2002) their CFD predictions do not balance mass through the Windcatcher. Hughes & Ghani (2009) also used CFD to estimate net flow rate through a 1000 mm Windcatcher, and normalised their results for comparison against the measurements of Elmualim & Teekaram (2002) and Awbi & Elmualim (2002), finding that the predictions were within 20% of the measured flow rates. An earlier study by Hughes & Ghani (2008) is designed to show that a Windcatcher can meet specific ventilation guidelines, here BB101 (DfES, 2006), although the predictions are not compared against measured flow rates or those estimated by another method.

The CFD models are found to be only partially successful in capturing the performance of a Windcatcher, perhaps because the very function of a Windcatcher is to create high levels of turbulence and early boundary layer separation, areas that CFD unsurprisingly struggles to model. Accordingly, Elmualim (2006a) and Kirk (2004a) have attempted to use an analytic model to estimate the performance of a Windcatcher. Elmualim (2006a) uses a so called explicit model based upon the power law (crack flow) equation (see Etheridge, 1998), and an overall representation of the area of a Windcatcher detailed by BS 5925 (BSI, 1991), although

there is no indication why this has been done or whether this is a viable method. Furthermore, heuristic constants are used to represent the flow regime and losses through the Windcatcher that appear to be based upon losses through a sharp edged opening (see Karava *et al.*, 2004) and not the array of components found in a Windcatcher. Here, it is doubtful that the crack flow equation should be applied to the Windcatcher element as a whole rather than across each quadrant, and the representation of losses and area appear to be inappropriate. It is not clear why some constants were chosen or how one should apply them to different Windcatcher designs. Perhaps fortuitously, limited agreement is reached between the predictions of the explicit model and the measured flow rates at low wind velocity. Kirk (2004a) carries out exactly the same process, although the values of the heuristic constants are slightly different, and he too finds limited agreement between predicted flow rates and those measured *in–situ*, see also Kirk & Kolokotroni (2004b). Elmualim (2006a) also uses an implicit analytic model, AIDA, which is well documented by Liddament (1996) and Orme & Leksmono (2002). The same heuristic constants were applied to the Windcatcher as a whole, not to each quadrant and poor agreement was found between predicted and measured flow rates.

Parker & Teekeram (2004b) produced a non–peer reviewed guide to the design of roof mounted natural ventilation systems, and outlines an empirical calculation method for a Windcatcher using the quadratic flow equations, see Etheridge (1998), which equate the pressure drop across each Windcatcher duct with the rate of air flow through it. An initial pair of quadratic equations for the supply and extract quadrants respectively are determined experimentally using a fan to blow air into and out of the top section and addition losses are added using the Darcy equation (see Munson *et al.*, 1998, Chapter 8) to create a plot of the pressure drop across each quadrant against flow rate through each quadrant. The plot is then used to determine the flow rate through each quadrant at a design wind speed by applying the static pressure on each Windcatcher face to it and then reading off the flow rate. The pressure drop is amended iteratively for all quadrants until the a state of mass equilibrium is achieved. The model is cumbersome, difficult to use, and is not seen anywhere else in the literature. It does not account for the turbulent flow around the Windcatcher, nor the effects of buoyancy that are shown to increase overall flow rates at low wind velocity. Furthermore, its predictions have not been compared against the measurements made in the wind tunnel or any of the estimations made by other predictive methods such as CFD.

Based upon the evidence presented here, there is a clear need for an analytic model from which estimations of Windcatcher performance can be quickly, easily, and reliably obtained. This would enable designers to accurately size a Windcatcher element for any particular application.

2.3.3 Investigations of a Windcatcher *In–Situ*

There is a general paucity of data for a Windcatcher operating *in–situ*. Kirk & Kolokotroni (2004b) and Kolokotroni *et al.* (2002b) both made individual assessments of the performance of a series of Windcatchers on a two storey office building located in the south of England. Each floor contains an open planned office space ventilated by two 600 mm and two 1200 mm square Windcatchers, although it is reported that each is sub–divided into two so that only half serves the first floor while the other serves the ground floor. Accordingly, Kirk & Kolokotroni (2004b) propose that the arrangement can be seen as one 1200 mm and one 600 mm Windcatcher serving each floor although the accuracy of this assumption is debatable. In addition to the Windcatchers, manually opening windows were present, and so measurements of the ventilation rate through each office was made using the tracer gas decay method for four configurations: all openings closed (background ventilation), Windcatchers open only, windows open only, and windows and Windcatchers open. The results show that the Windcatchers provide more than double the background ventilation which can be increased up to 5 or 6 times by opening 50% of the windows. The ventilation rates provided by Windcatchers and windows were between 50% to 80% greater than those provided by the windows alone. However, the number of occupants are not known as so these ventilation rates cannot be compared against the appropriate government standards. Kolokotroni *et al.* (2002b) also found that opening windows can significantly increase the ventilation rates, but noted that those measured on the ground floor were less than those measured on the first floor, which is confirmed by Kirk & Kolokotroni (2004b). Consequently, Kolokotroni *et al.* suggest that the length of the Windcatcher duct could be a confounding factor.

An advantage of the Windcatcher is that is can be opened at night to return the internal CO_2 concentration to the ambient, cool exposed thermal mass, and lower the initial and peak internal temperature during the following day. Night ventilation strategies may contribute highly to improved thermal comfort and towards a reduction in the energy consumption of air

conditioned buildings (Santamouris, 2004). However, the success of the strategy relies upon the magnitude of difference between the internal and external temperature, the heat convected from the thermal mass of the building to the incoming air, and the internal air velocity over the thermal mass (Santamouris & Asimakopoulos, 1996). Natural night ventilation strategies normally exploit the stack effect by using low openings to supply cool external air and high openings, such as a stack, to extract the warm internal air, see Pfafferott *et al.* (2004). An example of the potential for energy savings is given by Kolokotroni & Aronis (1999) who find that a 30% reduction in the cooling energy consumption of a UK air–conditioned office building is possible using natural night ventilation, while in a low energy building that uses both natural and mechanical ventilation, natural night cooling is found by Pfafferott *et al.* to improve IAQ without increasing electricity consumption. There are no studies in the academic literature that investigate night ventilation and cooling in buildings ventilated by a Windcatcher, but a non–peer reviewed document reports on a study by the Buildings Research Establishment (BRE) (Webb & White, 1998) who monitored the temperature over two nights in a room ventilated by an open Windcatcher and also in an equivalent room where the Windcatcher remained closed. In the room ventilated by the open Windcatcher, the lowest measured temperature was approximately 2°C below the temperature in the other room containing the sealed Windcatcher, on both nights.

To date there are no long term studies that quantify the performance of Windcatchers *in–situ* through the measurement of ventilation rates and IAQ parameters and their comparison against relevant building standards, nor have measurements been made in school classrooms where the vast majority of Windcatcher elements have been installed. Furthermore, there is no evidence that the data for a 500 mm square Windcatcher measured in a wind tunnel are applicable to those of another size.

2.4 Conclusions

This chapter has shown that poor IEQ in a building can have health and performance consequences for its occupants. However, occupants of naturally ventilated buildings show a greater tolerance to differing conditions when they are given control over their environment.

The IEQ is particularly important in schools where there is the potential for children to

sustain long lasting damage because their tissue and organs are still growing, they breath more air relative to their body mass than adults, and ventilation rates in school classrooms are often below those recommended by the various standards, such as BB101. Accordingly, the provision of good IAQ in schools is important both for the health of students and in maximising educational achievement. It is, however, common for school classrooms to be significantly under–ventilated and this can lead to high levels of CO_2 and other pollutants. Natural ventilation offers the potential to improve IAQ within schools whilst at the same time reducing running and maintenance costs. Most UK school classrooms are naturally ventilated using windows, but these are currently not functioning as they should. Therefore, if the requirements of BB101 are to be met consistently, an alternative to the natural ventilation strategies discussed here is required, such as the Windcatcher.

The literature reviewed in this chapter has outlined three key areas relevant to the study of a Windcatcher: indoor environment quality, the principals of natural ventilation, and investigations of vernacular and modern Windcatchers.

The indoor environment quality in a room ventilated by a Windcatcher is a function of the ventilation it provides and the noise it transmits, and so the control of a Windcatcher is important. However, the variable nature of the natural ventilation driving forces makes their design and measurement difficult. Consequently, there has been some research into the performance of a Windcatcher using a wind tunnel, and modelling of Windcatcher performance made using CFD and analytic modelling, but the state of the art of Windcatcher research is neither qualitative nor quantitative.

The literature shows that the functionality of the Windcatcher is not clearly understood and so a qualitative investigation into its physics is important for the development of its understanding. Furthermore, a method of quickly and reliably establishing the ventilation performance of a Windcatcher for a variety of locations is also needed. The literature also shows that there is a lack of data for a Windcatcher when measured *in–situ*. Consequently, a quantitative analysis of the performance of a Windcatcher *in–situ* would establish its performance when compared against the design criteria set by UK government standards for ventilation, indoor air quality, and noise.

Chapter 3

Theory: Modelling Flow Through a Windcatcher System

In Chapter 2 the need to provide a qualitative analysis of the physics of a Windcatcher and a simple analytic model from which Windcatcher performance can be quickly and reliably estimated was identified. Accordingly, this chapter addresses these needs by developing an analytic model that explicitly includes experimental data for a Windcatcher as part of the modelling methodology. Here, the experimental data for a Windcatcher measured under controlled conditions is used to quantify losses in the Windcatcher rather than using heuristic constants or CFD. Furthermore, the model addresses phenomena such as buoyancy, sealed and unsealed rooms, as well as façade openings, and delivers results for the wind incident at two angles, factors that were omitted from the analytic models of Elmualim (2006a) and Parker & Teekeram (2004b). In Section 3.1 an analytic model is developed based upon the principals of conservation of energy and mass for a Windcatcher ventilating both sealed and unsealed rooms, and in coordination with a single façade opening. In Section 3.2, the experimental data reported in the literature and obtained under controlled laboratory conditions is used to identify appropriate values for the constants such as the coefficient of pressure for each Windcatcher quadrant. Furthermore, by comparing predicted and measured flow rates through a Windcatcher, the losses in a Windcatcher are calculated and a semi–empirical model is formulated. The predictions of the semi–empirical model are then compared against other data in the literature and a simple relationship between the Windcatcher ventilation

rate, the wind velocity and the Windcatcher area is shown. Finally, the change in the overall ventilation rate that one would expect to find when a window or other façade opening is added to the system is estimated.

3.1 Analytic Model

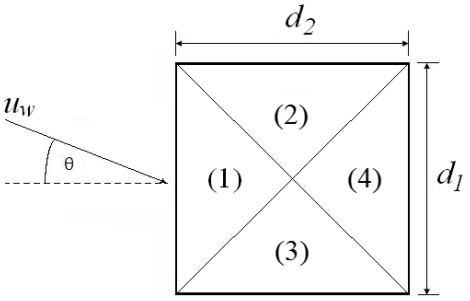

Figure 3.1: Plan view of Windcatcher.

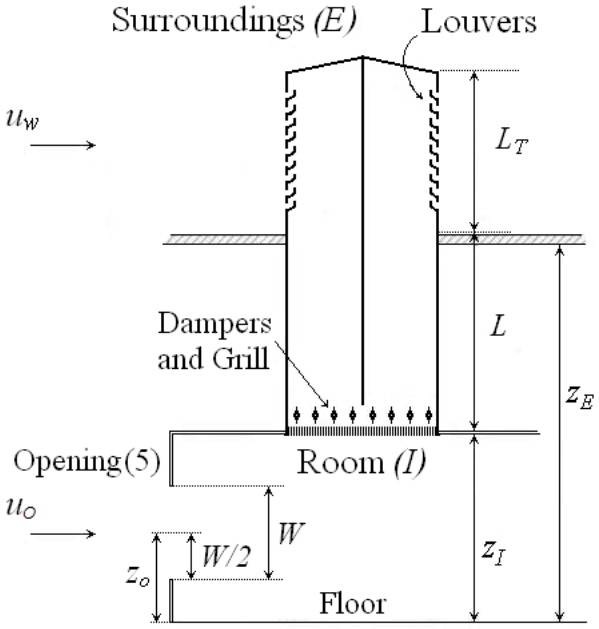

Figure 3.2: Side view of Windcatcher.

In the context of this chapter, a Windcatcher of rectangular cross–section is assumed to be diagonally divided into four quadrants of equal area. Each quadrant contains louvres at the top and volume control dampers and a security grill at the bottom, see Figures 3.1 and 3.2. The Windcatcher experiences a wind velocity u_w incident at an angle of θ degrees and has dimensions $d_1 \times d_2$, see Figure 3.1. The louvred section is of length L_T and the section from the louvres to the entrance to the room is of length L, see Figure 3.2.

The consideration of energy transfer in a fluid is fundamental to understanding the performance of a Windcatcher. For steady incompressible flow the difference between the pressure, kinetic, and potential energies of an element of fluid at two points in a finite region of space

(a control volume) is equal to the energy lost from the system and may be described by an energy Equation (see Munson *et al.*, 1998, for example). To model the performance of a Windcatcher, conservation of energy and mass are enforced using a method similar to that reported by Etheridge & Sandberg (1996) and CIBSE (2005a). For a quadrant that faces into the wind, flow is from the surroundings into the room and here conservation of energy yields (Etheridge & Sandberg, 1996)

$$\Delta p_{in} = p_E - p_I - \Delta\rho g z_I + p_w \tag{3.1}$$

where p_E is the external pressure measured at ground level immediately outside the building, p_I is the internal pressure measured at ground level inside the building, and Δp_{in} is the pressure drop over the Windcatcher quadrant, and assumes that all losses between the room and the surroundings are solely attributed to the Windcatcher. In addition, $\Delta\rho$ denotes the change in air density between the room and the surroundings, z_I is the height of the entrance to the Windcatcher relative to the floor of the room, and p_w denotes the pressure generated by the wind. Similarly, for a quadrant in which air moves from the room to the surroundings,

$$\Delta p_{out} = p_I - p_E + \Delta\rho g z_E - p_w \tag{3.2}$$

where Δp_{out} is the pressure drop over the outlet quadrant and z_E is the height of the top of the Windcatcher relative to the floor of the room.

The pressure generated by the action of the wind over the face of a Windcatcher quadrant is related to the velocity of the air flowing into or out of the quadrant by the coefficient of pressure C_p, which is defined as (Etheridge & Sandberg, 1996)

$$C_p = \frac{\Delta p}{\rho_E u_w^2/2} \tag{3.3}$$

Here, Δp is the difference between the static pressure on the face of the Windcatcher (p_w) and a reference pressure, and u_w is the wind speed measured at Windcatcher height on the windward side and in the free stream. So, for air that flows from the surroundings into the room (an "inlet" quadrant) Equation (3.1) may be re–written as (Etheridge & Sandberg, 1996)

$$\Delta p_{in} = \frac{1}{2}\rho_E u_w^2 C_p - g z_I(\rho_E - \rho_I) - p_I \tag{3.4}$$

where $\Delta\rho = \rho_E - \rho_I$ and the reference pressure is assumed to be atmospheric. Equation (3.4) makes several key assumptions: the first is that the ventilation is steady, which may seem unlikely if generated by a gusting wind, but Etheridge & Sandberg (1996) suggest that the ventilation rate is more likely to be steady in the mean rather than being truly steady and this is acceptable; second, the internal velocity is very small and thus negligible when compared to the wind velocity. Finally, changes in the density of the air caused by the variation of pressure with height may be neglected. So, for an outlet quadrant

$$\Delta p_{out} = p_I - g z_E(\rho_I - \rho_E) - \frac{1}{2}\rho_E u_w^2 C_p \tag{3.5}$$

Application of the ideal gas equation of state ($p = \rho RT$) to equations (3.4) and (3.5) gives

$$\Delta p_{in} = \frac{1}{2}\rho_E u_w^2 C_p - \frac{g z_I}{R}\left(\frac{p_E}{T_E} - \frac{p_I}{T_I}\right) - p_I \tag{3.6}$$

and

$$\Delta p_{out} = p_I - \frac{g z_E}{R}\left(\frac{p_I}{T_I} - \frac{p_E}{T_E}\right) - \frac{1}{2}\rho_E u_w^2 C_p \tag{3.7}$$

However, the changes in density that appear in equations (3.4) and (3.5) are assumed to be due solely to a change in temperature and so, following Etheridge & Sandberg (1996), an assumption of $p_I = p_E$ is made for the density components and equations (3.6) and (3.7) are re-written as

$$\Delta p_{in} = \frac{1}{2}\rho_E u_w^2 C_p - \frac{g z_I p_E}{R}\left(\frac{1}{T_E} - \frac{1}{T_I}\right) - p_I \tag{3.8}$$

and

$$\Delta p_{out} = p_I - \frac{g z_E p_E}{R}\left(\frac{1}{T_I} - \frac{1}{T_E}\right) - \frac{1}{2}\rho_E u_w^2 C_p \tag{3.9}$$

Here, T denotes the temperature, R is the specific gas constant for air, and Δp_{in} and Δp_{out} represent the drop in pressure over the supply and extract quadrants respectively. The losses imparted by the Windcatcher, and which cause the pressure to drop, may be expressed in a number of ways; for example, by using a standard loss coefficient C_d (see CIBSE, 2005a). However, the Windcatcher contains many different components and it is desirable to gain an appreciation of how each one impacts on the overall Windcatcher performance. Therefore, the losses are expressed in terms of a loss coefficient K, where in general

$$K_{in,out} = \frac{\Delta p_{in,out}}{0.5\rho u_{in,out}^2} \tag{3.10}$$

This allows Equations (3.8) and (3.9) to be re-written to give

$$\frac{1}{2}\bar{\rho}u_{in}^2 K_{in} = \frac{1}{2}\rho_E u_w^2 C_p - \frac{g z_I p_E}{R}\left(\frac{1}{T_E} - \frac{1}{T_I}\right) - p_I \tag{3.11}$$

and

$$\frac{1}{2}\bar{\rho}u_{out}^2 K_{out} = p_I - \frac{g z_E p_E}{R}\left(\frac{1}{T_I} - \frac{1}{T_E}\right) - \frac{1}{2}\rho_E u_w^2 C_p \tag{3.12}$$

Here, u_{in} and u_{out} represent the velocity inside the quadrant of an inlet and outlet quadrant respectively, and $\bar{\rho}$ is an average value for the density over the length of the quadrant.

For $\theta = 0°$, it may be assumed that one quadrant acts as an inlet [quadrant (1)] and the remaining three quadrants act as outlets, where quadrants 2 and 3 are assumed to be identical, see the experimental data of Elmualim (2006a) for example. After re-arranging, the conservation of energy for each inlet and outlet quadrant may be written as

$$\frac{1}{2}\bar{\rho}u_1^2 K_1 = \frac{1}{2}\rho_E u_w^2 C_{p1} - \frac{g z_I p_E}{R}\left(\frac{1}{T_E} - \frac{1}{T_I}\right) - p_I \tag{3.13}$$

$$\frac{1}{2}\bar{\rho}u_2^2 K_2 = p_I + \frac{g z_E p_E}{R}\left(\frac{1}{T_E} - \frac{1}{T_I}\right) - \frac{1}{2}\rho_E u_w^2 C_{p2} \tag{3.14}$$

and

$$\frac{1}{2}\bar{\rho}u_4^2K_4 = p_I + \frac{gz_Ep_E}{R}\left(\frac{1}{T_E} - \frac{1}{T_I}\right) - \frac{1}{2}\rho_E u_w^2 C_{p4} \tag{3.15}$$

where it is assumed that the external temperature is the same for each quadrant.

Similarly, these equations may also be used to describe energy conservation through an opening in the façade of a room containing a Windcatcher. Purpose provided openings, such as air vents, windows, and doors are generally characterised as sharp-edged openings with a negligible thickness (Etheridge & Sandberg, 1996). Accordingly, a rectangular opening located at the midpoint of the façade in both the vertical and horizontal planes is considered here. The vertical midpoint of the opening is assumed to be at a height z_O from the floor of the room (see Fig. 3.2), and it is assumed that the air flow incident to the opening is uniform.

The analysis of the flow through the Windcatcher follows Equations (3.11) and (3.12). For the opening, the flow of air around the building induces a change in pressure on each façade so that an opening with the wind incident upon it (located in the windward region) will have a higher pressure than the room, whilst an opening located in the leeward region will have a lower pressure because of energy dissipation through flow separation and turbulence. If the façade opening (designated the 5^{th} opening in Fig. 3.2) is in an area of positive pressure then conservation of energy gives

$$\frac{1}{2}\rho_E u_5^2 K_5 = \frac{1}{2}\rho_E u_w^2 \tilde{C}_{p5} - \frac{gz_Op_E}{R}\left(\frac{1}{T_E} - \frac{1}{T_I}\right) - p_I \tag{3.16}$$

and if the opening is in an area of negative pressure, then

$$\frac{1}{2}\rho_I u_5^2 K_5 = p_I - \frac{gz_Op_E}{R}\left(\frac{1}{T_I} - \frac{1}{T_E}\right) - \frac{1}{2}\rho_E u_w^2 \tilde{C}_{p5} \tag{3.17}$$

Here, $\tilde{C}_{p5}$ is introduced as a modified loss coefficient for the façade containing the opening and is used because it is convenient to refer the wind velocity incident at the opening back to the wind velocity at roof height used for the Windcatcher computations in Equations (3.13)—(3.15). This may be achieved using an appropriate correction equation to account

for the difference in height and the terrain. Accordingly, the equation of BS EN 5925 (BSI, 1991), Liddament (1996, Chapter 12), Etheridge & Sandberg (1996, Chapter 4), Santamouris & Asimakopoulos (1996, Chapter 9), and Orme & Leksmono (2002, Section 2.2.4) is used, although other conversion equations are available (see for example Etheridge & Sandberg, 1996, chapter 14), because it allows the velocity at roof level to be scaled using readily available conversion constants that are based upon a knowledge of the local terrain and the height of the building, so that

$$\frac{u_w}{u_{10}} = kz_E^a \tag{3.18}$$

where u_{10} is the wind velocity measured in open country at a height of 10 m, and k and a are topographically dependent constants where k has units m^{-a}. Equation (3.18) may now be re–written to form two simultaneous equations so that each accounts for the difference in wind velocity between heights z_E and z_O, respectively, and are then combined to eliminate u_{10} and k and give the following definition for $\tilde{C}_{p5}$

$$\tilde{C}_{p5} = C_{p5}[z_O/z_E]^{2a} \tag{3.19}$$

To solve Equations (3.13)—(3.17) it is necessary to enforce mass continuity, and how this is done depends upon the conditions assumed inside the room. Here, there are two limiting cases (i) a room in which air exchange with the surrounds is permitted, and (ii) a room that is perfectly sealed. For an autonomous Windcatcher, both scenarios are considered, with a sealed room studied first in Section 3.1.1, and an unsealed room studies in second in Section 3.1.2. However, when a Windcatcher is coupled with a façade opening the supplied room can no longer be considered to be truly sealed because it is expected that air flow through the opening will help to balance mass through the room. Furthermore, because air flow through adventitious openings is likely to be negligible when compared to the flow through the façade opening they may be ignored. Accordingly, a single scenario for a Windcatcher in coordination a façade opening is considered in Section 3.1.3.

3.1.1 Sealed Room Ventilated by an Autonomous Windcatcher

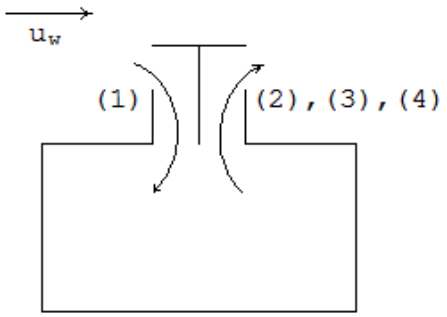

Figure 3.3: Primary flow paths for a sealed room ventilated by an autonomous Windcatcher with wind incident at $\theta = 0°$. Labelled quadrants.

For a sealed room ventilated by an autonomous Windcatcher when $\theta = 0°$, air flows in through quadrant 1 and out through quadrants 2, 3, and 4, see Figure 3.3, and so mass continuity gives

$$\dot{Q}_1 = 2\dot{Q}_2 + \dot{Q}_4 \tag{3.20}$$

where $\dot{Q}$ is the volume flow rate inside the Windcatcher, and quadrants 2 and 3 are assumed to be identical. The density (and therefore the temperature) of the air in each quadrant is assumed to be equal in order to be consistent with the average values for density used in Equations (3.13)—(3.15). Equation (3.20) is now rewritten in terms of the velocity in each quadrant so thatcher, and quadrants 2 and 3 are assumed to be identical. The density (and therefore the temperature) of the air in each quadrant is assumed to be equal in order to be consistent with the average values for density used in Equations (3.13)—(3.15). Equation (3.20) is now rewritten in terms of the velocity in each quadrant so that

$$u_1 A_1 = 2u_2 A_2 + u_4 A_4 \tag{3.21}$$

where A is the cross sectional area of a Windcatcher quadrant. Equations (3.13)—(3.15) and

(3.21) form four simultaneous equations that may be solved for the unknowns u_1, u_2, u_4, and p_I provided K and C_p are known. Here, the experimental data for a 500 mm square Windcatcher may be used to estimate values for K and C_p, and is considered later in Section 3.2.

Equations (3.13)—(3.15) and (3.21) can only be solved iteratively and it is common for this type of problem to successively change p_I until Equation (3.21) is satisfied; see for example the Air Infiltration Development Algorithm (Liddament, 1996). However, this method is rather cumbersome and it is more efficient to use a recognised root finding technique that may be easily automated, and so the Newton Raphson method is adopted (see Verbeke & Cools, 1995) which is a common method of solving an array of non-linear simultaneous equations (Boyer *et al.*, 1999).

In order to use the Newton Raphson method, the equations must be re-arranged. First, equation (3.21) is expanded to give

$$u_1^2 = 4u_2^2\left(\frac{A_2}{A_1}\right)^2 + u_4^2\left(\frac{A_4}{A_1}\right)^2 + 4u_2u_4\left(\frac{A_2A_4}{A_1^2}\right) \tag{3.22}$$

and incorporated into Equation (3.13) so that

$$\begin{aligned} p_I = {} & \frac{1}{2}\rho_E u_w^2 C_{p1} - \frac{gz_I p_E}{R}\left(\frac{1}{T_E} - \frac{1}{T_I}\right) \\ & -\frac{1}{2}\bar{\rho}\left[4u_2^2\left(\frac{A_2}{A_1}\right)^2 + u_4^2\left(\frac{A_4}{A_1}\right)^2 + 4u_2u_4\left(\frac{A_2A_4}{A_1^2}\right)\right]K_1 \end{aligned} \tag{3.23}$$

Equation (3.23) is now combined with Equations (3.14) and (3.15) to give

$$f_1(u_1, u_4) = u_2^2 + \left(\frac{A_4}{A_2}\right)u_2u_4 + a_4u_4^2 + b_4 \tag{3.24}$$

and

$$f_2(u_1, u_4) = u_4^2 + 4\left(\frac{A_2}{A_4}\right)u_2u_4 + a_2u_2^2 + b_2 \tag{3.25}$$

where the constants a_2 and a_4 are given by

$$a_2 = 4\left(\frac{A_2}{A_4}\right)^2 + \frac{K_2}{K_1}\left(\frac{A_1}{A_4}\right)^2 \tag{3.26}$$

$$a_4 = \frac{1}{4}\left(\frac{A_4}{A_2}\right)^2 + \frac{K_4}{4K_1}\left(\frac{A_1}{A_2}\right)^2 \tag{3.27}$$

and the constants b_2 and b_4 are given by

$$b_2 = \frac{1}{K_1[1+T_E/T_I]}\left(\frac{A_1}{A_4}\right)^2\left\{2(C_{p2}-C_{p1})u_w^2 - 4gL[1-T_E/T_I]\right\} \tag{3.28}$$

$$b_4 = \frac{1}{4K_1[1+T_E/T_I]}\left(\frac{A_1}{A_2}\right)^2\left\{2(C_{p4}-C_{p1})u_w^2 - 4gL[1-T_E/T_I]\right\}. \tag{3.29}$$

In general, if $\mathbf{u} = [u_2\ u_4]^T$, and $\mathbf{f} = [f_1\ f_2]^T$, the Newton Raphson method gives

$$\{\bar{\mathbf{u}}\} = \{\mathbf{u}\} - [\mathbf{J}]^{-1}\{\mathbf{f}\} \tag{3.30}$$

where $\mathbf{u}$ is an initial guess and $\bar{\mathbf{u}}$ is the new solution found after solving the right hand side of Equation (3.30). The Jacobian $[\mathbf{J}]$ is given by

$$[\mathbf{J}] = \begin{bmatrix} \frac{\partial f_1}{\partial u_2} & \frac{\partial f_1}{\partial u_4} \\ \frac{\partial f_2}{\partial u_2} & \frac{\partial f_2}{\partial u_4} \end{bmatrix} = \begin{bmatrix} 2u_2 + u_4A_4/A_2 & u_2A_4/A_2 + 2a_4u_4 \\ 4u_4A_2/A_4 & 2u_4 + 4A_2u_2/A_4 \end{bmatrix} \tag{3.31}$$

The Newton Raphson method requires the identification of an initial guess for $\mathbf{u}$. The measurements of a Windcatcher in a wind tunnel by Elmualim & Teekaram (2002) show that the velocity in quadrant 4 is small in comparison to those found in the other quadrants and so for an initial guess it is assumed that $u_4 \to 0$, which gives $\mathbf{u} = [\sqrt{-b_4}\ 0]$. Once Equation (3.30) has been solved for u_2 and u_4 it is then easy to return to Equation (3.21) to find u_1 and Equations (3.13)—(3.15) to find p_I. For further calculations, the value of $\mathbf{u}$ is calculated from a previous and preferably lower value of u_w, which is a more suitable initial guess.

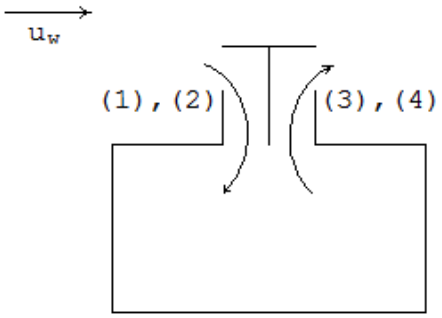

Figure 3.4: Primary flow paths for a sealed room ventilated by an autonomous Windcatcher with wind incident at $\theta = 45°$. Labelled quadrants.

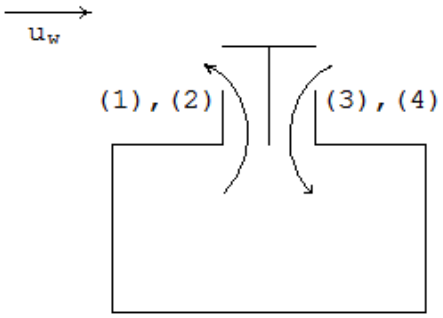

Figure 3.5: Secondary flow paths for a sealed room ventilated by an autonomous Windcatcher with wind incident at $\theta = 45°$ and $T_E > T_I$. Labelled quadrants.

When the wind is incident at $\theta = 45°$ it is assumed to enter through quadrants 1 and 2, and to extract through quadrants 3 and 4, see Figure 3.4. The energy carried by the wind now splits equally between the two inlet quadrants and so Equations (3.13) and (3.15) are re–written as

$$\frac{1}{2}\bar{\rho}u_{1,2}^2 K_{1,2} = \frac{1}{4}\rho_E u_w^2 C_{p1,2} - \frac{g z_I p_E}{R}\left(\frac{1}{T_E} - \frac{1}{T_I}\right) - p_I \tag{3.32}$$

and

$$\frac{1}{2}\bar{\rho}u_{3,4}^2 K_{3,4} = p_I + \frac{g z_E p_E}{R}\left(\frac{1}{T_E} - \frac{1}{T_I}\right) - \frac{1}{2}\rho_E u_w^2 C_{p3,4} \tag{3.33}$$

Here, the inlet quadrants 1 and 2, and the outlet quadrants 3 and 4, are assumed to be identical, and for a sealed room mass continuity gives

$$\dot{Q}_1 = \dot{Q}_4 \tag{3.34}$$

Now, Equation (3.34) is rearranged to give

$$u_1^2 = \left[u_4 \frac{A_4}{A_1}\right]^2 \tag{3.35}$$

and incorporated into Equation (3.32) so that explicit equations for flow into and out of the Windcatcher are given by

$$u_3 = u_4 = \sqrt{\frac{u_w^2(C_{p1} - 2C_{p4}) + 4gL(1 - T_E/T_I)}{\left(K_1\left(\frac{A_4}{A_1}\right)^2 + K_4\right)(1 + T_E/T_I)}} \tag{3.36}$$

and

$$u_1 = u_2 = \frac{A_4}{A_1}\sqrt{\frac{u_w^2(C_{p1} - 2C_{p4}) + 4gL(1 - T_E/T_I)}{\left(K_1\left(\frac{A_4}{A_1}\right)^2 + K_4\right)(1 + T_E/T_I)}} \tag{3.37}$$

The numerators of Equations (3.36) and (3.37) show that the direction of the flow in quadrants 3 and 4 and 1 and 2, respectively, will reverse when the buoyancy forces exceed those generated by the wind and when $T_E > T_I$, see Figure 3.5. Now, using the numerators of equations (3.36) and (3.36) this reversal is shown to occur when

$$u_w < \sqrt{\frac{4gL(T_E/T_I - 1)}{(C_{p1} - 2C_{p4})}} \tag{3.38}$$

Air is now extracted from the room through quadrants 1 and 2, and enters the room through quadrants 3 and 4 so that the flow equations are now given by

$$u_3 = u_4 = \sqrt{\frac{4gL(T_E/T_I - 1) - u_w^2(C_{p1} - 2C_{p4})}{\left(K_1\left(\frac{A_4}{A_1}\right)^2 + K_4\right)(1 + T_E/T_I)}} \tag{3.39}$$

and

$$u_1 = u_2 = \frac{A_4}{A_1}\sqrt{\frac{4gL(T_E/T_I - 1) - u_w^2(C_{p1} - 2C_{p4})}{\left(K_1\left(\frac{A_4}{A_1}\right)^2 + K_4\right)(1 + T_E/T_I)}} \tag{3.40}$$

3.1.2 Unsealed Room Ventilated by an Autonomous Windcatcher

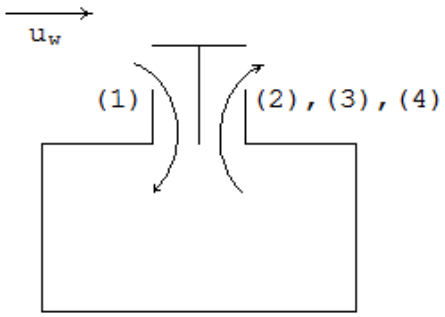

Figure 3.6: Primary flow paths for an unsealed room ventilated by an autonomous Windcatcher with wind incident at $\theta = 0°$. Labelled quadrants.

Current requirements dictate that a building should be as air–tight as possible so that air leakage, and thus energy losses, are kept to a minimum. Nevertheless, it is impossible to achieve a completely sealed building envelope and so there is always some air exchange between the supplied room and its surroundings that is through adventitious openings, and not through a Windcatcher. If this type of air exchange is considered by the model to balance mass rather than using a change to the internal pressure, then the analysis of Section 3.1.1 for a sealed room when $\theta = 0°$ simplifies because $p_I = 0$. First, the mass continuity equation becomes

$$\dot{Q}_I = 2u_2A_2 + u_4A_4 - u_1A_1 \tag{3.41}$$

where $\dot{Q}_I$ is the air exchange between supplied room and surroundings through adventitious openings, and the flow paths through the Windcatcher are shown in Figure 3.6. This now allows Equations (3.13)—(3.15) to be solved directly so that

$$u_1 = \sqrt{\frac{2u_w^2C_{p1} - 4gz_I(1 - T_E/T_I)}{K_1(1 + T_E/T_I)}} \tag{3.42}$$

$$u_2 = \sqrt{\frac{4gz_E(1 - T_E/T_I) - 2u_w^2C_{p2}}{K_2(1 + T_E/T_I)}} \tag{3.43}$$

$$u_4 = \sqrt{\frac{4gz_E(1 - T_E/T_I) - 2u_w^2 C_{p4}}{K_4(1 + T_E/T_I)}} \tag{3.44}$$

noting that flow reversal is possible in all quadrants and there are two exceptional cases.

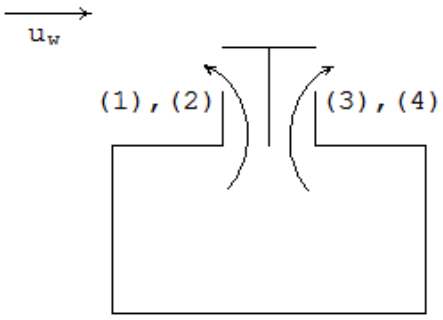

Figure 3.7: Secondary flow paths for an unsealed room ventilated by an autonomous Windcatcher with wind incident at $\theta = 0°$ and $T_I > T_E$. Labelled quadrants.

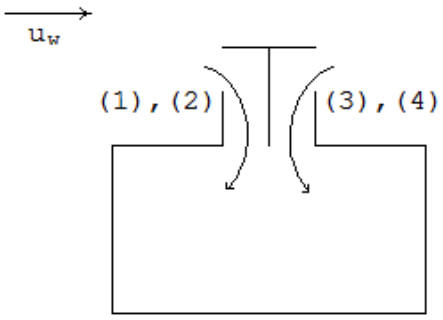

Figure 3.8: Secondary flow paths for an unsealed room ventilated by an autonomous Windcatcher with wind incident at $\theta = 0°$ and $T_E > T_I$. Labelled quadrants.

Firstly, if $T_I > T_E$ then flow may reverse in quadrant 1 so that air is extracted from the room through all quadrants and is supplied solely by infiltration, see Figure 3.7. The continuity equation then becomes

$$\dot{Q}_I = 2u_2A_2 + u_4A_4 + u_1A_1 \tag{3.45}$$

and the velocity in quadrant 1 is given by

$$u_1 = \sqrt{\frac{4gz_I(1 - T_E/T_I) - 2C_{p1}u_w^2}{K_1(1 + T_E/T_I)}} \quad \text{when} \quad u_1 < \sqrt{\frac{2gz_I}{C_{p1}}\left[1 - \frac{T_E}{T_I}\right]} \tag{3.46}$$

In this instance, a steady state is maintained by air infiltration into the room. However, if $T_E > T_I$ then flow may reverse in some or all of quadrants 2, 3, and 4. If the latter is true

then air is supplied to the room through quadrants 1, 2, 3, and 4, and extracted solely by exfiltration, see Figure 3.8, where the continuity equation becomes

$$-\dot{Q}_I = 2u_2A_2 + u_4A_4 + u_1A_1 \tag{3.47}$$

and

$$u_2 = \sqrt{\frac{4gz_E(1 - T_E/T_I) - 2C_{p2}u_w^2}{K_2(1 + T_E/T_I)}} \quad \text{when} \quad u_2 < \sqrt{\frac{2gz_E}{C_{p2}}\left[1 - \frac{T_E}{T_I}\right]} \tag{3.48}$$

$$u_4 = \sqrt{\frac{4gz_E(1 - T_E/T_I) - 2C_{p4}u_w^2}{K_4(1 + T_E/T_I)}} \quad \text{when} \quad u_4 < \sqrt{\frac{2gz_E}{C_{p4}}\left[1 - \frac{T_E}{T_I}\right]} \tag{3.49}$$

Here, the steady state is maintained by air exfiltration out of the supplied room.

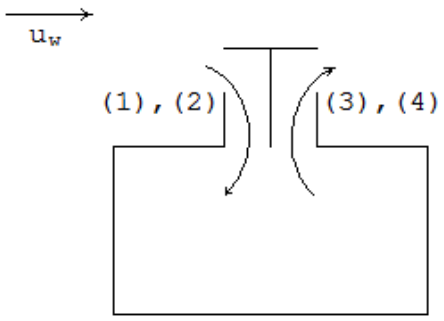

Figure 3.9: Primary flow paths for an unsealed room ventilated by an autonomous Windcatcher with wind incident at $\theta = 45°$. Labelled quadrants.

When the wind is incident so that θ =45 °, the initial continuity equation is given by

$$\dot{Q}_I = 2u_4A_4 - 2u_1A_1 \tag{3.50}$$

where air enters the room through quadrants 1 and 2, and is extracted through quadrants 3 and 4, see Figure 3.9 for the flow paths through the Windcatcher. Now, setting $p_I = 0$ in Equations (3.32) and (3.33) allows them to be solved directly so that

$$u_1 = u_2 = \sqrt{\frac{u_w^2 C_{p1} - 4gz_I(1 - T_E/T_I)}{K_1(1 + T_E/T_I)}} \tag{3.51}$$

and

$$u_3 = u_4 = \sqrt{\frac{4gz_E(1 - T_E/T_I) - 2u_w^2 C_{p4}}{K_4(1 + T_E/T_I)}} \tag{3.52}$$

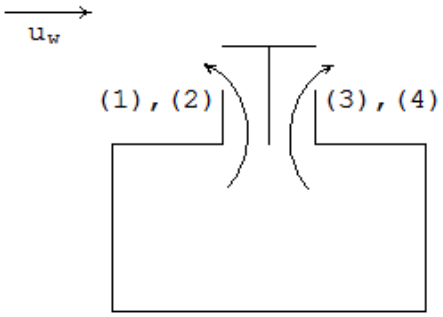

Figure 3.10: Secondary flow paths for an unsealed room ventilated by an autonomous Windcatcher with wind incident at $\theta = 45°$ and $T_I > T_E$. Labelled quadrants.

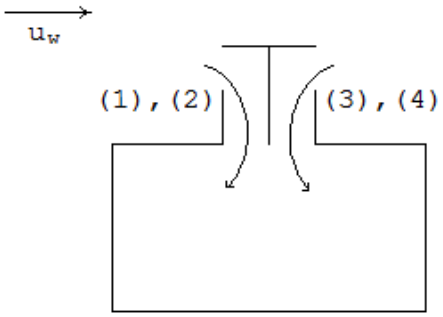

Figure 3.11: Secondary flow paths for an unsealed room ventilated by an autonomous Windcatcher with wind incident at $\theta = 45°$ and $T_E > T_I$. Labelled quadrants.

If $T_I > T_E$ then the flow direction in quadrants 1 and 2 may reverse so that air is extracted from the room through quadrants 1, 2, 3, and 4, and supplied solely by infiltration. The flow paths through the Windcatcher are now identical to those shown in Figure 3.10 and the continuity equation becomes

$$-\dot{Q}_I = 2u_4 A_4 + 2u_1 A_1 \tag{3.53}$$

The velocity in quadrants 1 and 2 is given by

$$u_1 = u_2 = \sqrt{\frac{4gz_I(1 - T_E/T_I) - u_w^2 C_{p1}}{K_1(1 + T_E/T_I)}} \quad \text{when} \quad u_w < \sqrt{\frac{4gz_I}{C_{p1}}\left[1 - \frac{T_E}{T_I}\right]} \tag{3.54}$$

Now, if $T_E > T_I$ then the flow direction flow in quadrants 3 and 4 may reverse so that air is supplied to the room through quadrants 1, 2, 3, and 4, and extracted solely by exfiltration. The flow paths through the Windcatcher are now identical to those shown in Figure 3.11 and the continuity equation becomes

$$\dot{Q}_I = 2u_4A_4 + 2u_1A_1 \tag{3.55}$$

The velocity in quadrants 3 and 4 is given by

$$u_3 = u_4 = \sqrt{\frac{2u_w^2C_{p4} - 4gz_E(1 - T_E/T_I)}{K_4(1 + T_E/T_I)}} \quad \text{when} \quad u_w < \sqrt{\frac{2gz_E}{C_{p4}}\left[1 - \frac{T_E}{T_I}\right]} \tag{3.56}$$

3.1.3 Room Ventilated by a Windcatcher in Coordination with a Façade Opening

When a room is ventilated by a Windcatcher in coordination with a façade opening, the continuity equation is complicated by the possibility of flow reversal in Windcatcher quadrants caused by the direction of the flow through the opening and the incidence of the flow to the Windcatcher. Consequently, this section is subdivided according to the the wind direction θ, and the polarity of the pressure on the façade containing the opening, expressed by C_{p5}. Within each section the initial continuity equation is given based upon the polarity of the coefficient of pressure on each face of the Windcatcher and the façade, and these "primary" flow paths are shown in a diagram where the quadrant and opening numbers are given in brackets, see for example Figure 3.12 (p. 89). If the magnitude of pressure on the façade containing the opening is large enough, it is sufficient to overcome the pressure differences in some of the Windcatcher quadrants so that the flow direction reverses and the initial continuity equation requires amendment. Then, in the same section a second diagram is presented that shows the new "secondary" flow paths (see Figure 3.13 for example, p. 89), the continuity equation is redefined, and a second set of flow equations are given.

It was noted earlier for the cases of an autonomous Windcatcher in an unsealed room, and in a sealed room when $\theta = 45°$, the governing equations can be solved explicitly, but for

all cases discussed in this section the equations reduce to a series simultaneous equations that must be solved iteratively, and some notes on how this may be done are offered in Section 3.1.3.5 (p. 101).

3.1.3.1 Wind Incident at $\theta = 0°$ with Positive Façade Pressure

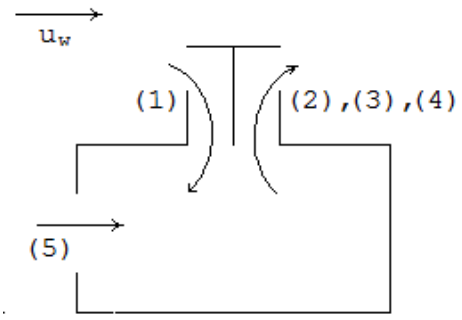

Figure 3.12: Primary flow paths for a room ventilated by a Windcatcher with wind incident at $\theta = 0°$, and a façade opening with $C_{p5} > 0$. Labelled quadrants.

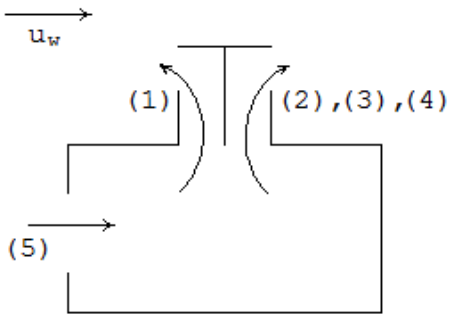

Figure 3.13: Secondary flow paths for a room ventilated by a Windcatcher with wind incident at $\theta = 0°$, and a façade opening with $C_{p5} > 0$. Labelled quadrants.

The typical continuity equation for for $\theta = 0°$ when $C_{p5} > 0$ is given by

$$\dot{Q}_5 = 2\dot{Q}_2 + \dot{Q}_4 - \dot{Q}_1 \tag{3.57}$$

so that air enters the room through quadrant 1 and the opening, and is extracted through quadrants 2 and 4, see Figure 3.12. Equation (3.57) may be expanded in terms of the velocity in each quadrant yielding

$$u_5 A_5 = 2u_2 A_3 + u_4 A_4 - u_1 A_1 \tag{3.58}$$

Here it is noted that energy Equation (3.16) uses the square of the velocity through the opening, and this is given by

$$\begin{aligned} u_5^2 = \Bigg[& 4u_1^2 \left(\frac{A_1}{A_5}\right)^2 + 4u_2^2 \left(\frac{A_2}{A_5}\right)^2 + 4u_4^2 \left(\frac{A_4}{A_5}\right)^2 + \\ & 2u_1 u_2 \left(\frac{A_1 A_2}{A_5^2}\right) - u_1 u_4 \left(\frac{A_1 A_4}{A_5^2}\right) - 2u_2 u_4 \left(\frac{A_2 A_4}{A_5^2}\right) \Bigg] \end{aligned} \tag{3.59}$$

Because the flow enters the room through the opening, Equation (3.16) is used to describe the energy transfer through the opening and equated to Equation (3.13) to give

$$\rho_E u_w^2 C_{p1} - \frac{2gz_I p_E}{R}\left(\frac{1}{T_E} - \frac{1}{T_I}\right) - \bar{\rho} u_1^2 K_1 = \rho_E u_w^2 \tilde{C}_{p5} - \frac{2gz_O p_E}{R}\left(\frac{1}{T_E} - \frac{1}{T_I}\right) - \rho_E u_5^2 K_5 \tag{3.60}$$

and then re-arranged so that

$$u_5^2 + \frac{u_w^2}{K_5}(C_{p1} - \tilde{C}_{p5}) - \frac{2g}{K_5}(z_I - z_O)(1 - T_E/T_I) - u_1^2(1 + T_E/T_I)\frac{K_1}{2K_5} = 0 \tag{3.61}$$

Now, by applying Equation (3.59), Equation (3.61) is rewritten to give

$$u_2^2 + u_4^2\frac{1}{4}\left(\frac{A_4}{A_2}\right)^2 + u_1^2\left[\frac{A_1}{4A_2^2} - \frac{(1 + T_E/T_I)K_1}{8K_5}\left(\frac{A_5}{A_2}\right)^2\right] - u_1u_2\frac{A_1}{2A_2} + u_2u_4\frac{A_4}{2A_2} - u_1u_4\frac{A_1A_4}{4A_2^2} + \left(\frac{A_5}{A_2}\right)^2\left\{\frac{u_w^2(C_{p1} - \tilde{C}_{p5}) - 2g(z_I - z_O)(1 - T_E/T_I)}{4K_5}\right\} = 0 \tag{3.62}$$

which may be simplified to

$$u_2^2 + u_4^2\frac{1}{4}\left(\frac{A_4}{A_2}\right)^2 + u_1^2 a_1 - u_1u_2\frac{A_1}{2A_2} + u_2u_4\frac{A_4}{2A_2} - u_1u_4\frac{A_1A_4}{4A_2^2} + b_1 = 0 \tag{3.63}$$

where the constants a_1 and b_1 are given by

$$a_1 = \frac{1}{4}\left[\left(\frac{A_1}{A_2}\right)^2 - \frac{(1 + T_E/T_I)K_1}{2K_5}\left(\frac{A_5}{A_2}\right)^2\right] \tag{3.64}$$

$$b_1 = \left(\frac{A_5}{A_2}\right)^2\left\{\frac{u_w^2(C_{p1} - \tilde{C}_{p5}) - 2g(z_I - z_O)(1 - T_E/T_I)}{4K_5}\right\} \tag{3.65}$$

Similarly, Equations (3.14), (3.16) and (3.59), and Equations (3.15), (3.16) and (3.59) also combine to give

$$u_4^2 + u_1^2 \left(\frac{A_1}{A_4}\right)^2 + u_2^2 a_2 - u_1 u_2 \frac{2A_1 A_2}{A_4^2} + u_2 u_4 \frac{2A_2}{A_4} - u_1 u_4 \frac{A_1}{A_4} + b_2 = 0 \tag{3.66}$$

and

$$u_1^2 + u_2^2\, 4 \left(\frac{A_2}{A_1}\right)^2 + u_4^2 a_4 - u_1 u_2 \frac{2A_2}{A_1} + u_2 u_4 \frac{2A_2 A_4}{A_1^2} - u_1 u_4 \frac{A_4}{A_1} + b_4 = 0 \tag{3.67}$$

where the constants a_2, a_4, b_2 and b_4 are given by

$$a_2 = \left[4 \left(\frac{A_2}{A_4}\right)^2 + \frac{(1 + T_E/T_I)K_2}{2K_5} \left(\frac{A_5}{A_4}\right)^2\right] \tag{3.68}$$

$$a_4 = \left[\left(\frac{A_4}{A_1}\right)^2 + \frac{(1 + T_E/T_I)K_4}{2K_5} \left(\frac{A_5}{A_1}\right)^2\right] \tag{3.69}$$

and

$$b_2 = \left(\frac{A_5}{A_4}\right)^2 \left\{\frac{u_w^2(C_{p2} - \tilde{C}_{p5}) - 2g(z_E - z_O)(1 - T_E/T_I)}{K_5}\right\} \tag{3.70}$$

$$b_4 = \left(\frac{A_5}{A_1}\right)^2 \left\{\frac{u_w^2(C_{p4} - \tilde{C}_{p5}) - 2g(z_E - z_O)(1 - T_E/T_I)}{K_5}\right\} \tag{3.71}$$

Equations (3.63), (3.66), and (3.67) now form three simultaneous equations that describe the air flow through the Windcatcher and opening described by continuity Equation (3.57). They cannot be solved explicitly, but notes on forming solutions are discussed in Section 3.1.3.5. Similar sets of equations are now derived for other values of θ, C_{p5}, and flow path combinations.

If there is a high positive pressure on the façade containing the opening when $\theta = 0°$ and $C_{p5} > 0$ then this may be sufficient to overcome the pressure difference in the inlet duct (quadrant 1) of the Windcatcher, and so a secondary scenario may exist where air is

supplied to the room solely through the opening and is extracted through all quadrants of the Windcatcher, see Figure 3.13. The new continuity equation gives

$$\dot{Q}_5 = \dot{Q}_1 + 2\dot{Q}_2 + \dot{Q}_4 \tag{3.72}$$

Here, it is relatively straightforward to determine the conditions under which this flow reversal will occur in quadrant 1 of the Windcatcher if the buoyancy forces are ignored in energy Equations (3.13)—(3.16). By using each energy equation it is straightforward to show that flow reversal will occur when

$$\frac{A_5^2}{K_5}(\tilde{C}_{p5} - C_{p1}) > \left[\frac{4A_2^2}{K_2}(C_{p1} - C_{p2}) + \frac{A_4^2}{K_4}(C_{p1} - C_{p4})\right] \tag{3.73}$$

Consequently, Equation (3.13) now becomes

$$\frac{1}{2}\bar{\rho}u_1^2 K_1 = p_I + \frac{gz_E p_E}{R}\left(\frac{1}{T_E} - \frac{1}{T_I}\right) - \frac{1}{2}\rho_E u_w^2 C_{p1} \tag{3.74}$$

and its combination with Equations (3.14)—(3.15) and (3.16) gives the following three simultaneous equations

$$u_2^2 + u_4^2\frac{1}{4}\left(\frac{A_4}{A_2}\right)^2 + u_1^2 a_1 + u_1 u_2\frac{A_1}{2A_2} + u_2 u_4\frac{A_4}{2A_2} + u_1 u_4\frac{A_1 A_4}{4A_2^2} + b_1 = 0 \tag{3.75}$$

$$u_4^2 + u_1^2\left(\frac{A_1}{A_4}\right)^2 + u_2^2 a_2 + u_1 u_2\frac{2A_1 A_2}{A_4^2} + u_2 u_4\frac{2A_2}{A_4} + u_1 u_4\frac{A_1}{A_4} + b_2 = 0 \tag{3.76}$$

and

$$u_1^2 + u_2^2\,4\left(\frac{A_2}{A_1}\right)^2 + u_4^2 a_4 + u_1 u_2\frac{2A_2}{A_1} + u_2 u_4\frac{2A_2 A_4}{A_1^2} + u_1 u_4\frac{A_4}{A_1} + b_4 = 0 \tag{3.77}$$

where the constants a_1, a_2, a_4, b_1, b_2, and b_4 are given by

$$a_1 = \frac{1}{4}\left[\left(\frac{A_1}{A_2}\right)^2 + \frac{(1+T_E/T_I)K_1}{2K_5}\left(\frac{A_5}{A_2}\right)^2\right] \tag{3.78}$$

$$a_2 = \left[4\left(\frac{A_2}{A_4}\right)^2 + \frac{(1+T_E/T_I)K_2}{2K_5}\left(\frac{A_5}{A_4}\right)^2\right] \tag{3.79}$$

$$a_4 = \left[\left(\frac{A_4}{A_1}\right)^2 + \frac{(1+T_E/T_I)K_4}{2K_5}\left(\frac{A_5}{A_1}\right)^2\right] \tag{3.80}$$

and

$$b_1 = \left(\frac{A_5}{A_2}\right)^2\left\{\frac{u_w^2(C_{p1}-\tilde{C}_{p5}) - 2g(z_I - z_O)(1-T_E/T_I)}{4K_5}\right\} \tag{3.81}$$

$$b_2 = \left(\frac{A_5}{A_4}\right)^2\left\{\frac{u_w^2(C_{p2}-\tilde{C}_{p5}) - 2g(z_E - z_O)(1-T_E/T_I)}{K_5}\right\} \tag{3.82}$$

$$b_4 = \left(\frac{A_5}{A_1}\right)^2\left\{\frac{u_w^2(C_{p4}-\tilde{C}_{p5}) - 2g(z_E - z_O)(1-T_E/T_I)}{K_5}\right\} \tag{3.83}$$

3.1.3.2 Wind Incident at $\theta = 0°$ with Negative Façade Pressure

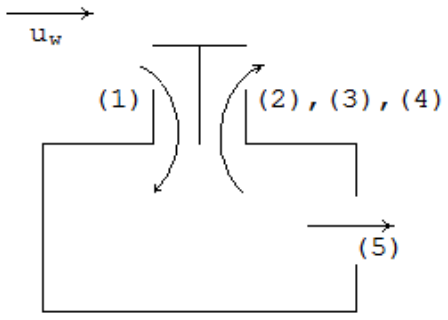

Figure 3.14: Primary flow paths for a room ventilated by a Windcatcher with wind incident at $\theta = 0°$, and a façade opening with $C_{p5} < 0$. Labelled quadrants.

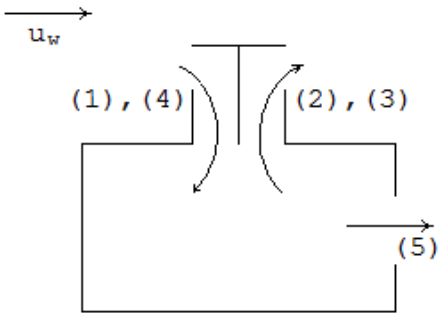

Figure 3.15: Secondary flow paths for a room ventilated by a Windcatcher with wind incident at $\theta = 0°$, and a façade opening with $C_{p5} < 0$. Labelled quadrants.

When the wind is incident at $\theta = 0°$ and $C_{p5} < 0$, the standard continuity equation is given by

$$\dot{Q}_5 = \dot{Q}_1 - 2\dot{Q}_2 - \dot{Q}_4 \tag{3.84}$$

so that air enters the room through quadrant 1 and is extracted through quadrants 2, 3, and 4, and the opening, see Figure 3.14. Therefore, Equations (3.13)—(3.15), (3.17) and (3.84) combine to give the following three simultaneous equations

$$u_2^2 + u_4^2 \frac{1}{4}\left(\frac{A_4}{A_2}\right)^2 + u_1^2 a_1 - u_1 u_2 \frac{A_1}{2A_2} + u_2 u_4 \frac{A_4}{2A_2} - u_1 u_4 \frac{A_1 A_4}{4A_2^2} + b_1 = 0 \tag{3.85}$$

$$u_4^2 + u_1^2 \left(\frac{A_1}{A_4}\right)^2 + u_2^2 a_2 - u_1 u_2 \frac{2A_1 A_2}{A_4^2} + u_2 u_4 \frac{2A_2}{A_4} - u_1 u_4 \frac{A_1}{A_4} + b_2 = 0 \tag{3.86}$$

and

$$u_1^2 + u_2^2 4\left(\frac{A_2}{A_1}\right)^2 + u_4^2 a_4 - u_1 u_2 \frac{2A_2}{A_1} + u_2 u_4 \frac{2A_2 A_4}{A_1^2} - u_1 u_4 \frac{A_4}{A_1} + b_4 = 0 \tag{3.87}$$

where the constants a_1, a_2, a_4, b_1, b_2, and b_4 are given by

$$a_1 = \frac{1}{4}\left[\left(\frac{A_1}{A_2}\right)^2 + \frac{(1 + T_I/T_E)K_1}{2K_5}\left(\frac{A_5}{A_2}\right)^2\right] \tag{3.88}$$

$$a_2 = \left[4\left(\frac{A_2}{A_4}\right)^2 - \frac{(1 + T_I/T_E)K_2}{2K_5}\left(\frac{A_5}{A_4}\right)^2\right] \tag{3.89}$$

$$a_4 = \left[\left(\frac{A_4}{A_1}\right)^2 - \frac{(1 + T_I/T_E)K_4}{2K_5}\left(\frac{A_5}{A_1}\right)^2\right] \tag{3.90}$$

and

$$b_1 = \left(\frac{A_5}{A_2}\right)^2 \left\{\frac{u_w^2(\tilde{C}_{p5} - C_{p1})(T_I/T_E) + 2g(z_I - z_O)(T_I/T_E - 1)}{4K_5}\right\} \tag{3.91}$$

$$b_2 = \left(\frac{A_5}{A_4}\right)^2 \left\{ \frac{u_w^2(\tilde{C}_{p5} - C_{p2})(T_I/T_E) + 2g(z_E - z_O)(T_I/T_E - 1)}{K_5} \right\} \tag{3.92}$$

and

$$b_4 = \left(\frac{A_5}{A_1}\right)^2 \left\{ \frac{u_w^2(\tilde{C}_{p5} - C_{p4})(T_I/T_E) + 2g(z_E - z_O)(T_I/T_E - 1)}{K_5} \right\} \tag{3.93}$$

The flow leaving the room through the opening may lower the pressure significantly to cause the flow in quadrant 4 of the Windcatcher to reverse so that air enters the room through quadrants 1 and 4, and is extracted through quadrants 2 and 3, and the opening, see Figure 3.15. The continuity equation is now given by

$$\dot{Q}_5 = \dot{Q}_1 + \dot{Q}_4 - 2\dot{Q}_2 \tag{3.94}$$

By using energy Equations (3.13)—(3.15) and (3.17), flow reversal is shown to occur when

$$\frac{A_1^2}{K_1}(C_{p1} - C_{p4}) > \left[\frac{4A_2^2}{K_2}(C_{p4} - C_{p2}) + \frac{A_5^2}{K_5}(C_{p4} - \tilde{C}_{p5}) \right] \tag{3.95}$$

and Equation (3.15) is rewritten as

$$\frac{1}{2}\bar{\rho}u_4^2 K_4 = \frac{1}{2}\rho_E u_w^2 C_{p4} - \frac{g z_I p_E}{R}\left(\frac{1}{T_E} - \frac{1}{T_I}\right) - p_I \tag{3.96}$$

which when combined with Equations (3.13)—(3.14), (3.17), and (3.94) gives the following three simultaneous equations

$$u_2^2 + u_4^2 \frac{1}{4}\left(\frac{A_4}{A_2}\right)^2 + u_1^2 a_1 - u_1 u_2 \frac{A_1}{2A_2} - u_2 u_4 \frac{A_4}{2A_2} + u_1 u_4 \frac{A_1 A_4}{4A_2^2} + b_1 = 0 \tag{3.97}$$

$$u_4^2 + u_1^2 \left(\frac{A_1}{A_4}\right)^2 + u_2^2 a_2 - u_1 u_2 \frac{2A_1 A_2}{A_4^2} - u_2 u_4 \frac{2A_2}{A_4} + u_1 u_4 \frac{A_1}{A_4} + b_2 = 0 \tag{3.98}$$

$$u_1^2 + u_2^2\, 4\left(\frac{A_2}{A_1}\right)^2 + u_4^2 a_4 - u_1 u_2 \frac{2A_2}{A_1} - u_2 u_4 \frac{2A_2 A_4}{A_1^2} + u_1 u_4 \frac{A_4}{A_1} + b_4 = 0 \tag{3.99}$$

where the constants a_1, a_2, a_4, b_1, b_2, and b_4 are given by

$$a_1 = \frac{1}{4}\left[\left(\frac{A_1}{A_2}\right)^2 + \frac{(1 + T_I/T_E)K_1}{2K_5}\left(\frac{A_5}{A_2}\right)^2\right] \tag{3.100}$$

$$a_2 = \left[4\left(\frac{A_2}{A_4}\right)^2 - \frac{(1 + T_I/T_E)K_2}{2K_5}\left(\frac{A_5}{A_4}\right)^2\right] \tag{3.101}$$

$$a_4 = \left[\left(\frac{A_4}{A_1}\right)^2 + \frac{(1 + T_I/T_E)K_4}{2K_5}\left(\frac{A_5}{A_1}\right)^2\right] \tag{3.102}$$

and

$$b_1 = \left(\frac{A_5}{A_2}\right)^2 \left\{\frac{u_w^2(\tilde{C}_{p5} - C_{p1})(T_I/T_E) + 2g(z_I - z_O)(T_I/T_E - 1)}{4K_5}\right\} \tag{3.103}$$

$$b_2 = \left(\frac{A_5}{A_4}\right)^2 \left\{\frac{u_w^2(\tilde{C}_{p5} - C_{p2})(T_I/T_E) + 2g(z_E - z_O)(T_I/T_E - 1)}{K_5}\right\} \tag{3.104}$$

$$b_4 = \left(\frac{A_5}{A_1}\right)^2 \left\{\frac{u_w^2(\tilde{C}_{p5} - C_{p4})(T_I/T_E) + 2g(z_I - z_O)(T_I/T_E - 1)}{K_5}\right\} \tag{3.105}$$

3.1.3.3 Wind Incident at $\theta = 45°$ with Positive Façade Pressure

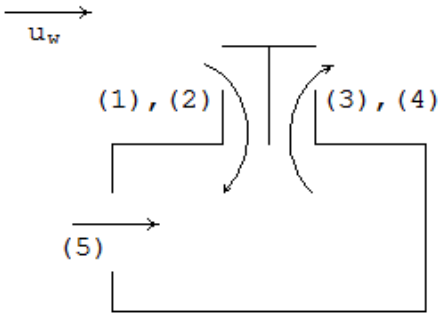

Figure 3.16: Primary flow paths for a room ventilated by a Windcatcher with wind incident at $\theta = 45°$, and a façade opening with $C_{p5} > 0$. Labelled quadrants.

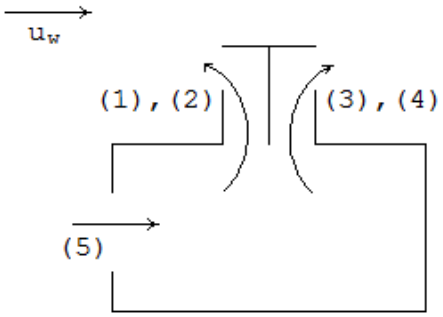

Figure 3.17: Secondary flow paths for a room ventilated by a Windcatcher with wind incident at $\theta = 45°$, and a façade opening with $C_{p5} > 0$. Labelled quadrants.

When the wind is incident at $\theta = 45°$ and $C_{p5} > 0$ the standard continuity equation is given by

$$\dot{Q}_5 = 2\dot{Q}_4 - 2\dot{Q}_1 \tag{3.106}$$

so that air enters the room through quadrants 1 and 2 and opening 5, and is extracted through quadrants 3 and 4, see Figure 3.16. Equation (3.106) is combined with Equations (3.13), (3.15), and (3.17) to give the following two simultaneous equations

$$u_4^2 + u_1^2 a_1 - u_1 u_4 \frac{A_1}{A_4} + b_1 = 0 \tag{3.107}$$

$$u_1^2 + u_4^2 a_4 - u_1 u_4 \frac{A_4}{A_1} + b_4 = 0 \tag{3.108}$$

where the constants a_1, a_4, b_1, and b_4 are given by

$$a_1 = \left[\left(\frac{A_1}{A_4} \right)^2 + \frac{(1 + T_E/T_I)K_1}{8K_5} \left(\frac{A_5}{A_4} \right)^2 \right] \tag{3.109}$$

$$a_4 = \left[\left(\frac{A_4}{A_1} \right)^2 + \frac{(1 + T_E/T_I)K_4}{8K_5} \left(\frac{A_5}{A_1} \right)^2 \right] \tag{3.110}$$

and

$$b_1 = \left(\frac{A_5}{A_4}\right)^2 \left\{ \frac{u_w^2(2\tilde{C}_{p5} - C_{p1}) + 4g(z_I - z_O)(1 - T_E/T_I)}{8K_5} \right\} \tag{3.111}$$

$$b_4 = \left(\frac{A_5}{A_1}\right)^2 \left\{ \frac{u_w^2(C_{p4} - \tilde{C}_{p5}) - 2g(z_E - z_O)(1 - T_E/T_I)}{4K_5} \right\} \tag{3.112}$$

The flow entering the room through the opening may raise the pressure significantly so as to reverse the flow in quadrants 1 and 2 of the Windcatcher so that air enters the room through the opening and leaves through all quadrants of the Windcatcher, see Figure 3.17. The continuity equation now gives

$$\dot{Q}_5 = 2\dot{Q}_4 + 2\dot{Q}_1 \tag{3.113}$$

By using energy Equations (3.15) and (3.16) flow reversal is shown to occur when

$$\frac{A_5^2}{K_5}(2\tilde{C}_{p5} - C_{p1}) > \frac{4A_4^2}{K_4}(C_{p1} - 2C_{p4}) \tag{3.114}$$

and by combining Equations (3.15), (3.16), (3.74), and (3.113), the following three simultaneous equations are given by

$$u_4^2 + u_1^2 a_1 + u_1 u_4 \frac{A_1}{A_4} + b_1 = 0 \tag{3.115}$$

$$u_1^2 + u_4^2 a_4 + u_1 u_4 \frac{A_4}{A_1} + b_4 = 0 \tag{3.116}$$

where the constants a_1, a_4, b_1, and b_4 are given by

$$a_1 = \left[\left(\frac{A_1}{A_4}\right)^2 + \frac{(1 + T_E/T_I)K_1}{8K_5} \left(\frac{A_5}{A_4}\right)^2 \right] \tag{3.117}$$

$$a_4 = \left[\left(\frac{A_4}{A_1}\right)^2 + \frac{(1 + T_E/T_I)K_4}{8K_5} \left(\frac{A_5}{A_1}\right)^2 \right] \tag{3.118}$$

and

$$b_1 = \left(\frac{A_5}{A_4}\right)^2 \left\{ \frac{u_w^2(C_{p1} - 2\tilde{C}_{p5}) - 4g(z_E - z_O)(1 - T_E/T_I)}{8K_5} \right\} \tag{3.119}$$

$$b_4 = \left(\frac{A_5}{A_1}\right)^2 \left\{ \frac{u_w^2(C_{p4} - \tilde{C}_{p5}) - 2g(z_E - z_O)(1 - T_E/T_I)}{4K_5} \right\} \tag{3.120}$$

3.1.3.4 Wind Incident at $\theta = 45°$ and Negative Façade Pressure

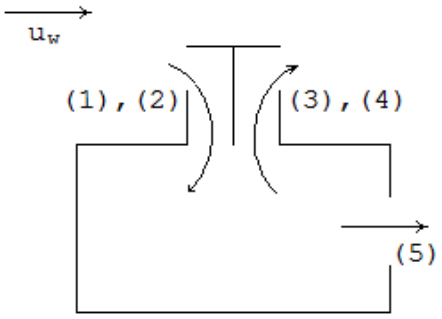

Figure 3.18: Primary flow paths for a room ventilated by a Windcatcher with wind incident at $\theta = 45°$, and a façade opening with $C_{p5} < 0$. Labelled quadrants.

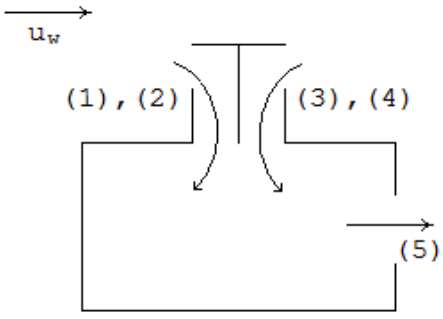

Figure 3.19: Secondary flow paths for a room ventilated by a Windcatcher with wind incident at $\theta = 45°$, and a façade opening with $C_{p5} < 0$. Labelled quadrants.

When the wind is incident at $\theta = 45°$ and $C_{p5} < 0$ the standard continuity equation is given by

$$\dot{Q}_5 = 2\dot{Q}_1 - 2\dot{Q}_4 \tag{3.121}$$

so that air is supplied to the room through quadrants 1 and 2 of the Windcatcher and extracted through quadrants 3 and 4 and the opening, see Figure 3.18. When Equation (3.121) is combined with Equations (3.13), (3.15), and (3.17) it gives the following two simultaneous equations

$$u_4^2 + u_1^2 a_1 - u_1 u_4 \frac{A_1}{A_4} + b_1 = 0 \tag{3.122}$$

$$u_1^2 + u_4^2 a_4 - u_1 u_4 \frac{A_4}{A_1} + b_4 = 0 \tag{3.123}$$

where the constants a_1, a_4, b_1, and b_4

$$a_1 = \left[\left(\frac{A_1}{A_4} \right)^2 + \frac{(1 + T_I/T_E)K_1}{8K_5} \left(\frac{A_5}{A_4} \right)^2 \right] \tag{3.124}$$

$$a_4 = \left[\left(\frac{A_4}{A_1} \right)^2 - \frac{(1 + T_I/T_E)K_4}{8K_5} \left(\frac{A_5}{A_1} \right)^2 \right] \tag{3.125}$$

and

$$b_1 = \left(\frac{A_5}{A_4} \right)^2 \left\{ \frac{u_w^2 (2\tilde{C}_{p5} - C_{p1})(T_I/T_E) + 4g(z_I - z_O)(T_I/T_E - 1)}{8K_5} \right\} \tag{3.126}$$

$$b_4 = \left(\frac{A_5}{A_1} \right)^2 \left\{ \frac{u_w^2 (\tilde{C}_{p5} - C_{p4})(T_I/T_E) + 2g(z_E - z_O)(T_I/T_E - 1)}{4K_5} \right\} \tag{3.127}$$

The flow leaving the room through the opening may lower the pressure significantly so as to reverse the flow in quadrant 4 of the Windcatcher so that air is supplied to the room through all quadrants of the Windcatcher and is extracted solely through the opening, see Figure 3.19. The continuity equation now becomes

$$\dot{Q}_5 = 2\dot{Q}_1 + 2\dot{Q}_4 \tag{3.128}$$

By using Equations (3.13), (3.15), and (3.17) flow reversal is shown to occur when

$$\frac{A_5^2}{K_5}(C_{p4} - \tilde{C}_{p5}) > \frac{4A_1^2}{K_1}(C_{p1} - 2C_{p4}) \tag{3.129}$$

The following three simultaneous equations are now given by combining Equations (3.13), (3.96), (3.17), and (3.128).

$$u_4^2 + u_1^2 a_1 + u_1 u_4 \frac{A_1}{A_4} + b_1 = 0 \tag{3.130}$$

$$u_1^2 + u_4^2 a_4 + u_1 u_4 \frac{A_4}{A_1} + b_4 = 0 \tag{3.131}$$

where the constants a_1, a_4, b_1, and b_4

$$a_1 = \left[\left(\frac{A_1}{A_4} \right)^2 + \frac{(1 + T_I/T_E)K_1}{8K_5} \left(\frac{A_5}{A_4} \right)^2 \right] \tag{3.132}$$

$$a_4 = \left[\left(\frac{A_4}{A_1} \right)^2 + \frac{(1 + T_I/T_E)K_4}{8K_5} \left(\frac{A_5}{A_1} \right)^2 \right] \tag{3.133}$$

and

$$b_1 = \left(\frac{A_5}{A_4} \right)^2 \left\{ \frac{u_w^2 (2\tilde{C}_{p5} - C_{p1})(T_I/T_E) + 4g(z_I - z_O)(T_I/T_E - 1)}{8K_5} \right\} \tag{3.134}$$

$$b_4 = \left(\frac{A_5}{A_1} \right)^2 \left\{ \frac{u_w^2 (\tilde{C}_{p5} - C_{p4})(T_I/T_E) + 2g(z_E - z_O)(T_I/T_E - 1)}{4K_5} \right\} \tag{3.135}$$

3.1.3.5 Notes on Obtaining Solutions

For the cases of an autonomous Windcatcher in an unsealed room and in a sealed room when $\theta = 45°$ the equations can be solved explicitly, but for all of the other cases discussed in this section the equations reduce to a series of two or three simultaneous equations where implicit methodologies must be employed to derive an estimate of the flow rate through a Windcatcher.

In Section 3.1.1, the Newton Raphson method (see Verbeke & Cools, 1995) was introduced as a common method of solving an array of non-linear simultaneous equations (see Boyer *et al.*, 1999), and for the case of a Windcatcher in coordination with an opening when $\theta = 45°$, equations (3.30)—(3.31) may be solved using the previously described method.

When $\theta = 0°$, the same method may be adapted to solve the three derived simultaneous equations. In general, if $\mathbf{u} = [u_1\ u_2\ u_4]^T$, and $\mathbf{f} = [f_1\ f_2\ f_4]^T$, the Newton Raphson method gives $\{\bar{\mathbf{u}}\} = \{\mathbf{u}\} - [\mathbf{J}]^{-1}\{\mathbf{f}\}$ where the Jacobian $[\mathbf{J}]$ is given by

$$[\mathbf{J}] = \begin{bmatrix} \frac{\partial f_1}{\partial u_1} & \frac{\partial f_1}{\partial u_2} & \frac{\partial f_1}{\partial u_4} \\ \frac{\partial f_2}{\partial u_1} & \frac{\partial f_2}{\partial u_2} & \frac{\partial f_2}{\partial u_4} \\ \frac{\partial f_4}{\partial u_1} & \frac{\partial f_4}{\partial u_2} & \frac{\partial f_4}{\partial u_4} \end{bmatrix} \tag{3.136}$$

Here, the initial guess will vary for each combination of wind incidence and façade pressure sign, but for the case of $\theta = 0°$ where $C_{p5} > 0$, the initial guess is given by $\mathbf{u} = [\sqrt{-b_4}\ 0\ 0]$ because the flow through quadrant 1 is typically significantly greater than through the other quadrants. However, for subsequent calculations of u_w, the chance of achieving convergence is significantly increase if the previous solution is used as the next estimation.

In some instances divergence occurs and a solution cannot be found using the Newton Raphson method, particularly when buoyancy forces are included. On these occasions another iterative method can be employed; for example, a method similar to that used by the Air Infiltration Development Algorithm (AIDA), see Orme & Leksmono (2002) and Liddament (1996) for an explanation of its capability and the code respectively. Here, the energy equations for each Windcatcher quadrant are calculated for an initial value of p_I, and the sum of the estimated flow rates through each Windcatcher quadrant $\sum \dot{Q}$ is made. The p_I term is then successively varied until $\sum \dot{Q} = 0$ and mass in and out of the Windcatcher element balances. The accuracy of the method becomes problematic when flow reversal occurs in a quadrant because the losses through it also change. On these occasions it may be necessary to compute the flow rate twice, varying the loss factor each time, and collating the data manually. Clearly then, there are computational advantages for ignoring buoyancy as well as those previously discussed that are more scientific.

3.2 Semi–Empirical Model

The model developed in the previous Section will calculate the ventilation rates generated by an autonomous Windcatcher or by a Windcatcher in combination with a single façade opening provided that one knows values of C_p and K. In Section 3.2.1 the experimental

data published in the literature for a 500 mm Windcatcher are used to quantify values of C_p and K for an autonomous Windcatcher so that they may later be substituted back into the theoretical model to form a semi–empirical model, while in Section 3.2.6 values for C_p and K that are specific to the opening are discussed.

3.2.1 Autonomous Windcatcher

The values of C_p are related to the geometry of the Windcatcher and the values of K to the losses incurred inside the Windcatcher itself. A variation in the value of C_p is considered here to be a function of the wind direction θ, whereas the values of K are assumed to be independent of θ. Accordingly, it is preferable to obtain these values under the controlled conditions provided by the laboratory. Here, Parker & Teekeram (2004b) obtained values for a 500 mm Windcatcher in a wind tunnel, while Elmualim (2006a) also used a wind tunnel with the Windcatcher connected to a sealed room of volume 15.25 m^3, and compared the results against CFD predictions. A comparison between these data for $\theta = 0°$ are shown in Table 3.1. Here, there is good agreement for the quadrant 1 (the windward quadrants when $\theta = 0°$, see Figure 3.2) although there are significant discrepancies between the predicted and measured values for the quadrants 2, 3, and 4 (side and leeward quadrants). There is reasonable agreement between the measured values for these quadrants—although Elmualim's measured value for quadrant 2 seems incorrect—and so this data seems to be consistent enough to be able to provide confidence when taking an average C_p for each Windcatcher quadrant.

Elmualim (2006a) also measured the C_p on the face of each quadrant for a 500 mm Windcatcher when the wind was incident at $\theta = 45°$ so that quadrants 1 and 2 act as inlets.

Table 3.1: C_p values for $\theta = 0°$.

Quadrant	Experiment Parker & Teekeram (2004b)	Experiment Elmualim (2006a)	CFD Elmualim (2006a)
1	0.853	0.830	0.840
2	-0.348	-0.034	-0.550
3	-0.348	-0.330	-0.550
4	-0.116	-0.100	-0.440

Once again, the data are compared against predictions made by CFD with varying levels of agreement, and a curious lack of symmetry in both sets of data that is inconsistent with the geometry of the Windcatcher, see Table 3.2. In view of these discrepancies, it appears sensible to follow the method used for $\theta = 0°$ and to use only the measured data when estimating an average C_p value for each Windcatcher inlet and outlet quadrant. The mean C_p values for each quadrant and for the wind incident at $\theta = 0°$ and $\theta = 45°$ used in the semi–empirical model are summarised in Table 3.3.

Now, it is necessary to assign appropriate values for the the loss coefficients K. One approach is to use standard values published in text books such as Douglas *et al.* (1995), or professional data books such as CIBSE (2001) and calculate their sum. However, this method is likely to lead to errors for two reasons: first, there is disagreement between the various sources for the losses through standard components such as a square elbow or sudden expansion, and secondly because these standard components bare little relation to those found in a Windcatcher. Therefore, it is arguably more consistent to analyse the losses across the Windcatcher element as a whole before assigning estimated values to each component or set of components. The measurement of a 500 mm Windcatcher in a wind tunnel by Elmualim & Awbi (2002a) and Elmualim & Teekaram (2002) shows the flow rates through a Windcatcher that may be expected with varying wind velocity and are made under controlled conditions. Accordingly, a semi–empirical model can be developed by comparing the predictions of the model against the empirical data and successively altering the values of K until acceptable agreement is reached. The values of K for a 500 mm Windcatcher are then assumed to be applicable to those of other geometries and over a wide range of conditions, such as those

Table 3.2: C_p values for $\theta = 45°$ (Elmualim, 2006a).

Quadrant	Experiment	CFD
1	0.510	0.300
2	0.110	0.200
3	-0.200	-0.580
4	-0.200	-0.058

Table 3.3: C_p values use in semi–empirical model.

	$\theta = 0°$	$\theta = 45°$
C_{p1}	0.84	0.31
C_{p2}	-0.34	0.31
C_{p3}	-0.34	-0.20
C_{p4}	-0.11	-0.20

experienced *in–situ*.

3.2.2 Determining Pressure Loss Coefficients

The data measured by Elmualim & Awbi (2002a) is presented in Figure 3.20 for a 500 mm Windcatcher with $L = 1\,\text{m}$ and $d_1 = d_2 = 0.5\,\text{m}$. Here, $\theta = 0°$ and the volume flow rate $\dot{Q}$ is plotted against the wind speed for a Windcatcher without its volume control dampers and grill. The C_p values given in Table 3.3 are used and values for K_1, K_2, and K_4 are successively altered until acceptable agreement between the predicted and estimated flow rates is reached. This is determined by the gradient m, where $m = \dot{Q}/u_w$, and it is assumed that the resulting straight line passes through the origin. The semi–empirical predictions for a sealed room [see Section 3.1.1 (p. 79) and Equations (3.20), (3.24)—(3.25)] are compared against the measured data of Elmualim & Awbi (2002a) in Figure 3.20 for $K_1 = 3.89$ and $K_2 = K_4 = 8.44$. The table shows that it is simple to vary the values for K until complete agreement is reached in the inlet quadrant and a maximum error of less than 7% for the other quadrants. However, the values of K for the inlet and outlet quadrants differ considerably;

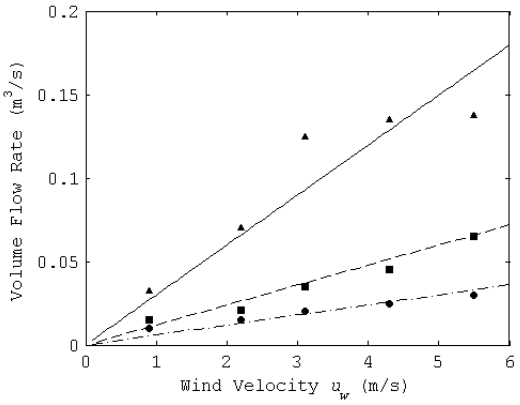

Figure 3.20: Comparison between semi–empirical predictions and the experimental measurements of Elmualim & Awbi (2002a) without dampers and grill for $\theta = 0°$. Quadrant 1, ——, prediction, ▲, experiment; quadrant 2, – – –, prediction, ■, experiment; quadrant 4, – · – ·, prediction, •, experiment.

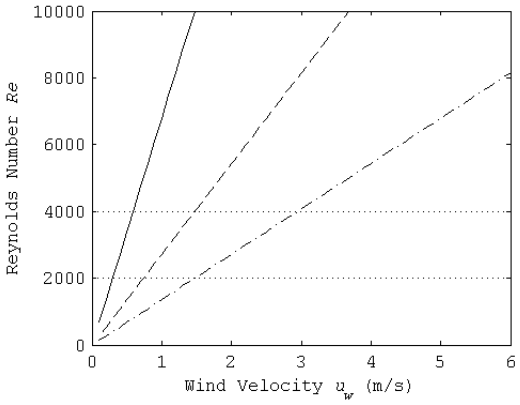

Figure 3.21: Predicted Reynolds Number in Windcatcher quadrants. Quadrant 1, ——; quadrant 2, – – –; quadrant 4, – · – · .

the value of $K = 3.89$ for the inlet quadrant seems plausible; a simple opening is suggested to be $K = 2.7$ (see CIBSE, 2001) and one would expect a Windcatcher to impart greater losses than this. The value of $K = 8.44$ chosen for the outlet quadrant is much higher however, and the reasons for this are unclear. Because the value for K has been successively iterated until acceptable agreement betweent the predicted and measured values is reached, its value is dependent upon the accuracy of the measured data. Here it is noted that significant concerns about the methodology employed by Elmualim & Awbi (2002a) have already been raised and discussed in Section 2.3.2 (p. 63).

Another possibility is that there may be physical reasons for the increased losses in the outlet quadrants that are attributable to the lower flow velocities found in these quadrants, see Figure 3.21 (p. 105). For a Reynolds number Re

$$Re = \frac{\rho\, u\, d_H}{\mu} \tag{3.137}$$

where u is the duct velocity, μ is the dynamic viscosity of the air, which at $T = 15°\mathrm{C}$ and $\rho = 1.225\,\mathrm{kg/m^3}$ is $\mu = 1.80 \times 10^{-5}\,\mathrm{kg/(m{\cdot}s)}$. The quadrants in a square Windcatcher are triangular and so Re is based upon the quadrant hydraulic diameter d_H where

$$d_H = \frac{4A}{P} \tag{3.138}$$

where P is the wetted perimeter for a right angled triangle given by

$$P = d\,(1 + \sqrt{2}) \tag{3.139}$$

Figure 3.21 shows that the flow in the outlet quadrants is more likely to lie in the transitional flow region; here its boundaries are indicated by horizontal lines. Furthermore, losses may be increased by interference of the flow leaving the room by the flow into it; for example, Hughes & Ghani (2008) show using a CFD analysis that short circuiting is often observed between the supply and extract quadrants.

Table 3.4: Gradient (m) of $\dot{Q}$ vs u_w.

Quadrant	m Damper and grill omitted			m Damper and grill included		
	Experiment[1]	Model	Error %	Experiment[2]	Model	Error %
1	0.0298	0.0298	0	0.0274	0.0277	1.1
2	0.0112	0.0119	6.3	0.0079	0.0112	42.4
3	0.0112	0.0119	6.3	0.0079	0.0112	42.4
4	0.0059	0.0060	1.7	0.0058	0.0052	9.6

[1]Elmualim & Awbi (2002a) [2]Elmualim (2005a)

The measurements made by Elmualim & Awbi (2002a) and presented in Table 3.4 show that more air enters the room through the Windcatcher than is extracted by it implying mass transfer with the surroundings other than through the Windcatcher, or errors in the experimental measurements (see Section 2.3.2, p. 63). However, the semi–empirical model must balance mass and the effect this has on the predicted pressure p_I in the supplied room is shown in Figure 3.22, where p_I is plotted against the same range of u_w studied in Figure

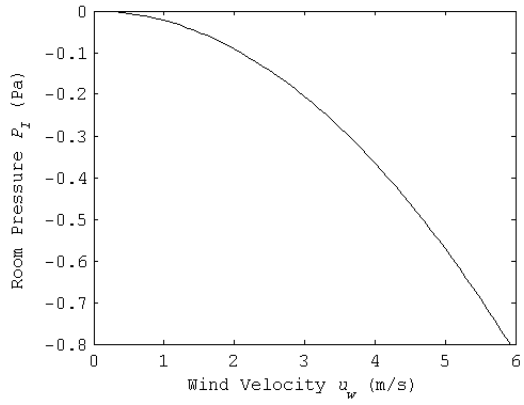

Figure 3.22: Predicted pressure in a sealed room without dampers and grill for $\theta = 0°$.

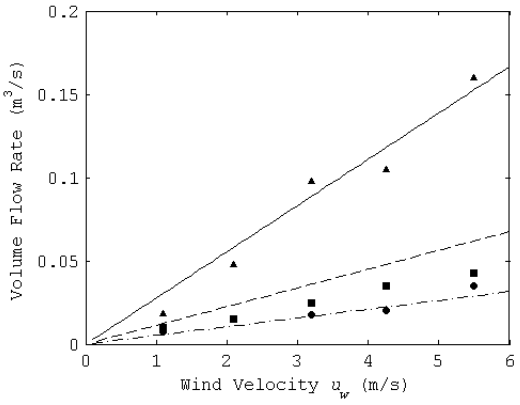

Figure 3.23: Comparison between semi–empirical predictions and the experimental measurements of Elmualim (2005a) with dampers and grill for $\theta = 0°$. Quadrant 1, ——, prediction, ▲, experiment; quadrant 2, – – –, prediction, ■, experiment; quadrant 4, – · – ·, prediction, ●, experiment.

3.20. Here, the solutions to Equations (3.20), (3.24), and (3.25) are applied to Equation (3.23) to calculate p_I, see Section 3.1.1 (p. 79). Figure 3.22 shows that p_I is negative for all wind speeds and that the Windcatcher is drawing more air from the room than it is supplying, thus causing the pressure to drop by a small amount.

The results presented in Figure 3.20 are for experimental data measured without the volume control dampers and grill (see Figure 3.2), but Elmualim (2005a) later measured flow rates through a 500 mm Windcatcher that included these components, see Figure 3.23. A comparison between the experimental data of Figures 3.20 and 3.23 is presented in Table 3.4 and shows that the losses in quadrant 1 increase by approximately 18% and are assumed to be attributed solely to the volume control dampers and grill. The inlet and outlet losses are now revised giving values of $K_1 = 4.59$ and $K_2 = K_4 = 9.14$. Table 3.4 and Figure 3.23 show that the agreement is good between the predicted and measured values in quadrants 1 and 4 where the error is less than 11%, although the model over-predicts the flow rates through quadrant 2 by 42%.

Figure 3.21 shows that the flow through the windward quadrants of a Windcatcher are likely to be fully turbulent while flow through the side and leeward ducts is more likely to lie in the lamina and transitional flow regions. Because the velocity profile of the air changes from one that is parabolic to become more blunt with increasing Re, the change in the total kinetic energy of the flow will also increase with Re. Therefore, in order to calculate the mean stream velocity, a Kinetic Energy Coefficient, α, may be introduced as a correction factor, and is a function of the velocity distribution found in the Windcatcher quadrant. Here, α is included in Equation (3.10) to give

$$\Delta p_{in,out} = \frac{1}{2}\rho u_{in,out}^2 K_{in,out}\alpha \tag{3.140}$$

and so is easily incorporated into the constants a_1, a_4, b_1, and b_4 [see Equations (3.26)—(3.29) for example]. To solve these new equations, the value of alpha is calculated from an initial prediction of the air velocity in each quadrant (without α), and then the model is re–computed including α. A single iteration is found to be sufficient to be determined the correct value of α for each Windcatcher quadrant.

For lamina flow ($Re < 2000$) α=2 while for turbulent flow ($Re > 4000$) α is shown by Fox & McDonald (1985) to be given by

$$\alpha = \left(\frac{2n^2}{(3+n)(3+2n)}\right)\left(\frac{(n+1)(2n+1)}{2n^2}\right)^3 \tag{3.141}$$

where

$$n = 0.817\ln(Re) - 2.0946 \tag{3.142}$$

When the flow through each Windcatcher quadrant is in the transitional region, α is assumed to vary linearly between the laminar and turbulent value, and so is described by

$$\alpha = 2.88 - 0.00044\,Re \tag{3.143}$$

The change of α with Re is presented in Figure 3.24 (where the vertical lines highlight the boundaries of the transitional region) shows that as Re increases, $\alpha \rightarrow 1$. Here, Figure 3.21 shows that the windward quadrant will only be effected by the value of α when $u_w < 0.3\,\mathrm{m/s}$, the side quadrant when $u_w < 1.4\,\mathrm{m/s}$, and the leeward quadrant when $u_w < 3.4\,\mathrm{m/s}$. However, this plot is for a 500 mm Windcatcher without dampers and grill, and so Figure 3.25

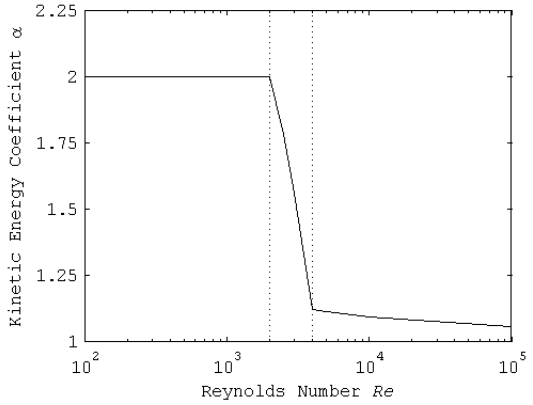

Figure 3.24: Change of Kinetic Energy Coefficient α with Reynolds Number Re.

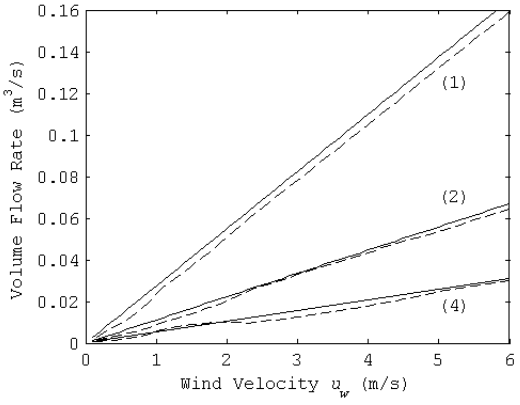

Figure 3.25: Comparison between semi–empirical predictions with and without the Kinetic Energy Coefficient α, with dampers and grill for $\theta = 0°$. Labelled quadrants; ——, prediction no α; – – –, prediction with α.

now shows the effect of applying α to the semi–empirical model for a sealed room ventilated by a 500 mm Windcatcher, with dampers and grill. Figure 3.25 shows that including α only has a minimal effect on the predictions of the semi–empirical model. Furthermore, this investigation shows that it would not help to reduce the value chosen for the losses imparted by the extract quadrants of the Windcatcher, and so it does not warrant inclusion in the semi–empirical model presented here.

3.2.3 Identification of Component Losses

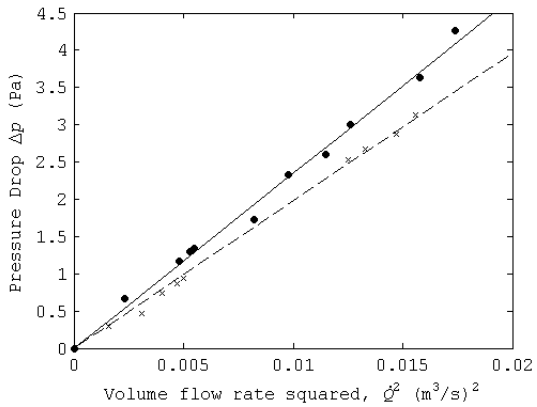

Figure 3.26: Measurements by Parker & Teekeram (2004b) of flow rate into and out of the top section of a Windcatcher. Air flow out through quadrant, • and ——; Air flow in through quadrant, × and – – –.

The values of loss for the inlet and outlet quadrants have been derived for the Windcatcher as a whole and give no information on the losses attributable to individual components of the Windcatcher apart from the estimation that the volume control dampers and grill contribute to 18% of the total losses. Here, measurements made by Parker & Teekeram (2004b) who used a fan to blow/draw air into and out of the top section of a 500 mm Windcatcher containing the louvres (see Figure 3.2, p. 73) are plotted in Figure 3.26 showing the pressure drop across the top section Δp against the square of the volume flow rate of air $\dot{Q}^2$ through it. Here, the losses are readily extrapolated from the gradients m obtained by linear data regression where $m = \Delta p/\dot{Q}^2$, and the Darcy–Weisbach equation (see Munson *et al.*, 1998) for the pressure loss over the Windcatcher section given as

$$\Delta p = \frac{1}{2}\rho u^2 K \tag{3.144}$$

Therefore, the loss imparted by the section K is easily derived and given as

$$K = \frac{2mA^2}{\rho} \tag{3.145}$$

Here, $K = 1.5$ for flow in through the Windcatcher and $K = 1.32$ for flow out of the Windcatcher.

Estimating the losses imparted by other Windcatcher components is less straightforward, and so estimations based upon standard values must be relied upon, which are presented in Table 3.5. It is assumed that the volume control dampers and grill make up 18% of the total losses (see the earlier discussion in Section 3.2.2, p. 105) and the frictional losses K_{fric} from the walls of each quadrant have been estimated from standard data for circular ducts using the hydraulic diameter for triangular ducts [see Equation (3.138)]. Furthermore, the large value given for the "inlet" of an extract quadrant refers to the discussion on p. 106 about possible interference of the flow leaving the room by the flow into it. Arguably, a standard

Table 3.5: Loss coefficients for the Windcatcher.

Section	Supply K_1	Extract $K_{2,4}$
Top section	1.50	1.32
Inlet	0.50	4.83
Outlet	1.00	1.00
Duct	$K_{frict} = 0.06L/d_H$	$K_{frict} = 0.06L/d_H$
Additional Losses	0.60	1.00
Grill	0.35	0.35
Dampers	0.35	0.35
Total	$4.30 + K_{frict}$	$8.85 + K_{frict}$

value for a sudden contraction could have been chosen (see value for the "inlet" of an supply quadrant in Table 3.5) with the additional losses placed in the "additional losses" losses section in Table 3.5, but this would not have reflected the hypothesis. Here, the "additional losses" represent the balance between the standard losses and those values of K derived earlier. They are attributed to frictional losses in the quadrants and to losses when entering the outflow quadrants, as was discussed previously, although there is clearly an element of guesswork in their derivation and a clear need for further experimental/modelling work to quantify this data with more certainty and to investigate the difference between K_{in} and K_{out}.

3.2.4 Corroborating the Predictions for an Autonomous Windcatcher

The semi–empirical model developed in Sections 3.1.1 and 3.1.2 is now applied to different scenarios in order to investigate its accuracy. Li & Mak (2007) generated CFD predictions of the net flow rate out of a 500 mm Windcatcher identical to the one studied by Elmualim (2006a) for a sealed room, and with the wind incident at $\theta = 0°$, $\theta = 15°$, $\theta = 30°$, and $\theta = 45°$. Their estimations of the total flow in and out of a Windcatcher ventilating a sealed room are given in Figure 3.27 (p. 113) where they are compared against the predictions of the sealed model (with $d_1 = d_2 = 0.5\,\text{m}$ $L = 1\,\text{m}$, and dampers and grill excluded). Here, Equations (3.20), (3.24), and (3.25) are used when $\theta = 0°$, and Equations (3.35), (3.36), and (3.37) are used when $\theta = 45°$, where all of the equations are found in Section 3.1.1 (p. 79). Good agreement is observed for $\theta = 0°$ (error of 3%), and for $\theta = 45°$ the error is still acceptable (error of 21%), especially when it is noted that the estimations for $\theta = 45°$ were made with the values of K_{in} and K_{out} generated for $\theta = 0°$.

Elmualim & Teekaram (2002) also examined the performance of a 500 mm Windcatcher with the wind incident at $\theta = 45°$ by obtaining experimental measurements; a comparison is shown in Figure 3.28 (p. 113). Scattering and a lack of symmetry is evident in the experimental data, although this is likely to be caused by experimental error. The predictions made by the semi–empirical model show relatively good agreement with the experimental data, with an overall error of 3.8% if the gradient of the semi–empirical model is compared against one based on linear data regression of all of the experimental data.

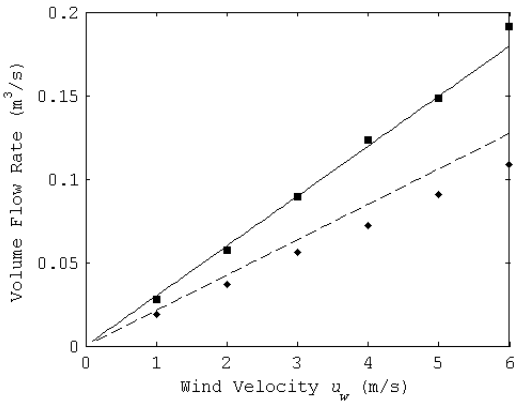

Figure 3.27: Comparison between semi–empirical predictions and the CFD predictions of Li & Mak (2007) for ventilation rates from a sealed room, without dampers and grill. $\theta = 0°$, ——, semi–empirical model, ■, CFD; $\theta = 45°$, – – –, semi–empirical model, ♦, CFD;

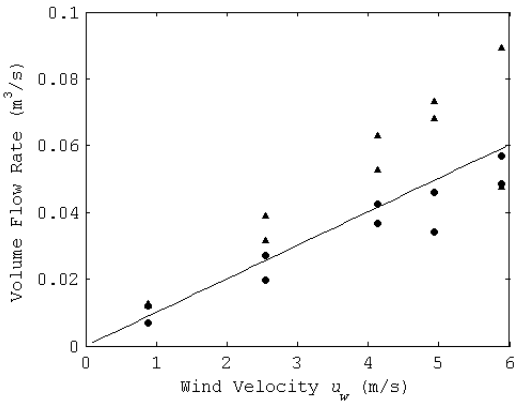

Figure 3.28: Comparison between semi–empirical predictions and the experimental measurements Elmualim & Teekaram (2002) for ventilation rates in each quadrant when ventilating a sealed room, without dampers and grill. $\theta = 0°$, ——, semi–empirical model; ♦ and • experiment.

Elmualim (2005b) measured the effect of a difference between the densities of the supplied room and the surroundings by placing an electric heater in a sealed room, and measuring the volume flow rates through each quadrant of a 500 mm Windcatcher. Here, a 10°C temperature difference between the room ($\Delta T = T_{in} - T_{out}$) and its surroundings was generated and in Figure 3.29 (p. 114) the predictions of the semi–empirical model are compared against Elmualim's data for $\theta = 0°$ (with $\Delta T = 10$°C and $T_{in} = 20$°C). Figure 3.29 shows good agreement between the predicted and measured data for quadrants 1 and 4, with an average error of 9% and 11% respectively, although the model over-predicts the flow rates in quadrant 2 (error of 52%). The key finding is that the model predicts that the change in density has a minimal influence on the overall performance of the Windcatcher. Because the supplied room is considered to be completely sealed, the internal pressure of the supplied room drops to compensate for the change in temperature and to maintain mass continuity. Consequently, changes to the volume flow rates of air through the quadrants are not observed (see Figure 3.29). This effect is observed in Figure 3.30 (p. 114) where the pressure in the room is seen to drop as the difference between the internal and external temperature increases.

The predictions presented so far have been compared to data obtained under controlled

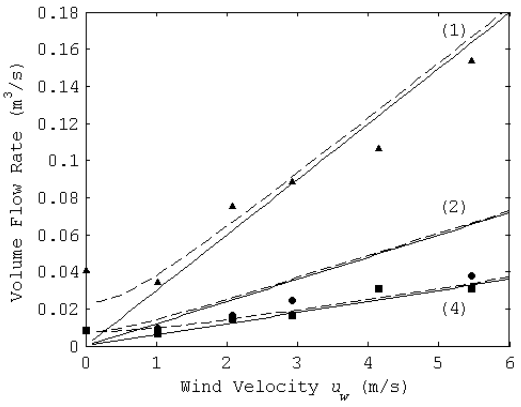

Figure 3.29: Comparison between semi–empirical predictions and the experimental measurements of Elmualim (2005b) without dampers and grill for $\theta = 0°$. Labelled quadrants; ——, prediction $\Delta T = 0°$C; – – –, prediction $\Delta T = 10°$C; ▲, quadrant 1; ■, quadrant 2; and •, quadrant 4.

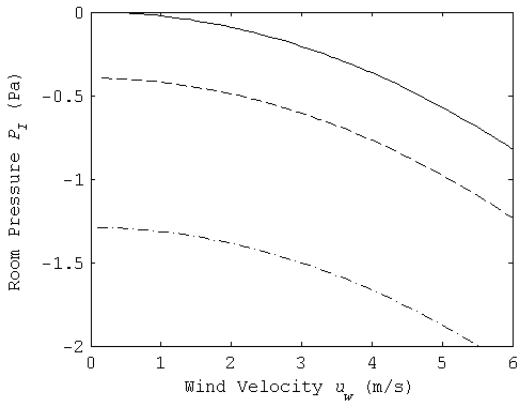

Figure 3.30: Predicted pressure in a sealed room. ——, $\Delta T = 0°$C; – – –, $\Delta T = 3°$C; – – –, $\Delta T = 10°$C.

conditions for a sealed room; however, when operating *in–situ*, the Windcatcher is likely to be ventilating a room that allows air exchange between it and its surroundings, however small they may be. In Figures 3.31 and 3.32, predictions are presented for flow rates in an unsealed room ventilated by a 500 mm Windcatcher that is identical to the type used in

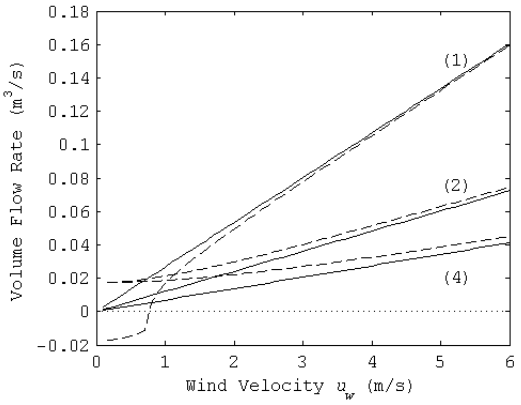

Figure 3.31: Predictions for an unsealed room when $\theta = 0°$. Labelled quadrants; ——, prediction $\Delta T = 0°$C; – – –, $\Delta T = 3°$C.

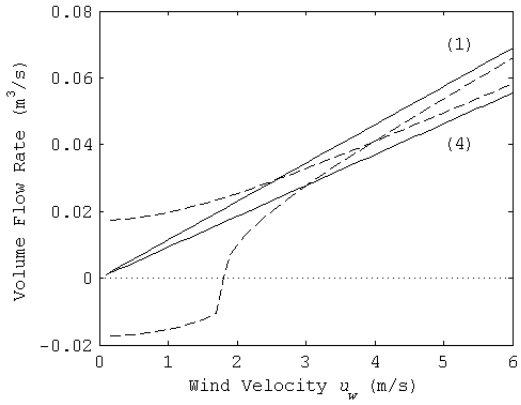

Figure 3.32: Predictions for an unsealed room when $\theta = 45°$. Labelled quadrants; ——, prediction $\Delta T = 0°$C; – – –, $\Delta T = 3°$C.

all the previous calculations, and also includes the volume control dampers and grill. The predictions are made with and without a difference between the temperature of the supplied room and its surroundings, where flow reversal in a quadrant is represented by a change in sign of the volume flow rate. Here, it can be seen that a temperature difference of $\Delta T = 3°\text{C}$ (where $T_{out} = 20°$) only significantly alters the the performance of the Windcatcher at low wind speeds, where a reversal of the flow direction is evident in quadrant 1. The effect is more noticeable when $\theta = 45°$ where the flow reversal in quadrant 1 occurs at a higher wind speed. This is thought to be because the Windcatcher is less efficient at gathering the incident energy from the wind when $\theta = 45°$ and so the buoyancy of the the air is larger relative to the wind energy. Consequently, the results presented here indicate that the effects of buoyancy can be ignored when $\Delta T < 10°\text{C}$ and the wind speed is greater than approximately 2 m/s.

It is interesting to compare of the volume flow rates found in each Windcatcher quadrant when ventilating an unsealed room with those previously found for a sealed room. Table 3.6 presents the gradient, m, of $\dot{Q}$ versus u_w for $\theta = 0°$ and $\theta = 45°$ (damper and grill included). Firstly, the gradients show that the predictions for an unsealed room and a sealed room are similar and when $\theta = 0°$ more air is predicted to flow out the an unsealed room than into it. The air flow rates predicted when $\theta = 45°$ are lower than those predicted when $\theta = 0°$, which is expected and tallies with the experimental findings of Elmualim & Teekaram (2002). However, when $\theta = 45°$ the sealed model now predicts the largest flow rates out of the Windcatcher, which is opposite to that seen for $\theta = 0°$, but it is not entirely clear why this should be the case.

In Section 3.2.2 the losses through the extract quadrants of the Windcatcher were found

Table 3.6: Predicted gradients (m) of $\dot{Q}$ vs u_w, damper and grill included.

Quadrant	m Unsealed		m Sealed	
	$\theta = 0°$	$\theta = 45°$	$\theta = 0°$	$\theta = 45°$
1	0.0267	0.0115	0.0277	0.0101
2	0.0121	0.0115	0.0113	0.0101
3	0.0121	0.0092	0.0113	0.0101
4	0.0069	0.0092	0.0052	0.0101

to be much greater than those for the supply quadrants, which is of some concern, especially for an unsealed room. In Table 3.7, the gradient m is plotted for differing losses through the extract quadrants $K_{2,4}$, and the effect this has on the predicted volume flow rate is investigated for an unsealed room ventilated by a 500 mm Windcatcher with dampers and grill. The table shows that as one reduces the value of $K_{2,4}$, the volume flow rate increases as one would expect. The lower limit used here is $K_{2,4} = K_1$ and the flow rates predicted at this limit are 40% higher than those when $K_{2,4} = 9.14$. This is a significant difference, and this highlights the need for further experimental data that can be used to determine confidence in the chosen values for $K_{in,out}$ (see Table 3.5). In particular, it is important to investigate the values presented in Table 3.5 under real operating conditions, because those value for K derived here may be influenced by the laboratory conditions under which the measurements were taken and may not reflect the behaviour of a Windcatcher *in–situ*. This is explored in greater deal in Chapter 6.

Table 3.7: Sensitivity of predicted volume flow rate to value of $K_{2,4}$.

$K_{2,4}$	Gradient m
$8.85+K_{fric}$	0.0310
$7+K_{fric}$	0.0347
$6+K_{fric}$	0.0373
$5+K_{fric}$	0.0407
K_1	0.0437

3.2.5 Simplifying the Semi–Empirical Model

The aim of this analysis is to provide a simple calculation method that estimates the performance of a Windcatcher. If the buoyancy forces can be neglected then a linear relationship is predicted between the wind velocity and the volume flow rate out of a Windcatcher. In Figure 3.29 the semi–empirical predictions for a sealed room with a 10°C temperature difference between the room and its surroundings has been shown to effect overall ventilation rates when $u_w < 1\,\mathrm{m/s}$. However, Figures 3.31 and 3.32 show that the semi–empirical predictions made for an unsealed room with a 3°C temperature difference between the room and its sur-

roundings when $\theta = 0°$ and $\theta = 45°$ are only effected by buoyancy forces when $u_w < 2\,\mathrm{m/s}$. Here, CIBSE (2005a) states that a mean wind velocity in excess of $3.5\,\mathrm{m/s}$ may be expected in all UK locations and so it seems plausible that buoyancy forces may be ignored for most UK locations. This makes the collapsing of data into simple expressions straightforward, and so the volume flow rates for a number of square Windcatchers of different dimensions, that contain a damper and gill, and ventilate an unsealed room, can be re-calculated for $\theta = 0°$ and $\theta = 45°$. When $\theta = 0°$ the flow out of a Windcatcher is through quadrants 2, 3, and 4 and so by using Equations (3.43)—(3.44) this is given by

$$\dot{Q}_{out} = \frac{A_T u_w}{4} \left\{ 2\sqrt{\frac{C_{p2}}{K_2}} + \sqrt{\frac{C_{p4}}{K_4}} \right\} \tag{3.146}$$

where $\dot{Q}_{out}$ is the air removed by a Windcatcher from a room, and A_T is the total cross sectional area of the Windcatcher given by

$$A_T = \sum_{n=1}^{4} A_n \tag{3.147}$$

Equation (3.146) is now simplified further by using the values for C_{p2} and C_{p4} given in Table 3.3 and typical values for K_2 and K_4 given in Table 3.5 for $L = 1\,\mathrm{m}$ and $d_H = 0.4\,\mathrm{m}$. Consequently, the following expression is obtained for $\theta = 0°$

$$\dot{Q}_{out} = 0.1251 A_T\, u_w \tag{3.148}$$

Similarly, Equation (3.52) is used to derive an expression for $\theta = 45°$ where flow out of the Windcatcher is through quadrants 3 and 4, and is given by

$$\dot{Q}_{out} = \frac{A_T u_w}{4} \left\{ 2\sqrt{\frac{C_{p4}}{K_4}} \right\} \tag{3.149}$$

Now, using the values for C_{p4} given in Table 3.3 for $\theta = 45°$ and typical values for K_4 given in Table 3.5 for $L = 1\,\mathrm{m}$ and $d_H = 0.4\,\mathrm{m}$, Equation (3.149) is simplified further and the following expression is obtained for $\theta = 45°$

$$\dot{Q}_{out} = 0.0747 A_T \, u_w \tag{3.150}$$

Equations (3.148)—(3.150) neglect buoyancy effects and assume that $L = 1\,\text{m}$. The latter assumption is possible because the effect of changing the length of the Windcatcher duct on Equations (3.148)—(3.150) is negligible; for example, by setting $L = 10\,\text{m}$, Equation (3.148) decreases by only 5%. However, the semi–empirical model is based upon measurements taken in a Windcatcher with a relatively short duct, and assumes that one may simply scaleup the frictional losses for a longer duct length. The accuracy of this assumption remains to be tested for Windcatchers with a longer duct length that span roof voids or a number of floors.

Equations (3.148)—(3.150) also assume that the C_p and K values obtained for a 500 mm Windcatcher may be applied to those of other geometries through the area A_T. The validity of this assumption can be explored further by comparing the short equations against the results of Hughes & Ghani (2009) who used CFD to predict the ventilation rates for a 1000 mm square generic modern wind-catcher that is similar to the Windcatcher studies here. If linear regression analysis is applied to Hughes and Ghani's CFD predictions for "counter-current flow", the expression $\dot{Q}_{out} = 0.116 u_w$ is obtained. For a 1000 mm Windcatcher Equation (3.148) gives $Q_{out} = 0.1251 u_w$, which is very close to the results of Hughes and Ghani, and further validates the expressions derived here.

3.2.6 Windcatcher with Façade Opening

In Section 3.2.1 the losses through a Windcatcher have been identified. Losses through a sharp-edged façade opening are shown by Karava *et al.* (2004) to be a function of its shape and location in the façade, angle of incidence of the wind, and Reynolds Number Re (based on d_H for the opening). Etheridge & Sandberg (1996) show that if Re is high ($\gg 100$) losses for a sharp-edged opening can be represented by a single discharge coefficient, which is often shown to be from 0.60 to 0.65 (Karava *et al.*, 2004). Professional guidelines CIBSE (2006a) suggest a discharge coefficient, $C_d = 0.61$, that correlates to a loss factor of $K = 2.69$ by virtue of the following relationship between the two representations of losses

$$C_d = \sqrt{\frac{1}{K}} \tag{3.151}$$

This latter value is now used by the semi–empirical model to estimate flow through a window while acknowledging that it is unfeasible to calculate the true losses through each window measured *in–situ*, and accepting that this method may be an over simplification that could be a source of error.

The C_p for each Windcatcher face with varying wind incidence are summarised in Table 3.3. The magnitude of C_{p5} for the façade of a building is a function of the geometry of the building, the angle of the wind incident to the façade, and the topography surrounding the building. Estimations of C_{p5} are commonly made from wind tunnel analysis, but can also be made using predictive software (see Sawachi *et al.*, 2006, for a discussion) or extracted from tables. For low rise buildings of up to three storeys, C_{p5} can be expressed as a mean value for each façade of a building because the influence of the wind velocity with changing height is relatively small. One may suggest that this assumption appears to contradict the inclusion of $\tilde{C}_{p5}$ and Equation (3.19) into the model but it is argued that although the variation in wind velocity with building height may not affect the mean C_{p5} for a building façade of up to three storeys, it will affect the wind velocity at the height of the opening significantly enough to alter estimations of flow rate through the opening. Consequently, the sensitivity of the semi-empirical model to its inclusion in Equation (3.19) for low rise buildings is investigated later through a sensitivity analysis of the C_{p5} parameter.

Values of C_{p5} for $\theta = 0^\circ$ to $\theta = 315^\circ$ at intervals of $\theta = 45^\circ$ are given by several sources and Liddament (1996), Orme & Leksmono (2002), and Santamouris & Asimakopoulos (1996) all quote similar values for buildings in a range of locations with an aspect ratio (length to width) of 1:1 and 2:1.

The aim of this section has been to develop a semi–empirical model that can predict ventilation rates through a room ventilated by a Windcatcher in coordination with a single façade opening, yet there are a considerable number of unknowns. For example, there is no guarantee that the angle of incidence of the wind on the façade will remain constant, and so limiting values of C_{p5} must be chosen so that estimations for the best and worst possible scenarios can be made. For example, for a sheltered building of aspect 2:1 that is surrounded by obstacles equivalent to its full height such that the aerodynamic flow fields from them and any surrounding buildings interact, Liddament (1996) shows that the limiting values are $C_{p5} = 0.06$ for the windward façade and $C_{p5} = -0.38$ for the leeward façade and are based

upon the assumption that the opening is located in the longest wall. Here, it is noted that the Air Infiltration and Ventilation Centre (Santamouris, 2004) shows that buildings with a height to separation distance ratio of less than 0.05 are disturbed by the flow regime known as isolated roughness flow.

Firstly, it is interesting to note the effect of increasing the opening area on the overall volume flow rate extracted from the room, $\dot{Q}_T$, via the Windcatcher and the opening. In Figure 3.33, the total extracted volume of air is normalised so that

$$\dot{Q}_0 = \frac{\dot{Q}_T}{u_w A_T} \tag{3.152}$$

and is plotted against a normalised façade opening area

$$A_0 = \frac{A_5}{A_T} \tag{3.153}$$

for $C_{p5} = 0.06$ and $C_{p5} = -0.38$, when $\theta = 0°$ and $\theta = 45°$. Here, $z_0 = 1.65\,\text{m}$, $z_I = 3.30\,\text{m}$, $z_E = 4.30\,\text{m}$, $a = 0.25$ for an urban building, and $L = 1\,\text{m}$. Note that a larger version of Figure 3.33 is given in Appendix A (p. 268). Figure 3.33 shows that when $\theta = 0°$, the total

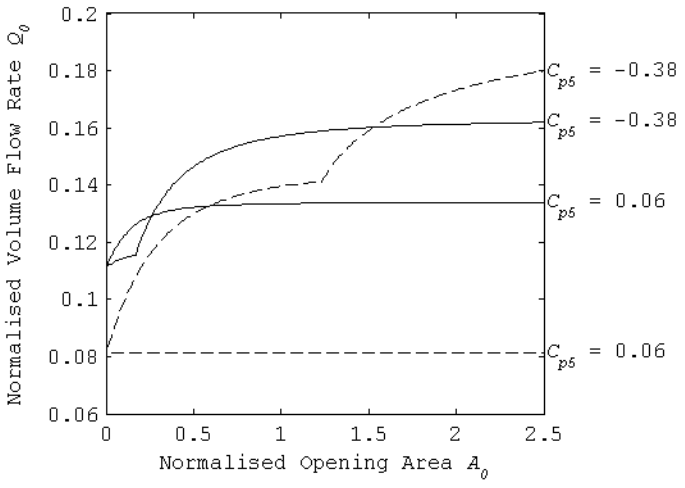

Figure 3.33: Prediction of the effect of the area of a shielded façade opening on Windcatcher ventilation rates. $\theta = 0°$, ——; $\theta = 45°$ – – –.

extracted flow rate $\dot{Q}_T$ increases significantly once an opening is present and this increase is maintained until a limiting open area of approximately $A_0 = 0.7$ is reached when $C_{p5} = 0.06$. However, when $C_{p5} = -0.38$, $\dot{Q}_0$ increases considerably when compared to $C_{p5} = 0.06$ and the flow rate is seen to rise steadily until $A_0 \approx 1.3$. When $\theta = 0°$, the predictions suggest that an opening will increase the flow rate through the room regardless of the value of C_{p5}, although to maximise the flow this opening should at least give $A_0 > 0.7$.

The relationship between A_0 and C_{p5} is less clear when $\theta = 45°$, for it is evident that when $C_{p5} = 0.06$ the change in $\dot{Q}_0$ is minimal. Conversely, a very large rise in $\dot{Q}_0$ occurs when $C_{p5} = -0.38$ and so under these conditions Figure 3.33 shows that $\dot{Q}_0$ is very sensitive to the value of C_{p5}. When $\theta = 45°$, this behaviour is thought to be a function of the losses through the inlet and outlet quadrants, as well as the number of quadrants that supply and extract air. Generally, when $C_{p5} = 0.06$ air is supplied by the façade opening and extracted through two Windcatcher quadrants, whereas when $C_{p5} = -0.38$ air is also extracted through the façade opening. This is significant because the losses through a Windcatcher are much lower when flow is from the surroundings into the room than when flow is from the room to the surroundings ($K_{out} > K_{in}$), and lower still when flow leaves the room through the opening ($K_{out} > K_{in} > K_5$). By using the values of C_p for a Windcatcher given in Table 3.3, Equation (3.73) shows that when $\theta = 0°$ and $C_{p5} = 0.06$, the façade supplies air and three Windcatcher quadrants extract air from the room, but when $\theta = 45°$ and $C_{p5} = 0.06$, Equation (3.114) shows that it is only possible for two Windcatcher quadrants to extract air, thus reducing the overall area of the extract quadrants and significantly reducing the extracted volume flow rate. However, when $\theta = 45°$ and $C_{p5} = -0.38$, Equation (3.129) shows that all of the Windcatcher quadrants will supply air into the room if $A_0 > 0.3$, which effectively overrides the normal function of the Windcatcher and reduces overall losses while maximising the ventilation rate $\dot{Q}_0$.

The influence of a difference between the internal and external temperatures ΔT, on the extracted flow rate $\dot{Q}_T$, is shown in Figure 3.34 for a 1000 mm Windcatcher with $A_5 = 1\,\mathrm{m}^2$, $\Delta T = T_{in} - T_{out} = -5°\mathrm{C}$ when $\theta = 45°$, for $C_{p5} = -0.38$ and $C_{p5} = 0.06$, and so represent a best and worst case performance scenario. All the other data is the same for Figure 3.33. Here, Figure 3.34 shows that as the wind speed increases, the estimated volume flow rates with and without buoyancy forces become similar, suggesting that the buoyancy forces are

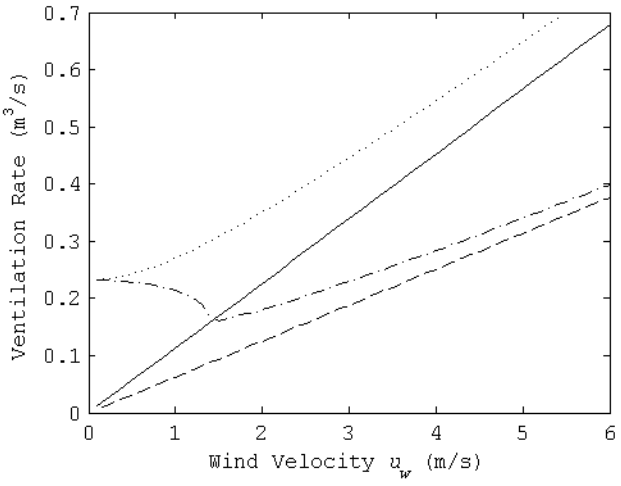

Figure 3.34: Prediction of ventilation rates for a 1000 mm Windcatcher with $A_5 = 1\,\mathrm{m}^2$ and $\theta = 45°$. ——, $\Delta T = 0°\mathrm{C}$ and $C_{p5} = -0.38$; – – –, $\Delta T = 0°\mathrm{C}$ and $C_{p5} = 0.06$; · · · · · ·, $\Delta T = -5°\mathrm{C}$ and $C_{p5} = -0.38$; — · — ·, $\Delta T = -5°\mathrm{C}$ and $C_{p5} = 0.06$.

only an important consideration at low wind velocity. This finding is also similar to those for an autonomous Windcatcher, where the effect of the buoyancy forces is found only to be significant when $u_w < 2\mathrm{m/s}$.

The accuracy of the prediction for a room ventilated by a Windcatcher in coordination with a façade opening are dependent upon the choices of value for K_5 and $\tilde{C}_{p5}$. Here, varying K_5 by $\pm 10\%$ had no discernible effect on the predicted ventilation rates, suggesting that inaccuracies in this value will not have significant consequences for the behaviour observed here. The variable $\tilde{C}_{p5}$ contains two constants, a and C_{p5}. Of these, C_{p5} is the most problematic, and Figure 3.35 (p. 123) shows the affect of varying its value for three different opening areas A_5, when $\theta = 45°$. The plot is asymmetric because the losses in the inlet and outlet quadrants are dissimilar (as discussed earlier), and so the model predicts greater ventilation rates when the opening is placed in an area of negative pressure. Initially this does not seem to agree with the CFD predictions of Su *et al.* (2008) who show that when a circular Windcatcher is mounted on the apex of a 30° pitched roof on an exposed square building, the opening located on the windward façade delivers the greatest ventilation rates through the supplied room. However, the critical factor here is that Su *et al.* (2008) examine an exposed building, and Liddament (1996) reports that the windward façade has the greatest magnitude of C_{p5}, where

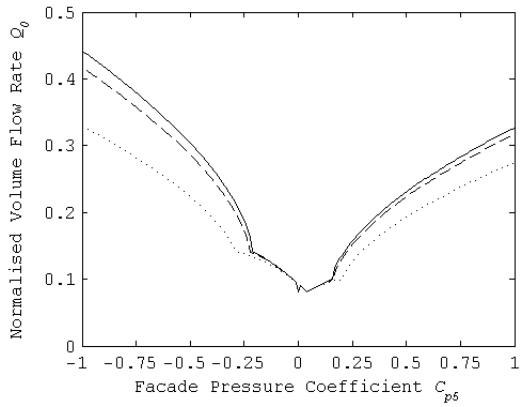

Figure 3.35: Prediction of ventilation rate from a room with varying C_{p5} for the façade opening. ——, $A_5 = 1.5\text{m}^2$; – – –, $A_5 = 1.0\text{m}^2$; ·····, $A_5 = 0.5\text{m}^2$.

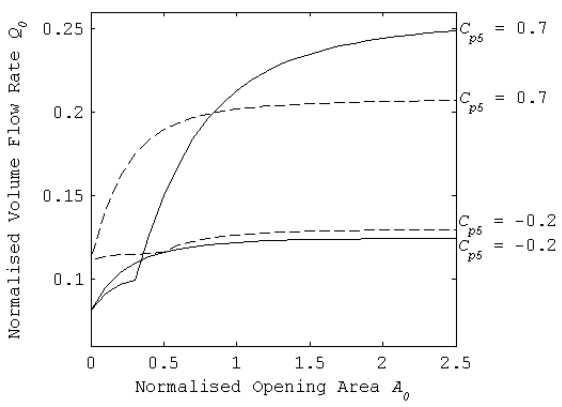

Figure 3.36: Prediction of the effect of the area of an exposed façade opening on Windcatcher ventilation rates. $\theta = 0°$, – – –; $\theta = 45°$ ——.

one would expect a value of $C_{p5} = 0.7$, and the leeward façade has the lowest magnitude of C_{p5}, where $C_{p5} = -0.2$. Accordingly, Figure 3.36 shows that for a square exposed building, the windward façade does deliver the greatest flow rates in accordance with the findings of Su *et al.* (2008). Note that a larger version of Figure 3.36 is given in Appendix A (p. 268).

It is evident from Figure 3.35 that the predicted volume flow rates are sensitive to the value chosen for C_{p5}; for example if $C_{p5} = -0.38$ is varied by $\pm 10\%$ when $A_5 = 1.5\text{m}^2$, the predicted ventilation rate changes by approximately $\pm 7\%$. Accordingly, when predicting the ventilation rates for a specific scenario the accuracy of the the model will depend upon the values chosen for C_{p5}. Accurately identifying values of C_p for a particular building represents a considerable challenge and also a limitation of the semi–empirical approach.

3.2.7 Comparing the Performance of Windcatcher Systems

The predictions made by the semi–empirical model suggest that a Windcatcher in coordination with a façade opening is able to provide greater ventilation rates than just a Windcatcher, and so demonstrates the benefit of combining a Windcatcher with open windows. Therefore, it is evident that this configuration could be used to achieve high levels of ventilation through a room in order to deliver good IAQ levels, as well as dissipate large heat gains and provide purge ventilation. For example, the purge ventilation requirement for a UK school classroom

with 30 occupants is $0.24\,\mathrm{m}^3/\mathrm{s}$ DfES (2006). In order to meet this flow rate using an 800 mm square Windcatcher, then if we choose, for example, $u_w = 3\,\mathrm{m/s}$, Figure 3.33 indicates that an opening of area $A_5 = 0.09\mathrm{m}^2$ is necessary for a shielded building, while Figure 3.36 suggests that $A_5 = 0.064\mathrm{m}^2$ is necessary for an exposed building. Therefore, this suggests that the requirement can be met with a relatively small open area, whatever the location of the building. The ventilation performance can clearly be improved if the building is located in a terrain with few obstacles or surrounding buildings, but in all but the most extreme cases this is not possible, and so Figure 3.33 shows that for a given C_{p5} value the windows should be located so that their orientation is normal or leeward to the prevailing wind, and are, therefore, in an area of negative pressure; however, what is important here is the magnitude of C_{p5} and so it is preferable to open windows that maximise this value and here the appropriate window will depend on the topography of the building as well as the prevailing wind conditions.

Figures 3.33 and 3.36 for shielded and exposed buildings suggest that only a small façade opening is required to significantly increase ventilation rates through a room ventilated by a Windcatcher, and perhaps suggest that a smaller purpose provided opening such as a trickle vent could also be used in coordination with a Windcatcher to meet ventilation requirements. Here, Karava *et al.* (2003) show that a simple slot ventilator has total losses of $K_5 = 8.65$ (or $C_d = 0.34$), and Figures 3.37 and 3.38 (p. 123) show the effect of a trickle vent opening on Windcatcher ventilation rates for shielded and exposed buildings respectively. If the purge ventilation requirement for a UK school classroom with 30 occupants is to be met with a trickle vent and an 800 mm Windcatcher, Figure 3.37 suggests that the area required is $A_5 = 0.26\mathrm{m}^2$ for a shielded building, and Figure 3.38 suggests that $A_5 = 0.096\mathrm{m}^2$ for an exposed building. If the trickle vent is, say, 30 mm high, the length of the vent would need to be approximately 8.5 m and 3.2 m long for shielded and exposed buildings respectively, suggesting that using trickle vents used in coordination with a Windcatcher to ventilate a room may only be suitable for the most exposed buildings.

The Windcatcher and vernacular wind–catcher are related to each other but they have several key differences and so their performance is now compared. The wind–catcher is used as an intrinsic part of the ventilation strategy of an Iranian house but other ventilation openings (such as windows) located in the façade of the house are also required. Generally, air enters

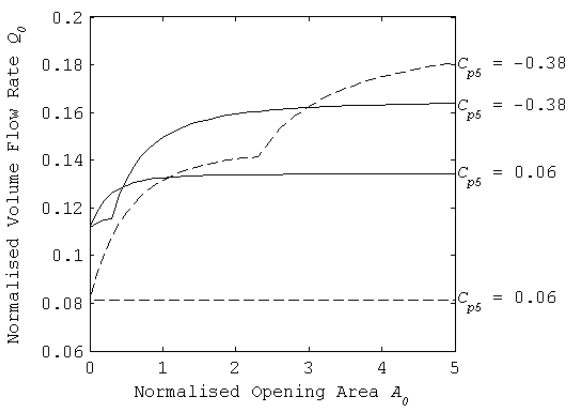

Figure 3.37: Prediction of the effect a shielded trickle vent opening on Windcatcher ventilation rates. $\theta = 0°$, ——; $\theta = 45°$ – – –.

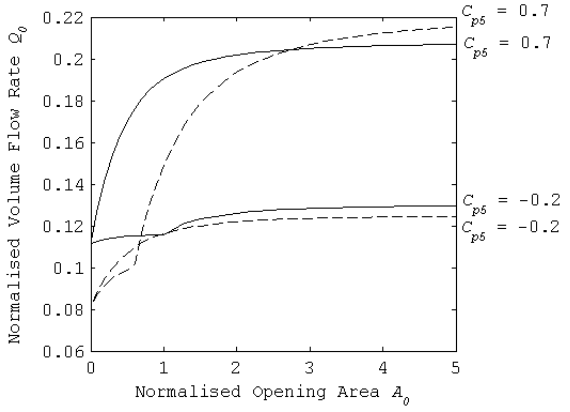

Figure 3.38: Prediction of the effect of an exposed trickle vent opening on Windcatcher ventilation rates. $\theta = 0°$, ——; $\theta = 45°$ – – –.

through the wind–catcher and is extracted through the ventilation openings. The side and leeward wind–catcher quadrants extract air in the same way as a modern Windcatcher but they are not designed to be the primary extraction paths from a room and at low wind speeds ($u_w < 0.3\,\mathrm{m/s}$) they can extract a significant proportion of the air entering a wind–catcher before it has a chance to flow into the house (Roaf, 1982). Accordingly, Karakatsanis *et al.* (1986) propose the implementation of a system that actively attenuates flow through the side and leeward wind–catcher quadrants and use an analytical approach to predict that ventilation rates can be significantly increased by them.

Modern Windcatchers are designed to operate autonomously providing top-down ventilation where best case ventilation performance (wind only) is shown to occur when $\theta = 0°$ and is estimated by Equation (3.148) to be $\dot{Q}_{out} = 0.1251 A_T\, u_w$. Similarly, Karakatsanis *et al.* use a scale model of a wind–catcher and a house (See Section 2.3.1 for a full description) and an analytic approach to predict that the highest ventilation rate supplied by the wind–catcher to the house occurs when $\theta = 90°$ and is given by $\dot{Q}_{out} = 0.0933 A_T\, u_w$. However, if a courtyard is included in the scenario the highest ventilation rate through the house increases to $\dot{Q}_{out} = 0.1022 A_T\, u_w$ when $\theta = 240°$. This latter equation for the best case performance of a wind–catcher, house and courtyard compares to that of an autonomous Windcatcher, but it should be noted that Equation (3.148) was derived from the measurements of Windcatcher performance in a wind tunnel where the element was located in a free stream of air

where it was not affected by environmental factors that could reduce its overall performance in-situ. Furthermore, Section 3.2.6 shows that Windcatcher performance can be significantly increased above those discussed here by the addition of façade openings, thus demonstrating versatility that the wind–catcher does not possess. However, without empirical measurements of the ventilation rates one may expect to find in a room ventilated by a vernacular wind–catcher an accurate comparison between the modern Windcatcher and its vernacular counterpart cannot be made.

3.3 Summary

This chapter has developed a semi–empirical model that combines a simple analytic model with experimental data reported in the literature. The model uses data measured in the laboratory for the coefficient of pressure on each face of a 500 mm square Windcatcher, and then calculates the losses in each Windcatcher quadrant using further laboratory measurements of ventilation rates. The semi–empirical model is developed here in the belief that this is the only practical approach to quickly and accurately estimate Windcatcher performance, especially in view of the highly turbulent nature of the flow round a typical Windcatcher and the problems this has been seen to cause for numerical models; however, this approach means that any errors present in the experimental measurements will also appear in the model and so the model can only be as good as the experimental data available. Moreover, the experimental data utilised here was obtained under laboratory conditions for a 500 mm square Windcatcher in a sealed room and so an assumption inherent in this approach is that this data may be extrapolated to real, *in–situ*, applications in which air transfer between the room and the surroundings is permitted and different Windcatcher geometries are present.

The semi–empirical model has been shown to perform well against a range of experimental data and CFD predictions, and so offers the potential for use as a quick iterative design tool. With this in mind, a very simple expression for extract ventilation rates is proposed that neglects buoyancy effects, and so provides a very quick estimate of Windcatcher performance requiring no computational effort.

The combination of a Windcatcher and open windows appears capable of significantly improving ventilation rates and delivering those rates typically required by building regula-

tions in the UK, although the semi–empirical model for a Windcatcher in coordination with a façade opening has not been corroborated against data measured *in–situ*, and this represents a significant knowledge gap. Accordingly, the semi–empirical model must be corroborated against quantitative data for a Windcatcher in coordination with a façade opening *in–situ* before the accuracy of its performance can be ascertained. This is done in Chapter 6.

Chapter 4

Case Studies

In this Chapter, seven schools and twenty four classrooms ventilated by a single Windcatcher are examined. Parameters relevant to the study of the schools, classrooms, and the performance of the Windcatcher that ventilate them are examined in detail in Sections 4.1—4.3. In addition, a methodology to measure the performance of the Windcatcher based ventilation strategies is explored in Section 4.4.

4.1 School Buildings

Seven schools have been chosen to test the performance of a Windcatcher based upon a number of beneficial criteria. The choice of a suitable school building is important because their study must give an indication of the performance of a Windcatcher *in–situ*, where the performance criteria are set by the relevant UK government guidelines for indoor air quality (IAQ) (DfES, 2006; ODPM, 2006), ventilation (DfES, 2006), and noise (DfES, 2003). All of the schools have a number of self–contained rooms that may be categorised as purpose provided classrooms. Each classroom contains a single roof–mounted Windcatcher element that is free from obvious shielding, obstacles, or architectural features at roof level. In addition, none of the classrooms incorporate supplementary mechanical supply or extract ventilation. Because of the highlighted difference in the performance of various geometries of Windcatcher (see Elmualim & Awbi, 2002a), the greater understanding of square Windcatchers, and the semi–empirical model of a square Windcatcher developed in Chapter 3, the majority of Windcatcher elements evaluated here are square. Pegg (2008) suggests that a sensible time between

the initial occupancy of a building post–construction and the evaluation of its performance is six months, although it is ideal to leave approximately three years. Although, all of these school buildings were designed and built after 2003, they have been operational for at least six months. All of the schools are located in urban areas of the south of England, and their Windcatcher systems were fitted during the construction phase. Relevant parameters are presented in Table 4.1 where each school is assigned an alphabetical prefix and each classroom studied within a school is given a numerical suffix. When a school has two storeys, classrooms with an odd suffix are located on the ground floor while those with a consecutive even suffix are located immediately above the ground floor classrooms.

It should be noted that none of the schools here have been designed to meet the standards set by BB101 but when Mumovic *et al.* (2009) recently measured the indoor air quality in classrooms of a similar age, they asserted that their ventilation strategies should still be able to comply with its operational performance criteria. In addition, the previous guidelines for air quality in schools given in BB87 (DfEE, 2003) are similar to those of BB101, specifying an identical minimum ventilation rate of 3 l/s – person and an identical achievable rate of 8 l/s – person. Moreover, it is the potential for the Windcatcher system to meet BB101 that is of interest here because the major components of a Windcatcher system have not changed since the implementation of the BB101 standard. Consequently, these results could effect the design of future Windcatcher systems.

Table 4.1: Building parameters.

School	Region	Terrain	Age	Type	Building Height (m)	Floors	Roof Type	Roof Pitch Pitch (°)
C	South East	Urban	New build	Secondary	7.9	2	Butterfly	-5
D	South West	Urban	New build	Secondary	4.9	1	Gable	15
E	South East	Urban	New build	Primary	8.0	2	Mono–pitch	10
F	South East	Urban	New build	Secondary	11.3	2	Mono–pitch	15
G	South East	Urban	New build	Lower	9.6	1	Gable	45
H	South East	Urban	New build	Primary	8.9	2	Mono–pitch	5
I	South East	Urban	New build	Primary	8.3	2	Mono–pitch	12

4.1.1 School C

Figure 4.1: School C, aerial view, 1.7 km by 0.9 km.

School C is a two storey building located between a hospital and a housing estate, and is adjacent to a busy road that leads to the M25 motorway. The case study building is part of a new mathematics, modern languages, and music block, and the four classrooms of interest are located on the ground and first floors where the first floor classrooms are positioned immediately above those on the ground floor. All of the Windcatchers enter the classrooms through the ceiling, and additional ventilation is provided by a series of manually opening windows. All of the classrooms contain under floor heating.

An aerial photograph covering a distance of approximately 1.7 km by 0.9 km is shown in Figure 4.1 where the planform of the building is shaded in white for clarity. The top of the photograph is orientated to the north and the sun can be considered to move from the right of the picture at sunrise, toward the bottom of the picture at midday, and then round to the left at sunset. Similar aerial photographs are given in Figures 4.2—4.7 for the other schools.

4.1.2 School D

Figure 4.2: School D, aerial view, 1.7 km by 0.9 km.

School D is located on the edge of an urban housing estate in Dorset. The classrooms of interest are contained in a single storey block of adjacent rooms that are entered via an external corridor on the south side. All of the classrooms are ventilated by a Windcatcher located on the apex of the roof and in the centre of each classroom. Additional ventilation is provided by manually opening windows located in the northern façade. All of the classrooms contain radiators.

4.1.3 School E

Figure 4.3: School E, aerial view, 1.7 km by 0.9 km.

School E is located at the centre of a brand new housing development near Milton Keynes. Here, Figure 4.3 shows a photograph taken immediately after construction of the school and so does not convey the density of new houses built immediately to the north of the site. The ground floor classrooms, which comprise this case study, are all ventilated by a Windcatcher and manually opening windows located in the south eastern façade. The first floor classrooms, which have not been analysed as part of this study, are ventilated by manually opening windows to the south east and clerestory windows to the north west. The Windcatchers are located just below the apex to its north west, and connected to the ground floor classrooms by a long duct before entering the classroom through the ceiling. All of the classrooms contain under floor heating.

4.1.4 School F

Figure 4.4: School F, aerial view, 1.7 km by 0.9 km.

School F is a two storey building located on the edge of an urban area, just north of the M25 motorway. The classrooms that comprise this study are located in a new art (1st floor) and design and technology (ground floor) block. The rooms are comparatively large and contain exposed thermal mass by avoiding the use of false ceilings. All classrooms are ventilated by a Windcatcher located on the apex of the roof, and air enters each classroom through the ceiling on their north east side. Although all of the classrooms are glazed none of the windows can be opened. All of the classrooms contain radiators.

4.1.5 School G

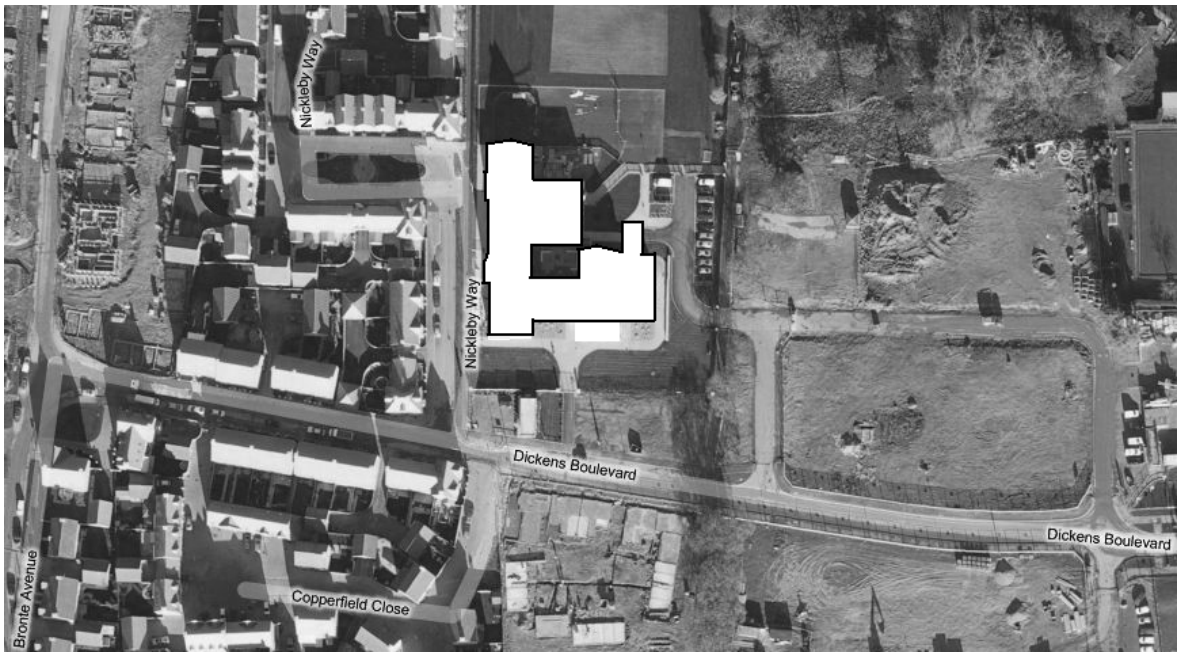

Figure 4.5: School G, aerial view, 0.6 km by 0.3 km.

School G is a single storey building located at the centre of a growing housing development. Like school E, the development of the area has been rapid and so the photograph in Figure 4.5 does not convey the density of new houses built on all sides of the school. All of the classrooms studied here are ventilated by a Windcatcher located on the apex of the roof and ducted to each room through a false ceiling. Furthermore, each classroom contains sash windows for additional ventilation that are housed the western façade and classroom G3 has an additional window located in the southern façade. All of the classrooms contain radiators.

An aerial photograph is shown in Figure 4.5, but when compared to the photographs of the other schools the scale has been increased to approximately 0.6 km by 0.3 km. This is because available satellite photographs predate the construction of the school and could mislead the reader at a larger scale. At the time of writing, on the vacant land located to the east and south east of the school are buildings with heights that are greater than, or equivalent to, the full height of the school.

4.1.6 School H

Figure 4.6: School H, aerial view, 1.7 km by 0.9 km.

School H is a two storey building located in a new housing development immediately north of the M4 motorway. Because of the high rate of development in the area, Figure 4.6 does quite convey the full extent of the existing development that extends from the south to the east in a clockwise direction. All of the classrooms are ventilated by a circular Windcatcher that enters the 1st floor classrooms through the ceiling, and the ground floor classrooms through their north wall. All of the classrooms contain under floor heating.

4.1.7 School I

Figure 4.7: School I, aerial view, 1.7 km by 0.9 km.

School I is a two storey building located in south London that is surrounded on all sides by housing, and is immediately adjacent to a busy main road. All of the classrooms are ventilated by a circular Windcatcher that enters the 1st floor classrooms through the ceiling, and the ground floor classrooms through their northern corner. Furthermore, each classroom contains manually opening windows that are located in the southern façade. All of the classrooms contain under floor heating.

4.1.8 Environmental Conditions

The climatic conditions expected at each site, given by the external temperature (°C) and wind speed (m/s), are presented in Figures 4.8—4.11 where the central bar denotes the mean value, the upper and lower bars denote the maximum and minimum values, respectively, and the dotted box denotes one standard deviation (σ) from the mean. The Figures are constructed using the CIBSE Test Reference Year database (CIBSE, 2005b), which provides typical weather conditions over a year taken from a number of sources surrounding a major land mark in each region of the UK In the south east of England, the database is solely from Heathrow Airport while in the south west of England measurements are made around the city of Plymouth. All of the schools located in the south east are all within approximately 65km (straight line distance) of Heathrow Airport while the school D is approximately 150km from the location of the south west data.

Figures 4.8—4.9 show that the temperature in the south east is expected to be both hotter in the summer and cooler in the winter than those expected in the south west of England. The summer, non–heating period, is defined by BB101 (DfES, 2006) to be from the beginning of May to the end of September. Here, the hottest months for both regions are projected to be in July and August, but all schools in England and Wales are unoccupied during the latter days of July and the whole of August for the summer vacation period, so the Windcatcher ventilation system only has to deal with the range of temperatures during the

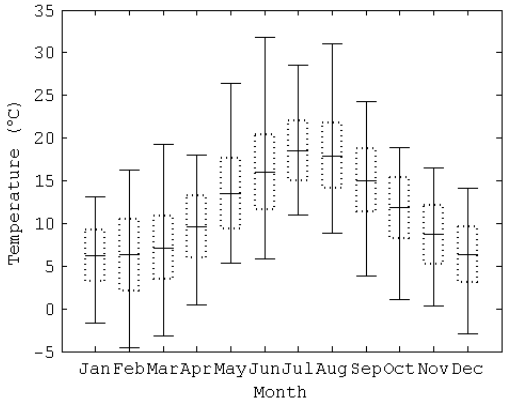

Figure 4.8: External temperature for the south east of England (CIBSE, 2005b).

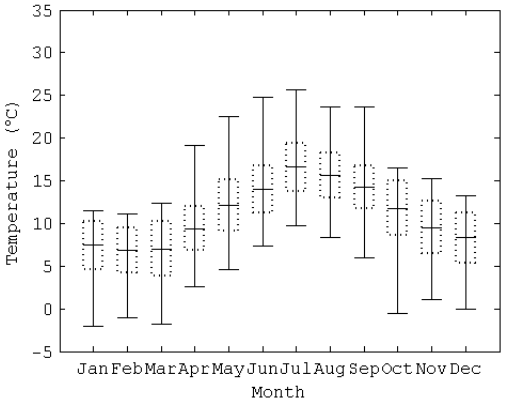

Figure 4.9: External temperature for the south west of England (CIBSE, 2005b).

remaining weeks. The maximum temperatures expected in the south east are approximately 32°C, which should not be exceeded inside a classroom if the BB101 temperature criteria are to be met. BB101 also states that 28°C should not be exceeded in any classroom for more than 120 hours over the summer months and here, Figure 4.8 suggests that the schools located in the south east may be exposed to temperatures that are greater than 28°C during the summer period. In the south west the maximum temperatures are expected to be much lower at around 26°C, and so the classrooms of school D should have fewer problems meeting the 28°C criteria set by BB101.

Figures 4.10–4.11 show that during the summer period when the external temperatures are expected to be at their highest, projected wind speeds are also expected to be at their lowest with an average of 3.26 m/s and 4.63 m/s for the south east and south west respectively. However, the difference between the expected wind speed in the summer and winter months is only 0.73 m/s in the south east and 1.28 m/s in the south west. In the summer months, the difference between the air temperature in a classroom and its surroundings is expected to be less than in the winter month, and so both of the natural driving forces of a Windcatcher are likely to be lower in the summer than in the winter.

The frequency of wind direction for the south east and south west of England are given in Figures 4.12 and 4.13 (p. 139), respectively. They show the percentage of annual hours that the wind comes from a particular direction, and demonstrate that the wind predominantly

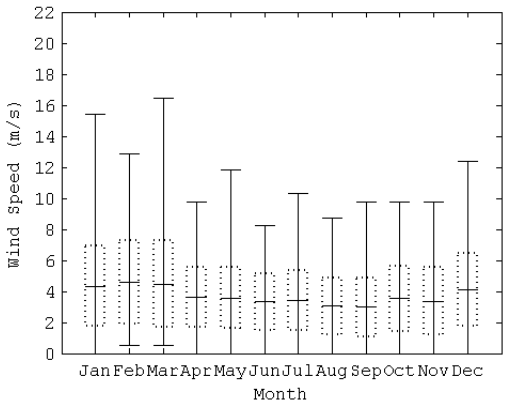

Figure 4.10: Wind speed for the south east of England (CIBSE, 2005b).

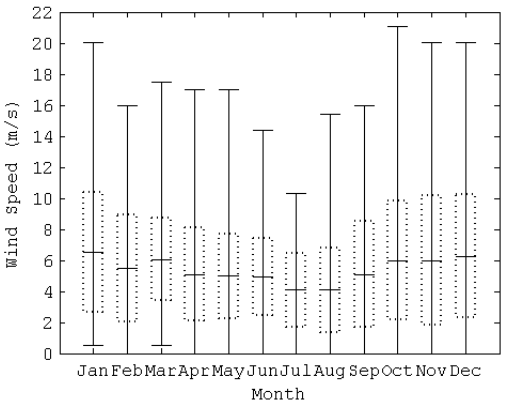

Figure 4.11: Wind speed for the south west of England (CIBSE, 2005b).

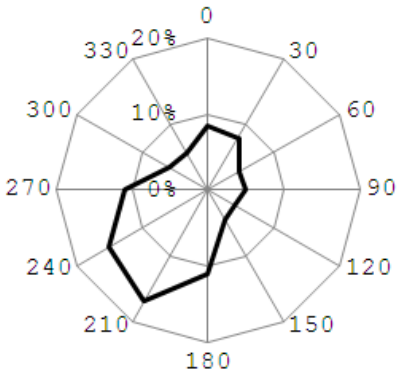

Figure 4.12: Frequency of wind direction for the south east of England (% annual hours) (CIBSE, 2005b).

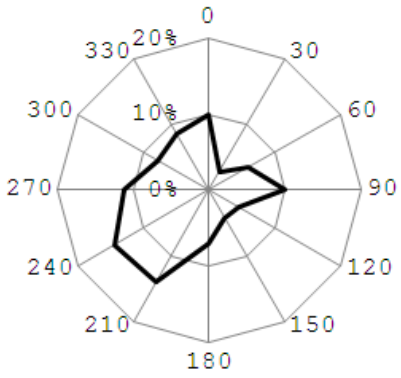

Figure 4.13: Frequency of wind direction for the south west of England (% annual hours) (CIBSE, 2005b).

blows from a south–westerly direction; for example, 32% of the time in the south east of England and 28% of the time in the south west of England.

4.2 School Classrooms

All of the classrooms evaluated here are self contained rooms of brick and concrete block construction. All rooms have false ceilings except those found in school F where concrete beams are left exposed to provide thermal mass. Parameters are presented in Table 4.2 (p. 140), which shows that the mean occupancy density of the classrooms is 0.43 persons/m^2. It was found in the review of literature (see Section 2.1.3, p. 40) that the occupancy density of an average UK school classroom is expected to be between 0.42—0.56 persons/m^2, and so Table 4.2 shows that these classrooms have an occupancy density that is generally at the lower end of the expected levels. The classrooms of school F have occupancy densities that are significantly lower than expected because they are specialised classrooms used for art and design and technology teaching where a greater floor area is required, whereas those of school H are higher than expected (approximately 3% greater). Furthermore, the classrooms have a mean volume of 229 m^3 which is approximately one third larger than those measured by Mumovic *et al.* (2009) at 170 m^3 and Beisteiner & Coley (2002) at 182 m^3. Here, the comparatively large volumes of the school F classrooms contort the mean volume because

Table 4.2: Classroom parameters.

School	Room	Type	Design Occupancy	Mean Height (m)	Depth:Height Ratio	Floor Area (m^2)	Volume (m^3)	Occupancy Density (persons/m^2)
C	1	GT	30	2.60	3.13	57.05	148.33	0.53
	2	GT	30	3.01	2.71	57.05	171.72	0.53
	3	GT	30	2.60	3.13	57.05	148.33	0.53
	4	GT	30	3.01	2.71	57.05	171.72	0.53
D	1	GT	30	3.90	2.36	69.84	272.38	0.43
	2	GT	30	3.90	2.36	69.84	272.38	0.43
	3	GT	30	3.90	2.36	69.84	272.38	0.43
E	1	GT	30	2.74	2.99	57.40	157.28	0.52
	3	GT	30	2.74	2.99	57.40	157.28	0.52
F	1	DT	20	3.10	2.26	104.30	323.33	0.19
	2	Art	30	5.92	1.26	92.75	548.65	0.32
	3	DT	20	3.10	2.26	104.30	323.33	0.19
	4	Art	30	5.37	1.39	92.75	497.97	0.32
G	1	GT	30	3.30	2.58	61.63	203.36	0.49
	2	GT	30	3.00	2.83	61.63	184.88	0.49
	3	GT	30	3.30	2.58	61.63	203.36	0.49
H	1	GT	30	3.00	2.67	52.22	156.67	0.57
	2	GT	30	3.00	2.67	52.22	156.67	0.57
	3	GT	30	3.00	2.67	52.22	156.67	0.57
	4	GT	30	3.00	2.67	52.22	156.67	0.57
I	1	GT	30	2.66	2.97	63.99	170.21	0.47
	2	GT	30	3.65	2.16	61.62	224.91	0.49
	3	GT	30	2.66	2.97	63.99	170.21	0.47
	4	GT	30	3.65	2.16	61.62	224.91	0.49
Mean						68.55	229.27	0.43

GT – General Teaching, DT – Design and Technology

the mean volume of all classrooms except those of school F is 189 m^3, which is much closer to those measured by Beisteiner and Coley, and Mumovic *et al.*

All of the classrooms have a single wall of double glazing, which in classrooms F2, F4, I2, and I4 is augmented by clerestory windows (here 77% and 45% of total glazing area at schools F and I respectively). The area of the façade to the total glazing area is given by the glazing ratio. Table 4.3 (p. 142) shows that classrooms with south facing classrooms generally have a lower glazing ratio (see schools C and F) although the glazing ratio of school H is very high and so its classrooms could experience over heating in the summer months. The windows of school F are all sealed, but at the other schools, a number of windows can be opened manually and so the estimated opening areas for these windows are presented in Table 4.3. The openable area has been calculated using CIBSE guidelines (CIBSE, 2005a) that for a top hung or bottom hung window takes into account the triangular area on each side of the window, and so their area is given by

$$A_5 = d_O(w_O + h_O) \tag{4.1}$$

where A_5 is the estimated open area of a window, w_O is the width of a window, h_O is the height of a window, and d_O is the opening depth of a window.

The estimated openable area is found to range from 0.46 m^2 to 3.88 m^2 with a mean value of 1.06 m^2 per classroom which is 18% smaller than those reported by Mumovic *et al.* (2009). Because openable windows are common in the majority of the classrooms and can be used to contribute to the ventilation strategy, estimations of the ventilation rates through them in coordination with a Windcatcher are made in Chapter 5, although it cannot be said if the windows are open or not during the monitored periods because their position was not recorded. Table 4.3 shows that some of the classrooms are south facing and although the windows of the classrooms of school G are not shielded, the classrooms of schools E and I (lower floor) are shielded by a balcony and those of school C, F, G, and I (upper floor) have solar fins or slats to reduce solar heat gains.

All of the openable windows are positioned adjacent to each other in one or two rows. In classrooms where two rows are found (schools E and I for example) the windows are

Table 4.3: Fenestration parameters.

School	Room	Total Glazing Area (m^2)	Glazing Ratio (%)	Openable Window Type	Estimated Openable Area (m^2)	Window Orientation (°)	Solar Shielding
C	1	3.15	17.31	TH	0.87	S	Fins
	2	3.15	14.95	TH	0.87	S	Fins
	3	3.15	17.31	TH	0.87	S	Fins
	4	3.15	14.95	TH	0.87	S	Fins
D	1	6.53	23.24	TH	1.53	N	None
	2	6.53	23.24	TH	1.53	N	None
	3	6.53	23.24	TH	1.53	N	None
E	1	7.87	41.03	BH	0.49	SE	Balcony
	3	7.87	41.03	BH	0.49	SE	Balcony
F	1	12.10	9.30	None	n/a	SW	Slats
	2	12.34	17.70	None	n/a	SW+NE(C)	Slats
	3	12.10	9.30	None	n/a	SW	Slats
	4	12.34	19.51	None	n/a	SW+NE(C)	Slats
G	1	4.61	19.26	Sash	1.84	W	None
	2	4.61	21.19	Sash	1.84	W	None
	3	9.69	18.64	Sash	3.88	W+S	None
H	1	14.30	78.15	TH	0.46	S	Fins
	2	14.30	78.15	TH	0.46	S	Fins
	3	14.30	78.15	TH	0.46	S	Fins
	4	14.30	78.15	TH	0.46	S	Fins
I	1	9.98	48.10	TH	0.77	E	Balcony
	2	13.40	39.05	TH,THC	1.47	E+W(C)	Fins
	3	9.98	48.10	TH	0.77	E	Balcony
	4	13.40	39.05	TH,THC	1.47	E+W(C)	Fins
Mean		9.18	35.23		1.06		

TH – Top Hung; BH – Bottom Hung; C – Clerestory.

N – North; S – South; E – East; W – West.

placed immediately on top of each other and so do not provide single–sided double–opening ventilation (see Figure 2.2, p. 48) because their separation is less than 1.5 m (CIBSE, 2005a). Therefore, in the absence of a Windcatcher they are only able to provide single–sided single–opening ventilation (see Figure 2.1). Here, rule–of–thumb guidelines (CIBSE, 2005a) for the effective penetration of air to the back of a room ventilated using single–sided single–opening ventilation suggest that the depth to height ratio should be no greater than 2, but Table 4.2 shows that none of the classrooms meet this criteria. Nevertheless, all of the classrooms meet the rule–of–thumb criteria (see CIBSE, 2005a) for successful cross–ventilation using windows because their depth to hight ratio is less than 5, see Figure 2.3.

4.3 Ventilation Strategy and Control

Of the twenty four classrooms examined here, sixteen contain a square Windcatcher while the remaining eight contain a circular Windcatcher, see Table 4.4 (p. 144). The ventilation strategies employed in each classroom are presented in Figures 4.14—4.21 (from p. 145), which show that the Windcatcher can be used to ventilate the classrooms autonomously and in coordination with open windows to provide cross–ventilation in all of the classrooms, except for those of school F, see Figure 4.17. In classrooms I2 and I4 the windows located in the façade in coordination with the upper clerestory windows can provide cross–ventilation without the Windcatcher, although this strategy relies upon the occupants to manually open these windows, see Figure 4.20. When a classroom is located on the lowest floor of a multi–storey building (see classrooms C1 and C3, Figure 4.14 for example), or where there is a significant roof void between the false ceiling and the roof top (see school G, Figure 4.18), the Windcatcher duct is generally much longer than those where there is a much smaller roof void (see Table 4.4 for duct lengths). Figure 4.21 shows a cross–section view of the duct transition in multi–storey buildings such as schools C, F, H, and I. The varying window area and duct length provide an opportunity to develop the findings of Kolokotroni *et al.* (2002b) who found that opening windows significantly increased the ventilation rates, and also noted that ventilation rates measured on the ground floor were less than those measured on the first floor, citing the length of the Windcatcher duct as a potential confounding factor.

All of the Windcatchers are diagonally divided for the length of the element, but not

Table 4.4: Windcatcher parameters.

School	Room	Floor	Side d_1, d_2 (mm)	Geometry	Acoustic Lining (mm)	CSA (m^2)	Duct Length (m)
C	1	Ground	1000	Square	25	0.77	4.80
	2	1st	1000	Square	25	0.77	1.00
	3	Ground	1000	Square	25	0.77	4.80
	4	1st	1000	Square	25	0.77	1.00
D	1	Ground	800	Square	0	0.64	1.00
	2	Ground	800	Square	0	0.64	1.00
	3	Ground	800	Square	0	0.64	1.00
E	1	Ground	800	Square	25	0.46	4.60
	3	Ground	800	Square	25	0.46	4.60
F	1	Ground	1200	Square	50	0.92	7.00
	2	1st	1000	Square	50	0.58	1.00
	3	Ground	1200	Square	50	0.92	7.00
	4	1st	1000	Square	50	0.58	1.00
G	1	Ground	800	Square	0	0.64	5.50
	2	Ground	800	Square	0	0.64	5.80
	3	Ground	800	Square	0	0.64	5.50
H	1	Ground	800	Circular	0	0.50	5.50
	2	1st	800	Circular	0	0.50	1.00
	3	Ground	800	Circular	0	0.50	5.50
	4	1st	800	Circular	0	0.50	1.00
I	1	Ground	800	Circular	0	0.50	5.25
	2	1st	800	Circular	0	0.50	1.00
	3	Ground	800	Circular	0	0.50	5.25
	4	1st	800	Circular	0	0.50	1.00

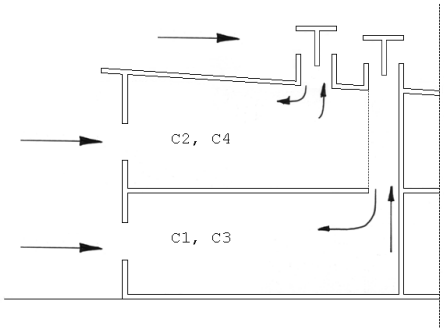

Figure 4.14: Ventilation strategy, school C. ·····, floor transition; – – –, line of symmetry.

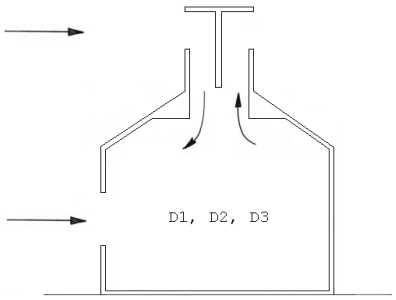

Figure 4.15: Ventilation strategy, school D.

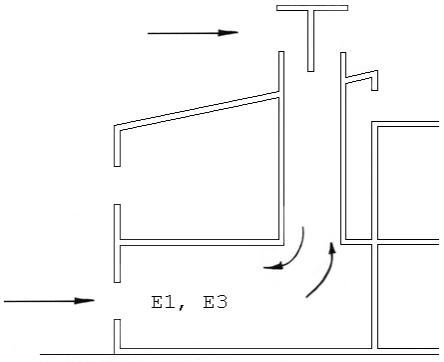

Figure 4.16: Ventilation strategy, school E.

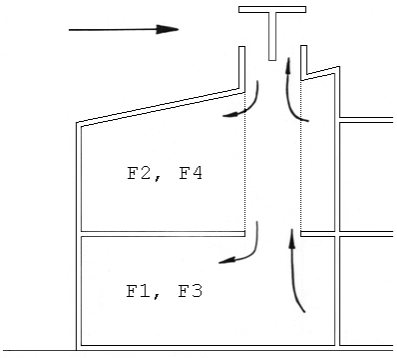

Figure 4.17: Ventilation strategy, school F. ·····, floor transition.

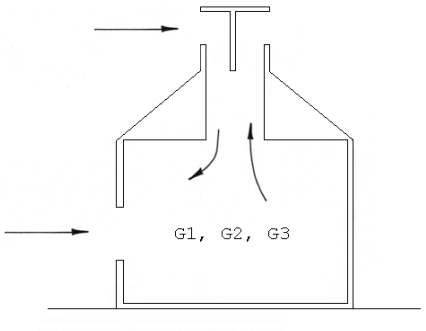

Figure 4.18: Ventilation strategy, school G.

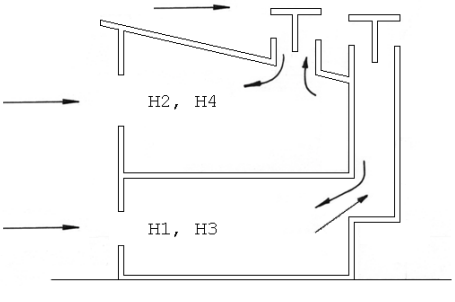

Figure 4.19: Ventilation strategy, school H.

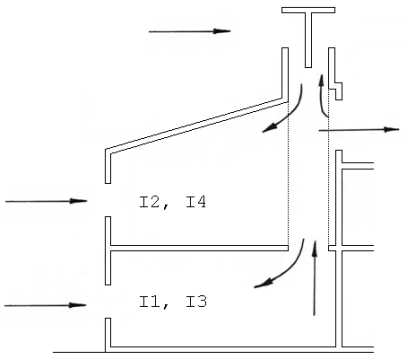

Figure 4.20: Ventilation strategy, school I. ·····, floor transition.

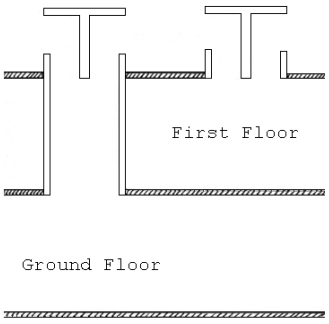

Figure 4.21: Floor transition, cross–section view.

through any additional duct work. The cross sectional area (CSA) of each Windcatcher takes into account the presence of an acoustic lining, which is normally made from foam and covers the duct walls and the diagonal dividers. The total cross section area of a square Windcatcher A_T lined with acoustic foam is given by

$$A_T = 4\left[\frac{d_1}{2} - t(1+\sqrt{2})\right]^2 \tag{4.2}$$

where $d_1 = d_2$ and is the side of a square Windcatcher, and t is the lining thickness.

The Windcatcher is automatically controlled and opens according to the room air temperature and the season. Volume control dampers at the base of the Windcatcher shaft control the flow of air into and out of the classroom, and when a prescribed opening temperature or set point is reached the dampers open 20% for every 1°C above the set point, which in the winter is 22°C, and in the summer is 16°C, see Table 4.5 (p. 147). Furthermore, in the summer the dampers open fully from midnight until 6 am to provide night–cooling unless the internal air temperature is at or below 15°C. Occupants may override the control settings at any time, using a wall–mounted override switch, by choosing to fully open or close the dampers but there is no way of tracking any input. The summer and winter set points are designed to modify the performance of a Windcatcher according to the heating season, and so monitoring was conducted during both the summer and winter seasons to determine the

Table 4.5: Seasonal set points for Windcatcher dampers.

Damper Position (%)	Summer set point (°C)	Winter set point (°C)
0	16	22
20	17	23
40	18	24
60	19	25
80	20	26
100	21	27

effectiveness of this ventilation strategy.

The volume control dampers rotate from a closed position where the angle of opening $\gamma = 0°$ to a fully open position where $\gamma = 90°$. When the dampers are said to be open 20%, this refers to γ and not the free area through the dampers. Here, the approximate free area through the dampers A_d, expressed as a fraction of the total area, is given by

$$A_d = 1 - \cos \gamma \tag{4.3}$$

This shows that when the dampers are open 20% ($\gamma = 18°$), the free area of the dampers is actually only 5% of the total available area. Clearly, this suggests that very little air flow through the dampers will occur when γ is low, which could have consequences during the winter when the set point is high. However, empirical measurements of air flow through the volume control dampers have only been made with the dampers fully open (see Elmualim & Awbi, 2002a) and not with varying γ, and so these assumptions are based upon a linear relationship between A_d and γ, which may not actually exist.

4.4 Measuring Indoor Environment Quality

4.4.1 Indoor Air Quality

The indoor environment quality guidelines for a school classroom set by BB101 (DfES, 2006) have been shown in Chapter 2 to vary according to the heating season. Furthermore, the

summer and winter set points are also designed to modify the performance of a Windcatcher according to the season, and so monitoring was conducted during both the summer and winter seasons to determine the effectiveness of this ventilation strategy, and its ability to meet the current BB101 standard. The high winter set point suggests that the Windcatcher dampers should remain closed for most of this season and so it is important to determine if this is true, and then to determine the overall air quality and ventilation rate in each classroom given that the Windcatcher is a significant part of the ventilation strategy and its inactivity could have a detrimental effect on the air quality in a classroom during the winter months. The dates when indoor air quality monitoring took place in the winter and summer months are presented in Table 4.6.

Internal air temperature, CO_2, and RH measurements were taken every minute for at least five working days during each season, and for each of thirteen classrooms; measurements of temperature only were taken in eleven other classrooms using the same time interval (see Table 4.7, p. 149). External air temperature was measured at 5 minute intervals for all classrooms. QTrak 8551 sensors were used to take measurements of temperature, RH, and CO_2. Here, the temperature measurements are accurate to $\pm 0.6°$, CO_2 measurements are accurate to $\pm 3\%$ and ± 50 ppm at 25°C, with an uncertainty of $\pm 0.36\%$ per °C change in temperature, and RH readings are accurate to $\pm 3\%$, with a $\pm 1\%$ hysteresis. Internal temperature was also measured using Onset U10 Hobo dataloggers that are accurate to

Table 4.6: Indoor air quality test dates.

School	Summer		Winter	
	Week	Year	Week	Year
C	27	2007	49	2008
D	25	2008	4	2009
E	24	2008	48	2008
F	19	2008	44	2008
G	22	2008	45	2008
H	28	2008	50	2008
I	29	2008	2	2009

Table 4.7: IAQ measurements made in each classroom.

School	Room	Temperature	CO_2	RH
C	1	✓	✓	✓
	2	✓	✓	✓
	3	✓		
	4	✓		
D	1	✓	✓	✓
	2	✓	✓	✓
	3	✓		
E	1	✓	✓	✓
	3	✓		
F	1	✓	✓	✓
	2	✓	✓	✓
	3	✓		
	4	✓		
G	1	✓	✓	✓
	2	✓	✓	✓
	3	✓		
H	1	✓	✓	✓
	2	✓	✓	✓
	3	✓		
	4	✓		
I	1	✓	✓	✓
	2	✓	✓	✓
	3	✓		
	4	✓		

± 0.4°C at 25°C. External temperature was measured using DS1921 iButton Dataloggers that are accurate to ± 1°C. BB101 guidelines recommend measurements are taken at seated head height, but in order to secure the equipment it was often necessary to place the equipment just above floor level, whereas on other occasions the equipment was placed at standing head height. However, in all cases effort was taken to place the equipment away from heat sources and in regions of free air flow in order to obtain reliable and accurate readings.

The IAQ data is processed so that it is directly comparable against the requirements of BB101. BB101 specifies its criteria for weekday occupied hours; occupied hours have previously been defined as 0900hrs to 1530hrs (see Section 2.1.2, p. 34) and "weekdays" are defined here as Monday to Friday inclusively. Accordingly, "unoccupied hours" comprise all other

hours of the day outside of occupied hours and the "weekend" encompasses Saturdays and Sundays. It should be noted that this does not necessarily mean that a classroom is unoccupied during "unoccupied" or "weekend" periods, but allows the IAQ data measured in each classroom to be subdivided into four time periods: weekday occupied hours, weekday unoccupied hours, weekend occupied hours, and weekend unoccupied hours. This methodology follows the presentation style of Kolokotroni *et al.* (2002a).

Indoor air quality data is presented in Chapter 5 for weekday occupied hours in both winter and summer months. The only exception to this is school D for the winter where three working days have been used. Examples of the internal temperature, RH, and CO_2 concentration measured over a full week are presented in Figures 4.22—4.24 where the continuous line shows the weekday occupied hours and the dotted line shows weekday unoccupied hours and all weekend hours. In the absence of another source, CO_2 production can be attributed solely to the occupants of a room. Therefore, a rise in CO_2 concentration above ambient levels indicates some level of occupancy, and the solid line in Figure 4.22 shows that the majority of the changes in CO_2 concentration occur during weekday occupied hours. Clearly, Figure 4.22 does show that the classroom is occupied during the weekday unoccupied period (before 0900 hrs and after 1530 hrs, Monday to Friday) and so a statistical analysis of the CO_2

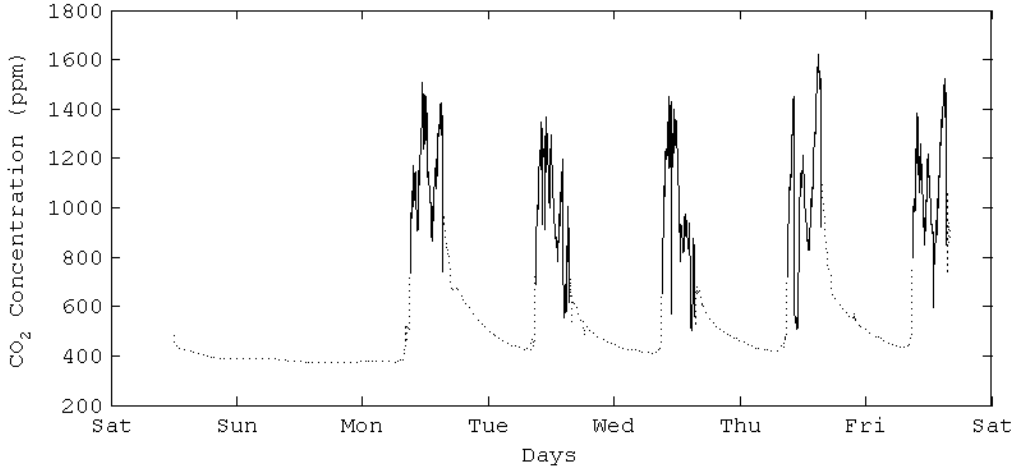

Figure 4.22: Example of CO_2 concentration in a classroom. ——, Occupied hours weekday; · · · · · ·, Unoccupied hours weekday and all hours weekend.

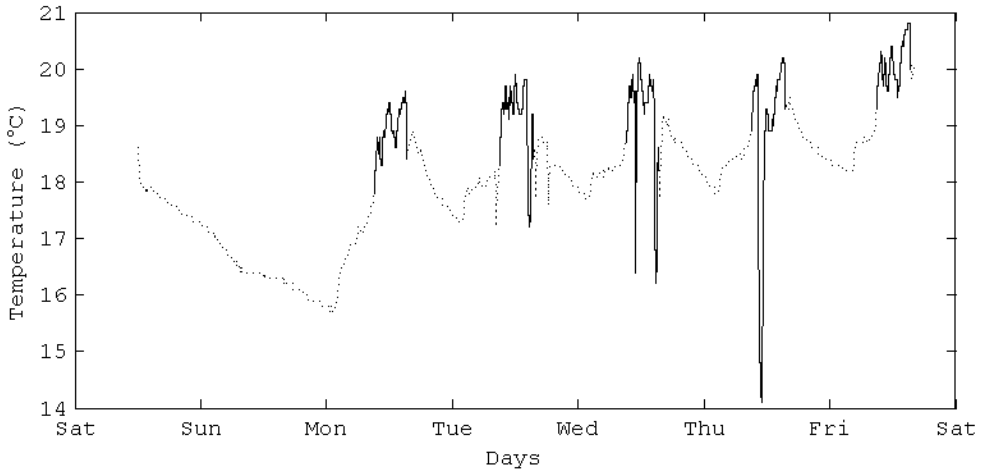

Figure 4.23: Example of air temperature in a classroom (°C). ——, Occupied hours weekday; · · · · · ·, Unoccupied hours weekday and all hours weekend.

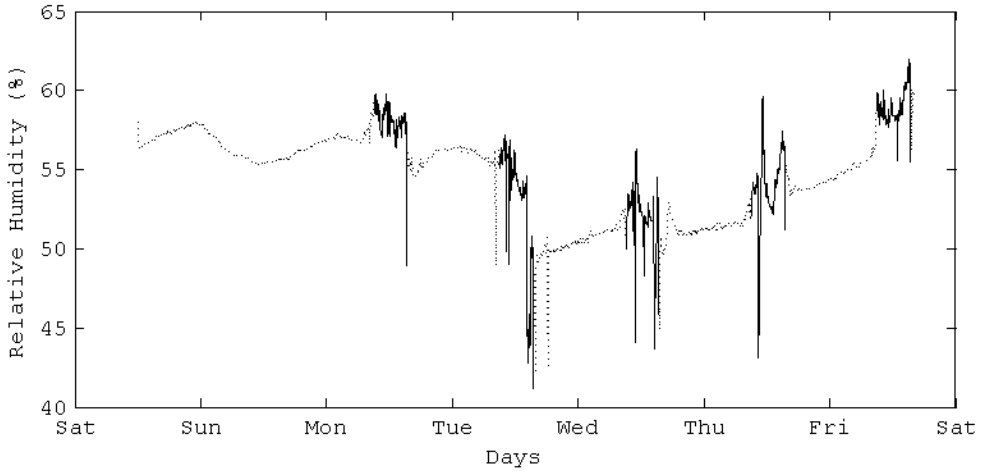

Figure 4.24: Example of relative humidity (%) in a classroom. ——, Occupied hours weekday; · · · · · ·, Unoccupied hours weekday and all hours weekend.

concentration during all periods of occupancy indicated by Figure 4.22 would give different results to those presented here.

Similarly, deviations away from smooth changes in air temperature and RH are also shown in Figures 4.23 and 4.24, respectively, to occur during weekday occupied hours.

All IAQ data are presented in Appendix C for occupied and unoccupied hours during

the working week and at the weekend. All calculations were made using MATLAB and have been corroborated using Microsoft Excel spreadsheets.

4.4.2 Ventilation Rate

The total ventilation rate in each classroom was measured using the tracer gas decay method, which is well documented by Etheridge & Sandberg (1996) and Liddament (1996). Here, a small amount of sulphur hexafluoride (SF_6) was chosen as a tracer gas and injected into a classroom where it was thoroughly mixed using fans to establish a uniform concentration. Then, its exponential decay was monitored every 45 seconds using an Innova 1312 dual gas analyser that has a repeatability of reading of 1%. Measurements were taken from the centre of the room for periods of no less than 20 minutes in accordance with the guidelines of Liddament. Mixing fans were not used during measurement periods because Liddament (1996) suggests that they create artificial flow paths so that measured conditions do not represent occupied conditions; this methodology is also followed by Kirk (2004a) and Pegg (2008). None of the classrooms measured here were interconnected except for those in School F. Here, classrooms F1 and F3, and classrooms F2 and F4 are interconnected but the doors were kept closed to replicated occupied conditions. Adjacent classrooms and corridoors were not seeded with the tracer gas, and so the measurement of ventilation rate does not distinguish between air supplied from outside, through a Windcatcher for example, or from adjacent classrooms.

The concentration of a gas at any instant in time is given by the following continuity equation (Coley & Beisteiner, 2002)

$$V\frac{\partial C(t)}{\partial t} = G + \dot{Q}_T\left[C_E - C(t)\right] \tag{4.4}$$

where V is the volume of the room (m^3), $\dot{Q}_T$ is the total air flow rate (m^3/s) into and out of the room, $C(t)$ is the concentration (ppm) of the gas at any moment in time t, $C(0)$ is the initial concentration of the gas (when time $t = 0$), C_E is the external concentration of the gas. Now, solving Equation (4.4) by integrating between $t = 0$ and a time t gives

$$C(t) = C_E + \frac{G}{\dot{Q}_T} + \left[C(0) - C_E - \frac{G}{\dot{Q}_T}\right] e^{-\frac{\dot{Q}_T}{V}t} \tag{4.5}$$

where $C(0)$ is the initial concentration of the tracer gas (when time $t = 0$), and $\dot{Q}_T/V$ is the air change rate (ACR) (h^{-1}). Because SF_6 is not generally found in the atmosphere and is released prior to its measurement and allowed to decay, $G = 0$ and $C_E = 0$. Accordingly, Equation (4.5) can be re–written to give

$$C(t) = C(0)e^{-\frac{\dot{Q}_T}{V}t} \tag{4.6}$$

An estimation of the ACR is now made by plotting the natural log of the concentration of SF_6 against time and obtaining the gradient of the resulting straight line of negative slope by linear data regression. An example is shown in Figure 4.25 where the equation of the line of best fit is given by $y = 2.41 - 2.75\,t$. The gradient at any point, and also the ACR, is found by differentiating the equation of the line with respect to t to give $\dot{Q}_T/V = 2.75 \pm 0.03\,h^{-1}$. The error is calculated from the coefficient of determination R^2, which indicates the accuracy of the linear data regression, and therefore, also indicates how well mixed the SF_6 was within the room and whether the decay of the SF_6 was truly exponential. Here, it is noted that classroom F2 has a volume of $549\,m^3$ that is greater than the maximum volume of $500\,m^3$

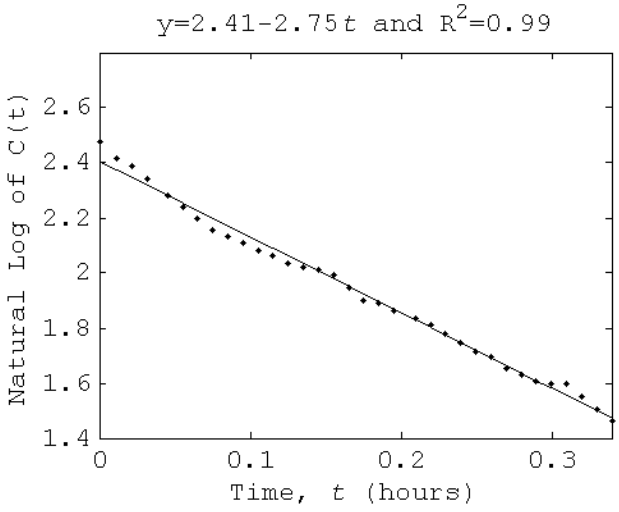

Figure 4.25: Example of the tracer gas decay method.

recommended for this type of test (see Liddament, 1996), although results were obtained with a confidence of between 76–93% indicating exponential decay and good mixing of the tracer gas.

The wind direction (°) and speed (u_{10}) are obtained from the Met Office (TMO, 2009) for the closest weather station (see Table 4.8) to each school and converted to an estimated speed (u_w) at roof height (z_E) using the corrective equation specified by BS EN 5925 (BSI, 1991), see Equation (3.18) on page 78, where for an urban setting (see Table 4.1, p. 129) the topographical constants are given by k=0.35 m^{-a} and a=0.25.

The ventilation rates for each classroom were measured for three different natural ventilation strategies: (i) all windows and Windcatcher closed (ii) windows closed and Windcatcher fully open (iii) all windows and Windcatcher fully open. Here, the term "fully open" means that the Windcatcher dampers are open to their full extent (100% and $\gamma = 90°$) and that all available openable window area was employed. In some limited instances, a further measurement was made of the ventilation provided by all of the windows with the Windcatcher dampers closed, and was designed to show the contribution of the Windcatcher to the cross–ventilation strategy employed in test (iii). Where more than one measurement has been made for a particular configuration of Windcatcher damper and window position, an average

Table 4.8: Weather stations.

School	Weather Station	Distance (km)
C	Wisley	10.0
	Heathrow	21.6
D	Portland	41.6
E	Bedford	11.2
F	Andrews Field	12.8
G	Andrews Field	22.4
H	Heathrow	12.8
I	Heathrow	22.4

value is used. Furthermore, where there are several variations of the same configuration, for example at schools G and I where windows are located on two façades, estimations of the ventilation rate using the maximum openable window area are used in Table 5.2, (p. 168). Estimates of background ventilation rates (with Windcatcher and windows closed) were not made in classrooms C3 and C4 due to time constraints, whereas in classrooms D2 and D3 the override controllers were damaged. In classroom G2, despite several attempts, a satisfactory estimate could not be made and so the classroom is considered to be tightly sealed with negligible background ventilation. It was also not possible to make estimations with the Windcatcher open and windows closed in classrooms I1 and I3 because the damper override was temporarily locked by the BMS in response to a boiler failure.

4.4.3 Noise

Acoustic measurements of the equivalent sound pressure level over 30 minutes ($L_{Aeq,30m}$) were made using a Cirrus CR262 Sound Level Meter that is accurate to ± 0.5 dB and DeafDefier software. The meter was placed in the centre of the room and measurements made with all windows closed and the Windcatcher dampers either open or closed. External $L_{Aeq,30m}$ was measured adjacent to the façade of the classroom. Here, it is noted that the upper limits specified by BB93 (DfES, 2003) are for an unoccupied and unfurnished classroom, but it was not possible to test the classrooms under these circumstances because, although the classrooms were unoccupied, they were not free from furnishings.

4.5 Summary

In Chapter 2 the indoor environment quality in a classroom ventilated by a Windcatcher was found to be a function of ventilation and noise, and the control of them. Furthermore, the literature also shows that there is a lack of data for a Windcatcher when measured *in–situ* and that a quantitative analysis of their performance would establish their performance when compared against the UK government standards for ventilation, indoor air quality, and noise. Accordingly, this Chapter has introduced seven case study buildings that have been chosen to demonstrate Windcatcher performance *in–situ* in a variety of environments and for a number of configurations. Because over 70% of Windcatcher systems are installed into

school buildings, all of the case study buildings are schools. Here, twenty four classrooms have been selected and their parameters have been compared against those found in the literature. A methodology for the measurement of IAQ, ventilation, and noise has been discussed, so that the findings may be compared against the current standards set by BB101 and BB93, and an indication of Windcatcher performance can be determined. Finally, the case studies also have a secondary function; the data collected from them will contribute to the limited number of published reviews of air quality and ventilation rates in UK school classrooms. The results are presented in Chapters 5 and 6.

Chapter 5

Results: IEQ in Case Study Classrooms

This chapter presents the measurements of key indoor air quality parameters, ventilation rates, and background noise for each classroom of the seven case study schools. Measurements of air temperature for twenty four classrooms, and CO_2 and RH for thirteen classrooms are presented in Section 5.1, and sound pressure levels are presented for twenty three classrooms in Section 5.3. The data is plotted so that it is easily compared with the requirements of BB101 (DfES, 2006), BB93 (DfES, 2003), or other relevant standards, and equivalent measurements for UK school classrooms available in the literature. Because the measurements of IAQ are largely determined by the ventilation rate delivered to each classroom, which in turn is an important indicator of the overall success of the ventilation strategy in each classroom, estimated ventilation rates for three key configurations are presented in Section 5.2.

5.1 Indoor Air Quality

The results presented in this section have been collated using the methodology described in Section 4.4 (p. 147).

5.1.1 Temperature

In Figures 5.1 and 5.2 temperature measurements for summer and winter, respectively, and are presented for all twenty four classrooms. Here, the central bar denotes the mean value and the upper and lower bars denote the maximum and minimum values respectively. The dotted box denotes one standard deviation (σ) from the mean value, and the horizontal dotted line denotes relevant criterion. The upper dotted line denotes the limit of 28°C set

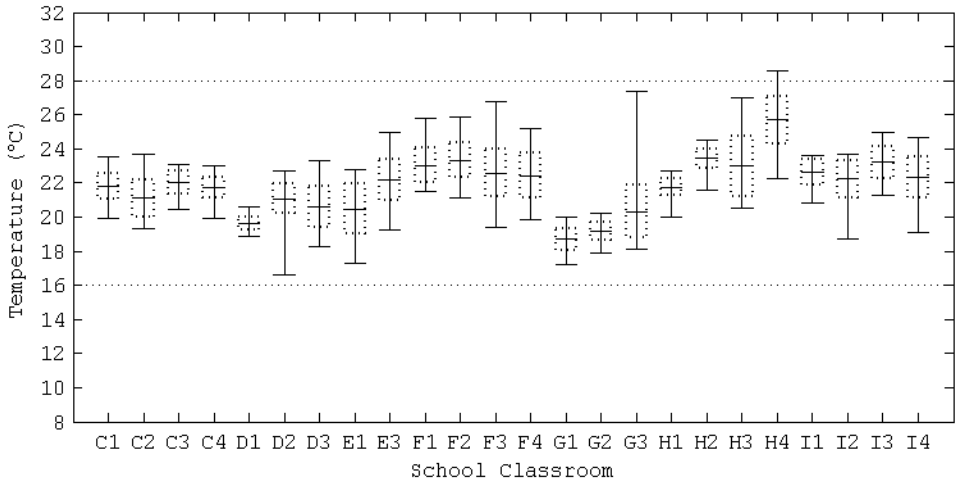

Figure 5.1: Measured air temperature for occupied hours in summer.

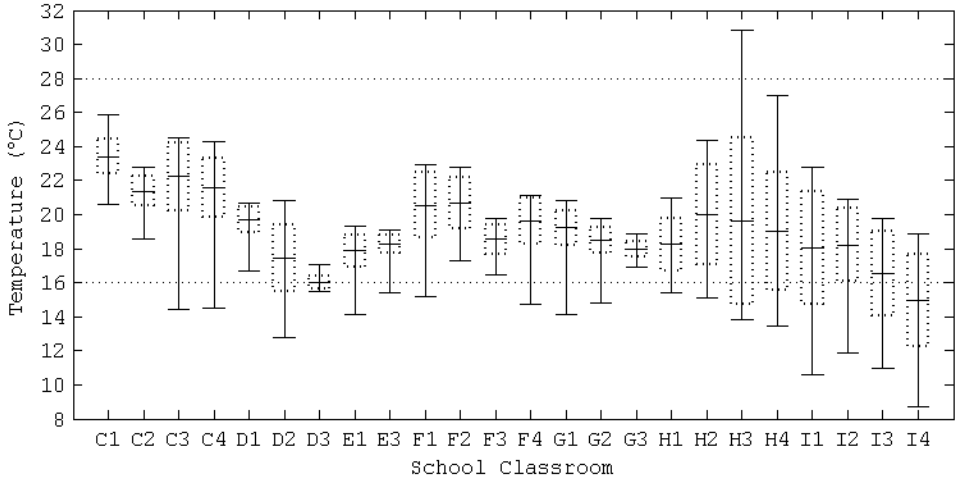

Figure 5.2: Measured air temperature for occupied hours in winter.

by BB101 (DfES, 2006), which must not be exceeded for more than 120 hours between 1st May to 30st September, and the lower indicates the minimum temperature of 16°C is set by the Health and Safety Executive (HSE, 1996) for office type accommodation. In Figure 5.3, the difference between the mean internal (T_I) and external (T_E) temperatures during the summer is presented since $\Delta T \leq 5$°C represents another important BB101 criterion.

The BB101 requirements for temperature only apply to the summer time, and Figure 5.1 shows that all of the classrooms did not exceed the maximum limit of 32°C, and only classroom H4 exceeded 28°C, which indicates that none of the classrooms would exceed 28°C for more than 120 hours during the summer time. However, it should be noted that the monitoring was only conducted over a representative working week and not for the whole summer season and so this remains only an indicator of compliance.

Figure 5.3 shows the difference between the mean internal and external temperatures, ΔT, which to be compliant must be less than 5°C. The classrooms of school F and the 1st floor classrooms of school H do not meet this requirement and this could be attributed to their comparatively large glazing areas and orientations (see Table 4.2 on p. 140 and Figures B.2—B.12 beginning on p. 272). The classrooms on the ground floor of school F are all south–west facing while the glazing on the 1st floor is split between the south–west and the

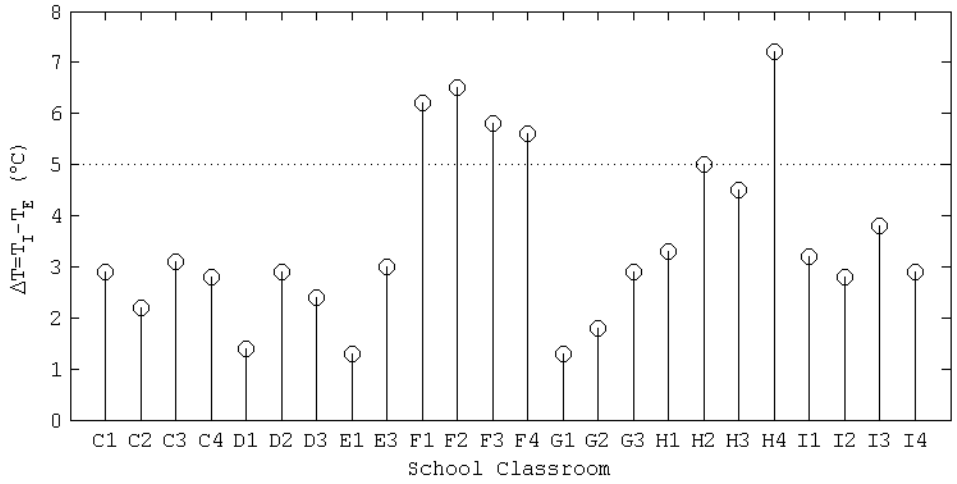

Figure 5.3: Difference between measured mean internal and external temperatures (ΔT) for occupied hours in summer.

north–east. The south facing windows do have solar shields and so the high values of ΔT are most likely to be due to the low mean external temperature for occupied hours of 16.81°C, with σ =3.45°C, see Table C.2. Although the ground floor classrooms in school F have a small number of mechanical items such as lathes and milling tools that together could produce an estimated 1.5 kW of heat energy, these are only sporadically used, and the difference in temperature between the ground and 1st floor classrooms does not reflect excessive heat gains from them. The classrooms of school H have a glazing area of 14.30 m^2 and a glazing ratio 78%, which is the largest of all the classrooms studied here, and although the windows are shielded, they are all south facing. In addition to the heat gains through the windows, Table 4.2 shows that the occupancy density is greatest in the classrooms of school H and so the comparative heat gains per unit of floor area are also likely to be the highest in these rooms. Consequently, Figure 5.3 indicates that classrooms H2 and H4 are likely to overheat in the summer.

The contribution of night cooling to the temperatures presented in Figures 5.1 and 5.1 are discussed in Section 5.4.

The internal temperature in each classroom is now used to estimate the position of the Windcatcher dampers based on an opening set point of 19°C in the winter and 16°C in the summer. Figure 5.4 shows the frequency of the damper angle ratio in all classrooms as a fraction of the total measured time for occupied hours and expressed as a percentage, where

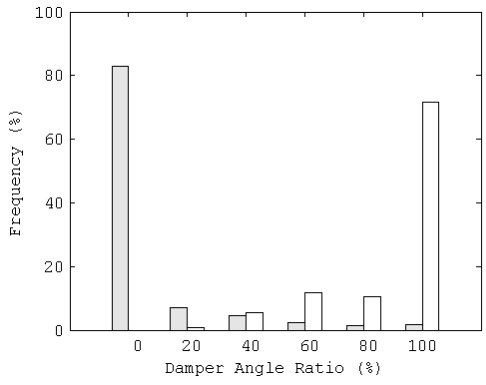

Figure 5.4: Frequency of Windcatcher damper position during occupied hours. Shaded bar, winter; clear bar, summer.

the damper angle ratio is given by $\gamma/90°$ and the dampers are considered to be fully or 100% open when $\gamma = 90°$. Figure 5.4 shows that the dampers are never closed during occupied hours in summer while they are closed for 83% of the time in winter. If all hours of the day are considered (not shown in Figure 5.4), the Windcatcher is found to be closed for less than 1% of the time in summer and 92% of the time in winter. Rijal *et al.* (2007) and Liddament (2001) suggest that the likelyhood of occupants opening windows in the winter is low based on the difference between internal and external temperature (ΔT), and so it is highly likely that the windows in these classrooms were closed through the winter. This could have an associated effect on the provision of ventilation to each classroom because Figure 5.4 suggests that ventilation in winter is controlled by background levels and not by the Windcatcher. Accordingly, internal CO_2 concentrations are expected to be highest in winter and lowest in summer.

In the winter, a statutory minimum temperature of 16°C is set by the Health and Safety Executive (HSE, 1996) for office type accommodation, but none is set by BB101 or Building Regulations, and a recommendation of 18°C is made by BB87. Here, Figure 5.2 shows that minimum temperatures fell below 16°C in eighteen of the classrooms during occupied hours, and classroom I4 has a mean temperature over occupied hours of 14.93°C while D3 and I3 were also particularly cold. However, the control strategy dictates that the dampers are closed when the classroom temperature is below 19°C and so the low temperatures found in these classrooms are unlikely to be related to the Windcatchers, whose dampers should have been closed.

5.1.2 Carbon Dioxide

The majority of building standards use CO_2 as the key indicator of performance, see ASHRAE (2007) for example, or Section 2.1.2 (p. 34) for a more detailed discussion.

In Figures 5.5 and 5.6 (p. 162), the measured data shows that all classrooms lie inside the BB101 maximum of 5000 ppm for summer and winter. In the summer months, all rooms meet BB101's mean limit of 1500 ppm, although only three meet the ASHRAE maximum of 1100 ppm [assuming an external concentration of 400 ppm (BSI, 2004)]. However, ten classrooms do have internal CO_2 concentrations of less than 1100 ppm for approximately 84% of the time in summer. This has been calculated by assuming that $\pm\sigma$ from the mean

includes approximately 68% of the data (see Ross, 2004) and a further 16% of all data also lies below the mean value.

Furthermore, mean CO_2 values also meet the requirements for category I of the European Standards 15251 (BSI, 2007) and 13779 (BSI, 2004) and so may be considered to have high IAQ. The CO_2 concentrations for the summer months also compare favourably with the equivalent data measured by Beisteiner & Coley (2002) who reported maximum and mean

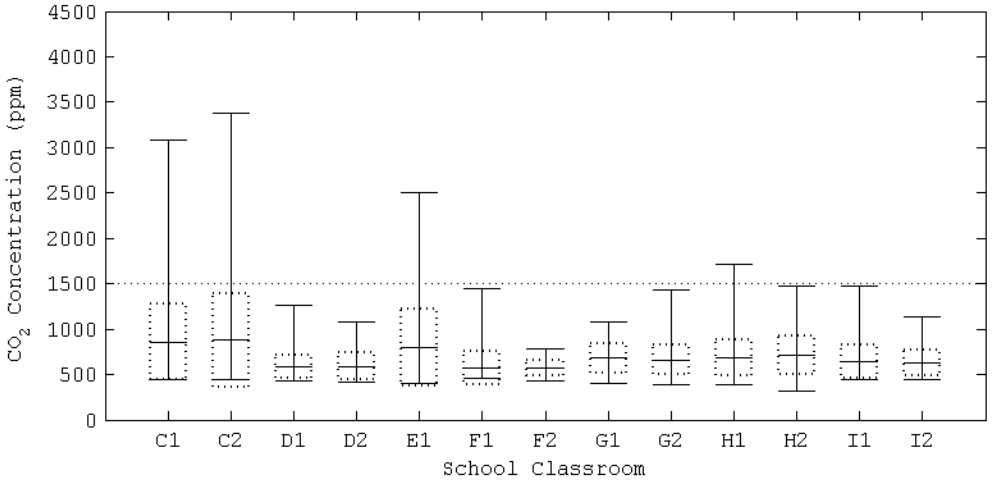

Figure 5.5: Measured CO_2 for occupied hours in summer.

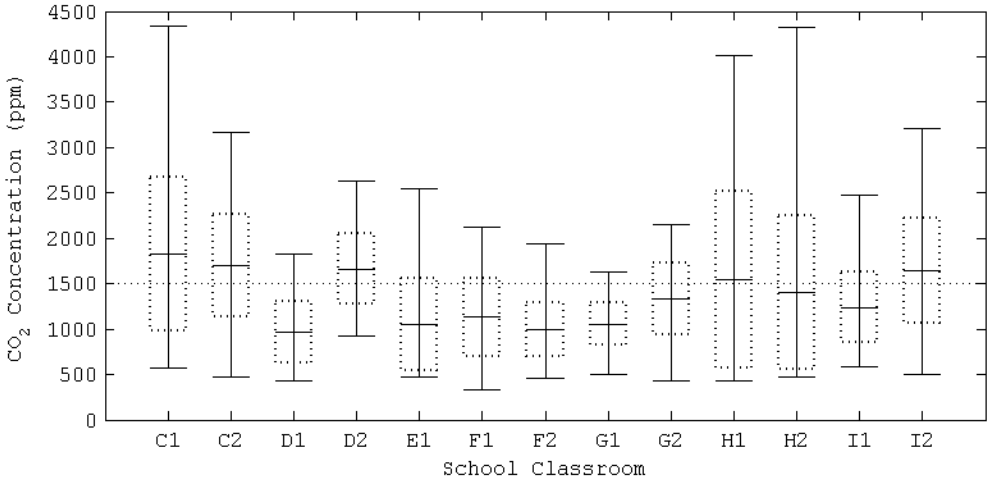

Figure 5.6: Measured CO_2 for occupied hours in winter.

CO_2 levels of 3756 ppm and 1570 ppm, respectively, with a standard deviation of 764 ppm when averaged over all of their measured classrooms. The equivalent values for the current study in the summer are: 3383 ppm, 682 ppm and 227 ppm. Beisteiner and Coley's NV strategy relies on opening windows, either on a single side of the building, or through cross–ventilation between two open sets of windows located on opposite façades. In the current study it is observed that the Windcatcher was, on average, fully open for over 70% (see Figure 5.4) of the time and never fully closed during the summer, and so an improvement in ventilation rates over and above those of Beisteiner and Coley appears possible using either a Windcatcher on its own, or in conjunction with open windows.

Table 4.4 (p. 144) shows that the geometry of the Windcatchers found in schools C—G is square, while those in schools H and I is circular. If CO_2 concentration is used as an indicator of the ventilation rate assuming a similar number of occupants in each classroom, Figure 5.5 indicates that there is no difference between the CO_2 concentrations found in each classrooms and, therefore, no difference in the ventilation rate found in each classroom in summer. However, a square Windcatcher is shown by Elmualim & Awbi (2002a) to outperform one of circular planform, and so it could be that the findings of Elmualim & Awbi (2002a), which were observed under controlled laboratory conditions, do not apply *in–situ*, or that another factor overrides their observations. Here, Rijal *et al.* (2007) and Liddament (2001) show that the use of openable windows is very common in the summer; for example, Liddament shows for a sunny day when the external temperature is $T_E = 20°C$, one may expect to find approximately 45% of all windows to be open. Therefore, it is possible that open windows have affected the overall ventilation rate in each classroom rendering it exclusive of Windcatcher geometry. Consequently, ventilation rates are discussed fully in Section 5.2.

In the winter months, Figure 5.6 shows that eight of the classrooms (62%) meet BB101 requirements wheras none meet the ASHRAE standards. The classrooms are classified as having low IAQ (category 4) when compared against BS EN 13779 (BSI, 2004), and an acceptable/moderate level (category III) when compared against the less stringent BS EN 15251 (BSI, 2007). Clearly, CO_2 levels are seen to rise in all classrooms during the winter when compared to the summer months. An examination of the room temperatures in winter suggests that, on average, the Windcatcher is closed for 83% of the time during occupied hours,

and it is highly likely that the windows remained closed throughout the testing period. Accordingly, in winter the CO_2 levels are largely controlled by background ventilation and this is the likely cause of the rise in CO_2 levels seen in the winter months. In Table 5.1 CO_2 levels for winter are compared with those measured by Mumovic *et al.* (2009) and Coley & Beisteiner (2002), and are shown to be higher than the MV classrooms and generally comparable to the NV classrooms reported by Mumovic *et al.*, but much lower than Coley and Beisteiner. Here, it seems likely that for each study the ventilation rates are dominated by background ventilation during the winter months, and so it is difficult to be certain why improvements have been found in the current study. Differences in ventilation rates may simply be caused by differences in the fabric of each building, although it is noticeable that in the two rooms studied by Mumovic *et al.* (2009) that adopt stack driven ventilation, CO_2 levels are similar to those found in the current study. What is clear, however, is that if one relies simply on opening windows to control CO_2 levels during the winter months then there is a significant risk of failure to meet BB101 requirements, see Coley & Beisteiner (2002). Therefore, a Windcatcher offers an alternative strategy with the potential of lowering CO_2 levels in winter by partially opening the Windcatcher dampers, although it would appear necessary to set the Windcatcher controls to open at a given CO_2 level rather than at a pre–determined temperature, which was the strategy employed by the classrooms measured here.

Santamouris *et al.* (2008) extensively reviewed the literature collating measurements of ventilation rate and internal CO_2 concentration during occupied hours from 1187 classrooms, of which 287 are NV and 900 are MV, to form a database that is presented in Figure 5.7 (p. 165). A comparison with the database of Santamouris *et al.* shows that in winter the mean

Table 5.1: CO_2 concentration in UK school classrooms in winter with ventilation type.

CO_2 (ppm)	Current Study NV	Mumovic *et al.* (2009) NV	Mumovic *et al.* (2009) MV/MM	Coley & Beisteiner (2002) NV
Mean	1350	1459	869	1957
σ	522	560	225	917
Max	4336	2917	1254	4108

NV, Natural ventilation; MV, Mechanical ventilation; MM, Mixed–mode ventilation

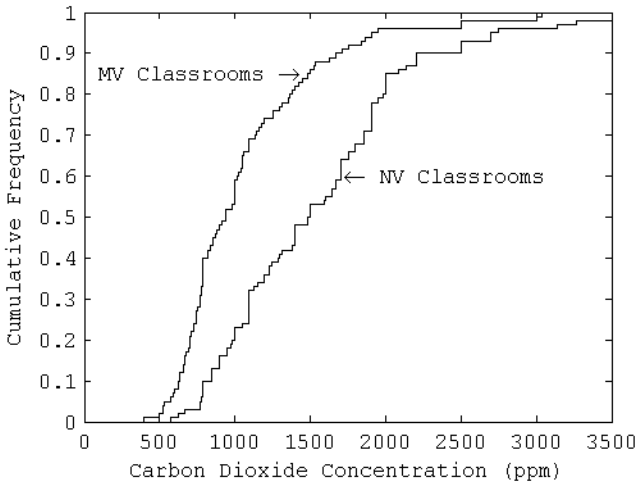

Figure 5.7: Cumulative frequency of mean carbon dioxide levels in mechanically and naturally ventilated school classrooms during occupied hours (Santamouris *et al.*, 2008).

CO_2 concentration of 1350 ppm measured here is lower than 58% of NV and 22% of MV data reported by Santamouris *et al.*; wheras in the summer the measured mean concentration of 682 ppm is lower than 97% of all NV classrooms and 83% of all MV classrooms. This indicates that, when compared against the 1187 classrooms in the database of Santamouris *et al.*, the twenty four classrooms monitored here perform very well.

5.1.3 Relative Humidity

Relative humidity levels in the summer and winter seasons are presented in Figures 5.8 and 5.9, respectively, and show that the mean levels are below 70% for both seasons and so demonstrate compliance with UK building regulations (ODPM, 2006). Here it is noted that the standard deviation box has not been included in Figures 5.9 and 5.8 because $\sigma < 10\%$. However, these limits are comparable to the findings of Mumovic *et al.* (2009) and Kolokotroni *et al.* (2002a), and fall withing the guidelines of 30—70% set by the Commission of the European Communities (CEC, 1992), so RH does not appear to be a significant cause for concern in any of the classrooms and warrants no further discussion.

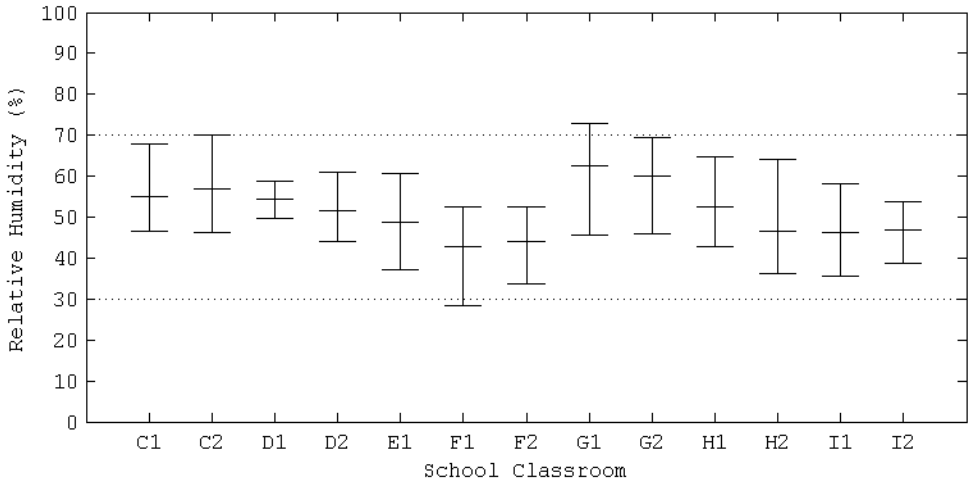

Figure 5.8: Measured relative humidity for occupied hours in summer.

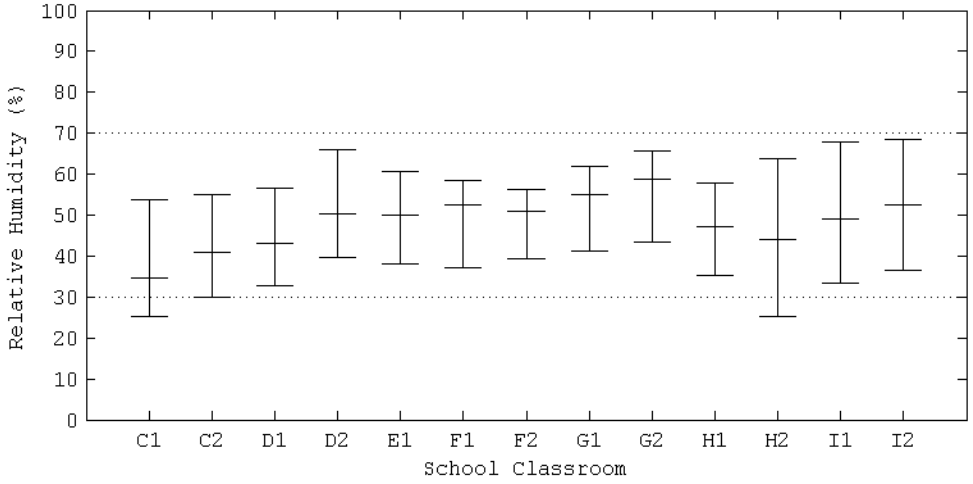

Figure 5.9: Measured relative humidity for occupied hours in winter.

5.2 Ventilation

In order to achieve the temperature, CO_2, and RH targets set by BB101, sufficient ventilation must be provided to each classroom and so measured ventilation rates are presented in Table 5.2 (p. 168) and provide an important indication of the performance of the Windcatcher. Aside from the errors presented in Table 5.2 that are an indication of the confidence in each

estimation based upon the coefficient of determination (R^2). Sherman (1990) suggests that $\pm 10\%$ is a reasonable assumption of overall error while Persily (2006) finds that typical field measurements have uncertainties of at least $\pm 20\%$ of the estimated value. The results of individual estimations of the ventilation rate, wind velocity, and temperature difference can be found in Appendix D. These estimations are only a snap–shot of expected ventilation rates in each classroom for a particular set of ventilation flow paths and are a function of the driving forces experienced at the time each measurement was made, and so these factors should be considered when interpreting the results in Table 5.2.

Background ventilation rates (with Windcatcher and windows closed) are given in Table 5.2 where it is noted that it was not possible to make estimates in classrooms C3, C4, D2, D3, and G2 for reasons discussed in Section 4.4.2. In the other classrooms, the estimations compare to those reported by Mumovic *et al.* (2009) of 12—60 l/s.

In general, Table 5.2 shows that the ventilation rate for a classroom ventilated by a square Windcatcher is increased approximately seven–fold once the Windcatcher is opened, although there are a few notable exceptions, such as in school G, and classroom C1 and C3 where lower values are observed. It is difficult to be certain about the reasons for this, although the classrooms in school G, and also rooms C1, C3, E1, and E3 all have long Windcatcher duct lengths, see Table 4.4 (p. 144). Kolokotroni *et al.* (2002a) noted a similar problem when studying ventilation rates from Windcatchers in a two storey office building, and so it appears that there may be operational problems with long Windcatcher duct lengths, although those long Windcatchers found in school F appear to be functioning satisfactorily. For a classroom ventilated by a circular Windcatcher, an increase in the ventilation rate once a the Windcatcher is opened is less obvious. Here it is noted that is was not possible to make estimations for this configuration in classrooms I1 and I3 (see Section 4.4.2 again), but Table 5.2 shows that in the other classrooms of schools H and I, the ventilation rate is increased by approximately two and a half times the background ventilation rate. This finding supports the difference in performance between Windcatchers of square and circular geometry noted by Elmualim & Awbi (2002a), but also suggests that the similar CO_2 levels for square and circular Windcatcher reported in Figure 5.5 are not the product of a Windcatcher operating autonomously.

Table 5.2: Volume flow rate (litres per second) measured for each classroom.

Windcatcher Dampers				Closed	Open	Open	Closed
Window Position				Closed	Closed	Open	Open
Room	Window Type†	Estimated Openable Window Area (m^2)	Windcatcher Side (mm) and Geometry‡				
C1	TH	0.87	1000 □	4.12 ± 0.19	30.80 ± 1.48	238.70 ± 3.76	
C2	TH	0.87	1000 □	4.12 ± 0.60	168.05 ± 3.10	247.80 ± 2.52	59.63 ± 4.19
C3	TH	0.87	1000 □		32.55 ± 2.62	393.90 ± 4.57	
C4	TH	0.87	1000 □		121.64 ± 2.82	320.31 ± 2.98	
D1	TH	1.53	800 □	25.72 ± 2.44	54.48 ± 45.76	234.55 ± 51.60	225.47 ± 31.57
D2	TH	1.53	800 □		168.72 ± 18.56	133.92 ± 68.30	
D3	TH	1.53	800 □		92.31 ± 38.77	254.22 ± 30.51	
E1	BH	0.49	800 □	1.75 ± 1.34	24.47 ± 2.84	395.37 ± 4.19	95.24 ± 1.89
E3	BH	0.49	800 □	10.05 ± 1.77	19.22 ± 2.06	352.56 ± 12.52	110.97 ± 1.18
F1	None	n/a	1200 □	72.75 ± 8.00	183.69 ± 6.89	n/a	n/a
F2	None	n/a	1000 □	62.48 ± 15.00	109.48 ± 8.12	n/a	n/a
F3	None	n/a	1200 □	73.65 ± 2.95	119.45 ± 7.17	n/a	n/a
F4	None	n/a	1000 □	30.43 ± 1.52	179.82 ± 8.99	n/a	n/a
G1	Sash	1.84	800 □	17.51 ± 7.53	16.38 ± 9.99	1245.60 ± 62.28	1037.15 ± 62.23
G2	Sash	1.84	800 □	Negligible	11.30 ± 3.16	432.92 ± 12.99	

† TH – Top Hung; BH – Bottom Hung; C – Clerestory.

‡ □, square geometry; ◯, circular geometry.

Table 5.2: Volume flow rate (litres per second) measured for each classroom, continued.

Windcatcher Dampers				Closed	Open	Open	Closed
Window Position				Closed	Closed	Open	Open
Room	Window Type†	Estimated Openable Window Area (m^2)	Windcatcher Side and Geometry‡				
G3	Sash	3.88	800 □	14.12 ± 2.40	16.38 ± 11.47	555.86 ± 11.12	
H1	TH	0.46	800 ◯	9.57 ± 0.97	18.71 ± 0.78	335.10 ± 3.69	113.15 ± 5.04
H2	TH	0.46	800 ◯	10.88 ± 0.25	19.15 ± 1.46	306.82 ± 2.49	102.71 ± 1.93
H3	TH	0.46	800 ◯	10.44 ± 1.53	23.07 ± 3.36	331.62 ± 4.87	112.28 ± 3.58
H4	TH	0.46	800 ◯	10.01 ± 0.31	25.24 ± 1.14	150.14 ± 2.40	65.72 ± 2.30
I1	TH	0.77	800 ◯	15.60 ± 2.40			137.59 ± 2.19
I2	TH,THC	1.47	800 ◯	21.24 ± 4.98	85.59 ± 3.18	466.07 ± 5.03	879.66 ± 5.54
I3	TH	0.77	800 ◯	17.02 ± 0.88			146.10 ± 3.40
I4	TH,THC	1.47	800 ◯	43.73 ± 1.22	121.20 ± 2.55	335.50 ± 15.27	604.14 ± 10.03

† TH – Top Hung; BH – Bottom Hung; C – Clerestory.

‡ □, square geometry; ◯, circular geometry.

For building and classroom parameters, see Tables 4.1 and 4.2 on pages 129 and 140, respectively.

For fenestration and Windcatcher parameters, see Tables 4.3 and 4.4 on pages 142 and 144, respectively.

For specific ventilation measurements, see Table D.1 on page 287.

In Table 5.2, is it evident that by opening windows as well as the Windcatcher it is possible to significantly increase the ventilation rate in a classroom, but here it is noted that it is not possible to open the windows in school F. In general, ventilation rates are seen to increase at least two–fold, although some very high multiples also appear possible, see classroom G1 for example. Here, it is interesting to isolate the effect of the Windcatcher by closing the dampers and opening the windows. In order to investigate this, specific tests were conducted in classrooms C1, D1, E1, E3, and G1, as well as all of the classrooms in schools H and I, to estimate the ventilation through the maximum openable window area with the Windcatcher closed. Table 5.2 shows that in classrooms C1, E1, E3, and H1–4, with the windows open and the Windcatcher closed, flow rates were between 64–76% less than the flow rates generated with the windows and the Windcatcher open, whereas in D1 and G1 flow rates were only 4–16% less. The greater openable window area is the likely explanation for the differences between these results and this has been demonstrated theoretically in Figure 3.33, which shows that when the wind speed is constant, the ventilation rate in a room increases with an increase in window area.

Classrooms I2 and I4 contain a Windcatcher and conventional windows that are augmented by clerestory windows located in the opposite façade, see Table 4.3 (p. 142) and Figure 2.4 (p. 49). Table 5.3 (p. 171) presents estimated ventilation rates measured for six different combinations of open or closed Windcatcher, façade windows, and clerestory windows. It shows that the greatest ventilation rate is achieved in these classrooms with the façade and clerestory windows open and the Windcatcher closed. In fact, the estimated ventilation rate with all windows and the Windcatcher open is approximately 50% less than that measured for the façade and clerestory windows open and the Windcatcher closed. This suggests that an open Windcatcher interferes with the air flow between the façade and clerestory windows, although it is unclear why this is so. When the Windcatcher is used in coordination with either the façade or the clerestory windows the estimated ventilation rate is greater than those measured when either the façade or the clerestory windows are used exclusively and the Windcatcher is closed. Table 4.4 (p. 144) shows that the CSA of the circular Windcatchers found in classrooms I2 and I4 is $0.5\,\mathrm{m}^2$, whereas Table 4.3 (p. 142) shows that the façade and clerestory windows have estimated opening areas of $9.98\,\mathrm{m}^2$ and $3.43\,\mathrm{m}^2$, respectively. The combined opening area of both window types far exceeds the opening area provided by a

Table 5.3: Volume flow rates (l/s) measured for various window configurations found in 1st floor classrooms of school I.

Room	Windcatcher Damper Position	Façade Window Position	Clerestory Window Position	Ventilation Rate $\dot{Q}$ (l/s)
I2	Open	Open	Closed	424.84 ± 6.92
I2	Open	Closed	Open	342.37 ± 2.12
I2	Open	Open	Open	466.07 ± 5.03
I2	Closed	Open	Closed	143.07 ± 3.92
I2	Closed	Closed	Open	154.32 ± 2.28
I2	Closed	Open	Open	879.66 ± 5.54
I4	Open	Open	Closed	504.18 ± 7.61
I4	Open	Closed	Open	248.03 ± 6.82
I4	Open	Open	Open	335.50 ± 15.27
I4	Closed	Open	Closed	264.90 ± 1.99
I4	Closed	Closed	Open	109.33 ± 1.90
I4	Closed	Open	Open	604.14 ± 10.03

Windcatcher in coordination with a single window type and so explains why this combination provides greater ventilation rates.

The Windcatchers in classrooms I2 and I4 may be superfluous; for example, Table 5.2 shows that the ventilation provided by an autonomous Windcatcher is less than those provided by just the façade windows, and Table 5.3 shows that the façade and clerestory windows are together capable of providing 8 l/s – person (assuming 30 occupants) to both classrooms, while the clerestory windows in I2 and the façade windows in I4 are capable of providing 5 l/s – person. However, such a strategy relies on the façade or clerestory windows being opened by the occupants because both types are manually operated. Here, it is noted that the clerestory windows can only opened by using a hook fixed at the end of a long pole, thus posing a real challenge to young school children. A significant advantage of the Windcatcher is its automation, whereby its dampers will open if the room air temperature is above an initial set point (see Table 4.5, p. 147) and so ensures that some rate of ventilation will take place. Therefore, if only daytime ventilation is required, the automatic control of the clerestory windows is likely to be the best solution in classrooms I2 and I4.

The results in Table 5.2 generally indicate that a Windcatcher operating in coordination with open windows located in a single façade will increase the ventilation rate over and above those provided by a Windcatcher or windows on their own, and so together provide a viable method for meeting BB101 ventilation requirements. These findings tally with the findings of Kirk & Kolokotroni (2004b) who measured flow rates in an office ventilated by several Windcatchers and found that ventilation rates increase when a Windcatcher operates in combination with open windows, and that ventilation through windows alone can be greater than those achieved through an autonomous Windcatcher. However, in this situation, the use of windows was disliked by the occupants because they caused uncomfortable draughts, although no such observations were found during the current study.

In order to compare the estimated ventilation rates presented in Table 5.2 against the requirements of BB101 it is necessary to assume the number of occupants in each classroom. Here, the design occupancy for each classroom given in Table 4.2 (p. 140) are assumed and so provide a worst case scenario. Accordingly, the estimated ventilation rates presented in Figures 5.10—5.12 may under–estimate the actual ventilation rate per person if class sizes are smaller, which is possible in Secondary schools. Figure 5.10 suggests that the minimum ventilation rate of 3 l/s – person cannot be met by background ventilation (through infiltration) alone, except in classrooms F1 and F3 that have a lower occupancy level. When using a Windcatcher on its own, Figure 5.11 shows that the minimum ventilation rate of 3 l/s – person is met in ten classrooms, and the required mean flow rate of 5 l/s – person is surpassed in five classrooms. When a Windcatcher is combined with fully open windows, then Figure 5.12 shows that 5 l/s – person is met in all classrooms except in D2 which is very close to the required value. It is also evident that the required purge ventilation rate of 8 ± 0.2 l/s – person is achieved in all rooms except D2 and I4. Here, there is no clear explanation for the lower ventilation rates found in these rooms, as the driving forces when the measurements were made do not differ greatly from those for other rooms, see Table D.1 in Appendix D.

In two similar studies, Mumovic *et al.* (2009) and Griffiths & Eftekhari (2008) found that the window area in naturally ventilated schools is insufficient for providing 8 l/s – person, and Figure 5.13 shows that the ventilation rates provided by single sided ventilation through open windows also cannot meet this standard. Consequently, Figures 5.10—5.12 (p. 173 and

p. 174) show that to consistently achieve the required mean and purge ventilation rates of 5 l/s – person and 8 l/s – person, respectively, it is necessary to use open windows in coordination with a Windcatcher, although the exact openable area required in a façade to meet the guidelines cannot be ascertained from the data. However, these results indicate that for the CO_2 results reported in Figure 5.5, windows were most probably open for a significant proportion of the occupied hours.

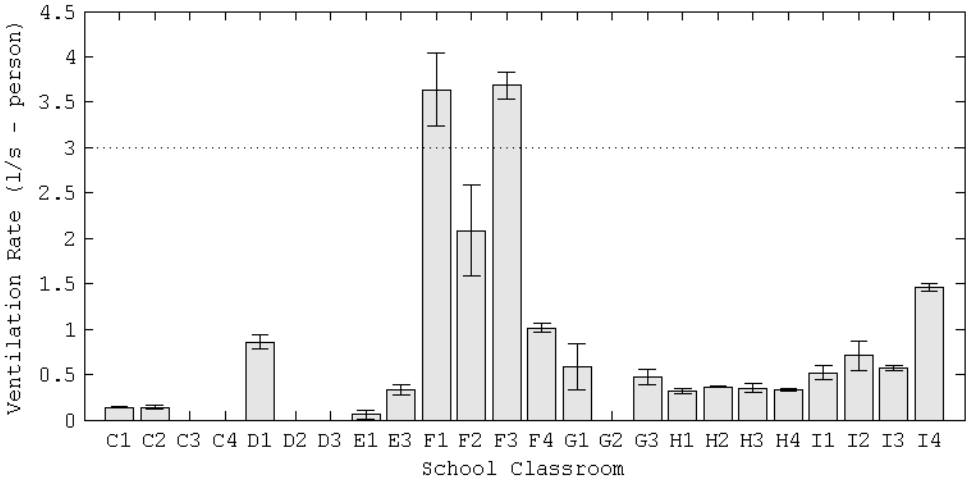

Figure 5.10: Estimated ventilation rate per person: Windcatcher closed and windows closed.

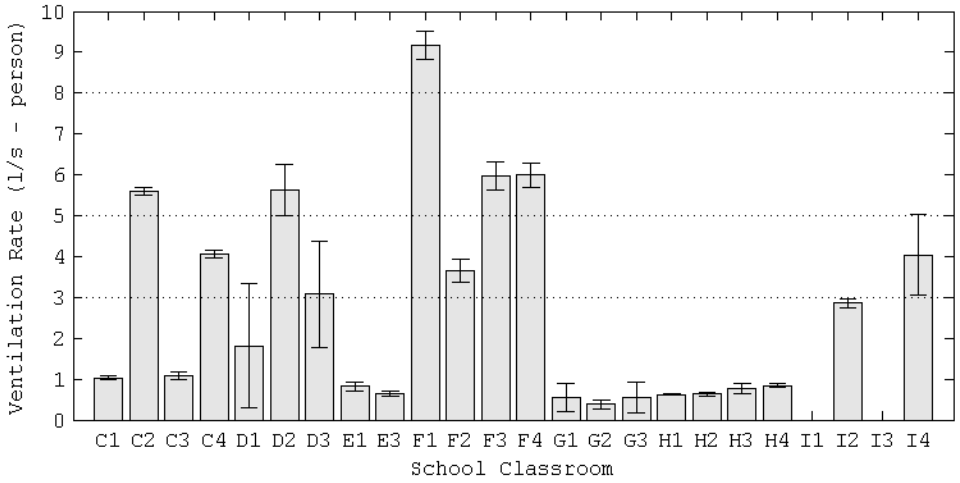

Figure 5.11: Estimated ventilation rate per person: Windcatcher open and windows closed.

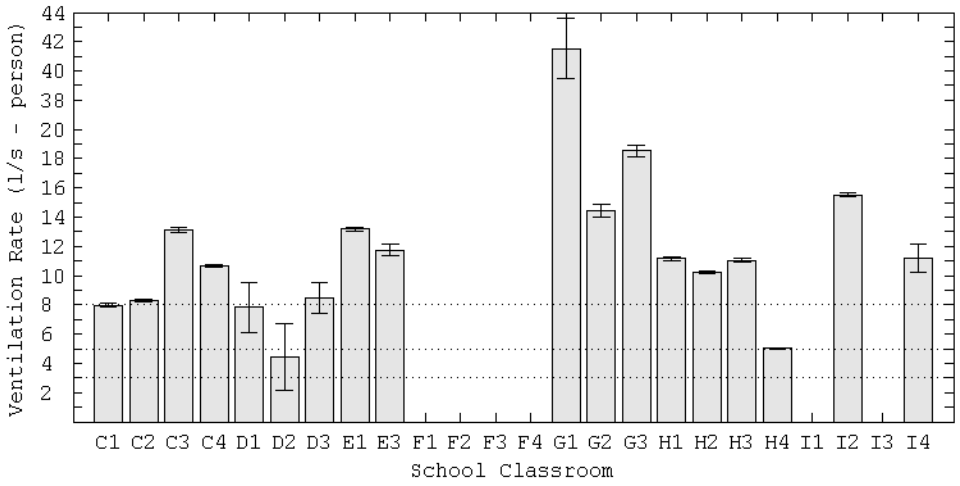

Figure 5.12: Estimated ventilation rate per person: Windcatcher open and windows open.

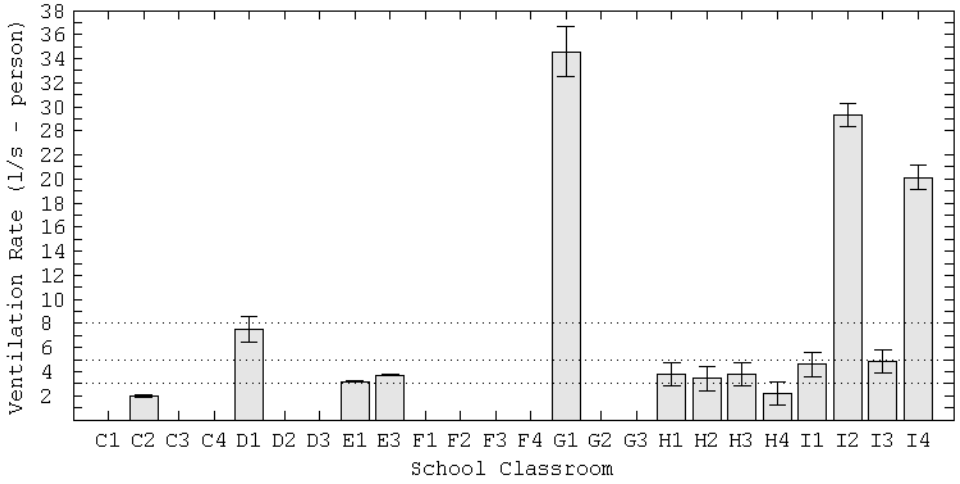

Figure 5.13: Estimated ventilation rate per person: Windcatcher closed and windows open.

The per capita ventilation rates reported in Figures 5.10—5.12 are now compared with the data of Santamouris *et al.* (2008) presented in Figure 5.14 (p. 175) using a mean ventilation rate for each figure. With a square Windcatcher operating autonomously, the mean ventilation rate is 3.1 l/s – person, which is greater than approximately 52% of NV and 28% of MV classrooms reported by Santamouris *et al.* For a circular Windcatcher operating autonomously, the mean ventilation rate is 1.6 l/s – person, which is greater than approxi-

mately 30% of NV and 13% of MV classrooms. With the windows open the geometry of the Windcatcher has not been shown to be a factor in the increase of overall ventilation rates, and so a combined mean ventilation rate of 12.5 l/s – person is found, which is greater than 94% of NV and 70% of MV classrooms. Accordingly, the Windcatcher is seen to perform well reative to the extensive database of Santamouris *et al.*, especially when the windows are opened. Therefore, these results demonstrate that combining a Windcatcher with open windows has the potential to provide relatively high per capita ventilation rates to school classrooms, which are greater than those specified by BB101 and ASHRAE Standard 62.1.

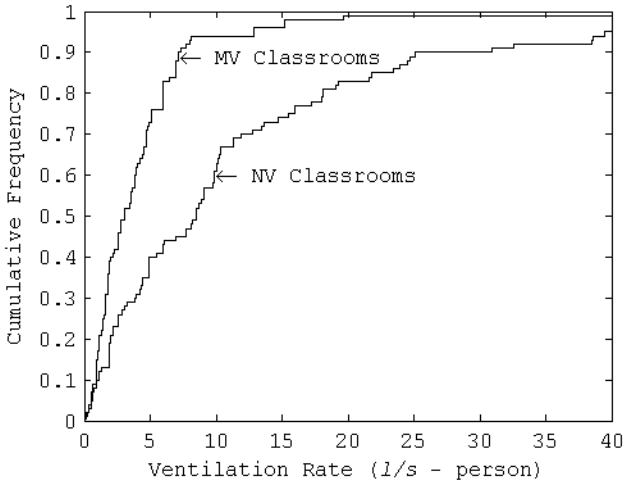

Figure 5.14: Cumulative frequency of mean flow rates in school classrooms during occupied hours (Santamouris *et al.*, 2008).

5.3 Ambient Noise

Ventilation systems such as a Windcatcher often generate noise or allow noise ingress, and so the contribution of the Windcatcher to the background noise level in each classroom is evaluated here. External ambient noise levels for each school are shown in Table 5.4 and the measured sound pressure level in each classroom with the Windcatcher dampers open and closed are given in Figure 5.15 as an average uninterrupted measurement of A weighted sound pressure level, L_{Aeq}, over 30 minutes. A full table of measurements is presented in Appendix E.

Table 5.4: Measured external sound pressure level $L_{Aeq,30m}$ (dBA).

School	$L_{Aeq,30m}$
C	57.5
D	44.4
E	38.4
F	42.9
G	50.9
H	53.5
I	66.6

In Table 5.4, the external sound pressure levels are shown to vary between 38.4—66.6 dB $L_{Aeq,30min}$, with a mean value across all of the schools of 50.6 dB $L_{Aeq,30min}$. Shield & Dockrell (2004) found a mean external sound pressure level of 57 dB $L_{Aeq,5min}$ outside 142 inner city schools and in this study the sound pressure level found outside schools C, H, and I are comparable, possibly because they located near to busy roads or motorways, while the remaining schools are much quieter. Figure 5.15 shows that for closed and open Windcatchers the internal ambient noise levels are below those required by BB93 (DfES, 2003)

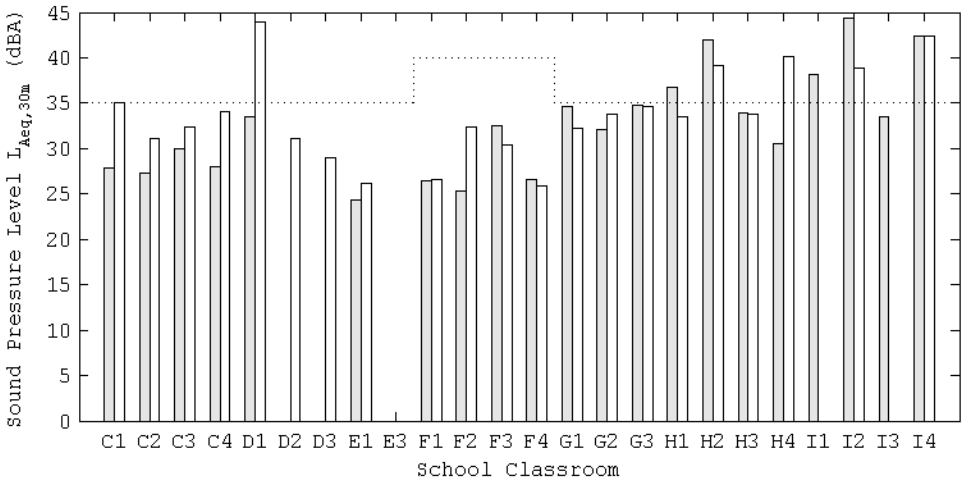

Figure 5.15: Measured internal sound pressure level $L_{Aeq,30m}$ (dBA). Filled, Windcatcher closed; clear, Windcatcher open; ·····, specified upper limit.

in sixteen classrooms, and exceeded in seven classrooms. The sound pressure levels range from 24.3 dB $L_{Aeq,30min}$ to 44.3 dB $L_{Aeq,30min}$, and the mean average for classrooms with an open or closed Windcatcher is 33.1 dB $L_{Aeq,30min}$. Here it is noted that it was not possible to take measurements in classrooms D2 and D3 with the Windcatcher dampers closed and the measurements made in classroom E3 have not been included because they were disturbed during the measurement. These values compare favourably to those of Mumovic *et al.* (2009) who measured sound pressure levels in twelve NV and MV classrooms that ranged from 24—71 dB $L_{Aeq,30min}$ and have a mean average of 43 dB $L_{Aeq,30min}$, and Shield & Dockrell (2004) who measured background sound pressure levels in 30 unoccupied classrooms reporting a mean level of 47 dB $L_{Aeq,5min}$.

By opening the Windcatcher dampers it is perhaps expected that the ambient sound pressure level measured in each classroom will increase because this exposes the large duct area that spans from the classroom to its surroundings. However, of the nineteen pairs of measurements made with the Windcatcher dampers open and closed, ten are highest with the Windcatcher dampers open, eight are highest with the Windcatcher dampers closed, and one pair is identical. Overall, the mean difference between the dampers being open and closed is +1.8 dB L_{Aeq} and so the difference between the sound pressure levels experienced in these classrooms with the Windcatchers open or closed can be considered to be negligible.

A number of the classrooms measured here are ventilated by a Windcatcher whose ducts contain an acoustic lining and so we cannot be certain of the noise transmitted by a Windcatcher on its own. Here, the Windcatcher ducts in schools C, E, and F all contained an acoustic attenuating duct lining, and Figure 5.15 shows that the sound pressure levels in these classrooms are all below those required by BB93, and so suggest that the duct lining may help meet requirements in these cases.

These results suggest that the classrooms generally conform to BB93, although the sample size is relatively small and so there is probably insufficient data to conclude that Windcatchers do not represent a problem when meeting noise targets in schools. Here, further testing that includes a detailed acoustic analysis of the Windcatcher using the frequency domain is probably necessary in order to draw more definitive conclusions.

5.4 Night Cooling

During the summer, the greatest difference between the internal and external air temperature occurs during the night and so this offers the opportunity to bring cold and fresh air into a room to cool any exposed thermal mass, and to lower the initial and peak internal air temperature during the following day. Consequently, the Windcatcher dampers are programmed to open fully from midnight until 6 a.m. to provide night cooling. This is important because night cooling via a Windcatcher may have influenced the summer temperature data presented in Section 5.1.1 and so this Section attempts to determine the extent of its contribution.

The ability of a Windcatcher to provide effective night cooling to a school classroom is a function of the background ventilation, the insulating capacity of the construction materials, the ability of the Windcatcher system to function autonomously, and the efficient mixing of incoming air within the classroom before it is extracted. Here, the ability of each Windcatcher system to function autonomously is shown by Figure 5.11 (p. 173) and it is expected that classrooms C2, D2, F1, F3, and F4 are the most effectively cooled at night. Specific evidence of night cooling comes from an identifiable change to the rate of cooling in a classroom after midnight. However, the measurements of internal temperature in each classroom tell us that, on average, the dampers were fully open for 73% of the time and never fully closed during occupied and unoccupied hours. Therefore, the Windcatcher dampers are likely have been fully open before midnight in most cases so that there is no observable difference to the rate of cooling that can be attributed solely to a Windcatcher. There are, however, two exceptions and the internal air temperatures measured in classrooms E3 and F1 are presented in Figures 5.16 and 5.17 (p. 179), respectively, where the vertical dotted lines indicate the midnight set point, and each example of night cooling is given by a bracketed number. Figures 5.16 and 5.17 show several clear incidences of an increase to the rate of cooling after midnight that may be attributed to the the automatic opening of the Windcatcher dampers. Now, using Figures 5.16 and 5.17 it is possible to calculate the rate of cooling (°C/hour) before and after midnight using linear data regression, and these values are given in Tables 5.5 and 5.6 where confidence in them is indicated by mean R^2 values of 94% for classroom E3 and 96% for classroom F1. Tables 5.5 and 5.6 (p. 180) show that the mean change to the cooling rate is 1.07 °C/hour in school E and 0.43 °C/hour in school F, or an approximate 7–fold and

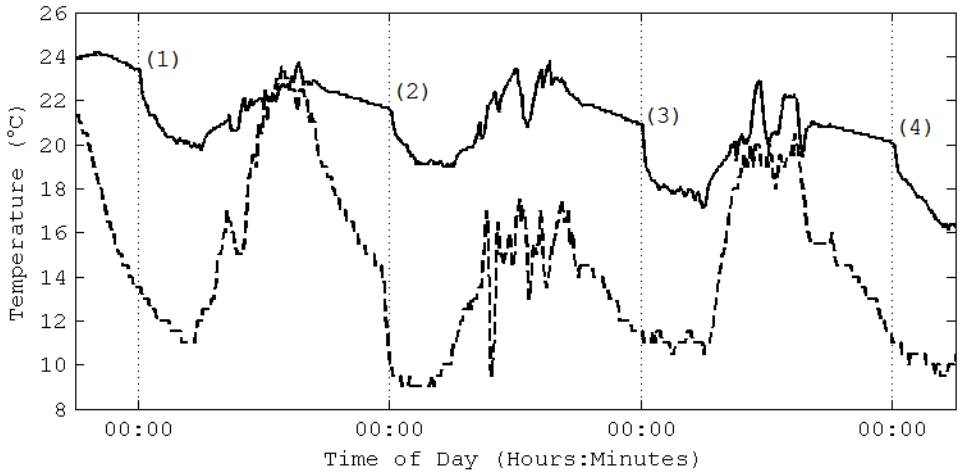

Figure 5.16: Identification of night cooling in classroom E3. ——, internal air temperature; – – –, external air temperature.

4–fold increase in cooling rates, respectively. Here, it is noted that the mean cooling rate is artificially high in school E because of the high value for night (3) and so a median value of 0.64 °C/hour is a more appropriate indication of the actual cooling rate in this classroom.

While it is expected that the Windcatcher system in classroom F1 is capable of provid-

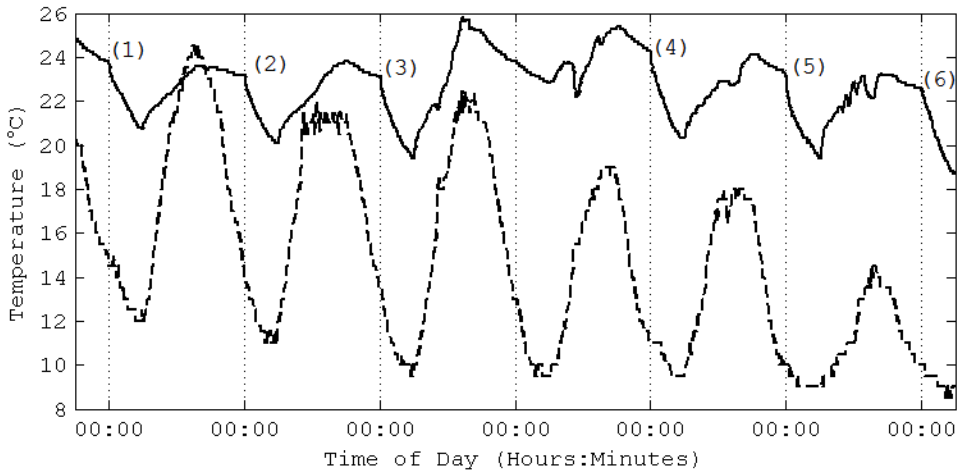

Figure 5.17: Identification of night cooling in classroom F1. ——, internal air temperature; – – –, external air temperature.

Table 5.5: Estimated cooling rate in classroom E3.

	Cooling rate (°C/hour)		
	Pre–midnight	Post–midnight	Difference
1	0.23	0.85	0.61
2	0.14	0.81	0.67
3	0.19	2.67	2.48
4	0.13	0.66	0.53
Mean	0.17	1.25	1.07
Median	0.17	0.83	0.64

Table 5.6: Estimated cooling rate in classroom F1.

	Cooling rate (°C/hour)		
	Pre–midnight	Post–midnight	Difference
1	0.18	0.49	0.30
2	0.06	0.50	0.44
3	0.13	0.59	0.46
4	0.21	0.64	0.43
5	0.16	0.51	0.35
6	0.12	0.68	0.57
Mean	0.14	0.57	0.43
Median	0.14	0.55	0.43

ing night cooling by virtue of its ability to provide an estimated 183.69l/s when operating autonomously (see Table 5.2, p. 168), it is perhaps surprising that the Windcatcher in classroom E3 is even more effective. Here, Table 5.2 suggests that its Windcatcher system is only capable of providing an estimated ventilation rate of 19.22l/s when operating autonomously and so an explanation of its ability to provide night cooling is necessary. Further examination of Table 5.2 shows that an 18–fold increase to the ventilation rate in classroom E3 may be delivered when the Windcatcher and windows are used in coordination, but the windows were almost certainly shut at night for security reasons. Therefore, the only plausible explanation is an additional untested ventilation flow path that initiated cross–ventilation. Accordingly, it is suggested that the classroom door was left propped open during the evenings and cross–ventilation was initiated via the corridor located behind the classroom, see Figure B.5 (p. 275). There is no specific evidence for this explanation although during visits to the school cleaners were observed propping doors open. A comparison between the temperature in classrooms E3 and E1, which are adjacent to each other, is given in Figure 5.18 (p. 181). Here, it shows that the rate of cooling in both classrooms is similar before midnight and so suggests similar ventilation rates in both rooms, but after midnight the rate of cooling in classroom E1 shows no change and therefore it likely that its did not have the same ventilation flow paths as classroom E3.

Further examination of Figures 5.16 and 5.17 shows that the temperature at midnight in

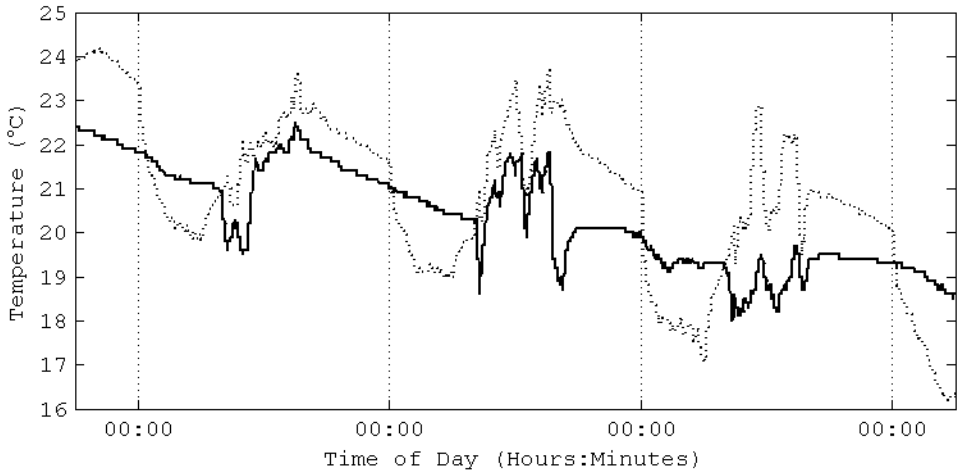

Figure 5.18: Air temperature in classrooms E1 and E3. ——, E1; · · · · · · , E3.

classrooms E3 and F1 is greater than 21 °C and so the Windcatcher dampers should already be fully open, which highlights a disagreement between the sensors used to measure the temperature and the thermostats present in the classrooms. The error for each calibrated sensor is described in Section 4.4.1 (p. 147) and is shown to be small, whereas the thermostats used in each classroom are more primitive and are, therefore, less accurate. Furthermore, the sensors were specifically placed in locations that were away from direct heat sources such as radiators, electronic equipment, or direct exposure to the sun. Consequently, trust is placed in the measurements made by the QTrak and Hobo sensors and concern is raised over the accuracy of the thermostats used in these two classrooms. Because there are no solar heat gains at night and a visual inspection showed no obvious local heat sources such as electronic equipment, the cause of their miss–measurement is likely to be a loss of calibration.

Finally, the data given in Tables 5.5 and 5.6 suggests that over a typical six hour cooling period from midnight until 6 am (see Section 4.3, p. 143) one may expect a reduction in air temperature of between 2.6°C and 3.8°C. Webb & White (1998) measured a drop in air temperature of approximately 1.5–2°C in a room ventilated by a single Windcatcher over the same period of time and on two consecutive nights. Similarly, Kolokotroni & Aronis (1999, Figure 1) show a 1–2°C reduction in air temperature in an open plan office that is directly attributed to night cooling ventilation over the same time period. The values

given here for the rate of cooling using a Windcatcher are quite high when compared against those in the literature and suggests that these Windcatchers perform comparatively well. However, the number of samples is limited and although Figures 5.16 and 5.17 show night cooling in classrooms E3 and F1, respectively, the true extent of the cooling provided by a Windcatcher can only be determined by intervention testing that isolates its contribution. Nevertheless, the evidence of Windcatcher performance presented in this chapter suggests that it is reasonable to expect Windcatcher systems to deliver ventilation at night if they are also capable of functioning autonomously. The internal air temperature is lowered if the external air temperature is lower than the internal temperature and the air mixes well inside the room. It is then possible to increase cooling rates over and above those delivered by an autonomous Windcatcher if cross–ventilation can be initiated at night. To improve energy savings from night ventilation Kolokotroni & Aronis (1999) suggest that a building should be western facing, the glazing ratio and internal heat gains should be reduced, and air tightness should be increased.

5.5 Summary

This chapter has reviewed the measurements of IAQ, ventilation, and noise made in twenty four classrooms of seven UK schools. Results demonstrate that a Windcatcher in coordination with windows is generally capable of meeting the UK BB101 standard for IAQ and a Windcatcher can meet the UK BB93 standard for noise.

For the summer months all classrooms were able to meet the CO_2 requirements indicating sufficient per capita ventilation. Measurements of the ventilation rate in each classroom with a Windcatcher operating autonomously show that 40% of measured classrooms meet the minimum 3 l/s – person requirement and 23% meet the 5 l/s – person requirement. If the Windcatcher is used in coordination with open windows, then all classrooms meet the 3 l/s – person requirement, 94% meet 5 l/s – person, and 77% meet 8 l/s – person under this arrangement. Furthermore, for the classrooms studied here, it is evident that a Windcatcher can aid in the delivery of ventilation rates that meet the UK standards during the summer time and this also extends to meeting European and US standards.

However, the analysis of actual Windcatcher performance shows that it is rarely open

during the winter months and although the maximum CO_2 limit of 5000 ppm is never reached, only 62% of classrooms meet the required mean CO_2 level of 1500 ppm and so the control strategy requires careful revision and is discussed in Chapter 7.

An increase in the rate of cooling at night that can be attributed to a Windcatcher is shown in two classrooms where the median cooling rate was found to be 0.64°C/hour and 0.43°C/hour. It is reasonable to expect other Windcatcher systems to deliver night cooling if they are also capable of functioning autonomously, the incoming air mixes well, and the external air temperature is less than the room air temperature. However, intervention testing is required to determine the exact contribution of a Windcatcher to a night ventilation strategy.

Measurements of ambient noise in twenty three classrooms with the Windcatcher dampers open suggest that the classrooms generally conform to BB93, although the sample size is relatively small and so there is probably insufficient data to conclude that Windcatchers do not represent a problem when meeting noise targets in schools. Further work using the frequency domain is necessary to draw more definitive conclusions and this is described in Chapter 9.

Finally, a Windcatcher is shown to offer the potential to significantly improve natural ventilation rates in school classrooms and to help comply with IAQ standards for schools.

Chapter 6

Results: A Comparison Between Predicted and Measured Ventilation Rates

In this chapter, the predictions of the semi–empirical model are compared against experimental measurements for a Windcatcher operating *in–situ* to determine its suitability for use in the design of a natural ventilation strategy that incorporates a Windcatcher. Two cases are considered: the first is for a Windcatcher functioning autonomously, and the second is for a Windcatcher in coordination with a single façade opening.

The semi–empirical model uses data measured in the laboratory for the coefficient of pressure on each face of a 500 mm square Windcatcher, and values for the losses in each Windcatcher quadrant derived from further laboratory measurements of ventilation rates through a 500 mm square Windcatcher. Therefore, its predictions can only be compared against those measurements made for a Windcatcher of similar geometry. Consequently, the predictions are compared against relevant measurements given in the literature, and because Section 2.3.2 (p. 63) shows that very little data currently appears in the literature for a Windcatcher, measurements made in four schools and twelve classrooms have also been selected from the case studies described in Chapter 4 to investigate further its performance. Here, all of the Windcatchers have a square cross–section and a comparable cross sectional area. All of the Windcatchers considered in this Chapter operate *in–situ* and so the total losses through

a Windcatcher identified in Table 3.5 (p. 111) are applied in each case. The relevant parameters for the classrooms and Windcatchers are given in Table 6.1, and additional information for the schools, classrooms, fenestration, and Windcatchers can be found in Tables 4.1, 4.2, 4.3, and 4.4 respectively (from p. 129). In Table 6.1, the cross sectional area (CSA) of each Windcatcher takes into account the presence of an acoustic lining, which covers the duct walls and diagonal partitions (see Figure 3.1, p. 73). Furthermore, the openable window area given in column 6 is the maximum area used when measuring the ventilation rate through a Windcatcher in coordination with windows located in a single façade and is not necessarily the maximum area available in the classroom, see classroom G3 for example. This is because the model makes predictions for open windows in a single façade and so those made with open windows in two façades have been excluded. It is noted that it would be relatively straight forward to add another façade opening to the model, although the mathematic solutions would be more complicated. At school F all of the windows are sealed, but at the other

Table 6.1: Classroom parameters.

School	Room	Windcatcher Side, $d_{1,2}$ (mm)	Actual Quadrant CSA, A_{1-4} (m^2)	Duct Length, L (m)	Openable Window Area, A_5 (m^2)
C	1	1000	0.193	4.8	0.9
	2	1000	0.193	1.0	0.9
	3	1000	0.193	4.8	0.9
	4	1000	0.193	1.0	0.9
D	1	800	0.160	1.0	1.5
	2	800	0.160	1.0	1.5
	3	800	0.160	1.0	1.5
F	2	1000	0.145	1.0	n/a
	4	1000	0.145	1.0	n/a
G	1	800	0.160	5.5	1.8
	2	800	0.160	5.8	1.8
	3	800	0.160	5.5	1.8

schools some or all of the available windows may be opened manually and the maximum openable area (A_5) is calculated using Equation (4.1) given on page 141.

A total of 56 measurements were made with the Windcatcher open and windows closed, and 21 measurements were made with the Windcatcher and windows open. These measurements were undertaken at times throughout the year (see Table 4.6, p. 148) in order to test a range of environmental and meteorological conditions. All measurements were made using the standard single–zone tracer gas decay method and weather data acquired from a local weather station in accordance with the procedures outlined in Section 4.4.2 (p. 152). Following the arguments made in Sections 3.2.6 (p. 118) and 4.4.2 (p. 152), terrain coefficients are assumed to be $k = 0.35\,\mathrm{m}^{-a}$ and $a = 0.25$, and limiting values of C_{p5} are chosen as $C_{p5} = -0.38$ and $C_{p5} = 0.06$. In addition, a duct length of $L = 1\,\mathrm{m}$ and the median classroom height of $z_I = 3.30\,\mathrm{m}$ are assumed, and the open windows are located at the midpoint of the façade where $z_O = 1.65\,\mathrm{m}$. Accordingly, limiting values of $\tilde{C}_{p5}$ become $\tilde{C}_{p5} = -0.24$ and $\tilde{C}_{p5} = 0.04$ using Equation (3.19) given on page 78. The relative merits of these assumptions are discussed in due course.

6.1 Autonomous Windcatcher

In Section 2.3 (p. 60), the review of literature shows that there is very little data that quantifies the performance of a Windcatcher operating *in–situ*, especially in schools. However, Kirk & Kolokotroni (2004b) have published data for Windcatchers similar to those investigated here, ventilating an open plan office. Kirk and Kolokotroni measured ventilation rates using the tracer gas decay method and measured the wind velocity at roof level using a portable weather station, or when this was not possible, similar data was obtained from the UK Meteorological Office for a local weather station. The office building studied by Kirk and Kolokotroni contained four square Windcatchers, and data is published for the first floor which contained two square Windcatcher elements with sides of $d_{1,2} = 1200\,\mathrm{mm}$ and two further two square Windcatchers with sides of $d_{1,2} = 600\,\mathrm{mm}$. Half of each Windcatcher serves the first floor while the other half serves the ground floor; Kirk and Kolokotroni propose that this arrangement of four Windcatchers effectively behaves as one 1200 mm and one 600 mm square Windcatcher to each floor. However, it was noted in Section 2.3.3 (p. 69) that

the accuracy of this assumption is debatable, but it does allow their data to be compared against the predictions of the semi–empirical model in conditions that are far removed from the idealised conditions of the laboratory, as well as using the losses derived for a 500 mm Windcatcher. The predictions in Figure 6.1 are the sum of the volume flow rates through a 1200 mm and a 600 mm square Windcatcher (calculated separately) in an unsealed room. The unsealed scenario, discussed in Section 3.1.2 (p. 84), is used because Kirk & Kolokotroni (2004b) show that the building is not perfectly sealed by measuring the background ventilation with the Windcatcher and windows closed and so Equations (3.41)—(3.44) are used for $\theta = 0°$, and Equations (3.50)—(3.52) are used for $\theta = 45°$. Here, it is noted that in Chapter 3 the findings of Figures 3.29, 3.31, and 3.32 (found on p. 114 and 114, respectively) suggest that the effects of buoyancy may be ignored if the wind velocity u_w, is greater than 2 m/s and because over 70% of Kirk and Kolokotroni's data has $u_w > 2$m/s, the effects of buoyancy are ignored here. Consequently, the two extremes of performance predicted by the semi–empirical model form two straight lines that are expected to encapsulate the measured data.

From Figure 6.1, it is evident that the predictions compare very well with the experimental

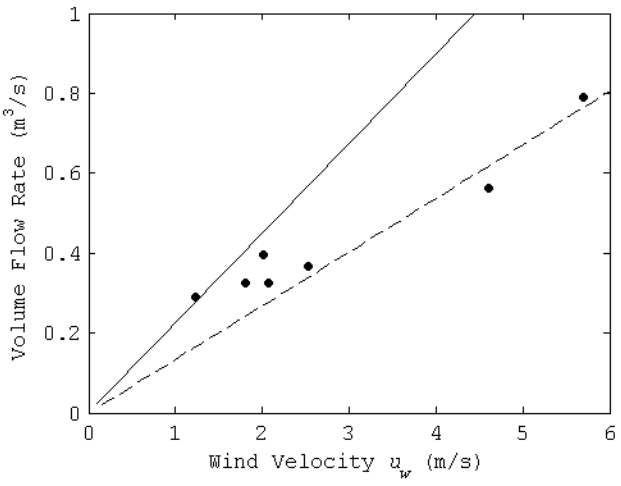

Figure 6.1: Comparison between semi–empirical predictions and the experimental measurements of Kirk & Kolokotroni (2004b) for ventilation rates from an unsealed room, with dampers and grill. ——, prediction $\theta = 0°$; – – –, prediction $\theta = 45°$; •, experiment.

measurements, particularly for lower wind velocities ($u_w < 3$m/s), although one may argue that this level of agreement is fortuitous. The wind direction is assumed to have varied during the measurements and so cannot be said to be at $\theta = 0°$ or $\theta = 45°$, although the measurements agree better with the predictions when $\theta = 45°$ (average error of 19%) than when $\theta = 0°$ (average error 41%). However, the results suggest that there is some merit in using the values for C_p and K determined from a square 500 mm Windcatcher to predict the performance of a square Windcatcher of other dimensions, but one cannot expect such good agreement all of the time, and so the predictions of the semi–empirical model must only be used as an estimate of true Windcatcher performance. Nevertheless, the predictions obtained for $\theta = 0°$ and $\theta = 45°$ both lie within a reasonable distance of the measured data, and so it seems sensible to use these as limiting cases where $\theta = 0°$ represents the best possible performance, and $\theta = 45°$ represents an estimation of a worst case performance.

The predictions of the semi–empirical model are now compared against the experimental measurements made *in–situ* for this study. All measurements of ventilation rates are given in Appendix D (p. 287), and for a Windcatcher operating autonomously, the predicted and measured ventilation rates are presented for 800 mm and 1000 mm Windcatchers in Figures 6.2 and 6.3 for the classrooms given in Table 6.1. The ventilation rates presented in Table 5.2

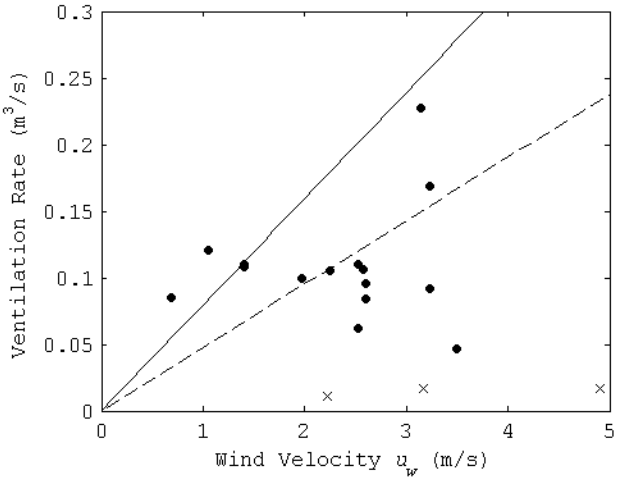

Figure 6.2: Ventilation rates for an autonomous 800 mm square Windcatcher. ——, prediction $\theta = 0°$; – – –, prediction $\theta = 45°$; •, measurement $L \leq 1$ m; ×, measurement $L > 1$ m.

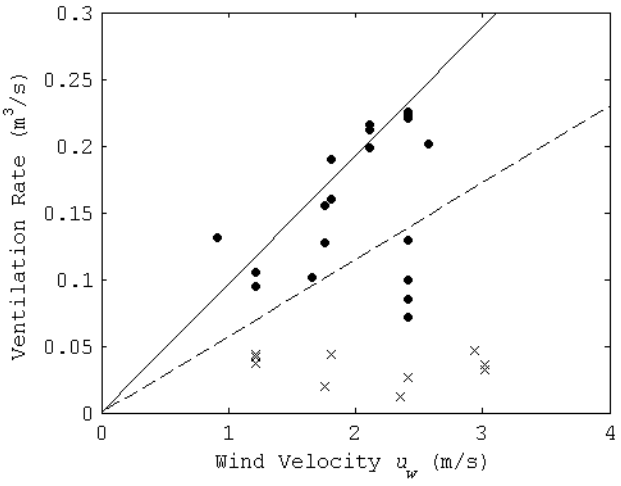

Figure 6.3: Ventilation rates for an autonomous 1000 mm square Windcatcher. ——, prediction $\theta = 0°$; – – –, prediction $\theta = 45°$; •, measurement $L \leq 1\,\text{m}$; ×, measurement $L > 1\,\text{m}$.

(p. 168) show that none of the classrooms given in Table 6.1 are perfectly sealed and so the unsealed scenario is used (see Section 3.1.2, p. 84) where Equations (3.41)—(3.44) are used for $\theta = 0°$, and Equations (3.50)—(3.52) for $\theta = 45°$.

The ventilation rates through a classroom containing an 800 mm Windcatcher comprise measurements made in Schools D, F, and G. Here, it is noted that the quadrant area of a Windcatcher located in school F is less than 10% below the area for a standard 800 mm Windcatcher and its equivalent side is $d_{1,2} = 762\,\text{mm}$. This represents a small difference ($<$ 5%) and so the measurements made at school F have been included with those made at schools D and G. The ventilation rates through a classroom containing a 1000 mm Windcatcher comprise measurements made in School C. In order to compare data measured in several classrooms against predictions of best possible and worst case performance for a Windcatcher, several assumptions must be made. Accordingly, the duct length is set to $L = 1\,\text{m}$ in the model because in Section 3.2.5 (p. 116) a ten–fold increase in the Windcatcher duct length is shown to affect the predictions of the semi–empirical model by less than 5%. However, the measured ventilation rates are separated in Figures 6.2 and 6.3 into dots for $L = 1\,\text{m}$ and crosses for $L > 1\,\text{m}$. It is immediately apparent that the measured ventilation rates for those Windcatchers with $L > 1\,\text{m}$ are much lower than the rates mesaured for $L = 1\,\text{m}$. The

reason for this is not categorically clear, but one explanation for this behaviour is that for Windcatchers with $L > 1\,\mathrm{m}$ the diagonal partition only extends through the upper louvred element and not for the whole length of the duct. Thus, the model does not fully replicate the geometry of this type of Windcatcher. Perhaps more importantly, it is possible that so–called short circuiting is occurring here, whereby a mixing of air is taking place in the lower half of the Windcatcher, and is extracted through the Windcatcher before it enters the room. Furthermore, it is possible that this is restricting the flow of air from the room through the outlet quadrants, and evidence for this is provided by the CFD analysis of Hughes & Ghani (2008, Figures 10 and 13).

The predictions presented in Figures 6.2 and 6.3 follow the same method used in Figure 6.1 for the analysis of the measurements of Kirk & Kolokotroni (2004b), whereby two lines are drawn, one for $\theta = 0°$ and one for $\theta = 45°$. This forms a "wedge" that is intended to encompass the two extremes of operation for a Windcatcher, depending on the incident wind conditions. Here, a further assumption made by the semi–empirical model is the exclusion of buoyancy, which is based upon the success at predicting the measurements of Kirk & Kolokotroni (2004b), shown in Figure 6.1, where buoyancy was also excluded. This decision is further justified by Figures 6.4 and 6.5 which show that there is no statistical link between the measured ventilation rates and the difference between internal and external temperatures

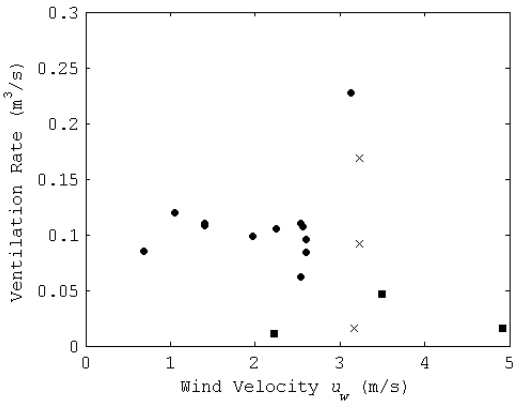

Figure 6.4: Measured ventilation rate and ΔT for autonomous 800 mm Windcatchers. ×, ($-5°\,\mathrm{C} < \Delta T < 0°\,\mathrm{C}$); ■, ($0°\,\mathrm{C} < \Delta T < 5°\,\mathrm{C}$); •, ($7°\,\mathrm{C} < \Delta T < 12°\,\mathrm{C}$).

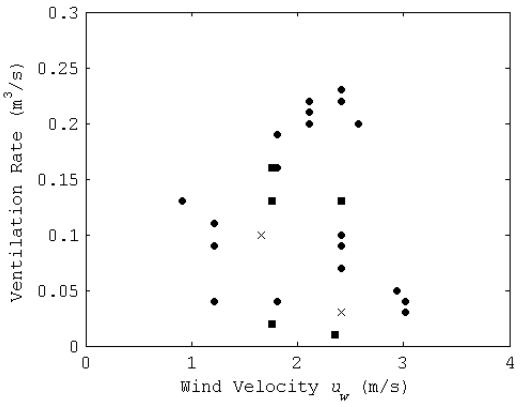

Figure 6.5: Measured ventilation rate and ΔT for autonomous 1000 mm Windcatchers. ×, ($0°\,\mathrm{C} < \Delta T < 5°\,\mathrm{C}$); ■, ($5°\,\mathrm{C} < \Delta T < 11°\,\mathrm{C}$); •, ($11°\,\mathrm{C} < \Delta T < 16°\,\mathrm{C}$).

(ΔT). If there was a relationship between ΔT and the measured ventilation rates one would expect to see the higher magnitudes of ΔT towards the top of the plots and the lower magnitudes of ΔT towards the bottom, and here it is evident that this is not the case. However, it is acknowledged that local environmental factors, unique to each measured Windcatcher, could also affect the overall ventilation rate supplied to a room through a Windcatcher by causing wind turbulence. Factors that may influence conditions include the proximity of surrounding buildings or obstacles, the shape of the roof, the juxtaposition of other Windcatcher elements, or the location of each measured Windcatcher with relation to the roof apex, see Shea *et al.* (2003) for example.

In Figure 6.2, 40% of the measured data lies within the "wedge" if one ignores data for $L > 1\,\mathrm{m}$, whereas in Figure 6.3 this figure is 60%. The success of these predictions is generally comparable to those made for the data of Kirk & Kolokotroni (2004b) in Figure 6.1; however, some of the measured data clearly shows that the Windcatcher is under–performing when compared to the predictions, especially for the 800 mm Windcatcher. Nevertheless, the action of the Windcatcher and its ability to act autonomously in the generation of ventilation in a room is clearly evident in Figures 6.2 and 6.3.

6.2 Windcatcher in Coordination with Open Windows

Predicted ventilation rates are now compared against measured data for a Windcatcher operation in coordination with open windows. In this case, the number of variables in the model increases and is greater than seen for an autonomous Windcatcher. In order to quantify the predicted limits of Windcatcher performance in the form of a "wedge" shown in Figures 6.1—6.3, it is necessary to make the following limiting assumptions: (i) for A_5 the maximum openable window area is used, and (ii) the maximum ventilation rate is predicted when $C_{p5} = -0.38$, and the minimum ventilation rate is when $C_{p5} = 0.06$ (see Section 4.4.2 on p. 152 for a discussion). In contrast, the measured ventilation rates were obtained with openable window areas ranging from $A_5 = 0.4\,\mathrm{m}^2$ to $A_5 = 0.9\,\mathrm{m}^2$ for a classroom containing a 1000 mm square Windcatcher, and from $A_5 = 0.3\,\mathrm{m}^2$ to $A_5 = 1.8\,\mathrm{m}^2$ for a classroom containing a 800 mm square Windcatcher. Using Equation (3.153) the normalised opening areas are calculated to be from $A_0 = 0.52$ to $A_0 = 1.17$ for a classroom containing a 1000 mm square

Windcatcher (with acoustic lining), and from $A_0 = 0.47$ to $A_0 = 2.81$ for a classroom containing a 800 mm square Windcatcher (with no acoustic lining). Figure 3.33 (see also Figure A.1 on p. 269 for an enlarged version of the same plot) shows that the maximum ventilation rates are achieved when $\theta = 0°$ for a classroom containing a 1000 mm square Windcatcher, and when $\theta = 45°$ for a classroom containing a 800 mm square Windcatcher. Furthermore, Figure 3.33 also shows that the difference between the estimated ventilation rates for the largest and smallest opening areas is 7% and 21% for a classroom containing a 1000 mm and an 800 mm square Windcatcher, respectively. Minimum ventilation rates are achieved when $\theta = 45°$ for all classrooms, and there is no difference in the predicted ventilation rate for the largest and smallest opening areas. Finally, the "wedge" is used to identify the predicted operating envelope for the Windcatcher with the expectation that the measurements should lie within it. In Figure 6.6, measured and predicted ventilation rates are presented for 800 mm and 1000 mm Windcatchers operating in combination with open windows. Here, Equations (3.94), and (3.97)—(3.105) (from p. 92) are used to calculate the upper bound for a classroom containing a 1000 mm square Windcatcher, Equations (3.128), and (3.130)—(3.135) (from p. 100) are used to calculate the upper bound for a classroom containing a 800 mm

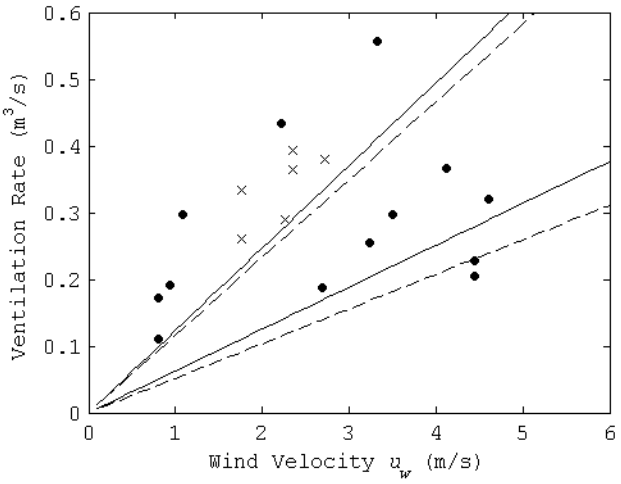

Figure 6.6: Ventilation rates for Windcatchers with open windows. ——, prediction (upper and lower bounds) for 1000 mm square Windcatcher with $A_5 = 0.9\,\mathrm{m}^2$; – – –, prediction (upper and lower bounds) for 800 mm square Windcatcher with $A_5 = 1.8\,\mathrm{m}^2$; •, measurement 800 mm square Windcatcher; × measurement 1000 mm square Windcatcher.

square Windcatcher, and Equations (3.106), and (3.107)—(3.112) (from p. 97) are used to calculate the lower bound for all classrooms.

It is noticeable here that the predictions for the 800 mm and 1000 mm Windcatchers are similar, although it is, perhaps, unsurprising to see the 1000 mm Windcatchers delivering greater ventilation rates. For the experimental data, Figure 6.6 shows that the thirteen measurements for a 800 mm Windcatcher are more widely dispersed than the six measurements for a 1000 mm Windcatcher, and this is likely to be a function of environmental factors and, consequently, the number of schools where measurements were made. In Figure 6.6, measurements of a 1000 mm Windcatcher are presented for only one school, while measurements of an 800 mm Windcatcher are presented for three schools. However, it is evident that when the windows are open the predictions are less successful and here it is common for the theory to under–predict the ventilation rates. This is in contrast to the findings of Section 6.1 where the over–prediction of ventilation rates was common for an autonomous Windcatcher. The cause of the under–prediction found in Figure 6.6 is likely to be an under–estimation of the values for C_{p5} used in the model (see Figure 3.35 on p. 123) rather than the selection of values for z_O, z_E, and a used to calculate $\tilde{C}_{p5}$ [see Equation (3.19)]. This is understandable given the difference in geometry between the building used to derive the values for C_{p5} given in the tables of Liddament and those measured here. This shows the importance of the selection of C_{p5} for a building. Figures 6.7—6.10 (p. 194) show that there are no statistical links between the measured ventilation rates and the duct length (L), the difference between internal and external temperatures (ΔT), the area of the opening (A_5), or the direction of the wind (θ), respectively. However, it is clear that opening a window, or windows, has the potential to significantly increase the ventilation rate in the classrooms studied here and the under–performance seen in Figures 6.2 and 6.3 has largely been eliminated.

To illustrate further the effect of opening windows it is effective to compare the measurements with and without open windows. Accordingly, in Figure 6.11 (p. 195) all of the measured ventilation rates are compared on a single plot. Here, ventilation rates are seen to increase significantly when a Windcatcher is used in combination with an open window. Interestingly, the measured volume flow rates for a Windcatcher with closed windows do not exceed $0.23\,\mathrm{m}^3/\mathrm{s}$, and appear to plateau when $u_w \geq 2\,\mathrm{m/s}$. This is not predicted by the model and the cause of this is unclear, but it may be a function of the internal dynamics of

the Windcatcher or an environmental problem such as roof level turbulence.

Figures 6.6 and 6.11 clearly demonstrate that opening a window as well as the Windcatcher significantly increases the ventilation rate in a classroom, however it is important to be sure that this is caused by the action of the window and the Windcatcher working together and cannot be obtained with a window on its own. Here, Table 5.2 (p. 168) shows

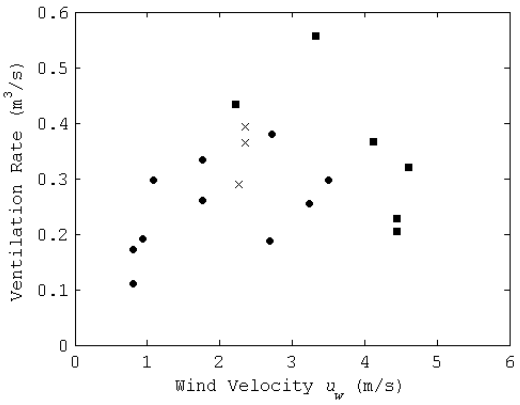

Figure 6.7: Measured ventilation rate and duct length for Windcatchers with open windows. ×, L =4.8 m; ■, L =5.5 m; •, $L = 1$ m.

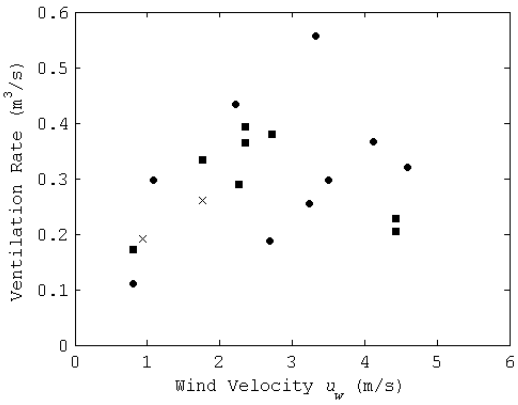

Figure 6.8: Measured ventilation rate and ΔT for Windcatchers with open windows. ×, ($-5°$ C < $\Delta T < 0°$ C); ■, ($0°$ C < $\Delta T < 5°$ C); •, ($5°$ C < $\Delta T < 15°$ C).

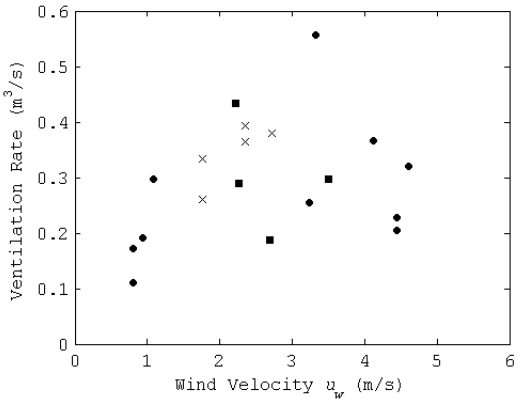

Figure 6.9: Measured ventilation rate and window area for Windcatchers with open windows. ×, (0.3 m < A_5 < 0.5 m); ■, (0.5 m < A_5 < 1 m); •, (1.5 m < A_5 < 2 m).

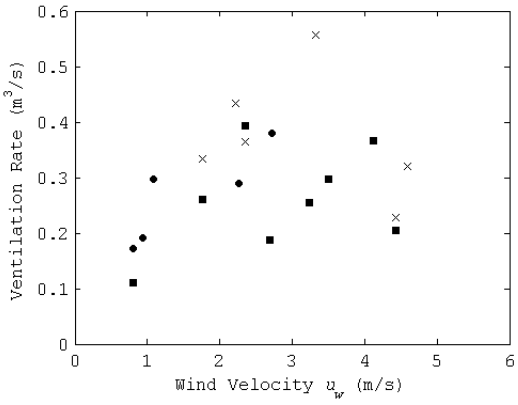

Figure 6.10: Measured ventilation rate and window location for Windcatchers with open windows. ×, front ($\theta = 0°$); ■, side ($\theta = 90°$ or $\theta = 270°$); •, rear ($\theta = 180°$).

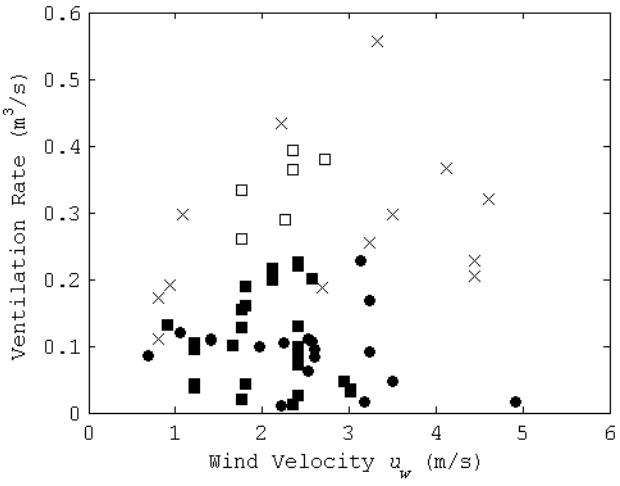

Figure 6.11: Measured ventilation rates for Windcatchers with and without open windows. •, 800 mm square Windcatcher with windows closed; ■, 1000 mm square Windcatcher with windows closed; ×, 800 mm square Windcatcher with windows open; □, 1000 mm square Windcatcher with windows open.

a comparison between the ventilation provided by a Windcatcher in coordination with the maximum available window area and the ventilation provided by the maximum available window area with the Windcatcher closed. For the schools listed in Table 6.1, results obtained indicate that the volume flow rates measured with the windows open and the Windcatcher closed were, on average, 32% less than those ventilation rates measured with the Windcatcher operating in coordination with the open windows. If all of the measurements made in schools A–I are considered, the difference is found to be 48%, and so this demonstrates the benefit of combining a Windcatcher with open windows. Therefore, it is evident that this configuration could be used to achieve high ventilation rates through a room in order to deliver good IAQ levels, as well as to dissipate large heat gains, and provide purge ventilation rates.

6.3 Application of the Semi–Empirical Model to Windcatcher Design

The findings of Sections 3.2.4, 6.1, and 6.2 suggest that the ventilation rates predicted by the semi–empirical model may be compared to those measured in real world situations, and so it has the potential to be used as a quick, iterative design tool.

In Section 4.1 (p. 128), climatic conditions are given for each of the case studies discussed in this chapter, and in Chapter 5, to show the wind velocity expected at each location. Calculations were made using the CIBSE Test Reference Year (TRY) database (CIBSE, 2005b) which is a synthesised typical weather year suitable for analysing environmental performance where relevant parameters are given hourly. The given wind speeds can, therefore, be considered to be steady–state values that are easily applicable to the semi–empirical model because a key assumption is that it predicts steady–state ventilation scenarios, see Section 3.1 (p. 73). Therefore, further validation of the semi–empirical model may be achieved by applying the wind parameters given by the TRY to predict the ventilation rate expected in a specific region. For example, this can be done using the parameters for a classroom assigned in Sections 6.1 and 6.2, where $L = 1\,\mathrm{m}$, $z_I = 3.30\,\mathrm{m}$, $z_O = 1.65\,\mathrm{m}$, $k = 0.35\,\mathrm{m}^{-a}$ and $a = 0.25$ for an urban environment. The TRY wind speed is converted to an estimated wind speed at Windcatcher height using Equation (3.18), here $z_E = 4.30\,\mathrm{m}$ (comparable to School D), and the appropriate continuity and flow equations are selected by considering the wind direction, which is also given by the TRY database. If the Windcatcher is oriented so that each of its faces are at the four cardinal points (0°, 90°, 180°, and 270°), then the wind is considered to be incident to the Windcatcher at $\theta = 0°$ if it originates from the direction of the cardinal points $\pm 22.5°$, otherwise it is considered to be incident at $\theta = 45°$. Therefore, for an autonomous Windcatcher ventilating an unsealed room, Equations (3.41)—(3.44) are used for $\theta = 0°$ and Equations (3.50)—(3.52) are used for $\theta = 45°$. In Figure 6.12 (p. 197), the TRY for London Heathrow Airport is used to predict ventilation rates in a classroom ventilated by an 800 mm Windcatcher and located in an urban area of the south–east of England. Here, the central bar denotes the mean value, the upper and lower bars denote the maximum and minimum values, respectively, the dotted boxe denotes one standard deviation (σ) from the mean, and the three horizontal dotted lines denote the minimum, mean, and purge ventilation rates of 0.09, 0.15, and $0.24\,\mathrm{m}^3/\mathrm{s}$ required by BB101 (DfES, 2006) if a class size of 30 occupants is assumed. Figure 6.12 shows that an 800 mm Windcatcher is likely to be able to meet the minimum ventilation requirement, but cannot meet the mean ventilation rate of $0.15\,\mathrm{m}^3/\mathrm{s}$. A further calculation for occupied hours [defined as 0900—1530 hrs (DfES, 2006)] is given in Figure 6.13 (p. 197) and shows that the ventilation rates supplied by an 800 mm Windcatcher are 16% greater annually and 17% greater during the non–heating season (see Section 2.1.3

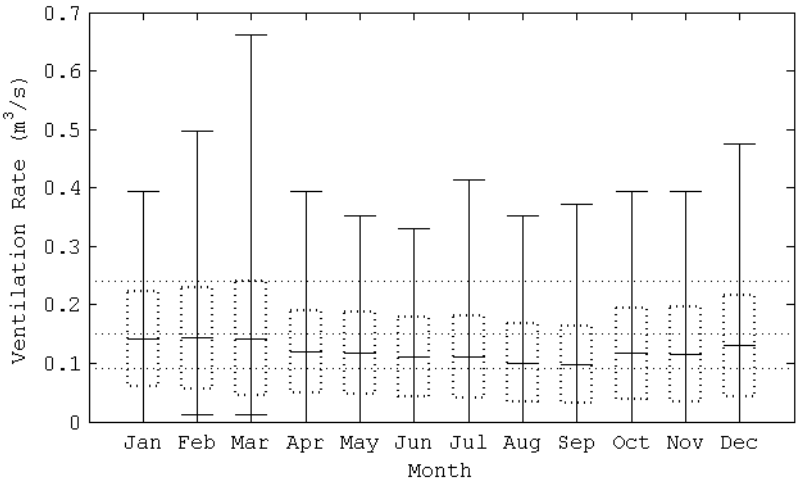

Figure 6.12: Predicted ventilation rates in a room ventilated by an autonomous 800 mm Windcatcher using TRY weather data (CIBSE, 2005b) for the south east of England.

on p. 40 for a definition) when the Windcatcher dampers can be expected to be open, but the conclusions drawn from Figure 6.12 remain unchanged. Furthermore, the effect of rotating the Windcatcher through 45° so that its four faces are now oriented halfway between the cardinal points (45°, 135°, 225°, and 315°), decreases the annual ventilation rate provided by the

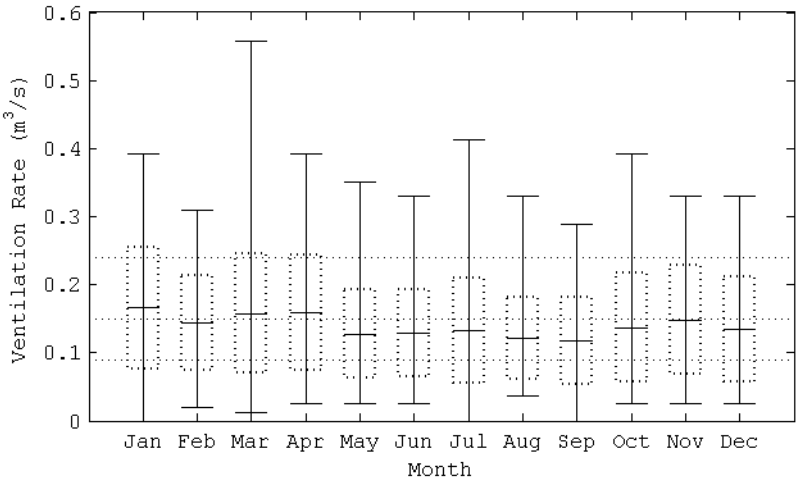

Figure 6.13: Predicted ventilation rates in a room ventilated by an autonomous 800 mm Windcatcher between 0900–1530 hrs using TRY weather data (CIBSE, 2005b) for the south east of England.

Windcatcher by 2% (for all hours). This result may seem surprising and even contradictory to the use of the "wedge", but further analysis of the weather data for the two Windcatcher orientations provides an explanation. If the Windcatcher faces are oriented normal to the cardinal points, the wind is normal to the a single Windcatcher quadrant for 57% of the time and incident to two quadrants for 47% of the time. However, the mean wind speed is 12.5% lower with the wind is normal to the a single Windcatcher quadrant the when it is incident to two Windcatcher quadrants. If the Windcatcher orientation is rotated through 45° the converse is true. Therefore, it is apparent that the lower wind speed experienced for the best case performance scenario for the majority of the time counter balances the higher wind speed experienced for the worse case performance scenario for the least amount of time, and so suggests that that the orientation of an autonomous Windcatcher is a relatively unimportant design consideration for the London TRY weather data when averaged over a twelve month period.

The effect of increasing the CSA of the Windcatcher is shown in Figure 6.14 for occupied hours. Here, a 1000 mm Windcatcher is shown to meet the mean ventilation requirement of 0.15 m^3/s during all months. In addition, the dotted boxes show that one standard deviation below the mean value lies above the minimum requirement for 0.09 m^3/s for all months, thus

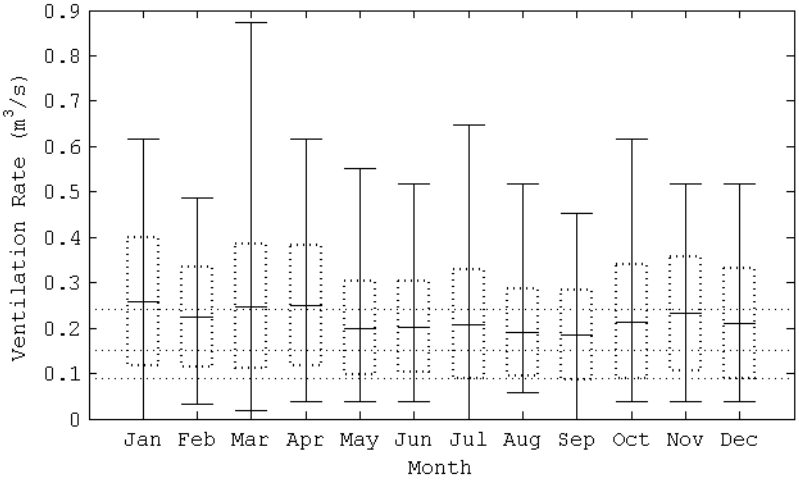

Figure 6.14: Predicted ventilation rates in a room ventilated by an autonomous 1000 mm Windcatcher between 0900–1530 hrs using TRY weather data (CIBSE, 2005b) for the south east of England.

suggesting that this requirement is likely to be met using the wind alone for approximately 84% of the time [assuming that 68% of data lies $\pm\sigma$ from the mean value and a further 16% of all data also lies above the mean value (Ross, 2004)] if the Windcatcher volume control dampers are fully open. The predictions presented in Figures 6.13 and 6.14 are for the south east of England and so should be comparable to measurements made *in–situ* of ventilation over time, indicated by internal CO_2 concentration for the classrooms measured in this study (see 5.5 5.6 from p. 162). However, a comparison is complicated by the the temperature based control strategy that is shown in Figure 5.4 (p. 160) to close the volume control dampers in the winter reducing ventilation rates below those that are actually obtainable, while in the summer Section 5.1.1 (p. 158) shows that available windows are very likely to be open, thus increasing the ventilation rates beyond those that can be achieved through an autonomous Windcatcher. Nevertheless, Figure 6.14 does show that during the heating season (October to April) the volume control dampers would have to remain fully open for a significant proportion of occupied hours in order to meet the mean ventilation requirement of BB101. This would, of course, increase energy losses and the need for additional heating, as well as the risk of thermal discomfort among occupants located in the draught–risk zone (see Schild, 2004) when cold air is brought into the room through the Windcatcher. These risks are discussed further in Chapter 7.

BB101 stipulates a purge ventilation rate of 8 l/s – person, which for a classroom of 30 occupants equates to a total ventilation rate of $0.24\,m^3/s$. Figure 6.14 shows that an average ventilation rate of $0.24\,m^3/s$ can be met in January, March, and April using an autonomous Windcatcher but at other times of the year it can only be achieved using a Windcatcher in coordination with open windows. Here, Figure 6.14 shows that this is most difficult to achieve in summer (1^{st} May to 30^{st} September) because the mean ventilation rates are lowest during these months. Therefore, the opening area of the windows should be selected based upon the conditions experienced during these month where the mean (scaled) wind speed is 1.95 m/s. The theory outlined in Section 3.1.2 (p. 84) shows that the wind incidence θ, is important for the calculation of ventilation rates through a room ventilated by a Windcatcher in coordination with open windows. Figure 6.6 suggests that there is value in predicting upper and lower boundaries using maximum and minimum values for the façade coefficient of pressure C_{p5}. For a sheltered building with an aspect ratio of 2:1,

Figure 3.33 (p. 120) shows that for the lower limit of C_{p5} ventilation rates are predicted to be only fractionally higher than those achieved using an autonomous Windcatcher when $\theta = 0°$ and so it seems sensible to calculate the window area required to supply $0.24\,\mathrm{m}^3/\mathrm{s}$ using only the upper boundary and the mean wind speed for summer months. For a 1000 mm Windcatcher, the required normalised flow rate is calculated using Equation (3.152) to be $Q_0 = 0.24/(1.95 \times 1) = 0.12$. Now, Figure 3.30 indicates that the normalised opening area required to deliver this ventilation rate is $A_0 = 0.20$, and is easily converted to an actual opening area of $A_5 = 0.20\,\mathrm{m}^2$ using Equation (3.153). This estimated openable window area is approximately 80% less than the average openable window area for all of the classrooms investigated in this study.

The Windcatcher CSA and openable window area calculated here seem plausible when compared to the existing scenarios outlined in Chapter 4. The similarity between the parameters provides the opportunity for cross reference and to learn more about the ventilation strategies used in the classrooms measured for this study. Here, Table 5.2 (p. 168) show that the ventilation rates measured in classrooms G1 and G2 for an autonomous Windcatcher is poor, and analysis showed that it is probably caused by their long duct lengths. But, with the windows and Windcatcher open, flow rates of $0.56\,\mathrm{m}^3/\mathrm{s}$ and $0.43\,\mathrm{m}^3/\mathrm{s}$ at wind speeds of 3.33 m/s and 2.22 m/s were measured for classrooms G1 and G2, respectively. In addition, Figure 5.5 (p. 162) shows that the mean CO_2 concentration was below 1000 ppm in all classrooms during the summer months suggesting that the ventilation rate was likely to be above 8 l/s – person and therefore, for a class of 30 occupants, the total ventilation was likely to be greater than $0.24\,\mathrm{m}^3/\mathrm{s}$. This seems to confirm that windows were open during the summer months and so their presence can be relied during the design process. A simple relationship between window opening behaviour of the occupants of a building, the external temperature T_E, and cloud cover is given in Figure 6.15 (p. 201), which shows that the proportion of open windows increases with as T_E rises and with a reduction in cloud over. For example, when $T_E = 0°\mathrm{C}$ one may expect approximately 2.5% of available windows to be open. This tells us that there are likely to be some windows open even on a cold winters day in the UK.

The estimates of ventilation rate in a classroom ventilated by an 800 mm or a 1000 mm Windcatcher in Figures 6.13 and 6.14 show that the wind speed may drop to zero on some occasions. The wind speed is estimated using the TRY database and when the wind speed is

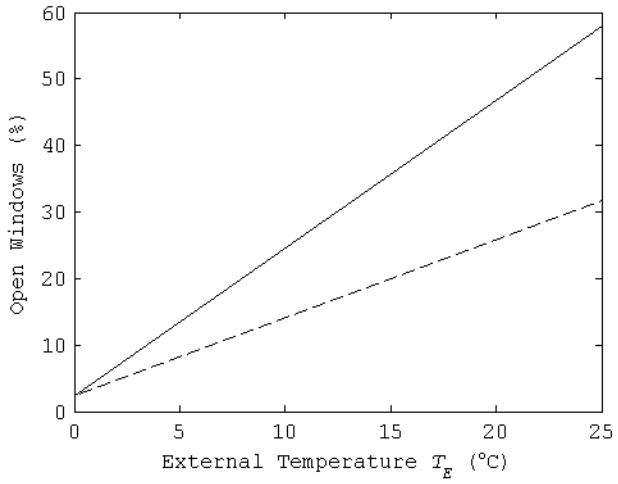

Figure 6.15: Predicted window opening behaviour related to external temperature and cloud cover (extrapolated from Liddament, 2001). ——, clear sky; – – –, overcast sky.

negligible, a natural ventilation system must use the difference between internal and external densities to induce air through a room and maintain thermal comfort and good IAQ. Now the semi–empirical model is used to investigate the effect of ΔT on flow rates when $u_w < 2\,\mathrm{m/s}$. There are currently no studies for a Windcatcher that only consider the effect of buoyancy on overall ventilation rates through a Windcatcher when $u_w \to 0\,\mathrm{m/s}$, and so the flow paths through the Windcatcher and their effect on the overall ventilation rate are unknown in this situation. Predictions have been made in Figures 3.29, 3.31, and 3.32 (from p. 114) for sealed and unsealed rooms and show that the effects of buoyancy are significant when $u_w < 2\,\mathrm{m/s}$, and so in these circumstances buoyancy forces could be used to provide the minimum ventilation rate, such as the 3 l/s – person specified by BB101. Accordingly, a wind speed of $u_w = 0\,\mathrm{m/s}$ is considered here and Figures 6.16 and 6.17 (p. 202) show the predicted ventilation rates through an unsealed and sealed room ventilated by 1000 mm Windcatcher, with a variation in the difference between the internal and external temperature, ΔT.

For the unsealed room, Equations (3.45)—(3.49) and Equations (3.53)—(3.56) would ordinarily be used when $\theta = 0°$ and $\theta = 45°$, respectively, but in the absence of wind forces either set of equations can be used because they yield the same result. When $T_E > T_I$ the unsealed model predicts that air is supplied to the room through all of the Windcatcher

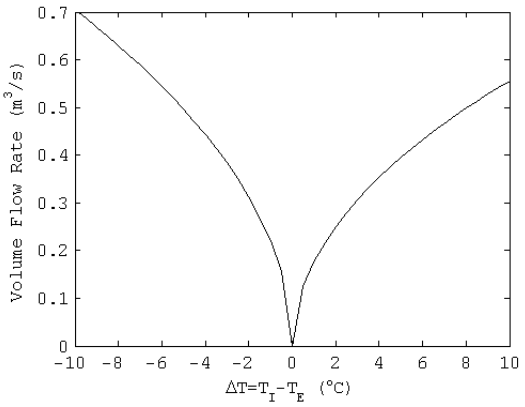

Figure 6.16: Prediction of ventilation rate from an unsealed room ventilated by a 1000 mm Windcatcher for $u_w = 0\,\mathrm{m/s}$ and varying ΔT.

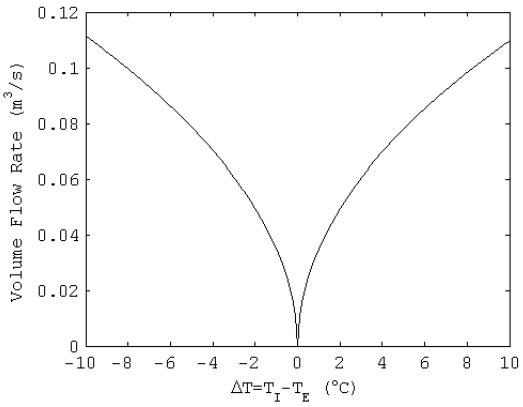

Figure 6.17: Prediction of ventilation rate from a sealed room ventilated by a 1000 mm Windcatcher for $u_w = 0\,\mathrm{m/s}$ and varying ΔT.

quadrants and extracted by exfiltration through adventitious openings, whereas when $T_I > T_E$, the model predicts that air is extracted from the room through all of the Windcatcher quadrants and is supplied by infiltration through adventitious openings. The predictions in Figure 6.16 do not exhibit symmetry because the estimated losses for a supply and an extract quadrant are different, see Table 3.5 (p. 111). Furthermore, the predictions suggest, unrealistically, that flow rates of up to $0.7\,\mathrm{m^3/s}$ are achievable when $-10°\mathrm{C} < \Delta T < 10°\mathrm{C}$. The scenario predicted by the unsealed model is unrealistic because in practice, neither exfiltration nor infiltration are likely to be able to match the mass flow in or out of the Windcatcher, and so here it is probable that the pressure of the supplied room would change to compensate for the temperature difference and to maintain mass continuity (see Section 3.2.4 on p. 112 and Figure 3.29 on p. 114 for a similar argument). This, implies that the unsealed model is unsuitable for modelling the effects of buoyancy at low wind velocity, and the sealed model is more likely to be applicable in this context.

Figure 6.17 shows predictions made for a sealed room ventilated by a 1000 mm Windcatcher for conditions that are identical to those used in Figure 6.16, and using the equations for continuity and flow given by Equations (3.32)—(3.38). Here, it has been assumed that air is supplied and extracted through two Windcatcher quadrants each and, although there is no empirical evidence for these flow paths, a similar example is given in AM10 (CIBSE, 2005a, example 4.7). The predictions of air flow rate by the sealed model are approximately

80% lower than those predicted by the unsealed model. Because mass flow through the Windcatcher does not balance, the pressure in the supplied room changes to compensate and maintain mass balance. For example, when $T_I > T_E$ more air is extracted from the supplied room through the Windcatcher than is supplied to it, thus causing the room pressure p_I to drop by a small amount, see Figures 3.22 (p. 107) and 3.30 (p. 114). This process restricts flow into and out of the supplied room through the Windcatcher, and is similar to the arguments made in Section 3.2.4 (p. 112). Finally, Figure 6.17 exhibits noticeable symmetry that is explained by the equal number of supply and extract quadrants for either sign of ΔT.

Figure 6.17 shows that the minimum ventilation rate of $0.09\,\mathrm{m}^3/\mathrm{s}$ specified by BB101 for a UK school classroom of 30 occupants is achievable when $\Delta T = \pm 6.6°\mathrm{C}$, but the mean and purge levels of $0.15\,\mathrm{m}^3/\mathrm{s}$ and $0.24\,\mathrm{m}^3/\mathrm{s}$, respectively, cannot be met.

The effect of opening windows in a single façade to ventilate a room in coordination with a 1000 mm Windcatcher is shown in Figure 6.18 for $u_w = 0\,\mathrm{m/s}$, $C_{p5} = -0.38$, and varying ΔT. The predictions are identical for $\theta = 0°$ and $\theta = 45°$ and so the following equations are used: Equations (3.128)—(3.135) for $T_E > T_I$, and Equations (3.113)—(3.120) for $T_I > T_E$. Here, the air is uniformly supplied or extracted through all of the Windcatcher quadrants

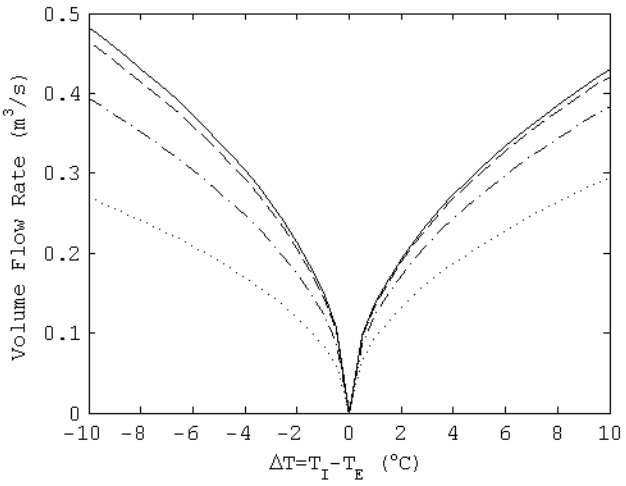

Figure 6.18: Prediction of ventilation rate from a room ventilated by a 1000 mm Windcatcher in coordination with open windows for $u_w = 0\,\mathrm{m/s}$ and varying ΔT. ——, $A_5 = 3\,\mathrm{m}^2$; – – –, $A_5 = 2\,\mathrm{m}^2$; – · – ·, $A_5 = 1\,\mathrm{m}^2$; · · · · · ·, $A_5 = 0.5\,\mathrm{m}^2$.

depending upon the sign of ΔT, and so the flow direction through the Windcatcher quadrants is the cause of the asymmetry. In Figure 6.18 the area of the open windows A_5, is also varied and shows that as A_5 increases the predicted flow rates plateau, thus agreeing with the findings of Figure 3.33 (p. 120), which also shows that for ever increasing values of A_5, the predicted flow rates reach a peak value. Figure 6.18 suggests that with an opening area of $A_5 = 0.5\,\mathrm{m}^3$ the background ventilation rate of $0.09\,\mathrm{m}^3/\mathrm{s}$ specified by BB101 for a UK school classroom of 30 occupants is achievable when $-1.5°\mathrm{C} > \Delta T > 1°\mathrm{C}$, the mean ventilation rate of $0.15\,\mathrm{m}^3/\mathrm{s}$ is achievable when $-3.5°\mathrm{C} > \Delta T > 3°\mathrm{C}$, and the purge ventilation rate of $0.24\,\mathrm{m}^3/\mathrm{s}$ is achievable when $-8°\mathrm{C} > \Delta T > 7°\mathrm{C}$.

Now, the data presented in Figure 6.15 is recalled that shows approximately 7%—15% of available openable windows can be expected to be open when the external temperature is $T_E = 5°\mathrm{C}$; a typical winter temperature. Figure 4.8 (p. 137) shows that the external temperatures expected in a British winter may cause a temperature difference in excess of $\Delta T > 10°\,\mathrm{C}$ and so may explain the comparably good measured mean CO_2 levels for winter discussed in Chapter 5 and presented in Figure 5.6 (p. 162). However, Figure 5.4 (p. 160) shows that Windcatcher volume control dampers were partially open ($20\% \leq A_d \leq 100\%$) for an average of 17% of occupied hours. Accordingly, the Windcatcher will only have contributed to the overall ventilation rate for 17% of the time, and ventilation in winter months was likely to have been provided by open windows and background ventilation for approximately 83% of occupied hours. This represents a missed opportunity for stack ventilation in winter, because the predictions given in Figures 6.17 and 6.18 suggest that a Windcatcher system can provide background ventilatation rates to a classroom autonomously, and mean and purge ventilation in coordination with open windows.

The methods of sizing a Windcatcher and the predictions of ventilation rates through a room ventilated by a Windcatcher discussed in this section have all been determined by the ventilation rates specified by BB101. However, with increasing internal heat gains reported in UK school classrooms (see Pegg, 2008) the ventilation rate required to dissipate total internal heat gains may actually be higher than those specified by government requirements for good IAQ. Therefore, an understanding of the total heat gains in each classroom, and their effect on the internal air temperatures must be determined. Thermal heat gains arise from solar heat gains, as well as those from occupants and ICT equipment, but their effect

can only be estimated by a thermal model, see Lomas & Ji (2009) for example. Here, CIBSE Guide A Section 5 (CIBSE, 2006a) gives thermal models for winter and summer design calculations, and more advanced commercial software is also available; for example, the Thermal Analysis Software (TAS) created by EDSL or Virtual Environment software developed by Integrated Environmental Solutions (IES). However, it is noted that, when selecting appropriate commercial software, it should conform to CIBSE TM33 (CIBSE, 2006b) accreditation standards.

In winter months it becomes more important to reduce heat lost from a room, and a primary source of heat loss is that dissipated by the ventilation through a room. Here, the total heat, H, dissipated from a room by ventilation is approximated by

$$H = \dot{Q}_T \, \rho_E \, c_p \, \Delta T \tag{6.1}$$

where c_p is the specific heat capacity of air at constant pressure [$c_p = 1004\,\mathrm{J/kg\,K}$ (see Fox & McDonald, 1985, Section 11.1 and Table A.6)]. For a temperature difference of $\Delta T = 5°\mathrm{C}$ where $T_E = 20°\mathrm{C}$, the minimum, mean, and purge ventilation rates specified by BB101 for a classroom containing 30 occupants are $0.09\,\mathrm{m^3/s}$, $0.15\,\mathrm{m^3/s}$, and $0.24\,\mathrm{m^3/s}$, respectively. Using Equation (6.1), these ventilation rates correspond to approximately 0.6 kW, 0.9 kW, and 1.5 kW of dissipated heat, respectively. This is discussed in greater detail, in Chapter 7, but it is noted here that Equation (6.1) does not account for the thermal characteristics of a room, its location, orientation, or occupancy patterns, and so it is argued that it is unsuitable for the calculation of temperature changes in a room when subject to known heat gains.

6.3.1 Design Steps

A series of processes have been tested and discussed in this section that can be employed to determine the correct CSA of a Windcatcher and openable windows for a particular application. These processes are now detailed in chronological order to provide supportive design steps for a Windcatcher designer. The steps are determined by the assumption that a mean, purge, and minimum ventilation rate must be provided to a room, in common with the requirements for BB101.

Below each test step is a worked example for a hypothetical 2nd floor school classroom of $z_I = 3.3\,\mathrm{m}$ in height, containing 30 students and staff, and with manually operable windows located in a single façade. It is ventilated by an unlined Windcatcher of duct length 1m, whose faces are normal to the cardinal points. The school is located in the south west of England, is z_E =10 m high, has topography defined as urban, is surrounded by obstructions equal to the height of the building, and has an aspect ratio of 2:1 with the windows located in the longer side. The ventilation rates and IAQ in the classroom must conform to those stated in BB101 and so a mean ventilation rate of 5 l/s – person, a purge ventilation rate of 8 l/s – person, and a minimum ventilation rate of 3 l/s – person must be supplied.

6.3.1.1 Providing a Mean Ventilation Rate

Firstly, the CSA of an autonomous Windcatcher to provide the required mean ventilation rate to a room is calculated.

1. Select required mean ventilation rate:

   (a) Using government ventilation guidelines, such as BB101 (DfES, 2006) or Building Regulations, Part F (ODPM, 2006).

   (b) To dissipate internal heat gains. An appropriate ventilation rate should be determined using a thermal model.

BB101 recommends a ventilation rate of 5 l/s – person, so for a room containing 30 occupants, the total required ventilation rate is 150 l/s (0.15 m^3/s). For the purposes of this example, the mean ventilation rate required to dissipate total heat gains in a room is supplied by the contractor and is calculated to be 0.14 m^3/s. Therefore, the greater ventilation rate of 0.15 m^3/s is used as the design ventilation rate.

2. Use aerial photographs or other relevant sources to determine the local topography and relevant topographical constants k and a, see those given by Orme & Leksmono (2002, Table 2) for example.

For an urban location Orme & Leksmono (2002) give $k = 0.35\,\mathrm{m}^{-a}$ and $a = 0.25$.

3. Select CIBSE TRY weather data (CIBSE 2005) for the relevant region and scale the wind speed data appropriately to determine the wind speed at roof level using Equation (3.18) and the topographical constants determined at Stage 2.

Figure 4.11 presents wind speeds for the south west of England and the mean wind speed is shown to be 5.91 m/s. The school building is $z_E = 10\,\text{m}$ high, and so using Equation (3.18)

$$u_w = u_{10} k {z_E}^a$$

$$5.91 \times 0.35 \times 10^{0.25} = 3.68\,\text{m/s}$$

the mean wind speed for the south east of England of $u_{10} = 5.91\,\text{m/s}$ equates to $u_w = 3.68\,\text{m/s}$ at roof level. CIBSE TRY data is given hourly, and all wind speeds are similarly scaled.

4. Determine the orientation of the Windcatcher faces relative to the points of a compass.

The Windcatcher faces are oriented to the cardinal points so that they face 0°, 90°, 180°, and 270°. Therefore, when the wind angle is at an angle of $\pm\,22.5$°C from the cardinal points the wind is considered to be normal to a single Windcatcher quadrant so that $\theta = 0°$. Otherwise the wind is considered to be incident to two Windcatcher quadrants so that $\theta = 45°$.

5. Select the initial CSA of the Windcatcher using the simplified semi–empirical model given by Equation (3.148).

Equation (3.148) is rearranged to give a simple relationship between the total cross sectional area of a Windcatcher, the flow rate out of it, and the wind speed.

$$A_T = \frac{\dot{Q}_T}{0.1251 u_w} \tag{6.2}$$

Application of the design flow rate and the scaled mean wind speed to Equation 6.2 gives

$$A_T = \frac{0.15}{0.1251 \times 3.68} = 0.33\,\mathrm{m}^2$$

The square root of A_T gives the length of the sides of a square Windcatcher so that $\sqrt{0.33} = 0.57\,\mathrm{m}$. Here, a 600 mm Windcatcher may seem the most suitable initial choice, but in months where the wind speed is below average the mean flow rates is likely to be less than $0.15\,\mathrm{m}^3/\mathrm{s}$. Therefore, an 800 mm Windcatcher is selected as the initial estimate of Windcatcher size.

6. Estimate monthly ventilation rates provided to the room using scaled TRY wind speeds, TRY wind direction, and the semi–empirical model to produce a plot similar to Figure 6.14, which shows predicted ventilation rates in a room per month during occupied hours. For an autonomous Windcatcher ventilating an unsealed room Equations (3.41)—(3.44) are used for $\theta = 0°$ and room Equations (3.50)—(3.52) are used for $\theta = 45°$.

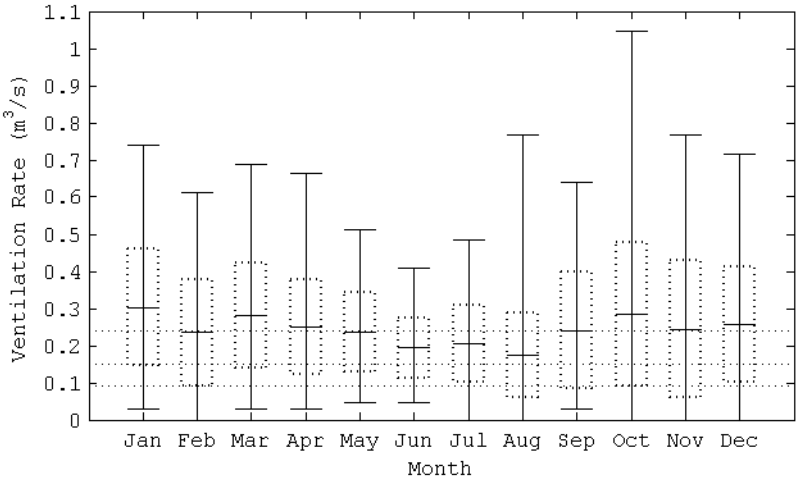

Figure 6.19: Predicted ventilation rates in a room ventilated by an autonomous 800 mm Windcatcher between 0900—1530hrs using CIBSE TRY weather data (CIBSE, 2005b) for the south west of England.

The scaled wind speeds calculated in Step 3 and the Windcatcher CSA determined in Step 5 are applied to the appropriate equations according to the wind angle and Windcatcher

orientation, see Step 4. The predictions of ventilation rate are parsed and split, first into occupied hours, and secondly into calendar months, to give Figure 6.19. Here, the central bar denotes the mean value, the upper and lower bars denote the maximum and minimum values, respectively, and the dotted box denotes one standard deviation from the mean.

7. Is the mean ventilation rate for each month greater than required?
   (a) If No, increase the Windcatcher CSA and return to stage 6.
   (b) If Yes, check that the estimated ventilation rates do not excessively exceed the required ventilation rate determined at stage 1.
      i. If the predicted ventilation rate is too large, reduce the Windcatcher CSA and return to stage 6.
      ii. If the predicted ventilation rates are satisfactory, continue to the next step.

Figure 6.19 shows that the required mean ventilation rate of $0.15\,m^3/s$ is exceeded in every month, and so an 800 mm Windcatcher is a suitable size for this application. Because the predicted ventilation rates are satisfactory, the design process can continue to the next section.

6.3.1.2 Providing Purge Ventilation

Next, the window area required to deliver purge ventilation rates in coordination with a Windcatcher is calculated.

1. Determine a purge ventilation rate using:
   (a) The number of occupants multiplied by the required ventilation rate per occupant, see the 8 l/s – person required by BB101 (DfES, 2006) for example.
   (b) Pre–determined rate specified by a third party.

BB101 requires a ventilation rate of 8 l/s – person, and so for a room containing 30 occupants, the total required ventilation rate is 240 l/s ($0.24\,m^3/s$).

2. Using the plot generated in Section 6.3.1.1 Step 6, determine the period of time where the worst ventilation performance occurs, and note the scaled mean wind speed. This

period will normally occur during the summer months, and so it is advisable to use the mean wind speed for May to September, inclusively.

Figure 6.19 shows that the worst ventilation performance occurs during summer months of May to September where the mean scaled wind speed is calculated to be 2.88 m/s.

3. Use the worst performance wind speed to calculate the required non–dimensional flow rate $\dot{Q}_0$ using Equation (3.152).

$$\dot{Q}_0 = \frac{Q_T}{u_w A_T}$$

Therefore, $\dot{Q}_0$ is calculated to be

$$\dot{Q}_0 = \frac{0.24}{2.88 \times 0.64} = 0.13$$

4. Apply $\dot{Q}_0$ to the non–dimensional plot of $\dot{Q}_0$ against A_0 (see Appendix A) for shielded façades to determine the required non–dimensional window area A_0.

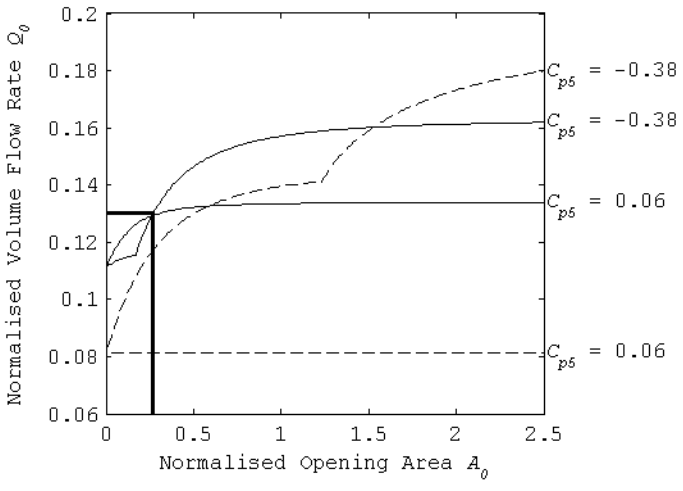

Figure 6.20: Prediction of the effect of the area of a shielded façade opening on Windcatcher ventilation rates. ——, $\theta = 0°$; – – –, $\theta = 45°$.

Figure A.1 is reproduced in Figure 6.20, where $\dot{Q}_0 = 0.13$ is applied to the y–axis, and $A_0 = 0.27$ is read from the x–axis.

5. Calculate the required opening area A_5, using Equation (3.151).

Equation 3.153 is rearranged to give

$$A_5 = A_0 A_T \tag{6.3}$$

and A_5 is calculated to be

$$A_5 = 0.27 \times 0.64 = 0.42\,\mathrm{m}^2$$

Therefore, it is predicted that a minimum window opening area of $0.42\,\mathrm{m}^2$ is required to meet the purge ventilation requirement of $0.24\,\mathrm{m}^3/\mathrm{s}$ with an 800 mm Windcatcher.

6.3.1.3 Providing Minimum Ventilation Rate

Finally, the ability of the Windcatcher to deliver a minimum ventilation rate in coordination with open windows when there is little or no wind speed must be found for a range of ΔT; for example $0°\mathrm{C} < \Delta T < 5°\mathrm{C}$ when $u_w = 0\,\mathrm{m/s}$.

1. Use the semi–empirical model for a room ventilated by a Windcatcher in coordination with a façade opening, and given in Section 3.1.3 to produce a plot similar to Figure 6.18, which shows ΔT versus $\dot{Q}_T$. Here, the chosen Windcatcher CSA and the opening area are applied.

BB101 specifies a minimum ventilation rate of 3 l/s – person, which for a class of 30 occupants equates to a total ventilation rate of 90 l/s ($0.09\,\mathrm{m}^3/\mathrm{s}$). Figure 6.19 (p. 208) shows that the lowest ventilation rates are predicted to be in summer months when the where wind speed can drop to $u_w = 0\,\mathrm{m/s}$. In addition, the difference in temperature between the classroom and its surroundings is also smallest at this time of year. Figure 6.21 (p. 212) shows the predicted ventilation rate in a classroom ventilated a 800 mm Windcatcher in coordination with an opening area of $A_5 = 0.42\,\mathrm{m}^2$ when $u_w = 0\,\mathrm{m/s}$ and for varying ΔT.

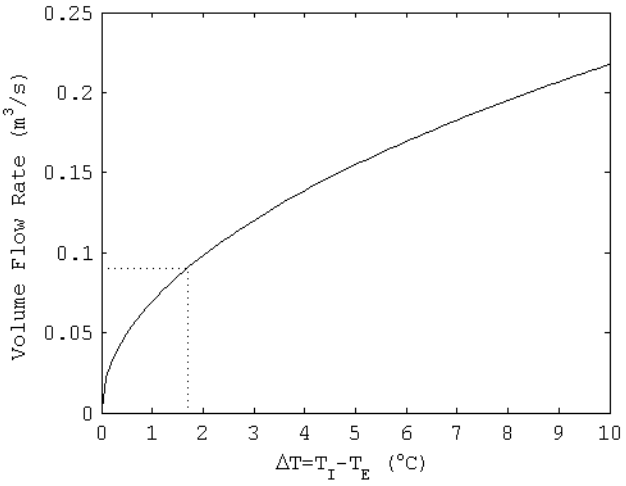

Figure 6.21: Prediction of ventilation rate from a room ventilated by an 800 mm Windcatcher in coordination with an opening area $A_5 = 0.42\,\mathrm{m}^2$ for $u_w = 0\,\mathrm{m/s}$.

2. Use the plot to determine compliance with the minimum ventilation rate target.

In summer months, BB101 states that the air temperature in a classroom must not exceed the external temperature by more than 5°C ($\Delta T \geq 5$°C) and so this temperature range is considered when interpreting Figure 6.21. Here, Figure 6.21 shows that the minimum ventilation rate of $0.09\,\mathrm{m}^3/\mathrm{s}$ can be achieved using an opening area of $A_5 = 0.42\,\mathrm{m}^2$ when $\Delta T = 1.7$°C.

3. Adjust the window area A_5, or Windcatcher CSA if necessary.

Figure 6.21 shows that the minimum flow rate of $0.09\,\mathrm{m}^3/\mathrm{s}$ can be achieved with an 800 mm Windcatcher and an opening area of $A_5 = 0.42\,\mathrm{m}^2$, calculated in Section 6.3.1.2 Step 5, and so does not need revision.

6.4 Summary

The theoretical predictions and experimental measurements presented here demonstrate that a Windcatcher is capable of delivering ventilation to a room when acting autonomously. The predictions of the semi–empirical model generally agree with the *in–situ* measurements, but

ventilation rates through a room ventilated by an autonomous Windcatcher are sometimes over–predicted and significant scatter in the experimental data is observed. The relatively poor performance of Windcatchers with long duct sections was not predicted and further investigation of such devices is required, see Chapter 7 for a discussion. Furthermore, the measured volume flow rates for a Windcatcher with closed windows do not exceed $0.23\,\mathrm{m}^3/\mathrm{s}$, and appear to plateau when $u_w \geq 2\,\mathrm{m/s}$. This too is not predicted by the model and its cause is unclear. Both the theoretical and experimental analysis of the Windcatcher demonstrate that Windcatcher performance can be significantly improved by the addition of open windows to a room. This aspect is likely to help rooms ventilated by a Windcatcher to meet ventilation standards for buildings, such as BB101 in the UK (DfES, 2006). In these circumstances the careful selection of C_{p5} for a building is important for the accuracy of the semi–empirical predictions.

Typical wind conditions for the south–east of England were applied to the semi–empirical model using the CIBSE TRY database to predict the ventilation performance of a room ventilated by a Windcatcher every month, and was shown to be a useful design tool. It also identified situations where the wind speed was negligible, and here the Windcatcher system must rely on buoyancy forces to generate ventilation through a room. When the semi–empirical model was used to investigate this situation, the unsealed model is found to be unsuitable for situations where $u_w < 2\,\mathrm{m/s}$ and $|\Delta T| > 0°\mathrm{C}$. The sealed model may be used to estimate ventilation rates under these circumstances and although the predictions seem plausible, they remain uncorroborated by empirical measurement. The predictions suggest that an autonomous Windcatcher is capable of providing minimum ventilation rates specified by BB101 for a class of 30 occupants, and a Windcatcher in coordination with open windows can provide minimum, mean, and purge ventilation rates.

Finally, the investigation of the capabilities of the semi–empirical model produced a series of steps that a designer may use to correctly size a Windcatcher for a particular application.

The ramifications of these findings are discussed in Chapter 7.

Chapter 7

Discussion of results

This chapter discusses issues raised during the course of this research, particularly methods of providing optimum thermal comfort and good IAQ to occupants, efficient flow paths for effective ventilation and energy conservation, improvements to Windcatcher system design and control, opportunities for the implementation of Windcatcher systems in building types other than schools, and immediate applications of this work. Finally, conclusions are proffered in Chapter 8.

7.1 Providing Thermal Comfort and Air Quality

It has been shown that a Windcatcher can provide a supply of fresh air to a room both autonomously and in coordination with open windows. External air is delivered to a room to maintain the quality of the indoor air and the thermal comfort of occupants. Indoor air quality is indicated by the concentration of carbon dioxide in a room, and in the classrooms measured for this study, mean CO_2 concentrations during occupied hours are shown in Chapter 5 to be 682 ppm in summer months and 1350 ppm in winter months. It is clear that the air quality and ventilation is better in these classrooms in summer months than in winter months, although the exact difference cannot be quantified by these values. The CO_2 concentration was found in Chapters 5 and 6 to be a function of the position of the Windcatcher dampers and the presence of open windows. The number of open windows is related to the external air temperature (see Figure 6.18, p. 203), and the position of the damper is determined by the internal air temperature. However, the ability of the dampers to regulate the rate of air flow

through the Windcatcher system is not yet quantified, despite a study by Hughes & Ghani (2009) who used CFD to investigate the effect that dampers have on overall flow rates through a Windcatcher. Their results confusingly suggest that a flow rate through the Windcatcher can be achieved when the dampers are fully closed. Furthermore, they model contra–rotating dampers, whereas the Monodraught Windcatcher system uses counter–rotating dampers. Hughes and Ghani also present several diagrams that indicate flow paths (see Figures 10 and 13, Hughes & Ghani, 2008) that clearly shows short circuiting in the space between the bottom of the duct partition and fully open dampers, but there is no indication of how this phenomena changes when the damper angle is reduced. Here, the quantity of short circuiting is expected to escalate with an increase in the space between the bottom of the duct partition and the dampers.

Currently, the control system increases the damper angle linearly at a rate of 20% per °C above the initial set point temperature, which corresponds to a non–linear increase in the free area of the damper. If it is assumed that the total flow rate through the damper is proportional to their free area ($\dot{Q}_T \propto A_d$), where A_d is the percentage free area of the volume control dampers, then the control system should be amended so that the free area of the dampers is increased linearly with each temperature set point, thus increasing the supply of air when the damper ange γ, is small (see Section 4.3, p. 143). The relationship between A_d and γ is described by Equation (4.3), which assumes that the dampers are flat plates of negligible thickness. Equation (4.3) is now rearranged to give

$$\gamma = \cos^{-1}(1 - A_d) \tag{7.1}$$

where, for a required damper free area of 20% ($A_d = 0.2$), the associated angle should be $\gamma = 37°$ rather than the value of $\gamma = 18°$ that is currently used. This simple change will allow more air to enter a room through the Windcatcher system at low damper angles, which is particularly important to ensure good IAQ in winter months when the temperature set point is higher than in summer months.

It may be argued that providing ventilation in the winter acts in opposition to the implementation of space heating. In Section 6.3 (p. 195) it was shown that for a class of 30 occu-

pants the minimum, mean, and purge ventilation rates of 0.09 m^3/s, 0.15 m^3/s, and 0.24 m^3/s, respectively, required by BB101 (DfES, 2006) will dissipate approximately 0.6 kW, 0.9 kW, and 1.5 kW of heat if $\Delta T = 5°C$. However, if occupancy levels falls below 30 then the required volume flow rate reduces, and so if the BB101 requirements are to be met while minimising heat losses by ventilation, a more intelligent control system is required that can implicitly determine the number of occupants in the room and calculate the volume flow rate required to deliver the per capita ventilation rate specified by BB101.

7.1.1 Demand Control Ventilation

Heiselberg (2004) suggests that increases in heating costs incurred from winter ventilation can be mitigated by demand controlled ventilation, thermal mass, embedded ducts, and/or heat recovery. Heat recovery systems are likely to be unfeasible for a Windcatcher because they would increase the pressure drop across the Windcatcher quadrants adversely affecting flow rates, and are also likely to be impractical because Windcatcher quadrants frequently switch from supplying to extracting air with small changes of wind incidence. Embedded ducts and thermal mass are architectural considerations and so are not considered here, although it is acknowledged that they may be useful. However, it is possible to control a Windcatcher using a demand control strategy, which has been shown to be effective by Haghighat & Donnini (1993) who controlled a mechanical ventilation system using a CO_2 based control strategy that did not worsen IAQ or thermal comfort and provided a 12% energy saving. Mysen *et al.* (2005) show a 28% reduction in the energy consumed by a mechanical ventilations system measured in 157 classroom from 81 schools when controlled by CO_2 based demand control ventilation. Applying a demand control strategy to a classroom would minimise heat losses; for example, the heat lost from a room with varying flow rate per occupant is given in Figure 7.1 (p. 217), and shows for a ventilation rate of 5 l/s – person (the mean rate required by BB101) and $\Delta T = 10°C$, the energy lost through ventilation is approximately 62 W – person. This loss could be recouped by incidental heat gains from ICT equipment and the metabolic heat of occupants. In fact, BB87 (DfEE, 2003) suggests that "pupils in a classroom will compensate for all fabric losses and a major part of ventilation heat losses." Heat gains from a child are not given in CIBSE environmental guidelines, but a single male or female adult occupant, seated and doing light work is estimated to generate a total heat

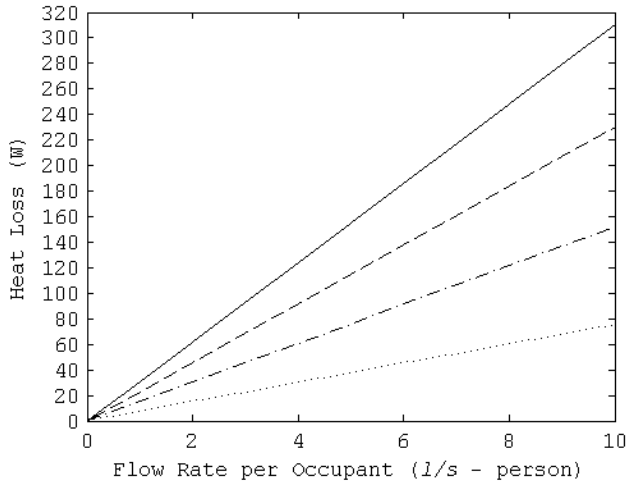

Figure 7.1: Heat lost from a room with varying ΔT. ——, $\Delta T = 20°C$; – – –, $\Delta T = 15°C$; – · – ·, $\Delta T = 10°C$; · · · · · ·, $\Delta T = 5°C$.

gain of 115 W (see Table 6.3 CIBSE, 2006a, for specific guidance). A similar argument is also made by Liddament (2009) who asserts that "provided the building is well insulated and the ventilation is occupant controlled, the energy impact of natural ventilation is manageable and does not require a complex mechanical strategy." As an example, Liddament discusses a new school built to the passivhaus air tightness standard but abandoned its original ventilation strategy that employed mechanical ventilation with heat recovery because the internal heat gains were found to be sufficient to overcome heat lost via the revised natural ventilation strategy, see also Bailey (2009).

A demand control strategy must provide a required ventilation rate and CO_2 concentration automatically using an autonomous Windcatcher. Here, it is expected that the use of manually opening windows in coordination with a Windcatcher will ensure that ventilation rates over and above the mean required rate are delivered, and so compliance with a purge ventilation requirement is assured. Figure 7.2 (p.218) describes a simple control logic for CO_2 based demand control ventilation. As the CO_2 concentration in a room rises from a prescribed minimum level $CO_{2\,min}$, to a prescribed maximum concentration $CO_{2\,max}$, the total ventilation rate $\dot{Q}_T$ through a room also increases until $CO_{2\,max}$ is maintained at a steady–state or diluted. In Section 6.3.1 (p. 205) it was recommended that the CSA of the

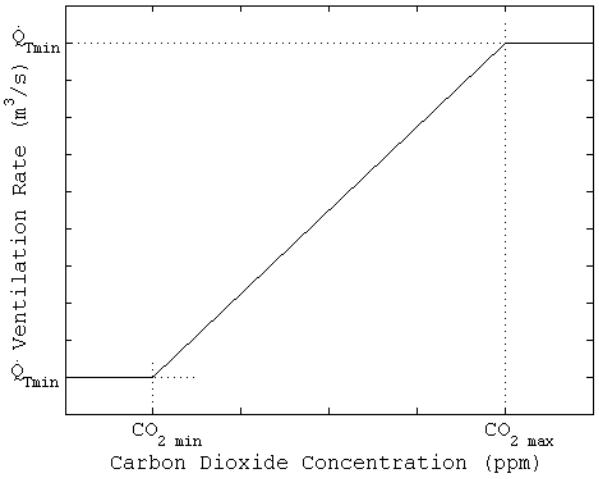

Figure 7.2: Control logic for CO_2 based demand control ventilation (Kolokotroni *et al.*, 2007)

.

Windcatcher is selected based upon its ability to supply a required mean ventilation rate autonomously, and so if the design procedure has been followed the required mean ventilation rate is supplied by a Windcatcher when its volume control dampers are fully open. Therefore, $CO_{2\,max}$ should correspond to the CO_2 concentration expected in a room when occupied by a prescribed number of occupants (design occupancy). The choice of $CO_{2\,min}$ is more arbitrary, but the dampers should start to open before $CO_{2\,max}$ is reached to give them and the system a chance to adjust. For example, the mean ventilation rate required in a classroom is 5 l/s – person, which for a class of 30 students and staff equates to a ventilation rate of approximately 0.15 m^3/s, and a steady–state CO_2 concentration of approximately 1500 ppm (see Liddament, 1996, Figure 2.4), and so $CO_{2\,max} = 1500$ ppm. Linear interim set points are now arbitrarily set at 100 ppm intervals giving $CO_{2\,min} = 1000$ ppm, with an increase of 20% free damper area at each additional increase of 100 ppm, see Table 7.1 (p. 219). Using Equation 4.5 and Table 7.1 the effect of using a CO_2 based control strategy in a classroom ventilated by an autonomous Windcatcher is estimated in Figure 7.3 and is compared in Figure 7.4 (both p. 219) against an identical classroom ventilated at a background ventilation rate. Here, each classroom has a volume V=230 m^3 and a background ventilation rate of 0.3 ACH or $\dot{Q}_I = 0.0191 m^3/s$, which are equal to the mean volume and background ventilation rate for the case study classrooms, see Tables 4.2 (p. 140) and D.1 (p. 287). The

Table 7.1: Control set points for CO_2 based strategy.

Setpoint	CO_2 Concentration (ppm)	Damper Free Area A_d (%)	Damper Angle γ (°)
$CO_{2\,min}$	1000	0	0
	1100	20	37
	1200	40	53
	1300	60	66
	1400	80	78
$CO_{2\,max}$	1500	100	90

external CO_2 concentration is assumed to be $C_E = 400\,\text{ppm}$, and a rate of CO_2 production of $G = 5.5\,\text{cm}^3/\text{s}$ has been chosen to achieve a steady state CO_2 concentration of 1500 ppm when the maximum possible ventilation rate is $\dot{Q}_{Tmax} = 0.15\,\text{m}^3/\text{s}$. The choice of value for G is used to illustrate a point rather than for complete accuracy, but Griffiths & Eftekhari (2008) show that $G = 5.4\,\text{cm}^3/\text{s}$ is typical for an adult and $G = 4.1\,\text{cm}^3/\text{s}$ is typical for a child, and so demonstrates that the value chosen for G is realistic. Finally, the ventilation rate $\dot{Q}_T$ through the demand controlled classroom is estimated by

$$\dot{Q}_T = \dot{Q}_I + \left(\dot{Q}_{Tmax} - \dot{Q}_I\right) A_d \tag{7.2}$$

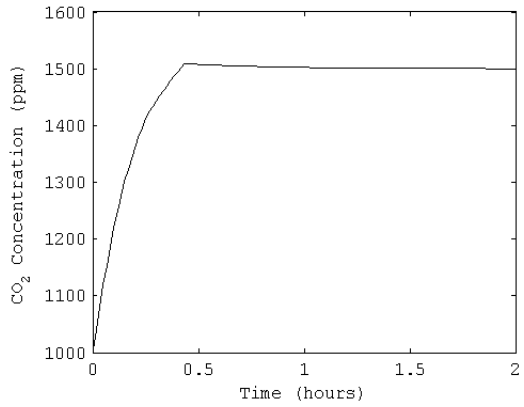

Figure 7.3: Predicted CO_2 concentration in a classroom with demand controlled ventilation.

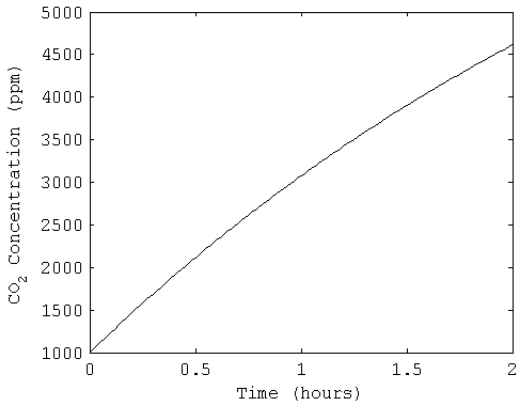

Figure 7.4: Predicted CO_2 concentration in a classroom with background ventilation.

where A_d is the free area of the damper (%), and the ventilation rate $\dot{Q}_T$ is assumed to be steady–state, see Figure 7.2 for further clarification. Figure 7.4 shows that with no Windcatcher ventilation the CO_2 concentration continues to rise past the required mean concentration of 1500 ppm and will eventually pass the maximum level of 5000 ppm specified by BB101. Using Equation (4.5) it is possible to show that the concentration in a room will eventually reach a steady–state C_{ss}, when

$$C_{ss} = \frac{G}{\dot{Q}_I} + C_E \tag{7.3}$$

and so in the classroom ventilated by background ventilation $C_{ss} = 9040$ ppm. Figure 7.3 predicts that by opening the Windcatcher dampers in accordance with Table 7.1 the increase in Windcatcher ventilation fully arrests the increase in CO_2 concentration so that it settles at a steady–state concentration of 1500 ppm. A ventilation effectiveness of unity [uniform mixing throughout a room, see CIBSE (2006a, Table 1.10)] has been assumed during this example, but in reality the mixing ventilation effectiveness could be less than unity and so it may be prudent to reduce $CO_{2\,max}$ to 1400 ppm, see Mysen *et al.* (2005).

A further improvement to the strategy is the addition of a fail–safe system that automatically opens a number of windows to provide purge ventilation when a dangerously high CO_2 level is reached. In a school classroom this would occur when the CO_2 concentration reaches 5000 ppm, the maximum value specified by BB101. Such a concentration will arise if the conditions in the room deviate away from those considered during the design process. Firstly, if the ventilation rate falls below the required mean rate, the CO_2 is not adequately diluted. Secondly, if the occupancy levels increase above those that have been designed for, the generation of CO_2 by occupants G, also increases and so Equation (7.3) shows that the steady–state level will rise above CO_{2max}. Finally, if the metabolic rate of the occupants increases, perhaps because of an increase in activity intensity, then G and the steady–state CO_2 level C_{ss}, increase similarly. Consideration should also be given to the provision of automatic purge ventilation during unoccupied periods to bring the internal CO_2 concentration back to ambient levels. This could be done during break times or at night, but the current control

system only allows an occupant to either activate the manual override that fully opens the Windcatcher flow control dampers or to open a window. Therefore, automatically opening façade windows in coordination with the Windcatcher dampers will deliver purge ventilation without occupant input.

A cheaper alternative to demand control ventilation is to engage the occupants; for example, an intervention study in The Netherlands (Geelen *et al.*, 2008) shows that occupant engagement produced a limited improvement in the IAQ of 81 primary school classrooms using a teaching package and/or a CO_2 indication device. However, an educational strategy is only likely to have limited application, because it faces challenges from staff turnover and the high levels of class rotation by teachers of secondary (high) school children. Education is certainly required to inform occupants on the Windcatcher system's capability and how the override system functions, and this could have an important part to play in the management of occupant expectations. Although it may be reasoned that the teachers and students who occupy a school classroom should concentrate on the processes of learning rather than managing their ventilation system, giving them control over their environment is very important, see Brager & De Dear (1998). In fact, Mavrogianni (2007) suggests that the efficient control of a natural ventilation system translates into an increase in operability and is the most important way to enhance thermal comfort in school environments. The CO_2 indication device used by Geelen *et al.* (2008) is a traffic light warning system that displays a green, amber, or red light emitting diode to indicate optimal, moderate, or poor IAQ. While it could be argued that warning occupants of poor IAQ may have commercial implications for a product such as a Windcatcher, recognition of the limitations of natural ventilation suggests that this is a sensible option which would guide occupants to open windows in coordination with the Windcatcher. In a school classroom the traffic light warning system could be used to indicate amber when the internal CO_2 concentration exceeds 1500 ppm and red when it exceeds 5000 ppm. Alternatively, in an office environment the warning system could be indicate air quality categories given by BS EN 15251 (BSI, 2007). If the office was designed to meet category II conditions (normal level of expectation, 7 l/s – person) the warning device could indicate amber for category III conditions (acceptable level of expectation, 4 l/s – person) and red for category IV conditions (acceptable at limited times of the year, <4 l/s – person).

Finally, it should be noted that if an occupant activates the Windcatcher override, the

Windcatcher dampers open fully for a pre–defined period of time (15 minutes in winter months) which could be draughty and/or lead to excessive heat loss. This highlights the argument for the use of CO_2 sensors and a full demand control strategy.

7.1.2 Dynamic Comfort Control

The literature review (see Section 2.1.1, p. 29) shows that the thermal comfort of occupants is related to links with the outdoor environment visually through windows, and thermally by wearing seasonal clothing and by making use of environmental adjustments by opening or closing windows. CIBSE Guide A (CIBSE, 2006a, Table 1.5) recommends a bandwidth of internal operative temperatures for heated buildings in winter months and air conditioned buildings in summer months. The operative temperature T_O, also known in the UK as the dry resultant temperature, is often used to show thermal comfort and is defined by Santamouris & Asimakopoulos (1996) as the uniform temperature of a hypothetical space at which a person will exchange the same dry heat by convection and radiation as that in the actual environment. It calculated by a weighted average of the internal air temperature T_I, and the mean radiant temperature T_R, which encompasses the average effect of radiation from surfaces in a room (McMullan, 2002). T_O should be measured at several points around the room (CIBSE, 2006a), so that an accurate value is derived, using a thermometer whose sensor is situated inside a blackened globe with an optimum diameter of 40 mm (see Humphreys, 1977). The operative temperature is given by

$$T_O = \frac{T_I\sqrt{10\,u_I} + T_R}{1 + \sqrt{10\,u_I}} \tag{7.4}$$

where u_I is the air speed in a room, which has a recommended upper limit of 0.8 m/s (Santamouris & Asimakopoulos, 1996). For an air conditioned (mechanically ventilated) school classroom T_O is recommended to be between 19–21°C in the heating season and 21–23°C in the cooling season (CIBSE, 2006a). Specific temperatures are not given by CIBSE Guide A for free–running, naturally ventilated, buildings because T_O is known to be related to an exponentially weighted running mean of external temperature, see McCartney & Nicol (2002). The running mean $\bar{T}_{rm}$, is given by

$$\bar{T}_{rm} = (1 - \alpha_{rm})\,(\bar{T}_{E-1} + \alpha_{rm}\bar{T}_{E-2} + \alpha_{rm}^2\bar{T}_{E-3}\,\cdots) \tag{7.5}$$

but may be simplified to [see Lomas & Ji (2009)]

$$\bar{T}_{rm} = (1 - \alpha_{rm})\,\bar{T}_{E-1} + \alpha_{rm}\,\bar{T}_{rm-1} \tag{7.6}$$

where α_{rm} is the running mean constant (normally $\alpha_{rm} = 0.8$), $\bar{T}_{E-1}$ is the daily mean external temperature for the previous day, and $\bar{T}_{rm-1}$ is the running mean for the previous day.

CIBSE Guide A (CIBSE, 2006a) gives two simple algorithms for the heating and free–running (no heating or cooling) seasons that apply the running mean $\bar{T}_{rm}$, to determine an upper operative temperature limit T_{Omax}, and a lower limit T_{Omax} in a naturally ventilated building. For a naturally ventilated building operating in free–running mode, the upper and lower limits are

$$T_{Omax} = 0.33\,\bar{T}_{rm} + 18.8 + 2^{\circ}\mathrm{C} \tag{7.7}$$

and

$$T_{Omin} = 0.33\,\bar{T}_{rm} + 18.8 - 2^{\circ}\mathrm{C} \tag{7.8}$$

whereas during the heating season the limits are amended to

$$T_{Omax} = 0.09\,\bar{T}_{rm} + 22.6 + 2^{\circ}\mathrm{C} \tag{7.9}$$

and

$$T_{Omin} = 0.09\,\bar{T}_{rm} + 22.6 - 2^{\circ}\mathrm{C}. \tag{7.10}$$

These algorithms are illustrated in Figure 7.5 showing a bandwidth of 4°C for both seasons, and is noted as being identical to a category I (high level of expectation) building for $X = 2$°C, see BS EN 15251 (BSI, 2007). In summer, the gradient of the relationship is 0.33 and so the daily change to the internal operative temperature is limited to 33% of a change in the rolling mean $\bar{T}_{rm}$, whereas in winter the daily change in the internal operative temperature is limited to 9% of a change in the rolling mean $\bar{T}_{rm}$, see Figure 7.5. The limits of the internal operative temperature will vary throughout the year and this is illustrated in Figure 7.6 (p. 225) which uses the CIBSE TRY data base (CIBSE, 2005b) for London to calculate the daily mean temperature $\bar{T}_E$, running mean $\bar{T}_{rm}$, and upper and lower limits of operative temperature, T_{Omax} and T_{Omin} where $\alpha_{rm} = 0.8$ and $X = 2$°C. $\bar{T}_{rm}$ is calculated using Equation (7.6), $\bar{T}_E$ is calculated from 0000–2359 hrs each day, and the free–running period is set from April to October inclusively when Equations (7.7) and (7.8) are used to calculate T_{Omax} and T_{Omin}, respectively. At all other times Equations (7.9) and (7.10) are used.

Figure 7.6 shows that $\bar{T}_{rm}$ lags behind changes in $\bar{T}_E$ with the hottest day occurring on the 26$^{\text{th}}$ June, whereas the hottest rolling mean day arises on the 20$^{\text{th}}$ August after a

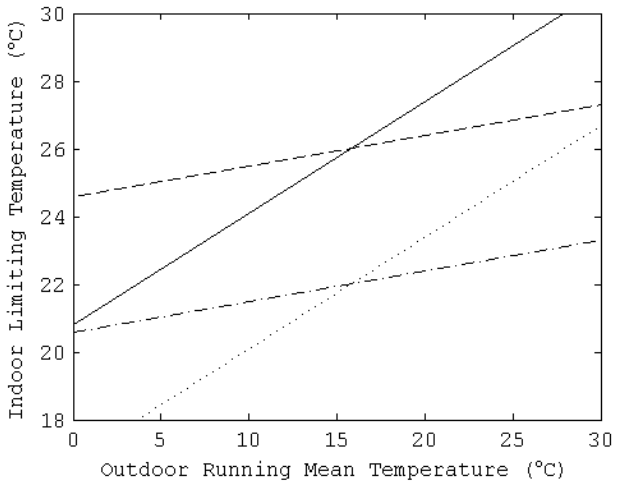

Figure 7.5: Operative temperature related to the outdoor running mean temperature (CIBSE, 2006a). ——, free–running upper limit; · · · · · ·, free–running lower limit; – – –, heated upper limit; – · – ·, heated lower limit.

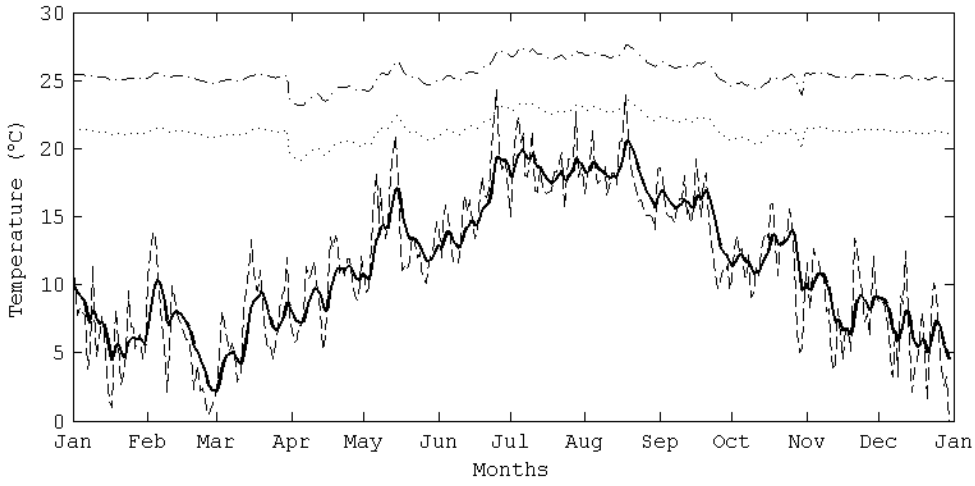

Figure 7.6: Relationship between the external temperature and the indoor comfort temperature (CIBSE, 2006a). ——, running mean external temperature; – – –, daily mean external temperature; – · – ·, upper limit internal operative temperature; · · · · · ·, lower limit internal operative temperature.

more prolonged period of high temperatures. This demonstrates that it is more important to provide efficient cooling to a building when the rolling mean is high rather than when the daily temperature is high because the rolling mean value is an historic indicator of temperature. BB101 sets the threshold air temperatures for a classroom at 32°C, which must never be exceeded, and 28°C, which must not be exceeded for more than 120 hours during summer months to avoid over heating. In Figure 7.6 the maximum upper operative temperature limit T_{Omax} is predicted to be 28.6°C. The corresponding internal air temperature T_I, is shown by Equation (7.4) to depend upon the internal air speed u_I, and the radiant temperature T_R. In a well sealed building T_R is expected to be similar to the T_I (CIBSE, 2006a) and so T_I can also be expected to be approximately equal to 28.6°C. However, the cooling effect of air moving over the skin is not accounted for by Equation (7.4), and so a corrective elevation must be applied, see Figure 7.7 (p. 226). Therefore, for an operative temperature of $T_O = 28.6$°C and $u_I = 0.8$ m/s Figure 7.7 shows that T_O must be elevated by 2.4°C so that $T_O = 31$°C. This calculated example illustrates that comfortable temperatures in a naturally ventilated room are broad and cannot be encapsulated by a single value. It also shows that the two upper temperatures set by BB101 are perhaps restrictive because it is shown here that when $T_I > 28$°C occupants can still be comfortable if the internal air speed is significant,

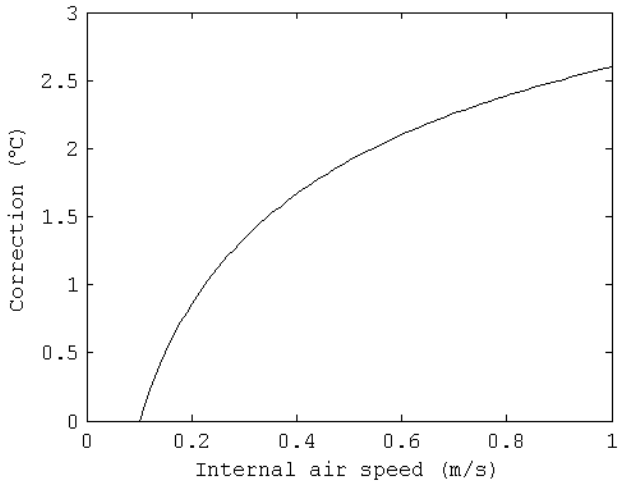

Figure 7.7: Correction to operative temperature to account for air movement (Extrapolated from CIBSE, 2006a).

$0.1 < u_I \leq 0.80$.

BS EN 15251 (BSI, 2007) also uses Equations (7.7) and (7.8) to determine T_{Omax} and T_{Omin}, but are applied according to the magnitude of the running mean $\bar{T}_{rm}$, where,

$$T_{Omax} = 0.33\,\bar{T}_{rm} + 18.8 + X°\text{C} \quad \text{when} \quad 10°\text{C} < \bar{T}_{rm} < 30°\text{C} \tag{7.11}$$

and

$$T_{Omin} = 0.33\,\bar{T}_{rm} + 18.8 - X°\text{C} \quad \text{when} \quad 15°\text{C} < \bar{T}_{rm} < 30°\text{C} \tag{7.12}$$

The variable X is determined by the category of the room and is 2, 3, or 4°C for a category I, II, or III space, respectively. When the running mean is outside of the ranges given in Equations (7.11) and (7.12) the operative temperature limits for an air conditioned building are applied. Here, CIBSE Guide A (CIBSE, 2006a) sets the temperature bandwidth for a category II room such as school classroom to be T_O =19–21°C, and this is shown in Figure 7.8 (p. 227). The limits of operative temperature vary throughout the year and so the calculations of daily mean temperature $\bar{T}_E$, running mean $\bar{T}_{rm}$ made using the CIBSE TRY

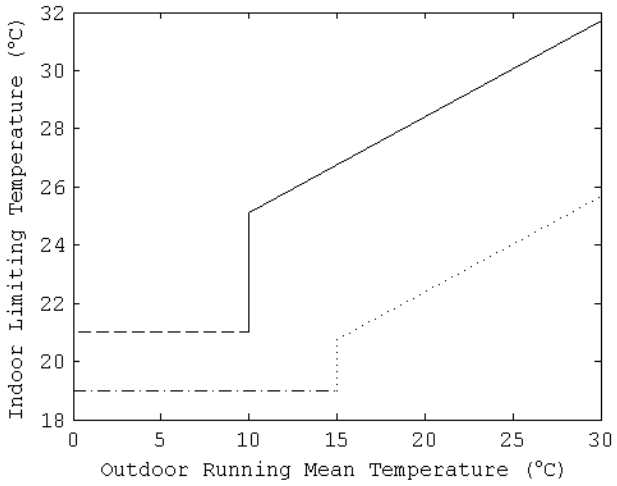

Figure 7.8: Operative temperature related to the outdoor running mean temperature for a category II building (BSI, 2007). ——, free–running upper limit; · · · · · ·, free–running lower limit; – – –, heated upper limit; – · – ·, heated lower limit.

database (CIBSE, 2005b) for London and given in Figure 7.6 are re–presented in Figure 7.9. The upper and lower limits of operative temperature, T_{Omax} and T_{Omin} are predicted using

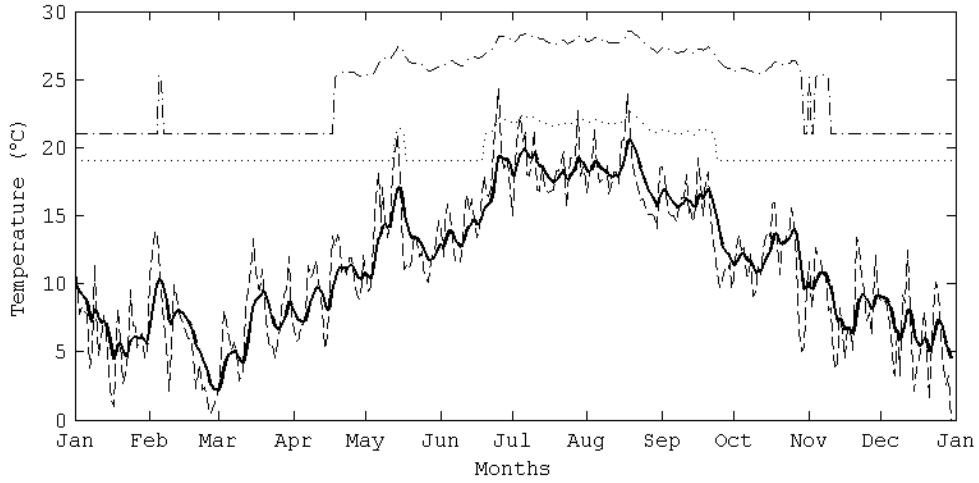

Figure 7.9: Relationship between the external temperature and the indoor comfort temperature (BSI, 2007). ——, running mean external temperature; – – –, daily mean external temperature; – · – ·, upper limit internal operative temperature; · · · · · ·, lower limit internal operative temperature.

Equations (7.11) and (7.12) where and $X = 3°C$ for a category II (normal level of expectation) school classroom.

Figure 7.9 shows a clear difference between the upper and lower operative temperatures for the summer and winter months. In the summer the bandwidth is given by $X = 3°C$ for a category II building, whereas in the winter Equations (7.11)—(7.12) do not apply and the difference between the upper and lower limits is fixed at 2°C. Based on these limits, providing thermal comfort in the winter using a natural ventilation strategy is a real challenge, and in an effort to maintain such a narrow temperature range the consequence is low ventilation and poor indoor air quality.

A comparison of the two adaptive models shows that the BS EN 15251 model predicts a greater temperature tolerance in early and late summer months (according to the category of the space), but also predicts a narrower temperature tolerance in winter months. The CIBSE model is restrictive in its application to different types of building giving category I bandwidth throughout the year. Furthermore, the model is unable to automatically determine the season requiring direct user input or pre–definition of the seasons. The winter operative temperature bandwidth is very high (21–25°C) and so controlling a Windcatcher using the current temperature set points (outlined in Table 4.5, p. 147) will vary the angle of the volume control dampers between 0–60°, equivalent to 0–50% of free damper area. The primary advantage of the BS EN 15251 adaptive model over the CIBSE model is its ability to predict appropriate heating and free–running seasons using the temperature ranges given in Equations (7.11) and (7.12), but the full application of either model into a Windcatcher system is impracticle at the present time.

The first argument against full implementation is the difficulty in measuring the internal operative temperature. Clear advice is given for the size of the blackened globe, which should be 40 mm in diameter with a the thermometer placed at its centre (Humphreys, 1977), and international standard BS EN 7726 (BSI, 2001) suggests that when the internal air speed is low (u_I <0.1 m/s) T_O can be approximated by the radiant temperature T_R. However, in a naturally ventilated building u_I is not normally low; Santamouris & Asimakopoulos (1996) suggest that air speeds can gust to much higher magnitudes. Secondly, there is little advice on how many thermometers are required in a room or where should they be placed. Finally, the cost, security, and size of radiative and operative thermometers are prohibitive—the former

thermometer uses a heated sensor consisting of a reflective gold–plated disc and an absorbing matt black painted disc (see BSI, 2001, Section C.2.1).

The partial incorporation of an adaptive model into the Windcatcher control system is a more expedient option. Lomas & Ji (2009) use the BS EN 15251 adaptive model to predict over heating in hospitals in summer months as part of the design process. Similarly, it could be incorporated into the Windcatcher design process to ensure that thermal comfort requirements are met, thus giving customers an indication of compliance with thermal standards. However, its most useful trait is its ability to predict changes in the season and unseasonal hot and cold spells. It should also be applied to trigger additional night cooling ventilation, which it is currently implemented congruous to a pre–defined summer season and not according to the actual need for it. For example, a cold summer requires less additional cooling whereas an unseasonal hot spell requires additional cooling. Givoni (1994) states that night ventilation should be implemented when the measured internal operative temperature exceeds the upper comfort limit T_{Omax}, however he remains sceptical about the benefits of this type of strategy in warm humid environments where the diurnal temperature difference is less than 15–20°C, as it is in the UK. The Windcatcher systems offer night ventilation as a by–product of its daytime capability, and so it is sensible to make use of this capacity to cool exposed thermal mass in medium and heavyweight buildings or to temper the air temperature in lightweight buildings such as schools. The first determining factor for night cooling should be the heating strategy; if the heating is off, then night cooling can be considered. The second determining factor should be the season; Figure 7.9 indicates that the building should enter free–running mode around the middle of April when $\bar{T}_{rm} > 10$°C—see the condition for Equation (7.11)—and at this point the summer strategy should start. The third consideration should be the maximum internal operative temperature T_{Omax}; if the internal operative temperature $T_O > (T_{Omax} - Y)$, where Y°C is a tolerance variable, then the night ventilation strategy should be implemented. The exact value of Y is not absolute and must be determined by empirical and/or theoretical experimentation. The full potential of night cooling using a Windcatcher system can only be realised using a cross–ventilation strategy, and this is discussed in Section 7.3.

This section has shown that the optimum temperature for the maintenance of thermal comfort among occupants is not only related to an air temperature, such as those specified

by BB101, but also to the radiant temperature T_R, and the air speed in a room, u_I. Their joint effect is combined in a weighted average known as the operative temperature, T_O. Furthermore, occupants of naturally ventilated buildings can adapt to their environment as the external temperature T_E, changes over time. When a naturally ventilated building is in free–running mode, T_O is also shown to be related to a weighted running mean $\bar{T}_{rm}$, of the daily mean external temperature, $\bar{T}_E$. Upper and lower limits of T_O are proposed by CIBSE (2006a) and, more recently, by BS EN 15251 (BSI, 2007) for the heating and free–running seasons. These temperatures can be applied to ensure the successful control of a Windcatcher system; for example $\bar{T}_{rm}$ can be used to show when night cooling is appropriate and to automatically determine the heating season. Here, Figure 7.9 has been used to show that the summer season starts around the middle of April when $\bar{T}_{rm} > 10$°C because after this point $\bar{T}_E$ continues to rise steadily. Similarly, Figure 7.9 can also be used to estimate the start of the heating season, which occurs in late September when $\bar{T}_{rm} < 15$°C, because after this point the $\bar{T}_E$ continues to fall steadily. In Section 7.1.1 demand control ventilation was discussed and it was proposed that the Windcatcher dampers should open based upon the per capita ventilation rate indicated by the internal CO_2 concentration. Currently, the summer temperature set point is 16°C and the results presented in Chapters 5 and 6 show no reasons why this should be changed. However, heat energy must be conserved in winter and so the temperature set point should be higher than that used in the summer. CIBSE Guide A (CIBSE, 2006a) suggests that the upper operative temperature limit for a school classroom in winter should be 21°C, and currently the Windcatcher system uses an air temperature of 21°C as an initial set point, see Table 4.5 (p. 147). It is suggested that this set point should not be changed. Note that the BS EN 15251 standard is considered here because it is the most recent and may be considered to be a revision of the CIBSE adaptive model. When the Windcatcher dampers are closed the initial air temperature and the prescribed operative temperature can be considered to be the same because u_I is be expected to be low. Therefore, if the air and operative temperatures rise above the prescribed upper limit of 21°C for a school classroom (see CIBSE Guide A and Figure 7.9) then some discomfort can be expected to occur, and so the Windcatcher dampers should open to dissipate unwanted heat and provide a limited increase in the internal air speed. Here, the winter set points given in Table 4.5 (p. 147) that specify a 20% increase in free damper area per °C above 21°C should

be used and the correct damper angle calculated using Equation (7.1).

These recommended applications allow the current system to remain relatively unchanged physically, but will require some new firmware. The changes will produce an improvement in performance over the current system providing adequate ventilation for the maintenance of personal performance, health, and thermal comfort.

7.2 Providing Efficient Ventilation Flow Paths

Thermal comfort issues often arise when naturally ventilating a room in winter because the difference between the internal and external air temperatures is large ($T_I \gg T_E$). This is particularly relevant for occupants located in the region close to the diffuser, known as the draught–risk zone (Schild, 2004). The Windcatcher diffuser is a grill that acts more as a security system than as a nozzle designed to affect changes in the dynamic properties of the incoming air. The grill directs the incoming air down towards the floor (see Elmualim, 2005b, Figure 6) where it could be uncomfortable for occupants situated nearby because it raises the required operative temperature. For example, Figure 7.7 shows that an air speed of 0.2 m/s raises the required operative temperature in a room by around 1°C and so a Windcatcher diffuser should dissipate incoming flow away from the occupants. However, there is an advantage to the provision of top–down mixing–ventilation by an autonomous Windcatcher in winter because it allows cold incoming air to gradually dilute the warm internal air (see Gage *et al.*, 2001). Furthermore, mixing–ventilation is shown by Woods *et al.* (2009) to be a more energy efficient method of introducing cold air into a room when compared to displacement ventilation. Therefore, mixing ventilation should be encouraged in the winter months to reduce energy consumption and thermal discomfort, while providing good IAQ.

To achieve both thermal comfort and energy savings it is recommended that the design of the diffuser is investigated. Here, it is possible to convert the incoming flow of air into a jet using a radial nozzle. A jet is defined by Etheridge & Sandberg (1996, Section 7.10) as "the discharge of a fluid from an opening into a larger body of the same or similar fluid [...] driven by the momentum of the discharged fluid." When a jet is directed close to a surface such as a ceiling, it causes high speed rotational turbulence in the area between the edge of

the jet plume and the surface, which is shown by the Bernoulli equation to be at a lower pressure than the jet, see Figure 7.10. Accordingly, the jet entrains itself to the surface of the ceiling and the phenomena is known as the "Coanda effect" (see Etheridge & Sandberg, 1996, Section 7.10.2). Utilising the Coanda effect can increase the penetration or "throw" of a jet of air into the room and its mixing effectiveness (see Figure 7.11), while reducing uncomfortable draughts (Kolokotroni *et al.*, 2007).

The location of the diffuser determines the proportion of the room that is covered by the supplied air. Figure 7.12 (p. 233) shows a single diffuser located in a large room, where the penetration of the incoming air is insufficient to give adequate mixing and distribution. Here, Kolokotroni *et al.* (2007) suggest that a second diffuser should be added to spread the incoming air across a greater proportion of the room, see Figure 7.13. There are occasions where a room is better served by two smaller Windcatchers rather than a single large Windcatcher, and this should be investigated using CFD or empirical measurements to determine the mixing efficiency of air supplied from different diffuser locations and using different diffuser designs. The location of the diffuser may be restricted by the location of the duct in some instances; for example, if a room is located on the ground floor of a two (or more)

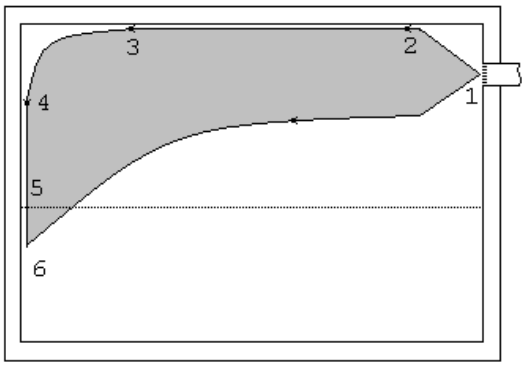

Figure 7.10: Mixing and distribution of supplied air using the Coanda effect. 1–2, near zone; 2–3, jet attached to ceiling; 3, jet detaches from ceiling; 4, jet attached to wall; 5, jet reaches occupied zone; 6, jet is mixed totally with room air (Kolokotroni *et al.*, 2007).

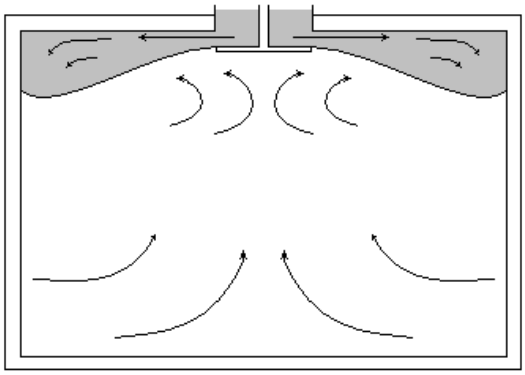

Figure 7.11: A diffuser that encourages jet attachment using the Coanda effect [Adapted from Etheridge & Sandberg (1996, Figure 7.27)].

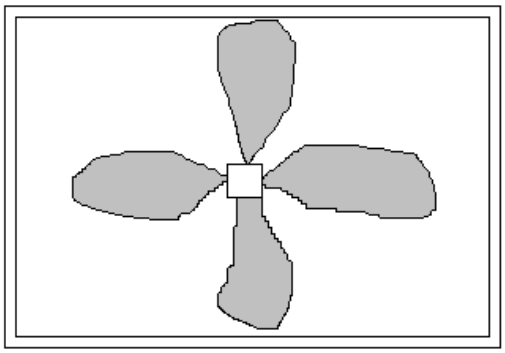

Figure 7.12: Plan view of the distribution of air in the occupied zone using ventilation from a single source (Kolokotroni *et al.*, 2007).

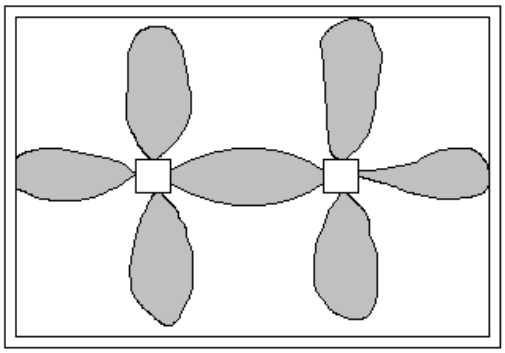

Figure 7.13: Plan view of the distribution of air in the occupied zone using ventilation from two sources (Kolokotroni *et al.*, 2007).

storey building, it is common practice to place the duct inside an extended cavity in the wall of the rooms on the higher floors. This places the diffuser at the edge of the room and may lead to poor air penetration and distribution when operating autonomously. This practice can be seen in fourteen of the twenty four classrooms studied here, see Appendix B (p. 271) for the floor plans of classrooms C1, C3, E1, E3, F1—4, H1, H3, and I1—4. Although such a location is less than ideal for mixing ventilation, if the diffuser is situated at the furthest possible distance from openable windows it is perfectly placed for effective cross/displacement ventilation. Section 2.1.3 and Figure 2.3 (p. 49) show that this distance should be less than 5 times the height of the room.

Displacement ventilation is provided by a Windcatcher in coordination with a low opening, such as an open window, located in an area of positive pressure so that air enters the room through the opening and leaves through all Windcatcher quadrants, see for example the flow paths given in Figure 3.17 (p. 97). When the supplied air is cold, it sinks under gravity spreading out across the floor rather than mixing with the warm air already present in the room, and so leads to a continuous upwards displacement of the warmer air that is analogous to filling a bath with water (Schild, 2004), see Figure 7.14 (p. 234). The rate at which the room is emptied under steady–state conditions is described by Hunt & Linden (1999), but in the presence of a continuous heat source, the supplied and extract zones of cold and hot air, respectively, form distinct and stable layers, see Figure 7.15 (p. 234) and Cook (1998,

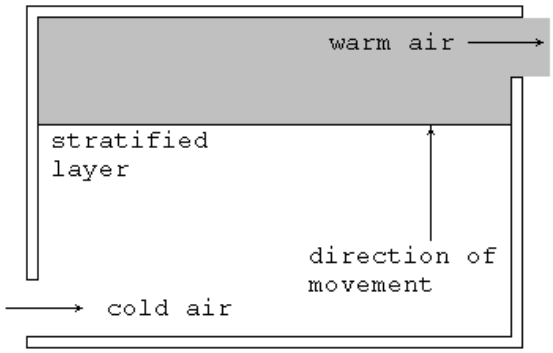

Figure 7.14: Removing warm air using displacement ventilation.

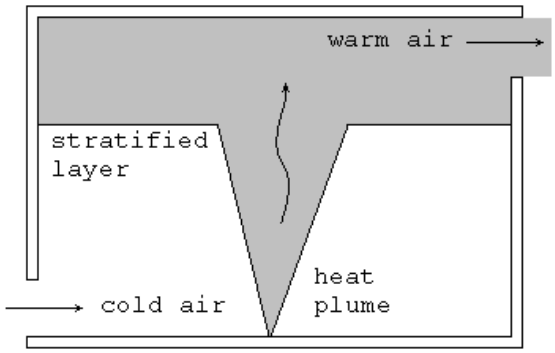

Figure 7.15: Removing warm air from a room with steady–state heat gains using displacement ventilation.

chapter 3). In the winter, cold air entering at low level is uncomfortable for occupants and energy inefficient. Figures 7.14 and 7.15 show simplified scenarios with a single opening on opposite façades, but the four quadrants of the Windcatcher can either supply or extract air according to a large number of factors that include the geometry of the building, direction of the wind, the strength of the wind driven and buoyancy forces, the cross section area of the Windcatcher, and the total area of the façade openings. Therefore, predicting the presence of either mixing or displacement ventilation is extremely difficult because some of these parameters can vary over a short period of time. In winter months, occupants should be advised that opening windows may cause thermal discomfort and waste energy, and so if additional ventilation is required they should be instructed to fully open the Windcatcher dampers using the wall mounted override control.

In summer months, displacement ventilation is the most suitable strategy because it enables hot stale air to be removed from a room at a greater rate than by using a mixing ventilation strategy. Displacement ventilation is achieved by using a Windcatcher in coordination with open windows when the wind is incident to the façade containing the windows so that $\tilde{C}_{p5} > 0$, where $\tilde{C}_{p5}$ is the scaled coefficient of pressure on the façade (see Figure 3.1, p. 73). Clearly, this cannot always be guaranteed; for example consider the flow paths given in Figures 3.12 and 3.13 (p. 89), which show that flow is not always uniformly extracted by the Windcatcher when $\tilde{C}_{p5} > 0$. Furthermore, Equation (3.73) shows that when $\theta = 0°$

displacement ventilation may only be achieved if $\tilde{C}_{p5} > C_{p1}$. Tables of façade wind pressure coefficients C_{p5}, given by Liddament (1996) show that the greatest value for a windward façade is $C_{p5} = 0.7$, which is found on a building of square aspect located in open countryside. Similarly, pressure coefficients for a Windcatcher are given in Table 3.3 showing $C_{p1} = 0.83$ when $\theta = 0°$. These values for C_{p1} and C_{p5} suggest that displacement ventilation is unlikely to be achieved when $\theta = 0°$, because $C_{p5} < C_{p1}$. It should also be noted that when C_{p5} is converted to $\tilde{C}_{p5}$ it reduces in magnitude, see Equation (3.19), making the condition more difficult to achieve. However, if $\theta = 45°$ when the wind is incident to two Windcatcher quadrants, Equation (3.114) shows that displacement ventilation is only possible when $2\tilde{C}_{p5} > C_{p1}$. Table 3.3 (p. 104) gives $C_{p1} = 0.31$ when $\theta = 45°$, and so displacement may only be achieved when $\tilde{C}_{p5} > 0.16$ which compares the pressure coefficient measured on the windward façade of a building of square aspect surrounded by obstacles equivalent to the height of the building, or a building of 2:1 aspect surrounded by obstacles equivalent to half the height of the building. Once this condition is met, Equation (3.114) gives a further requirement related to the CSAs of, and the losses through, the façade opening and the leeward Windcatcher quadrants. This relationship is displayed graphically in Figure 3.36 (p. 123) which shows the effect of the an increase in the opening A_5, located in an exposed façade on the overall ventilation rates. For $C_{p5} = 0.7$ and $\theta = 45°$ Figure 3.36 shows a sharp increase in the predicted flow rates when $A_0 \geq 0.4$, and this change in the gradient shows the transition from mixing to displacement ventilation. So, for a room in a building located in an exposed environment where $C_{p5} = 0.7$, if displacement ventilation is to be achieved the required opening area is $A_5 = 0.27\,\mathrm{m}^2$ or $A_5 = 0.40\,\mathrm{m}^2$ if the room is ventilated by an 800 mm or a 1000 mm Windcatcher, respectively. This shows that it is easier to achieve displacement ventilation with a Windcatcher of smaller CSA. Table 4.3 (p. 142) shows that the mean opening area of the windows in the case study classrooms is $A_5 = 1.06\,\mathrm{m}^2$, and so suggests that they are all capable of achieving displacement ventilation when $\theta = 45°$. To encourage displacement ventilation in summer months, occupants should be advised to open all available windows.

7.3 Improving the Windcatcher System

Table 3.5 on (p. 111) shows the predicted loss coefficients for a Windcatcher. The component that is estimated to cause the greatest losses in the Windcatcher system is the top (louvred) section, which converges, turns, and then diverges the flow of air as it enters the Windcatcher element. Losses in this section have to be balanced against the ingress of rain and debris, and their design has evolved over time to avoid this. Therefore, any changes aimed at lowering the head loss through this section are likely to increase the amount of rain and debris that enters through the louvres, which would be commercially unsatisfactory. Moreover, the addition of fittings designed to reduce head loss are unlikely to be of benefit. For example, turning vanes (see CIBSE, 2001) are designed to avoid the formation of eddies in an elbow, but would require modification to fit into the Windcatcher's triangular ducts. Their efficiency increases with higher flow rates, but because the Windcatcher is subject to gusts of wind and the air speed is relatively low in the ducts (see Figure 3.21, p. 105), the addition of turning vanes is very likely to be unsuccessful in consistently lowering the head loss. Consideration should also be given to the cost of installing precision fittings such as vanes because the Windcatcher is designed to be a relatively low cost–natural ventilation system, and so capital spent to gain relatively small reductions in head loss will compromise this business model.

One of the major issues highlighted in Chapter 6 is the reduced performance of autonomous Windcatchers with duct lengths greater than 1 m. It has been suggested in Section 6.1 (p. 186) that this is due to the short length of the partition, which does not extend for the full length of the duct. Consequently, the supplied air is simply taking the path of least resistance and is extracted by the Windcatcher through the leeward quadrants long before it reaches the room. Evidence for this is provided by the CFD analysis of Hughes & Ghani (2008, Figures 10 and 13) who show that short circuiting occurs between the area between the bottom of the partition and the top of the open dampers. To increase bi–directional flow through a Windcatcher and, therefore, to increase total ventilation rates through a room, the solution is to partition the ducts along their whole length. However, Hughes & Ghani (2008) show that short circuiting occurs even when the duct length is apparently short; the duct length is not given but diagrams intimate that they tested a duct with a length that was approximately 33% of the total element height. This suggests that if the partition is extended

to cover the whole length of a duct, then short circuiting will occur no matter how long the duct is. The source of this problem is the gap between the partition and the dampers. A solution is to remove this gap by connecting the partition directly to the diffuser. Clearly, this requires the removal of the dampers and eliminates the ability to control the volume of air entering a room, which is unsatisfactory. Another solution is a reduction in the gap loacted between the dampers and the diffuser so that when the dampers are fully open they are flush to both components.

Yet another possibility is to control the flow of air elsewhere, and here the Windcatcher element louvres could be used. A system of movable louvres would control air into the element in the same way that venetian blinds vary the amount of light entering a room through a window. When used with a rain sensor, the louvres would close in bad weather sealing the Windcatcher protecting the supplied room from rain, hail, sleet, or snow. Moreover, this would allow the louvres to be completely redesigned so that they are aerodynamically more efficient. A notable drawback in winter months is heat loss, and although this is to be expected when the Windcatcher is actively ventilating, unnecessary heat loss will occur through the duct to the loft cavity and the Windcatcher element when the Windcatcher is intentionally inactive and the the louvres are closed. Here, the duct can be lagged, but an efficient seal at ceiling level using dampers may still be required to avoid heat loss through the Windcatcher element.

The Windcatcher system is marketed and sold as a top–down ventilation system but the *in–situ* measurements and the semi–empirical predictions show that a Windcatcher used in coordination with façade openings can double the ventilation rate, see Section 6.2 (p. 191). In Section 7.1.1 the use of automatically opening windows was proposed to provide purge ventilation at break times or at night. Adding façade openings to the existing flow paths would accord greater control of the system and allow it to cope with deviations from the design criteria. There are security issues when opening windows at night and so an alternative is to use a duct through the façade wall protected by a security grill, see Cook & Short (2005). The volume of air though the opening is then controlled using a damper arrangement similar to that used by the Windcatcher, but with significantly improved insulating properties so that they conform to thermal and pressure test standards. The Queens Building at De Montfort University uses a retro–fitted radiator array in front of the opening to temper incoming air

in winter months, however Section 7.2 shows that it is not simple to predict the direction of the flow through the opening and so it is highly likely that this solution is inefficient for a Windcatcher system and should only be used in summer months. Then, it would significantly improve the ability of the Windcatcher system to perform night cooling, particularly when wind speeds are low.

7.4 Application of the Windcatcher to Other Non–Domestic Building Types

This thesis has explored the use of Windcatchers in schools, and specifically in school classrooms. The characteristics of a school classroom are reported in Chapter 4 and show that occupancy densities are very high when compared to other non–domestic building types such as offices (Clements-Croome *et al.*, 2008), and so a Windcatcher ventilation system must deliver a greater net ventilation rate to a classroom than is required by another type of room, such as an office. Accordingly, it can be reasoned that because a carefully designed Windcatcher system has been shown to provide sufficient ventilation to a classroom under specific conditions (see Chapters 5 and 6), it can also ventilate other non–domestic building types where the required net ventilation is lower; for example, offices, factories, and retail outlet all require 10 l/s – person (see CIBSE, 2006a) but have lower occupancy densities. However, the biggest opportunity for future applications of Windcatcher systems is likely to remain within the public sector because the British Government is committed to take action against climate change which includes a major reduction in energy consumption, see the NHS Carbon Reduction Strategy for England for example (NHS, 2009). It is highly likely that Windcatchers will continue to be installed in schools because the school construction programme will continue until 2020 (Mumovic *et al.*, 2009), see Section 2.1.2 (p. 34).

A further opportunity lies in healthcare buildings; the National Health Service (NHS) is the largest employer in Europe employing 1.3 million people and 5% of the UK work force. It currently occupies and manages 14,040 sites and is responsible for 3% of all UK CO_2 emissions and 30% of all public sector emissions. Approximately 44% of energy consumed in a typical NHS hospital is used for air and space heating and so one may expect climatic warming to lead to reduced consumption in winter months. However, an assessment of energy consumed

between 1999 and 2005 shows that overall consumption increased by 7% per annum; see Lomas & Ji (2009) for references of all figures. At this rate of growth, and at fixed prices, its energy costs are likely to double every 10 years. Accordingly, the Department of Health (DoH) has set stringent energy targets for all new and refurbished buildings and an energy reduction target of 15% from 2000 to 2010; a target which the NHS trusts are struggling to meet (NHS, 2009). Most NHS trust buildings are not air conditioned, which helps to reduce their energy demand, but renders their buildings potentially susceptible to climate change. Whereas healthy occupants can adapt to higher than normal temperatures and to heat waves, this is not necessarily so for the the occupants of a hospital who are sick, confined to bed, or have suppressed thermoregulatory systems. Furthermore, hospitals must provide a comfortable working environment for staff who may be involved in life threatening work. The challenge of reconciling the competing demands of curbing energy use and improving resilience to climate change is one that must be met by modern hospitals and the building services products that they employ.

A recent health technical memorandum (DoH, 2007) states that "natural ventilation is always the preferred solution for a space, provided that the quantity and quality of air required, and the consistency of control to suit the requirements of the space, are achievable." Some concern over airborne disease and cross infection in naturally ventilated buildings has, in the past, been a driver for the installation of mechanical ventilation systems in healthcare premises (NHS, 2009). However, current academic research suggests that there are a number of coexisting factors that can contribute to infection transmission and so it is difficult to completely rule out the possibility of transmission by routes unrelated to the type of ventilation, or to quantify the impact of ventilation on infection transmission rates (Li *et al.*, 2007). It is also suggested by the Patient Safety Agency that "true airborne infection is rare, what is fairly common is the direct route of infection" (Short & Al-Maiyah, 2009). In fact, there is growing concern about the healthiness of many mechanical ventilation systems because poor indoor air quality and unhygienic air supply conditions have been directly associated with poor maintenance (Roaf, 2007). In addition, pressurised mechanical ventilation systems have been linked in scientifically robust studies to the spread of a range of infectious diseases (Kumari *et al.*, 1998; Cotterill *et al.*, 1996). Clearly, there is scope to employ natural ventilation intelligently and a study by Short & Al-Maiyah (2009) suggests that up to 70% of net floor

area could be wholly or partly naturally ventilated.

Following the formation of the NHS Sustainable Development Unit (NHSSDU) and recent consultation with NHS stakeholders, it is recommended by Short & Al-Maiyah (2009) that displacement ventilation is used for clinical areas and mixing ventilation is reserved for non–clinical areas. Accordingly, a Windcatcher system should only be installed in non–clinical areas because it provides mixing ventilation when operating autonomously and pure displacement ventilation cannot be guaranteed when it is used in coordination with façade openings.

7.5 Immediate Application of this Work

Monodraught Ltd. are currently the market leader in the design and manufacture of advanced (top–down) natural ventilation systems for non–domestic buildings. It has sought to stay ahead of the competition by commissioning small pieces of academic work from Brunel (Kirk & Kolokotroni, 2004b; Kirk, 2004a), Reading (Elmualim & Awbi, 2002a), and Nottingham (Su *et al.*, 2008) Universities to investigate the performance of the Windcatcher system. Moreover, the research given here is now part of a long term company strategy that puts research at its core. Previously sales have driven the research, but now the opposite is true. This includes the way that Windcatcher strategies are designed and tendered. With increased market place competition and a desire by customers to be given more information, this strategy makes complete sense. For example, the steady–state semi–empirical model described in Chapter 3 and corroborated in Chapter 6 is now central to the Monodraught design strategy. It was shown in Section 6.3 that by applying weather data suitable for analysing the environmental performance of buildings, the semi–empirical model can be used to predict ventilation rates over a period of time, thus becoming a quasi–dynamic model. This idea is now being implemented further by applying the semi–empirical model to an independent steady–state thermal model (not discussed here), which when used in conjunction with TRY and DRY weather data (CIBSE, 2005b) will also make quasi–dynamic predictions.

It is predicted that this knowledge, which has been derived independently from Monodraught, and with academic rigor, will have a positive impact by

- Giving context to Windcatcher systems and their performance (see Chapters 1 and 2);

- Quantifying the performance of a Windcatcher system *in–situ* (see Chapters 4, 5, and 7);
- Predicting the performance of a Windcatcher system and corroborating the predictions using measurements made *in–situ* (see Chapters 3 and 6);
- Presenting a simple, straight forward design process (see Chapter 6);
- Showing how the Windcatcher system can be used effectively and efficiently according to the season (see Chapter 7), which will lead to improved performance;
- Identifying future development work and research projects (see Chapters 7 and 9);
- Invoking confidence in stakeholders when specific claims about the Windcatcher system are made;
- Producing marketing material;
- Contributing to increased sales.

When tendering Windcatcher strategies for UK buildings there is an increasing number of requirements to be met, and this is particularly so for school buildings. The statutory requirements have been discussed in Chapter 2 and the Windcatcher performance compared against them throughout this document. However, school designs now have to be reviewed by the Commission for Architecture and the Built Environment CABE (2009a,b,c) and must achieve a *very good* rating when assessed against the Buildings Research Establishment Environmental Assessment Method (BREEAM) criteria. BREEAM (BRE, 2008) is a measure of sustainability made at the design stage and credit is earned by implementing natural ventilation systems where possible. However, it remains only an aspiration because it does not close the loop by testing the performance of the building, although the presence of the measures that earned credits at the design stage are checked when the building is handed over. There may be many buildings that have received a *very good* rating but there is no indication that they achieve the awarded level of performance and sustainability in practice. The post occupancy assessment of the Windcatcher technology given here shows that if it is implemented using the methodology outlined in Section 6.3.1 then the building will conform

to the current standards. Furthermore, the expertise in measuring a Windcatcher system *in–situ*, developed during this project, can be applied if the loop is ever closed and the post occupancy assessment of a building and its systems becomes mandatory.

Chapter 8

Conclusions

The research has made a number of significant advances in the understanding of the performance of a natural ventilation Windcatcher. These conclusions are made in an order that allow direct comparison, where applicable, against the objectives of this thesis (see Section 1.5).

An analysis of existing literature that investigates Windcatcher performance empirically and theoretically is used to quantify and understand the performance of a Windcatcher. The flow rates one may expect through a Windcatcher and the coefficient of pressure on each Windcatcher face are identified and an assessment of the accuracy of this data is made.

A semi–empirical model is developed that combines a simple analytic model with experimental data reported in the literature. It is shown to perform well against a range of experimental data and CFD predictions and can be used as a quick iterative design tool. With this in mind, a simple expression for extract ventilation rates is proposed that neglects buoyancy effects, and so provides fast estimates of Windcatcher performance requiring no computational effort. The semi–empirical model predicts ventilation rates through a room ventilated by a Windcatcher in coordination with open windows, and estimates that this configuration is capable of significantly improving ventilation rates over and above those provided by an autonomous Windcatcher, and of delivering those rates typically required by building regulations in the UK.

Measurements of IAQ, ventilation, and noise made in twenty four classrooms of seven UK schools show that that a Windcatcher is generally capable of meeting the requirements

of UK standards BB101 and BB93. In summer months all classrooms met the CO_2 requirements indicating sufficient per capita ventilation. Measurements of the ventilation rate in each classroom with a Windcatcher operating autonomously show that 40% of measured classrooms meet the minimum 3 l/s – person requirement and 23% meet the 5 l/s – person requirement. If the Windcatcher is used in coordination with open windows, then all classrooms meet the 3 l/s – person requirement, 94% meet 5 l/s – person, and 77% meet 8 l/s – person under this arrangement. Furthermore, for the classrooms studied here, it is evident that a Windcatcher can aid in the delivery of ventilation rates that meet the UK standards during the summer time and this also extends to meeting European and US standards. However, the Windcatcher is rarely open during the winter months and although the maximum CO_2 limit of 5000 ppm is never reached, only 62% of classrooms meet the required mean CO_2 level of 1500 ppm. Measurements of ambient noise in twenty three classrooms with the Windcatcher dampers open suggest that the classrooms generally conform to BB93, although the sample size is relatively small and so there is probably insufficient data to conclude that Windcatchers do not represent a problem when meeting noise targets in schools. Finally, a Windcatcher is shown to offer the potential to significantly improve natural ventilation rates in school classrooms and to help them comply with IAQ standards for UK schools.

The predictions of ventilation rate by the semi–empirical model generally agree with those measured *in–situ*, but with three notable exceptions for a room ventilated by an autonomous Windcatcher. Firstly, ventilation rates are sometimes over–predicted. Secondly, the measured volume flow rates do not exceed $0.23\,\mathrm{m^3/s}$, and appear to plateau when $u_w \geq 2\,\mathrm{m/s}$. This is not predicted by the model and its cause is unclear. Thirdly, Windcatchers with long duct sections exhibit relatively poor performance and this was also not predicted by the model. In addition, when the Windcatcher is used in coordination with open windows the semi–empirical model tends to under–predict the ventilation rates. The experimental analysis of the Windcatcher demonstrates that Windcatcher performance can be significantly improved by the addition of open windows to a room, thus confirming the earlier theoretical prediction. This aspect is likely to help rooms ventilated by a Windcatcher meet ventilation standards for buildings, such as BB101 in the UK. In these circumstances the careful selection of C_p for a building is important for the accuracy of the semi–empirical predictions.

Typical wind conditions given by the CIBSE TRY weather series are applied to the semi–

empirical model to predict the ventilation performance of a room ventilated by a Windcatcher over any period of time, and is shown to be a useful design tool. It also identifies situations where the wind speed is negligible, and here the Windcatcher system must rely on buoyancy forces to generate ventilation through a room. When the semi–empirical model is used to investigate this situation, the unsealed model is found to be unsuitable for situations where $u_w \to 0\,\mathrm{m/s}$ and $|\Delta T| > 0°\mathrm{C}$. Instead, the sealed model may be used to estimate ventilation rates under these circumstances and although the predictions seem plausible, they remain uncorroborated by empirical measurement. Here, the predictions suggest that an autonomous Windcatcher is capable of providing minimum ventilation rates specified by BB101 for a class of 30 occupants, and a Windcatcher in coordination with open windows could provide the required minimum, mean, and purge ventilation rates. The investigation of the capabilities of the semi–empirical model has enabled the development of a series of steps that a designer can use to correctly size a Windcatcher for a particular application.

Chapter 9

Further Work

This chapter proposes further work based upon the analysis of Windcatcher performance presented in Chapters 2—7. Firstly, Section 2.3.2 highlights several key problems with the existing empirical measurements of a Windcatcher made in a wind tunnel. Therefore, the following research should be undertaken to:

- Re–evaluate the performance of a square Windcatcher ventilating a sealed room under controlled conditions, such as those experienced in a wind tunnel. Here, the equipment should be updated to use omni–directional velocity sensors, such as hot–wire anemometers, and state of the art pressure sensors.
- Extend the empirical analysis to re–analyse the performance of a Windcatcher with circular geometry, with and without fins.

Secondly, Chapters 6 and 7 shows gaps in the current knowledge of Windcatcher performance, and so research should be undertaken in the following areas:

- Investigate the reduced performance of a Windcatcher with a long duct section to determine the capability of a Windcatcher to provide bi–directional flow in these circumstances. Here, the partition should be extended for the full length of the duct and the possibility of connecting the partition to the diffuser should be considered.
- Quantify the flow attenuation of the volume control dampers for different free areas and angles.

- Investigate Windcatcher performance for buoyancy driven ventilation establishing flow paths and flow rates for varying ΔT.

- Determine methods of quickly calculating the coefficient of pressure (C_{p5}) on the façade of a building to help increase the accuracy of the predictions of the semi–empirical model for a Windcatcher ventilating a room in coordination with façade openings.

Thirdly, Chapter 7 suggests improvements to the Windcatcher system and identifies gaps in the current knowledge of Windcatcher performance. Therefore, further research should be undertaken in the following areas:

- The design of a diffuser to provide the efficient mixing of incoming air should be investigated, and should utilising the Coanda effect.

- The current louvre profile of a square Windcatcher has evolved to reduce the intake of water, debris, birds, and insects. The ability to seal the louvres in adverse weather would allow the most aerodynamic louvre profile to be used and eliminate the ingress of foreign bodies. Here, this research may utilise aerodynamic fins to increase the negative pressure areas on side and leeward Windcatcher faces.

Fourthly, Chapter 5 suggests that there is "probably insufficient data to conclude that Windcatchers do not represent a problem when meeting noise targets in schools." Accordingly, the following research into the acoustic properties of a Windcatcher system is proposed:

- Further measurements of continuous sound pressure levels measured over 30 minutes, in accordance with BB93, would help to provide a firm conclusions.

- This study concentrates on the comparison of noise transmission through a Windcatcher with the volume control dampers open and closed. The noise transmitted by open windows would provide a useful counterpoint to the data provided here by comparing the noise transmitted through a Windcatcher system with conventional ventilation openings.

- Further testing is required that includes a detailed acoustic analysis of the Windcatcher *in–situ* using the frequency domain. This would help to determine the frequencies that

are most readily transmitted from the surroundings into a room by a Windcatcher system. Furthermore, Section 2.1.4 shows that the polyurethane foam acoustic used to line Windcatcher duct sections is designed to attenuate mid and high frequencies and is expected to have mixed effects on low frequency traffic noise. This could also be quantified by a frequency analysis.

Finally, Chapter 5 shows that the Windcatcher is closed for the majority of the time in winter months. Consequently , Chapter 7 recommends the use of a demand control system that opens the Windcatcher volume control dampers according to the number of occupants present in a room, thus ensuring that per capita flow rates are provided. The following further research is proposed:

- Develop a suitable demand control natural ventilation system and test its performance by measurement and modeling. Here, an intervention testing methodology should be used to compare the performance of (i) a system offering no ventilation (ii) a temperature controlled system (iii) a demand controlled CO_2 based system. (iv) a demand and thermally controlled CO_2 and temperature based system. The performance in the summer and winter months should be verified and heat losses in winter shown by accurate modeling of the measured conditions using thermal modeling and CFD software.

- Further investigation into the measurement of the external temperature and the calculation of a rolling mean temperature is required. This would enable seasonal switch points to be incorporated into the control algorithm giving flexibility; for example, the Windcatcher would be able to adapt to an Indian summer, or provide night–cooling only when it is required to do so.

- Chapter 6 shows that the the most efficient ventilation strategy is that provided by a Windcatcher in coordination with façade openings such as windows. The addition of automatically opening windows, controlled by the Windcatcher system, would provide highly effective cross–ventilation for summer time heat dissipation and night cooling, see Chapter 7.

References

Ackermann, ME. 2002. *Cool Comfort: America's Romance with Air Conditioning*. Washington and London: Smithsonian Institution Press.

Andersen, A, & Hopkins, C. 2005. Sound Measurements and Natural Ventilation in Schools. *International Journal of Ventilation*, **4**(1), 57–70.

ANSI. 2002. *ANSI Acoustical Performance Criteria, Design Requirements, and Guidelines for Schools (S12.60–2002)*. Tech. rept. American National Standards Institute.

Apte, MG, Fisk, WJ, & Daisey, JM. 2000. Associations Between Indoor CO_2 Concentrations and Sick Building Syndrome Symptoms in U.S. Office Buildings: An Analysis of the 1994–1996 BASE Study Data. *Indoor Air*, **10**(4), 246–257.

ASHRAE. 2007. *ANSI/ASHRAE Standard 62.1: Ventilation for Acceptable Indoor Air Quality*. Atlanta, USA: American Society of Heating, Refrigeration, and Air–Conditioning Engineers.

Auliciems, A. 2001. Towards a Psycho–Physiological Model of Thermal Perception. *International Journal Biometeorology*, **25**(2), 109–122.

Awbi, HB, & Elmualim, AA. 2002. Full Scale Model Windcatcher Performance Evaluation Using a Wind Tunnel. *In: World Renewable Energy Conference VII*.

Aynsley, R. 2008. Quantifying the Cooling Sensation of Air Movement. *International Journal of Ventilation*, **7**(1), 67–76.

Bahadori, Mehdi N. 1994. Viability of wind towers in achieving summer comfort in the hot arid regions of the middle east. *Renewable Energy*, **5**(5-8), 879–892.

Bailey, C. 2009. Learning from passive action. *CIBSE Journal*, **1**(6), 28–31.

Bakó-Biró, Z. 2004. *Human Perception, SBS Symptoms and Performance of Office Work During Exposure to Air Polluted by Building Materials and Personal Computers.* Ph.D. thesis, Technical University of Denmark.

Bakó-Biró, Z, Wargocki, P, Weschler, CJ, & Fanger, PO. 2004. Effects of Pollution from Personal Computers on Perceived Air Quality, SBS Symptoms and Productivity in Offices. *Indoor Air*, **14**(3), 178–187.

Bakó-Biró, Z, Kochhar, N, Clements-Croome, DJ, Awbi, HB, & Williams, M. 2008. Ventilation Rates in Schools and Pupil's Performance Using Computerised Assessment Tests. *In: Indoor Air 2008.*

Bartlett, KH, Martinez, M, & Bert, J. 2004. Modeling of Occupant–Generated CO2 Dynamics in Naturally Ventilated Classrooms. *Journal Of Occupational and Environmental Hygeine*, **1**(3), 139–148.

Beisteiner, A, & Coley, DA. 2002. Carbon Dioxide Levels and Summertime Ventilation Rates in UK Schools. *International Journal of Ventilation*, **1**(3), 181–187.

Boyer, H, Lauret, AP, Adelard, L, & Mara, TA. 1999. Building Ventilation: A Pressure Airflow Model Computer Generation and Elements of Validation. *Energy and Buildings*, **29**(3), 283–292.

Brager, GS, & De Dear, RJ. 1998. Thermal Adaptation in the Built Environment: A Literature Review. *Energy and Buildings*, **27**(1), 83–96.

Brager, GS Schiller, & De Dear, RJ. 2000. A Standard for Natural Ventilation. *ASHRAE Journal*, **42**(10), 21–28.

BRE. 2005 (24th March 2005). *Test Report: Laboratory Sound Insulation of Monodraught G.R.P. Square Windcatcher System.* Private Report 222354. Buildings Research Establishment.

BRE. 2008. *BRE Environmental and Sustainability.* Tech. rept. BRE.

BSI. 1991. *BS 5925. Code of Practice for Ventilation Principles and Designing for Natural Ventilation.* Tech. rept. BSI.

BSI. 2001. *BS EN 7726. Ergonomics of the thermal environment. Instruments for measuring physical quantities.* Tech. rept. BSI.

BSI. 2004. *BS EN 13779. Ventilation for Non–Residential Buildings — Performance Requirements for Ventilation and Room–Conditioning Systems.* Tech. rept. BSI.

BSI. 2007. *BS EN 15251. Indoor Environment Input Parameters for Design and Assessment of Energy Performance of Buidlings Addressing Indoor Air Quality, Thermal Environment, Lighting and Acoustics.* Tech. rept. BSI.

CABE. 2009a. *Effective School Design — Effective Graphic Approaches.* Tech. rept. Commission for Architecture and the Built Environment.

CABE. 2009b. *Effective School Design — How CABE's Schools Design Panel Works.* Tech. rept. Commission for Architecture and the Built Environment.

CABE. 2009c. *Effective School Design — Questions to Ask.* Tech. rept. Commission for Architecture and the Built Environment.

Carbon Trust. 2007 (March). *Air Conditioning. Maximising Comfort, Minimising Energy Consumption.* Tech. rept. Carbon Trust.

CEC. 1992. *Indoor Air Quality and Its Impact on Man.* Tech. rept. 2. Commission of the European Communities.

Chaichongrak, R, Nil-athi, S, Panin, O, & Posayanonda, S. 2002. *The Thai House: History and Evolotion.* Bangkok, Thailand: River Books.

Chaloulakou, A, & Mavroidis, I. 2002. Comparison of Indoor and Outdoor Concentrations of Carbon Dioxide at a Public School. Evaluation of an Indoor Air Quality Model. *Atmospheric Environment*, **36**(11), 1769–1781.

Chappells, H, & Shove, E. 2005. Debating the Future of Comfort: Environmental Sustainability, Energy Consumption and the Indoor Environment. *Building Research and Information*, **33**(1), 32–40.

Chen, L, Jennison, BL, Yang, W, & Omaye, ST. 2000. Elementary School Absenteeism and Air Pollution. *Inhalation Toxicology*, **12**(11), 997–1016.

Chen, Qingyan. 2009. Ventilation Performance Prediction for Buildings: A Method Overview and Recent Applications. *Building and Environment*, **44**(4), 848–858.

Chenvidyakarn, T, & Woods, A. 2005. Multiple Steady States in Stack Ventilation. *Building and Environment*, **40**(3), 399–410.

CIBSE. 2001. *Guide C — Reference Data.* London: CIBSE Publications.

CIBSE. 2003. *The Energy Performance of Buildings Directive.* Tech. rept. CIBSE.

CIBSE. 2004. *Guide F — Energy Efficiency in Buildings.* London: CIBSE Publications.

CIBSE. 2005a. *AM10 — Natural Ventilation in Non–Domestic Buildings.* London: CIBSE Publications.

CIBSE. 2005b. *Current DSY/TRY Hourly Weather Data.*

CIBSE. 2005c. *Sustainable Low Energy Cooling: An Overview.* Tech. rept. Chartered Institute of Building Services Engineers.

CIBSE. 2006a. *Guide A — Environmental Design.* London: CIBSE Publications.

CIBSE. 2006b. *TM33 – Tests for software accreditation and verification.* 7 edn. Vol. 1. London: CIBSE Publications.

Clements-Croome, DJ, Awbi, HB, Bakó-Biró, Z, Kochhar, N, & Williams, M. 2008. Ventilation Rates in Schools. *Building and Environment*, **43**(3), 362–367.

Coley, DA, & Beisteiner, A. 2002. Carbon Dioxide Levels and Ventilation Rates in Schools. *International Journal of Ventilation*, **1**(1), 45–52.

Conceição, EZE, & Lucio, MMJR. 2006. Air Quality Inside a School Building: Air Exchange Monitoring, Evolution of Carbon Dioxide and Assessment of Ventilation Strategies. *International Journal of Ventilation*, **5**(2), 259–270.

Cook, MJ. 1998. *An Evaluation of Computational Fluid Dynamics for Modelling Buoyancy–Driven Displacement Ventilation.* Ph.D. thesis, De Montfort University.

Cook, MJ, & Short, CA. 2005. Natural Ventilation and Low Energy Cooling of Large, Non–Domestic Buildings Four Case Studies. *International Journal of Ventilation*, **3**(4), 283–294.

Cook, MJ, Ji, Y, & Hunt, GR. 2003. CFD Modelling of Natural Ventilation: Combined Wind and Buoyancy Forces. *International Journal of Ventilation*, **1**(3), 169–179(11).

Costola, D, & Etheridge, DW. 2008. Unsteady Natural Ventilation at Model Scale–Flow Reversal and Discharge Coefficients of a Short Stack and an Orifice. *Building and Environment*, **43**(9), 1491–1506.

Cotterill, S, Evans, R, & Fraise, AP. 1996. An Unusual Source for an Outbreak of Methicillin–Resistant Staphylococci Aureus on an Intensive Therapy Unit. *Journal of Hospital Infection*, **32**(3), 217–227.

Daisey, JM, Angell, WJ, & Apte, MG. 2003. Indoor Air Quality, Ventilation and Health Symptoms in Schools: An Analysis of Existing Information. *Indoor Air*, **13**(1), 53–64.

De Dear, RJ, & Brager, GS. 2002. Thermal Comfort in Naturally Ventilated Buildings: Revisions to ASHRAE Standard 55. *Energy and Buildings*, **34**(6), 549–561.

De Salis, M.H.F., DJ, DJ Oldham, & Sharples, S. 2002. Noise Control Strategies for Naturally Ventilated Buildings. *Building and Environment*, **37**(5), 471–484.

DfEE. 2003. *Building Bulletin 87 — Ventilation of School Buildings.* London: Department for Education and Employment.

DfES. 2002. *Building Bulletin 95 — Schools for the Future.* London: Department for Education and Skills.

DfES. 2003. *Building Bulletin 93 — Acoustic Design of Schools.* London: Department for Education and Skills.

DfES. 2005. *Class Vent (version 0702).* London: Department for Education and Skills.

DfES. 2006. *Building Bulletin 101 — Ventilation of School Buildings.* London: Department for Education and Skills.

Dockrell, JE, & Shield, BM. 2006. Acoustical Barriers in Classrooms: The Impact of Noise on Performance in the Classroom. *British Educational Research Journal*, **32**(3), 509–525.

DoH. 2007. *Health Technical Memorandum, 03–01: Specialised Ventilation for Healthcare Premises.* Tech. rept. Department of Health, The Stationary Office.

Douglas, J.F., Gasiorek, J.M., & Swaffield, J.A. 1995. *Fluid Mechanics.* Longman.

DTI. 2003. *Our Energy Our Future.* Tech. rept. Department of Trade and Industry.

DUKES. 2006. *Digest of United Kingdom Energy Statistics.* Tech. rept. The Stationary Office.

Elmualim, AA. 2005a. Effect of Damper and Heat Source on Wind Catcher Natural Ventilation Performance. *Energy and Buildings*, **38**(8), 939–948.

Elmualim, AA. 2005b. Effect of damper and heat source on wind catcher natural ventilation performance. *Energy and Buildings*, **38**(8), 939–948.

Elmualim, AA. 2006a. Dynamic Modelling of a Wind Catcher/Tower Turret for Natural Ventilation. *Building Services Engineering Research and Technology*, **27**(3), 165–182.

Elmualim, AA, & Awbi, HB. 2002a. Wind Tunnel and CFD Investigation of the Performance of Windcatcher Ventilation Systems. *International Journal of Ventilation*, **1**(1), 53–64.

Elmualim, AA, & Teekaram, AJ. 2002 (February 2002). *Natural Ventilation Testing Carried out for: Monodraught Ltd.* Tech. rept. 16270/1. BSRIA.

Elmualim, AA, Awbi, HB, Teekaram, AJ, & Brown, RG. 2001. Evaluating the Performance of a Windcatcher System Using Wind Tunnel Testing. *In: 22nd Annual AIVC Conference.*

Erdmann, CA, & Apte, Michael G. 2004. Mucous Membrane and Lower Respiratory Building Related Symptoms in Relation to Indoor Carbon Dioxide Concentrations in the 100–Building BASE Dataset. *Indoor Air*, **14**(s8), 127–134.

Etheridge, D, & Sandberg, M. 1996. *Building Ventilation: Theory and Measurement.* John Wiley and Sons.

Etheridge, DW. 1998. A Note on Crack Flow Equations for Ventilation Modelling. *Building and Environment*, **33**(5), 325–328.

Etheridge, DW. 2002. Non–Dimensional Methods for Natural Ventilation Design. *Building and Environment*, **37**(11), 1057–1072.

Etheridge, DW. 2004. Natural Ventilation through Large Openings — Measurements at Model Scale and Envelope Flow Theory. *International Journal of Ventilation*, **2**(4), 325–342.

Etheridge, DW. 2009. Wind Turbulence and Multiple Solutions for Opposing Wind and Buoyancy. *International Journal of Ventilation*, **7**(4), 309–319.

Evola, G, & Popov, V. 2006. Computational Analysis of Wind Driven Natural Ventilation in Buildings. *Energy and Buildings*, **38**(5), 491–501.

Fang, L, Clausen, G, & Fanger, PO. 1998. Impact of Temperature and Humidity on the Perception of Indoor Air Quality. *Indoor Air*, **8**(2), 80–90.

Fanger, PO. 1970. *Thermal Comfort — Analysis and Applications in Environmental Engineering.* New York: McGraw–Hill.

Fanger, PO. 2006. What is IAQ? *Indoor Air*, **16**(5), 328–334.

Fisk, WJ. 2000. Health And Productivity Gains From Better Indoor Environments And Their Relationship With Building Energy Efficiency. *Annual Review of Energy and the Environment*, **25**(1), 537.

Fitzgerald, SD, & Woods, AW. 2007. On the Transition from Displacement to Mixing Ventilation with a Localized Heat Source. *Building and Environment*, **42**(6), 2210–2217.

Fox, RW, & McDonald, AT. 1985. *Introduction to Fluid Mechanics.* New York: John Wiley and Sons.

Gage, SA, & Graham, JMR. 2000. Static Split Duct Roof Ventilators. *Building Research and Information*, **28**(4), 234–244.

Gage, SA, Hunt, GR, & Linden, PF. 2001. Top Down Ventilation and Cooling. *Journal of Architecture and Planning Research*, **18**(4), 286–301.

Geelen, LMJ, Huijbregts, MAJ, Ragas, AMJ, Bretveld, RW, Jans, HWA, van Doorn, WJ, Evertz, SJCJ, & van der Zijden, A. 2008. Comparing the effectiveness of interventions to improve ventilation behavior in primary schools. *Indoor Air*, **18**(5), 416–424.

Givoni, B. 1994. *Passive and Low Energy Cooling of Buildings*. John Wiley and Sons Inc.

Godwin, C, & Batterman, S. 2007. Indoor Air Quality in Michigan Schools. *Indoor Air*, **17**(2), 109–121.

Griffiths, M, & Eftekhari, M. 2008. Control of CO_2 in a Naturally Ventilated Classroom. *Energy and Buildings*, **40**(4), 556–560.

Grimsrud, D, Bridges, B, & Schulte, R. 2006. Continuous measurements of air quality parameters in schools. *Building Research & Information*, **34**(5), 447–458.

Haghighat, F, & Donnini, G. 1993. Conventional vs CO_2 Demand–Controlled Ventilation Systems. *Journal of Thermal Biology*, **18**(5–6), 519–522.

Heiselberg, P. 2004. Natural Ventilation Design. *International Journal of Ventilation*, **2**(4), 295–312.

Heiselberg, P, Li, Y, Andersen, A, Bjerre, M, & Chen, Z. 2004. Experimental and CFD Evidence of Multiple Solutions in a Naturally Ventilated Building. *Indoor Air*, **14**(1), 43–54(12).

Hellwig, RT, Antretter, F, Holm, A, & Sedlbauer, K. 2009a. Investigations into Indoor Environment Conditions and Natural Ventilation in School Buidlings. *Bauphysik*, **31**(2), 89–98.

Hellwig, RT, Kersken, M, & Schmidt, S. 2009b. Equipment of Classrooms with Systems for Maintaining Temperature, Ventilation, and Illumination. *Bauphysik*, **31**(3), 157–162.

Horan, JM, & Finn, DP. 2005. CFD Reliability Issues in the Prediction of Airflows in a Naturally Ventilated Building. *International Journal of Ventilation*, **4**(3), 255–268.

HSE. 1996. *Workplace Health, Safety and Welfare. Workplace (Health, Safety and Welfare) Regulations 1992 (As Amended by the Quarries Miscellaneous Health and Safety Provisions Regulations 1995).*

Hughes, BR, & Ghani, SAA. 2008. Investigation of a Windvent Passive Ventilation Device Against Current Fresh Air Supply Recommendations. *Energy and Buildings*, **40**(9), 1651–1659.

Hughes, BR, & Ghani, SAA. 2009. A Numerical Investigation into the Effect of Windvent Dampers on Operating Conditions. *Building and Environment*, **44**(2), 237–248.

Hummelgaard, J, Juhl, P, Sæbjörnsson, KO, Clausen, G, Toftum, J, & Langkilde, G. 2007. Indoor Air Quality and Occupant Satisfaction in Five Mechanically and Four Naturally Ventilated Open–Plan Office Buildings. *Building and Environment*, **42**(12), 4051–4058.

Humphreys, M. A. 1977. The optimum diameter for a globe thermometer for use indoors. *Annals of Occupational Hygiene*, **20**(2), 135–140.

Humphreys, MA. 2005. Quantifying Occupant Comfort: Are Combined Indices of the Indoor Environment Practicable? *Building Research and Information*, **33**(4), 317–325.

Humphreys, MA, & Nicol, FJ. 1998. Understanding the Adaptive Approach to Thermal Comfort. *ASHRAE Transactions*, **104**(1), 991–1004.

Hunt, GR, & Linden, PF. 2000. Multiple Steady Airflows and Hysteresis When Wind Opposes Buoyancy. *Air Infiltration Review*, **21**(2), 1–3.

Hunt, GR, & Linden, PP. 1999. The Fluid Mechanics of Natural Ventilation—Displacement Ventilation by Buoyancy–Driven Flows Assisted by Wind. *Building and Environment*, **34**(6), 707–720.

Hurst, KS, & Rapley, CW. 1991. Turbulent Flow Measurements in a 30/60 Degree Right Triangular Duct. *Journal of Heat Mass Transfer*, **34**(3), 739–748.

IIF. 2002. *Industry as a Partner for Sustainable Development Report Card of the Sector: Refrigeration in Preparation for CSD–14 on "Industrial Development"*. Tech. rept. International Institute of Refrigeration.

ISO. 1991. *140–10: Acoustics — Rating of Sound Insulation in Buildings and of Building Elements*. Tech. rept. International Standards Organisation.

ISO. 1997. *717–1: Acoustics — Rating of Sound Insulation in Buildings and of Building Elements*. Tech. rept. International Standards Organisation.

ISO. 2005. *7730: Ergonomics of the Thermal Environment*. Tech. rept. International Standards Organisation.

Jaakkola, JJK, & Miettinen, P. 1995. Type of Ventilation System in Office Buildings and Sick Building Syndrome. *American Journal of Epidemiology*, **141**(8), 755–765.

Jones, AP. 1999. Indoor Air Quality and Health. *Atmospheric Environment*, **33**, 4535–4564.

Karakatsanis, C., Bahadori, M. N., & Vickery, B. J. 1986. Evaluation of pressure coefficients and estimation of air flow rates in buildings employing wind towers. *Solar Energy*, **37**(5), 363–374.

Karava, P, Stathopoulos, T, & Athienitis, AK. 2003. Investigation of the performance of trickle ventilators. *Building and Environment*, **38**(8), 981–993.

Karava, P, Stathopoulos, T, & Athienitis, AK. 2004. Wind Driven Flow Through Openings–A Review of Discharge Coefficients. *International Journal of Ventilation*, **3**(3), 255–266.

Khan, N, Su, Y, & Riffat, SB. 2008. A Review on Wind Driven Ventilation Techniques. *Energy and Buildings*, **40**(8), 1586–1604.

Kinsler, LE, Frey, AR, Coppen, AB, & Sanders, JV. 1982. *Fundamentals of Acoustics*. John Wiley and Sons.

Kirk, S. 2004a. *Top Down Natural Ventilation in Non–Domestic Buildings*. M.Phil. thesis, Brunel University.

Kirk, S, & Kolokotroni, M. 2004b. Windcatchers in Modern UK Buildings: Experimental Study. *International Journal of Ventilation*, **3**(1), 67–78.

Kolokotroni, M, & Aronis, A. 1999. Cooling–Energy Reduction in Air–Conditioned Offices by Using Night Ventilation. *Applied Energy*, **63**(4), 241–253.

Kolokotroni, M, Ge, YT, & Katsoulas, D. 2002a. Monitoring and Modelling Indoor Air Quality and Ventilation in Classrooms within a Purpose–Designed Naturally Ventilated School. *Indoor Built Environment*, **11**, 316–326.

Kolokotroni, M, Ayiomamitis, A, & Ge, YT. 2002b. The Suitability of Wind Driven Natural Ventilation Towers for Modern Offices in the UK: A Case Study. *In: World Renewable Energy Congress.*

Kolokotroni, M, Shilliday, J, Liddament, M, Santamouris, M, Farrou, I, Seppänen, O, Brown, R, Parker, J, & Guarracino, G. 2007. *Energy Efficient Ventilation for Buildings.* Vol. 2. Uxbridge: Brunel University.

Kumari, DNP, Haji, TC, Keer, V, Hawkey, PM, Duncanson, V, & Flower, E. 1998. Ventilation Grilles as a Potential Source of Methicillin–Resistant Staphylococcus Aureus Causing an Outbreak in an Orthopaedic Ward at a District General Hospital. *Journal of Hospital Infection*, **39**(2), 127–133.

Laxen, DPH, & Noordally, E. 1987. Nitrogen Dioxide Distribution in Street Canyons. *Atmospheric Environment*, **21**(9), 1899–1903.

Lee, SC, & Chang, M. 1999. Indoor Air Quality Investigations at Five Classrooms. *Indoor Air*, **9**(2), 134–138.

Lee, SC, & Chang, M. 2000. Indoor and Outdoor Air Quality Investigation at Schools in Hong Kong. *Chemosphere*, **41**(1–2), 109–113.

Li, L, & Mak, CM. 2007. The Assessment of the Performance of a Windcatcher System using Computational Fluid Dynamics. *Building and Environment*, **42**(3), 1135–1141.

Li, Y, & Heiselberg, P. 2002. Analysis Methods for Natural and Hybrid Ventilation — A Critical Literature Review and Recent Developments. *International Journal of Ventilation*, **1**(4), 3–20.

Li, Y, Delsante, A, Chen, Z, Sandberg, M, Andersen, A, Bjerre, M, & Heiselberg, P. 2001. Some Examples of Solution Multiplicity in Natural Ventilation. *Building and Environment*, **36**(7), 851–858(8).

Li, Y, Leung, M, Tang, J W, Yang, X, Chao, CYH, Lin, JZ, Lu, JW, Nielsen, PV, Niu, J, Qian, H, Sleigh, AC, Su, HJJ, Sundell, J, Wong, TW, & Yuen, PL. 2007. Role of Ventilation in Airborne Transmission of Infectious Agents in the Built Environment — A multidisciplinary Systematic Review. *Indoor Air*, **17**(1), 2–18.

Liddament, M. 2001. *Occupant Impact on Ventilation.* Tech. rept. AIVC.

Liddament, M. 2009. The Applicability of Natural Ventilation — Technical Editorial. *International Journal of Ventilation*, **8**(3), 189–199.

Liddament, MW. 1996. *AIVC: A Guide to Energy Efficient Ventilation.* Oscar Faber.

Linden, PF. 1999. The Fluid Mechanics of Natural Ventilation. *Annual Review of Fluid Mechanics*, **31**(1), 201.

Ling, MK. 2001. *Technical Note 52: Acoutics and Ventilation.* Tech. rept. AIVC.

Lomas, KJ, & Ji, Y. 2009. Resilience of naturally ventilated buildings to climate change: Advanced natural ventilation and hospital wards. *Energy and Buildings*, **41**(6), 629–653.

Mavrogianni, A. 2007. *Impact Assessment of Climate Change on Thermal Comfort in a Naturally Ventilated School.* M.Phil. thesis, University College London.

McCarthy, C. 1999. *Wind Towers.* Wiley–Academy.

McCartney, KJ, & Nicol, JF. 2002. Developing an Adaptive Control Algorithm for Europe. *Energy and Buildings*, **34**(6), 623–635.

McMullan, R. 2002. *Environmental Science in Building.* Basingstoke: Palgrave.

Mendell, MJ, & Heath, GA. 2005. Do Indoor Pollutants and Thermal Conditions in Schools Influence Student Performance? A Critical Review of the Literature. *Indoor Air*, **15**(1), 27–52.

Milton, DK, Glencross, PM, & Walters, MD. 2000. Risk of Sick Leave Associated with Outdoor Air Supply Rate, Humidification, and Occupant Complaints. *Indoor Air*, **10**(4), 212–221.

Mølhave, L. 2003. Organic Compounds as Indicators of Air Pollution. *Indoor Air*, **13**(s6), 12–19.

Monodraught. 2009. *The Importance of Natural Ventilation and Daylight in Schools*. Tech. rept. Monodraught Ltd.

Montazeri, H, & Azizian, R. 2008. Experimental Study on Natural Ventilation Performance of One–Sided Wind Catcher. *Building and Environment*, **43**(12), 2193–2202.

Mumovic, D, Palmer, J, Davies, M, Orme, M, Ridley, I, Oreszczyn, T, Judd, C, Critchlow, R, Medina, HA, Pilmoor, G, Pearson, C, & Way, P. 2009. Winter Indoor Air Quality, Thermal Comfort and Acoustic Performance of Newly Built Secondary Schools in England. *Building and Environment*, **44**(7), 1466–1477.

Munson, B, Young, D, & Okiishi, T. 1998. *Fundamentals of Fluid Mechanics*. John Wiley and Sons.

Myhrvold, AN, Olsen, E, & Lauridsen, O. 1996. Indoor Environment in Schools — Pupils Health and Performance in Regard to CO_2 Concentrations. *In: Indoor Air '96: The 7th International Conference on Indoor Air Quality and Climate.*

Mysen, Mads, Berntsen, Sveinung, Nafstad, Per, & Schild, Peter G. 2005. Occupancy density and benefits of demand–controlled ventilation in Norwegian primary schools. *Energy and Buildings*, **37**(12), 1234–1240.

NHS. 2009 (January 2009). *Saving Carbon, Improving Health. NHS Carbon Reduction Strategy for England*. Tech. rept. NHS Sustainable Development Unit.

Nicol, JF. 1974. An Analysis of Some Observations of Thermal Comfort in Roorkee, India and Baghdad, Iraq. *Annals of Human Biology*, **1**(4), 411–426.

Nicol, JF, & Humphreys, MA. 2002. Adaptive Thermal Comfort and Sustainable Thermal Standards for Buildings. *Energy and Buildings*, **34**(6), 563–572.

Nicol, JF, & Roaf, S. 2005. Post–Occupancy Evaluation and Field Studies of Thermal Comfort. *Building Research and Information*, **33**(4), 338–346.

Nicol, JF, Raja, IA, Allaudin, A, & Jamy, GN. 1999. Climatic Variations in Comfortable Temperatures: The Pakistan Projects. *Energy and Buildings*, **30**(3), 261–279.

Niemelä, R, Lefevre, A, Muller, JP, & Aubertin, G. 1991. Comparison of Three Tracer Gases for Determining Ventilation Effectiveness and Capture Efficiency. *Annual of Occupational Hygiene*, **35**(4), 405–417.

NOAA. 2009. *National Oceanic and Atmospheric Administration, Earth System Research Laboratory, Global Monitoring Division, Trends in Atmospheric Carbon Dioxide — Mauna Loa (Hawaii).*

ODPM. 2006. *Building Regulations 2000, Part F (Ventilation).*

Oldham, DJ, De Salis, MH, & Sharples, S. 2004. Reducing the Ingress of Urban Noise Through Natural Ventilation Openings. *Indoor Air*, **14**(2), 118–126.

Olesen, BW. 2007. The Philosophy Behind EN15251: Indoor Environmental Criteria for Design and Calculation of Energy Performance of Buildings. *Energy and Buildings*, **39**(7), 740–749.

Orme, M, & Leksmono, N. 2002. *Ventilation Modelling Data Guide — GU05.* Tech. rept. Air Infiltration and Ventilation Centre.

Parker, J. 2004a (February). *Performance Testing of a Modified Circular Windcatcher.* Tech. rept. 18537/1. BSRIA.

Parker, J, & Teekeram, AJ. 2004b (May). *Design and Application Guide for Roof Mounted Natural Ventilation Systems.* Tech. rept. 70205/5. BSRIA.

Pegg, I. 2008. *Assessing the Role of Post–Occupancy Evaluation in the Design Environment: A Case Study Approach.* Ph.D. thesis, Brunel Univeristy.

Persily, A. 1997. Evaluating Building IAQ and Ventilation with Indoor Carbon Dioxide. *ASHRAE Transactions*, **103**(2), 193–204.

Persily, A. 2006. What We Think We Know about Ventilation. *International Journal of Ventilation*, **5**(3), 275–290.

Persily, A, Stanke, D, Holness, G, & Hermans, R. 2007. Standard 62.1 Problems, Perceptions & Panaceas. *ASHRAE Journal*, **49**(3), 34–44.

Persily, AK. 1996. Relationship Between Indoor Air Quality and Carbon Dioxide. *In: Indoor Air Quality and Climate, 7th International Conference. 21–26 July 1996.*

Pfafferott, J, Herkel, S, & Wambsganß, M. 2004. Design, Monitoring and Evaluation of a Low Energy Office Building with Passive Cooling by Night Ventilation. *EPIC — 3rd European Conference on Energy Performance and Indoor Climate in Buildings*, **36**(5), 455–465.

Porritt, J. 2005. *Capitalism as If the World Matters.* London: Earthscan Publications Ltd.

Prill, R, Blake, D, & Hales, D. 2002. School Indoor Air Quality Assessment and Program Implementation. *In: Indoor Air 2002.*

Raja, IA, Nicol, JF, McCartney, KJ, & Humphreys, MA. 2001. Thermal Comfort: Use of Controls in Naturally Ventilated Buildings. *Energy and Buildings*, **33**(3), 235–244.

Rijal, HB, Tuohy, P, Humphreys, MA, Nicol, JF, Samuel, A, & Clarke, J. 2007. Using Results from Field Surveys to Predict the Effect of Open Windows on Thermal Comfort and Energy Use in Buildings. *Energy and Buildings*, **39**(7), 823–836.

Roaf, S. 1982. Wind–catchers. *Pages 57–72 of:* Beazley, Elisabth, & Harverson, Michael (eds), *Living With the Desert.* London: Aris and Phillips Ltd.

Roaf, S. 2007. Resilient Hospital Design: The Zero Carbon Cooling Challenge. *In: 2nd PALENC and 28th AIVC Conference on Building Low Energy Cooling and Advanced Ventilation Technologies in the 21st Century.*

Ross, SM. 2004. *Introduction to Probability and Statistics for Engineers and Scientists*. Elsevier Academic Press.

Roulet, CA, & Foradini, F. 2002. Simple and Cheap Air Change Rate Measurement Using CO_2 Concentration Decays. *International Journal of Ventilation*, **1**(1), 39–44.

Rudofsky, B. 1977a. *Architecture without Architects: A Short Introduction to Non–Pedigree Architecture*. Bath: The Pitman Press.

Rudofsky, B. 1977b. *The Prodigious Builders*. London: Martin Secker and Warburg Ltd.

Santamouris, M. 2004. *Night Ventilation Strategies (VIP04)*. Tech. rept. Air Infiltration and Ventilation Centre.

Santamouris, M., & Asimakopoulos, D. 1996. *Passive Cooling of Buildings*. London: James and James (Science Publishers) Ltd.

Santamouris, M, Synnefa, A, Asssimakopoulos, M, Livada, I, Pavlou, K, Papaglastra, M, Gaitani, N, Kolokotsa, D, & Assimakopoulos, V. 2008. Experimental Investigation of the Air Flow and Indoor Carbon Dioxide Concentration in Classrooms with Intermittent Natural Ventilation. *Energy and Buildings*, **40**(10), 1833–1843.

Sanz, SA, García, AM, & García, A. 1993. Road Traffic Noise Around Schools: A Risk for Pupils' Performance? *International Archives of Occupational and Environmental Health*, **65**(3), 205–207.

Sawachi, T, Maruta, E, Takahashi, Y, & Sato, KI. 2006. Wind Pressure Coefficients for Different Building Configurations with and without an Adjacent Building. *International Journal of Ventilation*, **5**(1), 21–30.

Schild, PG. 2004. *Displacement Ventilation (VIP05)*. Tech. rept. Air Infiltration and Ventilation Centre.

Seppänen, O, & Fisk, WJ. 2002. Association of Ventilation System Type with SBS Symptoms in Office Workers. *Indoor Air*, **12**(2), 98–112.

Seppänen, O, Fisk, WJ, & Mendell, MJ. 2002. Ventilation Rates and Health. *ASHRAE Journal*, **44**(8), 56–58.

Seppänen, O, Fisk, WJ, & Lei, QH. 2006. Ventilation and Performance in Office Work. *Indoor Air*, **16**(1), 28–36.

Seppänen, OA, & Fisk, WJ. 2004. Summary of Human Responses to Ventilation. *Indoor Air*, **14**(s7), 102–118.

Seppänen, OA, Fisk, WJ, & Mendell, MJ. 1999. Association of Ventilation Rates and CO_2 Concentrations with Health and Other Responses in Commercial and Institutional Buildings. *Indoor Air*, **9**(4), 226–252.

Shaughnessy, RJ, Haverinen-Shaughnessy, U, Nevalainen, A, & Moschandreas, D. 2006. A Preliminary Study on the Association Between Ventilation Rates in Classrooms and Student Performance. *Indoor Air*, **16**(6), 465–468.

Shea, AD, Robertson, AP, Aston, WI, & Rideout, NM. 2003. The Performance of a Roof–Mounted Natural Ventilator. *In: 11th International Conference on Wind Engineering.*

Shendell, DG, Prill, R, Fisk, WJ, Apte, MG, Blake, D, & Faulkner, D. 2004. Associations Netween Classroom CO_2 Concentrations and Student Attendance in Washington and Idaho. *Indoor Air*, **14**(5), 333–341.

Sherman, MH. 1990. Tracer–Gas Techniques for Measuring Ventilation in a Single Zone. *Building and Environment*, **25**(4), 365–374.

Shield, BM, & Dockrell, JE. 2003. The Effects of Noise on Children at School: A Review. *Building Acoustics*, **10**(2), 97–116.

Shield, BM, & Dockrell, JE. 2004. External and Internal Noise Surveys of London Primary Schools. *The Journal of the Acoustical Society of America*, **115**(2), 730–738.

Short, C. Alan, & Al-Maiyah, Sura. 2009. Design strategy for low–energy ventilation and cooling of hospitals. *Building Research and Information*, **37**(3), 264–292.

Simons, MW, & Maloney, BJ. 2003. Comfort and Acoustic Monitoring in a Large Naturally Ventilated Technically Advanced Building. *International Journal of Ventilation*, **2**(1), 1–13.

Smedje, G, & Norback, D. 2000. New Ventilation Systems at Select Schools in Sweden — Effects on Asthma and Exposure. *Archives of Environmental Health*, **55**(1), 18–25.

Smedje, G, Norback, D, & Edling, C. 1997. Subjective Indoor Air Quality in Schools in Relation to Exposure. *Indoor Air*, **7**(2), 143–150.

Stansfeld, SA, & Matheson, MP. 2003. Noise Pollution: Non–Auditory Effects on Health. *British Medical Bulletin*, **68**(1), 243–257.

Stranger, M, Potgieter-Vermaak, SS, & van Grieken, R. 2008. Characterization of indoor air quality in primary schools in Antwerp, Belgium. *Indoor Air*, **18**(6), 454–463.

Su, Y, Riffat, SB, Lin, YL, & Khan, N. 2008. Experimental and CFD Study of Ventilation Flow Rate of a Monodraught^{TM} Windcatcher. *Energy and Buildings*, **40**(6), 1110–1116.

Sundell, J. 2004. On the History of Indoor Air Quality and Health. *Indoor Air*, **14**(s7), 51–58.

Thörn, A. 2000. Case Study of a Sick Building. Could an Integrated Bio–Psychosocial Perspective Prevent Chronicity? *European Journal of Public Health*, **10**(2), 133–137.

TMO. 2009. *Weather Data and Historic Weather Data.*

TSI. 1995. *Model 9355/8357 VelociCalc and VelociCalc Plus Air Velocity Meters: Operation and Service Manual.*

van Dijken, F, van Bronswijk, JEMH, & Sundell, J. 2006. Indoor Environment and Pupils' Health in Primary Schools. *Building Research and Information*, **34**(5), 437–446.

Verbeke, J, & Cools, R. 1995. The Newton–Raphson Method. *International Journal of Mathematical Education in Science and Technology*, **26**(2), 177–193.

Wargocki, P, & Wyon, DP. 2007a. The Effects of Moderately Raised Classroom Temperatures and Classroom Ventilation Rate on the Performance of Schoolwork by Children. *HVAC&R Research*, **13**(2), 193–220.

Wargocki, P, & Wyon, DP. 2007b. The Effects of Outdoor Air Supply Rate and Supply Air Filter Condition in Classrooms on the Performance of Schoolwork by Children. *HVAC&R Research*, **13**(2), 165–191.

Wargocki, P, Wyon, DP, Sundell, J, Clausen, G, & Fanger, PO. 2000. The Effects of Outdoor Air Supply Rate in an Office on Perceived Air Quality, Sick Building Syndrome (SBS) Symptoms and Productivity. *Indoor Air*, **10**, 222–236.

Wargocki, P, Sundell, J, Bischof, W, Brundrett, G, Fanger, PO, Gyntelberg, F, Hanssen, SO, Harrison, P, Pickering, A, Seppänen, O, & Wouters, P. 2002. Ventilation and Health in Non–Industrial Indoor Environments: Report from a European Multidisciplinary Scientific Consensus Meeting (EUROVEN). *Indoor Air*, **12**(2), 113–128.

Webb, BC, & White, M. 1998 (September). *Performance of Windcatcher Units at University of Hertfordshire.* Tech. rept. TCR 186/98. Buildings Research Establishment.

WHO. 1946. Preamble to the Constitution of the World Health Organization as Adopted by the International Health Conference. *In: International Health Conference.*

WHO. 1999. *Guidelines for Community Noise.* Tech. rept. World Health Organisation.

WHO. 2000. The Right to Healthy Indoor Air. *In: Report on a WHO Meeting.*

Woods, Andrew W., Fitzgerald, Shaun, & Livermore, Stephen. 2009. A comparison of winter pre–heating requirements for natural displacement and natural mixing ventilation. *Energy and Buildings*, **41**(12), 1306–1312.

Yaghoubi, M. A., Sabzevari, A., & Golneshan, A. A. 1991. Wind towers: Measurement and performance. *Solar Energy*, **47**(2), 97–106.

Appendix A

Predicting Ventilation Rates Through a Room Ventilated by a Windcatcher in Coordination with a Façade Opening.

This appendix reproduces Figures 3.33 and 3.36 found on pages 120 and 123, repectively, which are used through out the document for calculation purposes. In addition they may be useful to those who want to design a Windcatcher in coordination with open windows located in a façade.

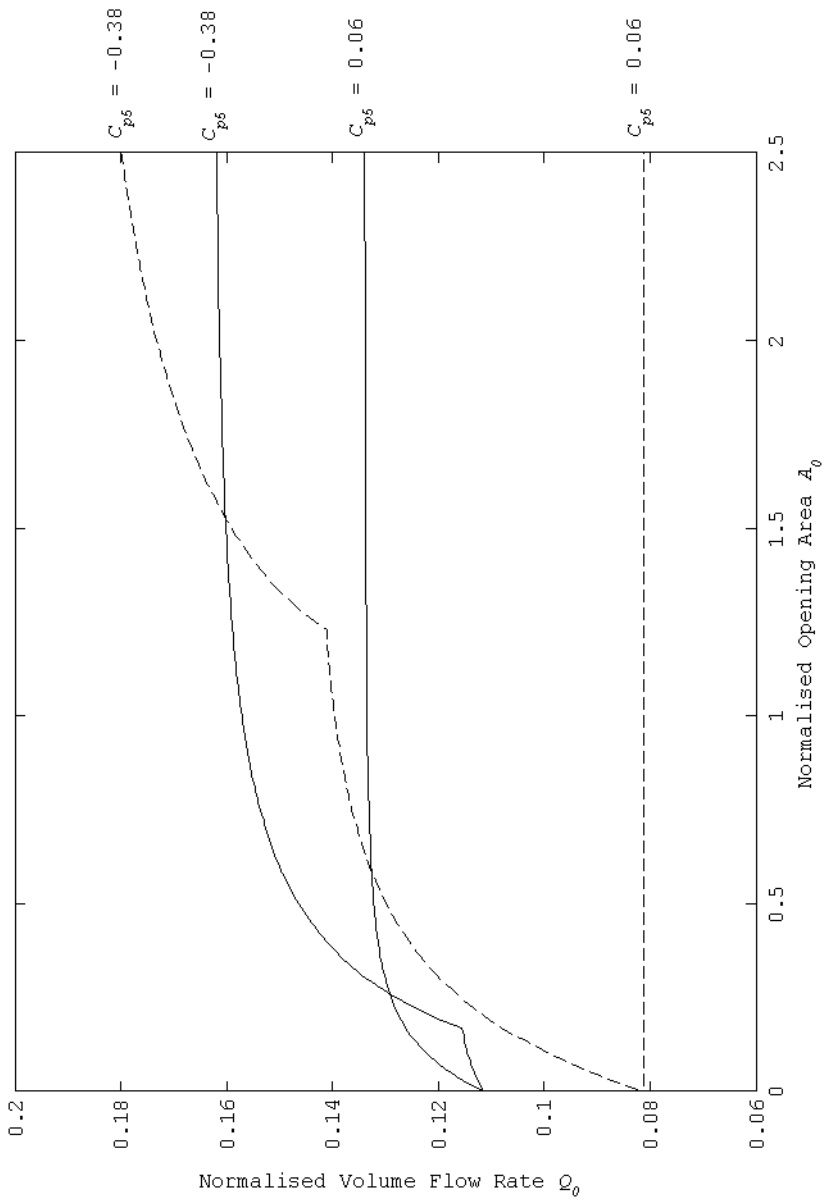

Figure A.1: Prediction of the effect of the area of a shielded façade opening on Windcatcher ventilation rates. $\theta = 0°$, ——; $\theta = 45°$ – – –.

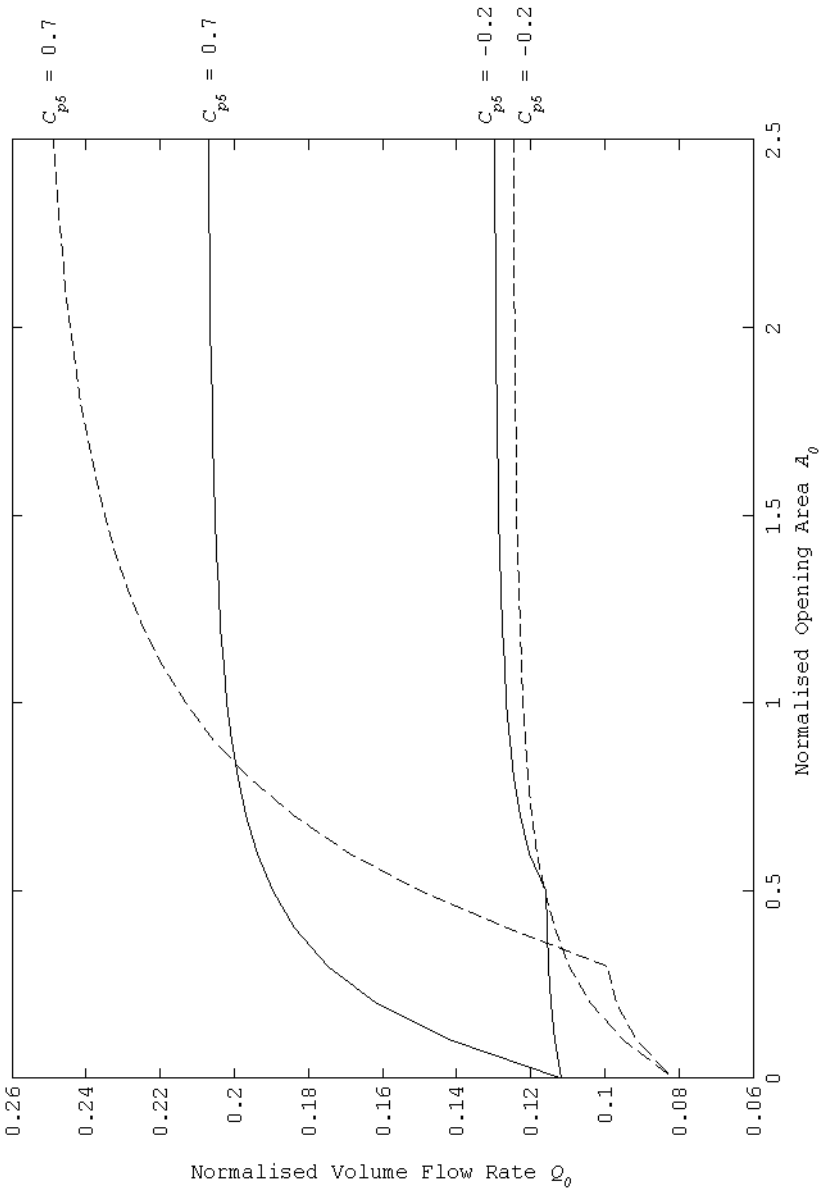

Figure A.2: Prediction of the effect of the area of an exposed façade opening on Windcatcher ventilation rates. $\theta = 0°$, ——; $\theta = 45°$ – – –.

Appendix B

Case Study Details

This appendix presents additional details of the case study buildings described in chapter 4. The floor plans of each classroom are clearly marked with the school prefix letter and classroom suffix number. Within each classroom the position of the thermostat is denoted by •, the Windcatcher by ■, and for 1st floor classrooms any ducting from the roof to a lower floor classroom is denoted by □. Also included with each floor plan is a directional wind rose, similar to those presented in Chapter 4, which show the orientation of the building and the frequency of the wind direction (% of annual hours). Finally, where appropriate, an elevation view has been included. Here, it should be noted that Figure B.1 is typical of the multi–storey duct work between a Windcatcher located at roof level and the ground floor classrooms of schools C, E, F, H, and I.

B.1 School C

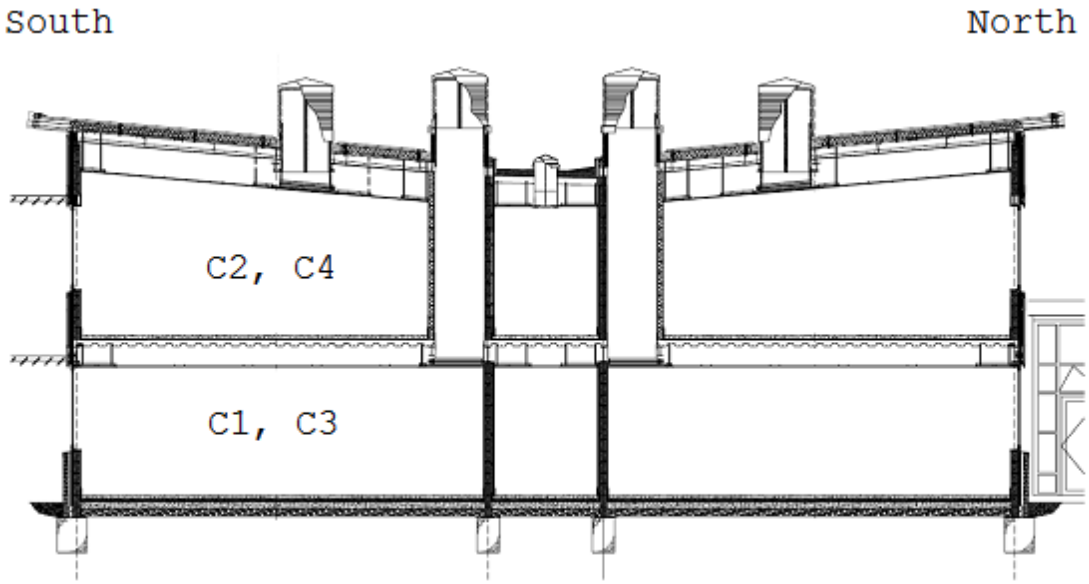

Figure B.1: School C, elevation view.

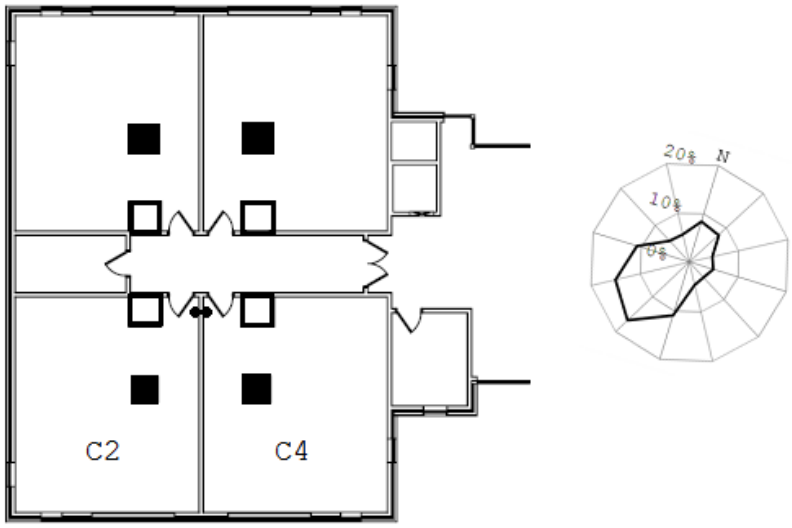

Figure B.2: School C, plan view, first floor. C2 and C4, floor area 57.05 m^2.

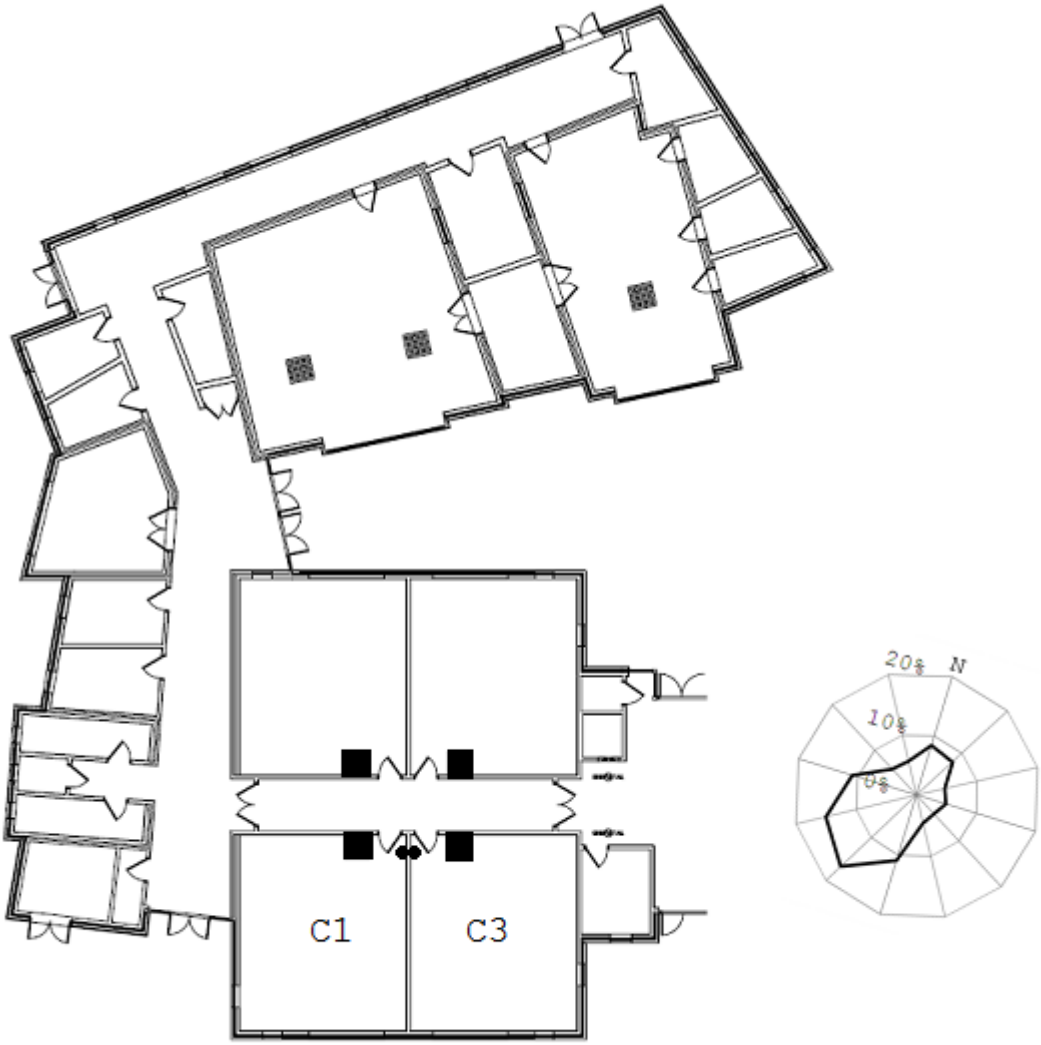

Figure B.3: School C, plan view, ground floor. C1 and C3, floor area 57.05 m^2.

B.2 School D

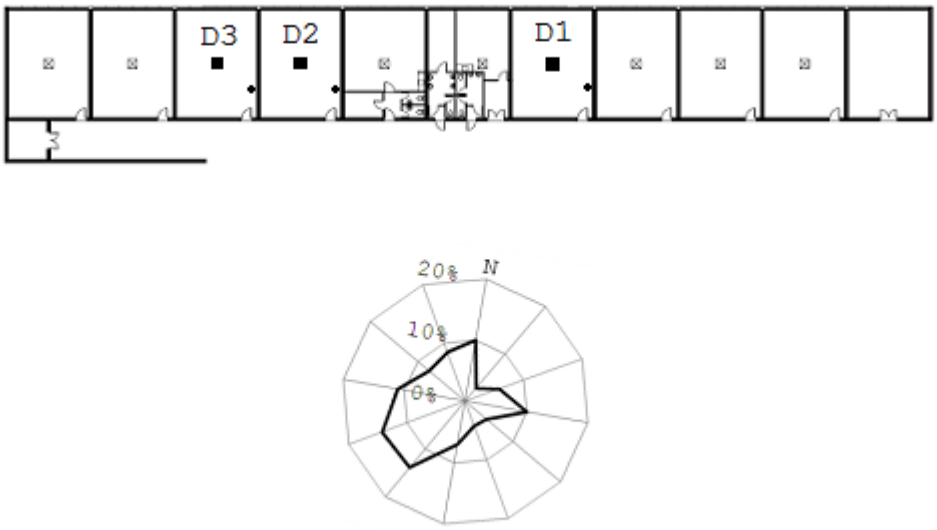

Figure B.4: School D, plan view, ground floor. D1, D2, and D3, floor area 69.84 m^2.

B.3 School E

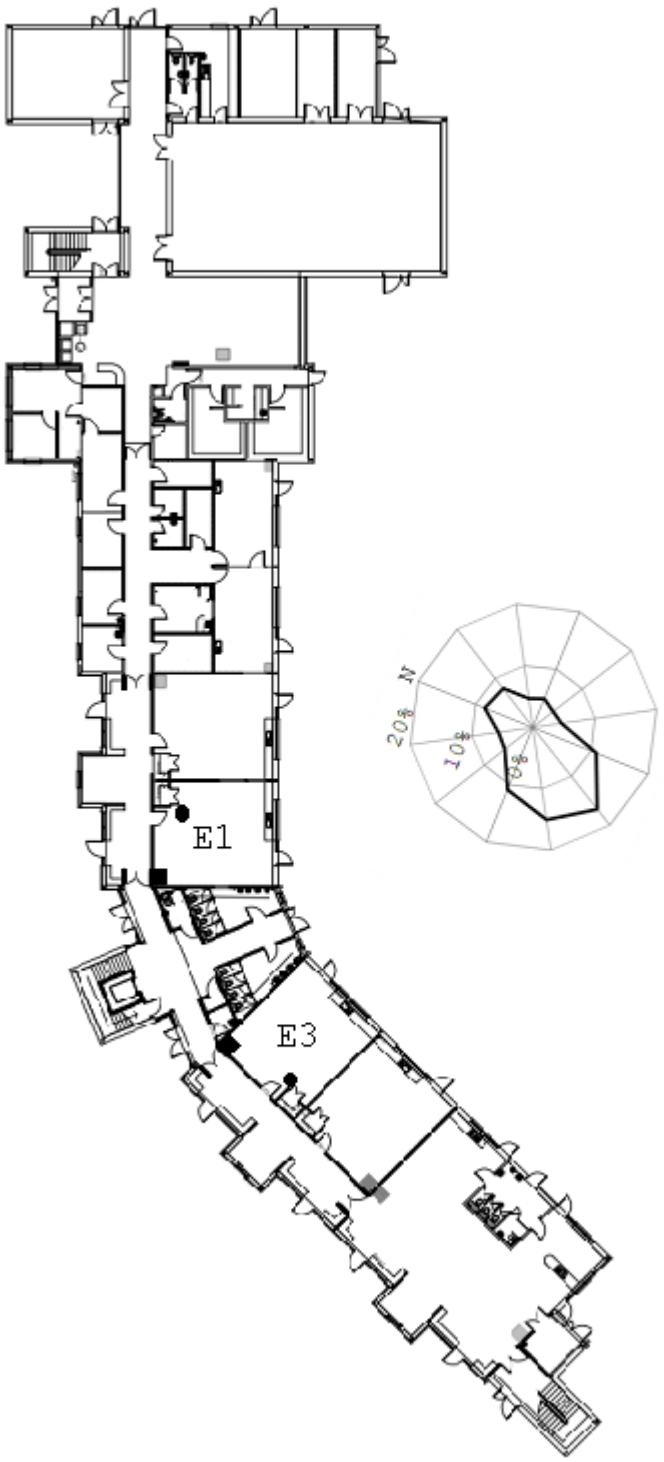

Figure B.5: School E, plan view, ground floor. E1 and E3, floor area 57.40 m^2.

B.4 School F

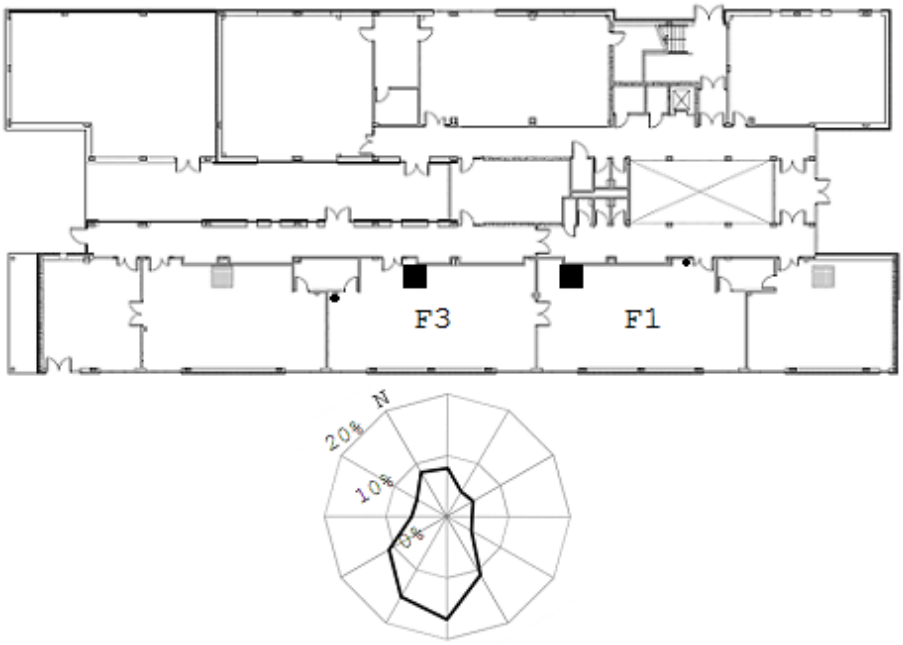

Figure B.6: School F, plan view, ground floor. F1 and F3, floor area 104.30 m^2.

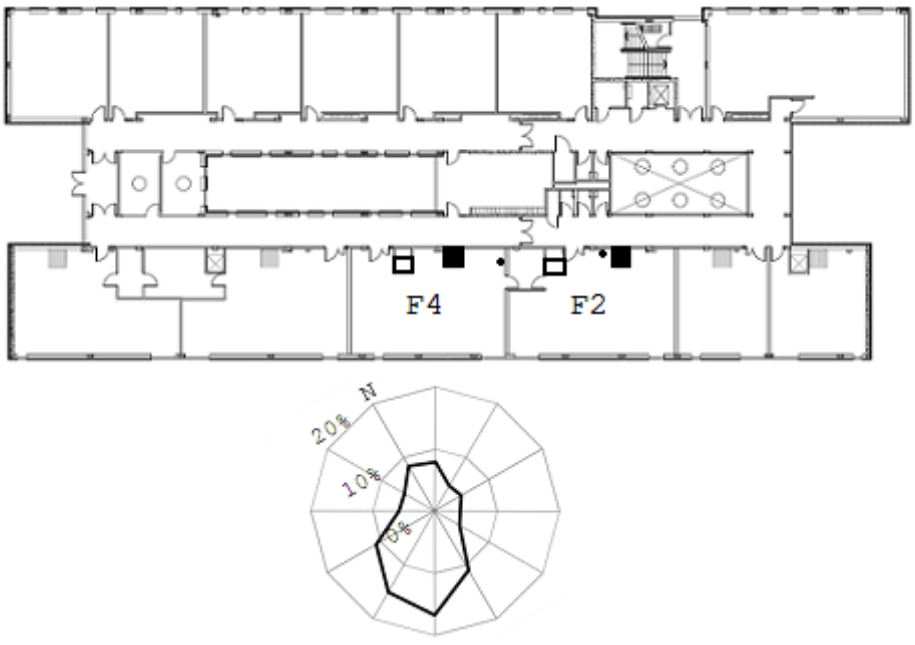

Figure B.7: School F, plan view, first floor. F2 and F4, floor area 92.75 m^2.

B.5 School G

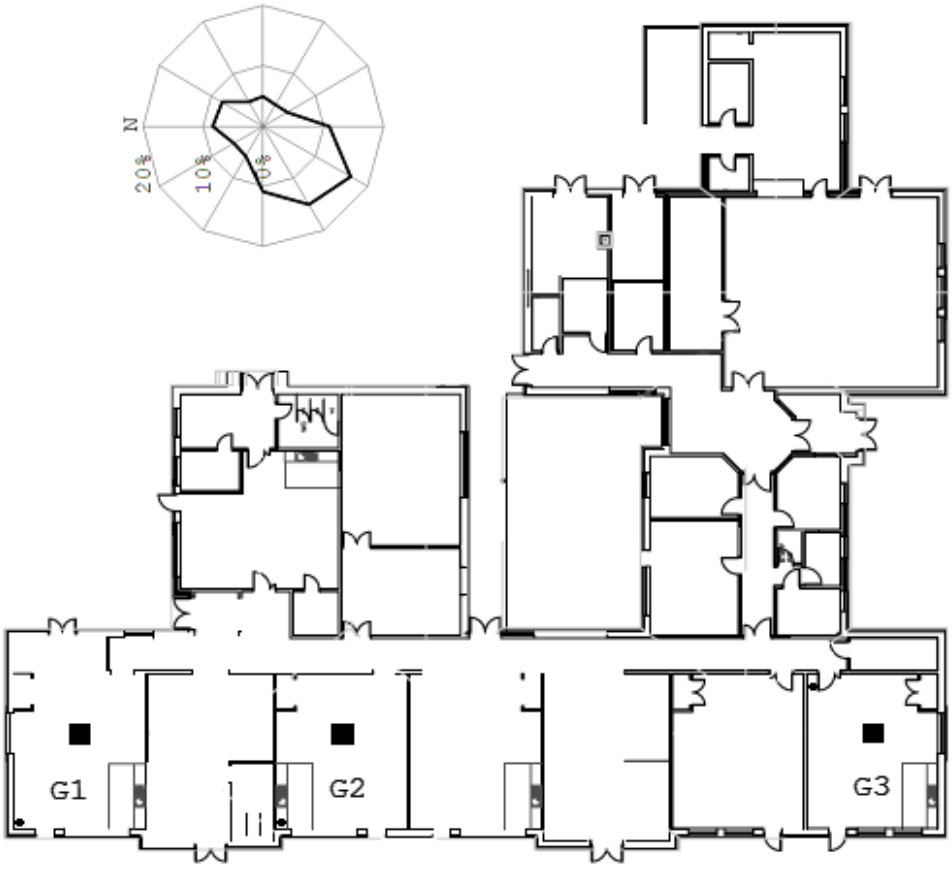

Figure B.8: School G, plan view, ground floor. G1, G2, and G3, floor area 61.63 m^2.

B.6 School H

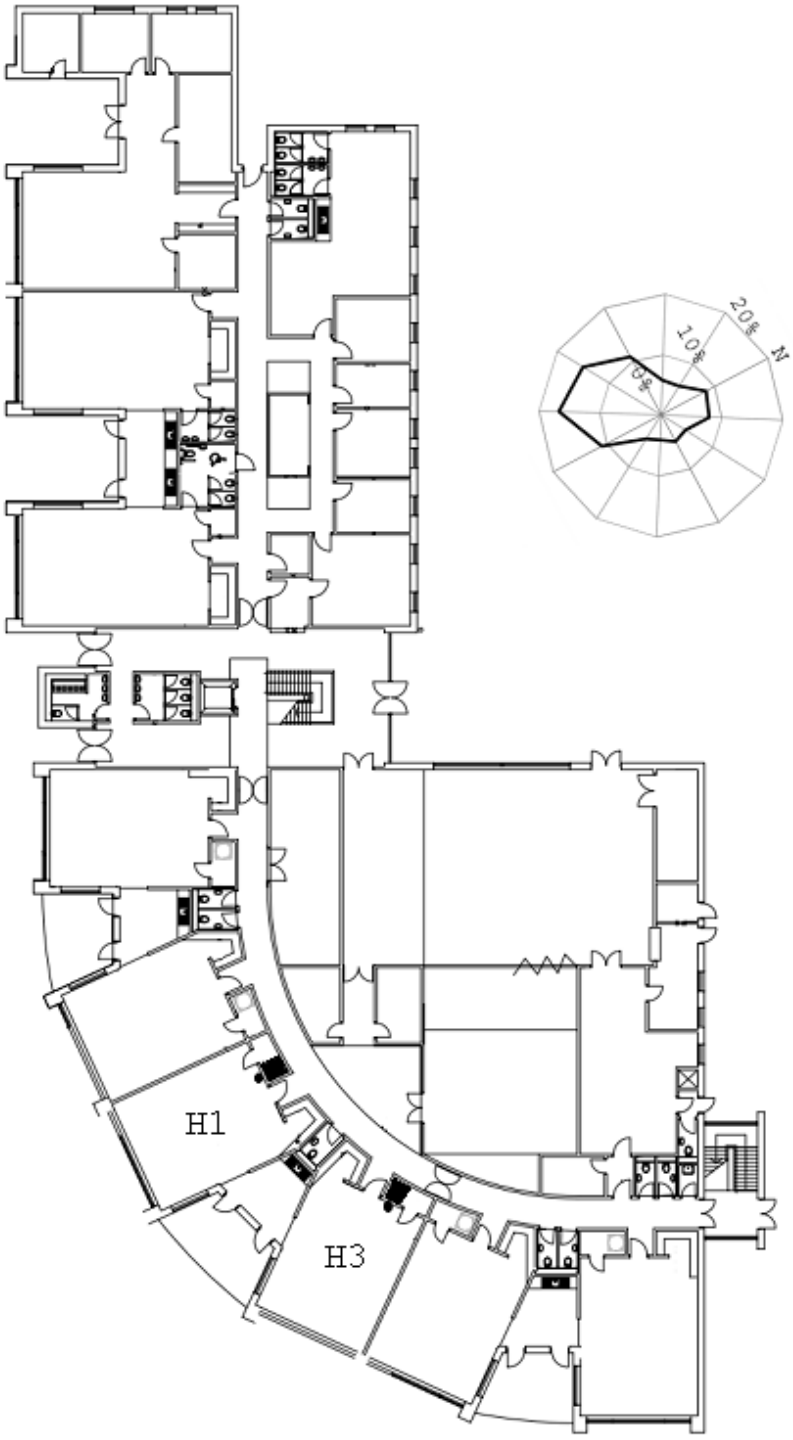

Figure B.9: School H, plan view, ground floor. H1 and H3, floor area 52.22 m^2.

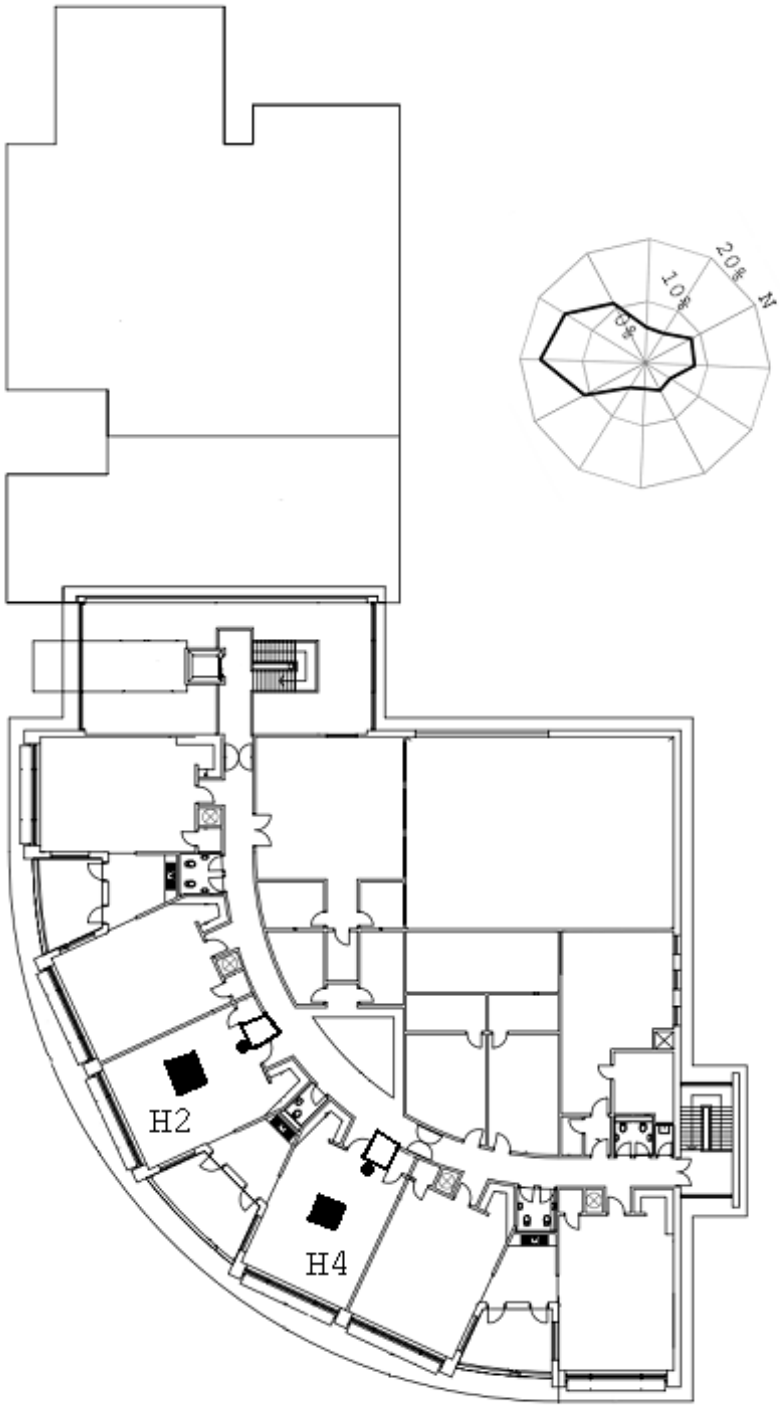

Figure B.10: School H, plan view, first floor. H2 and H4, floor area 52.22 m^2.

B.7 School I

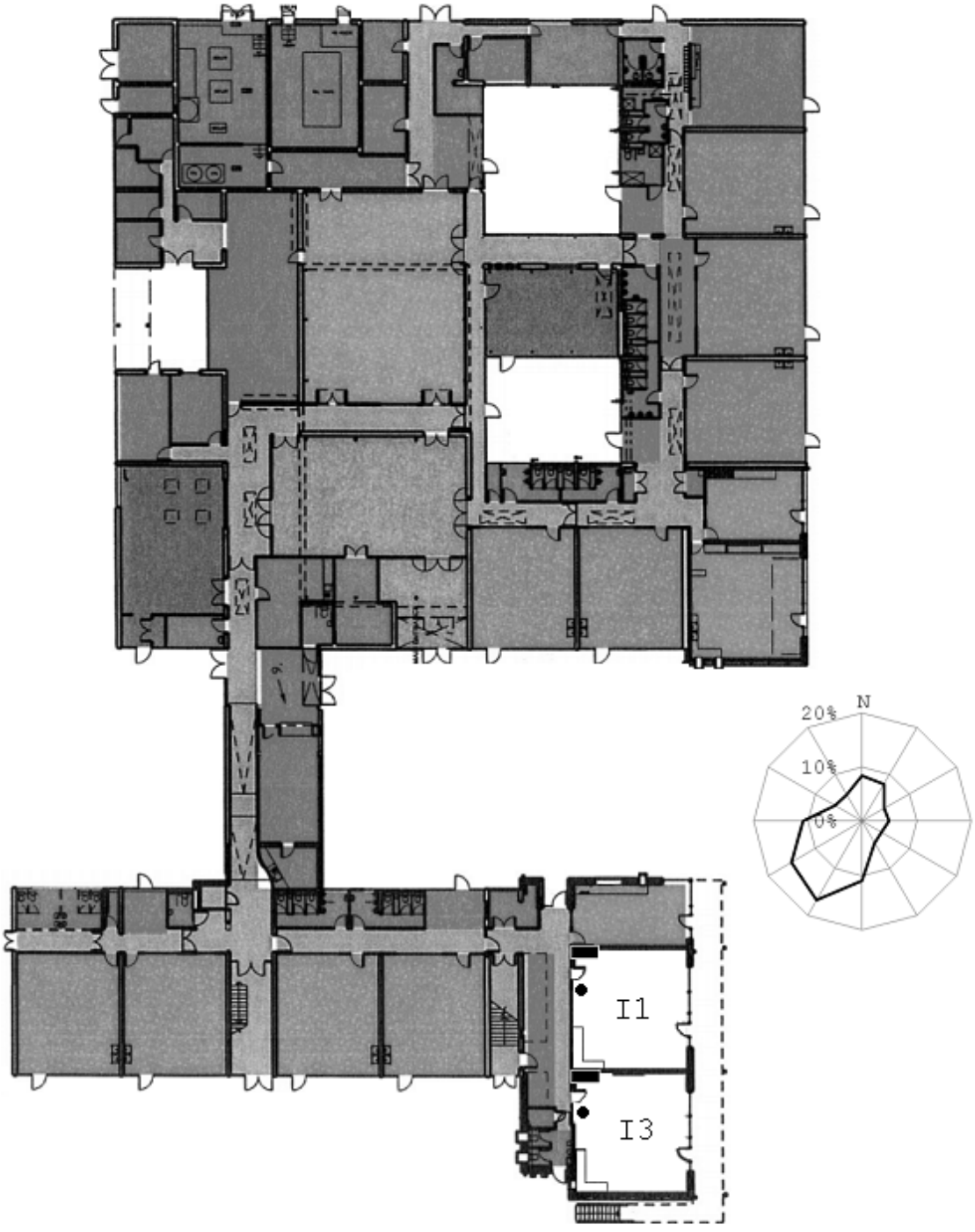

Figure B.11: School I, plan view, ground floor. I1 and I3, floor area 63.99 m^2.

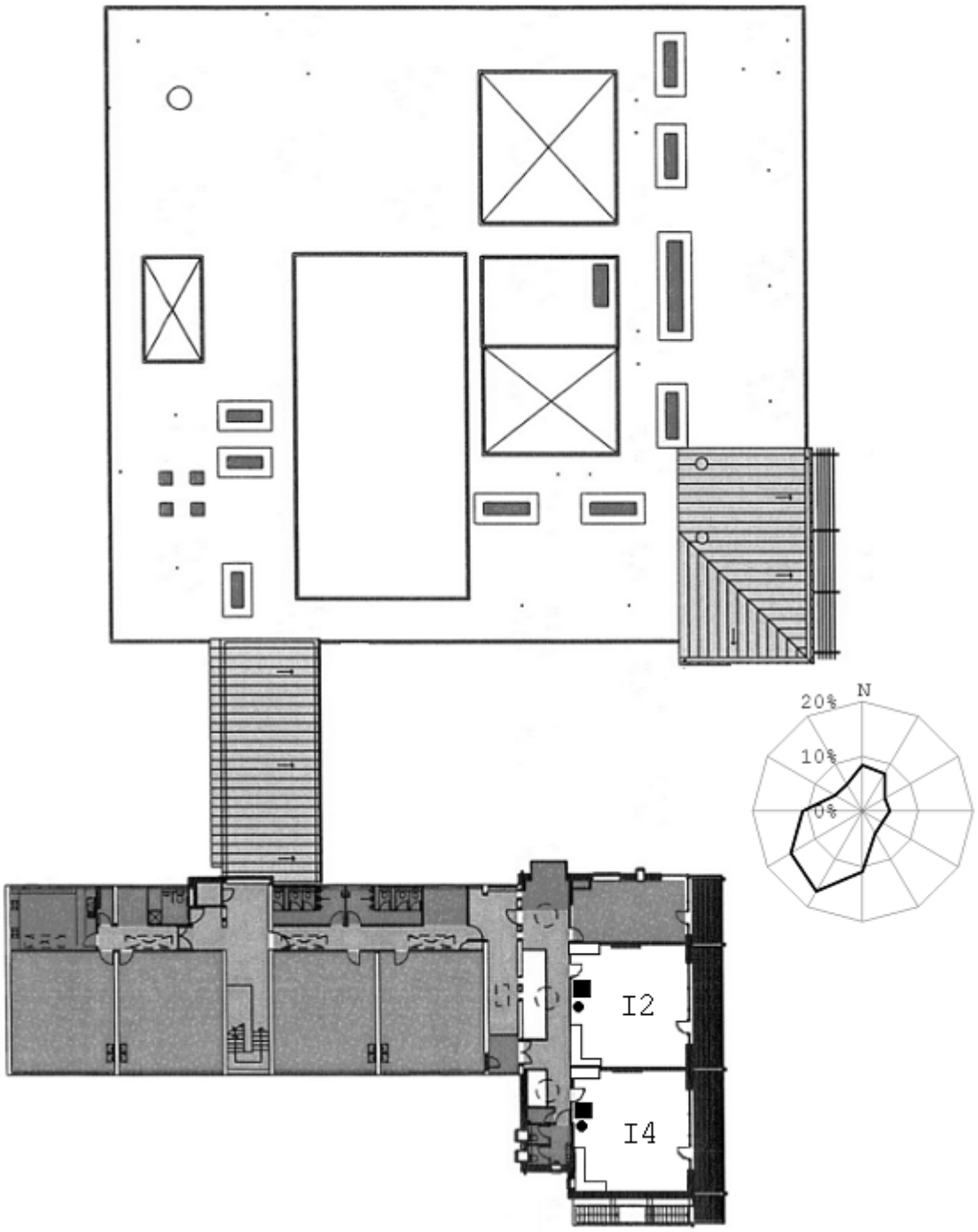

Figure B.12: School I, plan view, first floor. I2 and I4, floor area 61.62 m^2.

Appendix C

Indoor Air Quality

Appendix C provides full tables of results for internal and external temperature, carbon dioxide concentration, and relative humidity for all classrooms during occupied and unoccupied hours, and for weekdays and weekends. For further details on the collection of this data see Chapter 4.

C.1 Temperature

Table C.1: Measured air temperature in winter (°C).

	Weekday Occupied				Weekday Unoccupied				Weekend Occupied				Weekend Unoccupied			
	Mean	Stdev	Max	Min	Mean	Stdev	Max	Min	Mean	Stdev	Max	Min	Mean	Stdev	Max	Min
C1	23.40	1.01	25.90	20.60	21.99	0.91	24.90	19.70	19.32	1.11	20.80	17.10	19.03	1.17	21.30	17.00
C2	21.37	0.87	22.80	18.60	19.85	1.13	22.20	16.30	18.72	1.23	20.20	16.90	18.46	1.36	20.60	16.30
C3	22.24	2.01	24.55	14.42	22.06	1.43	24.55	18.62	19.32	1.29	20.90	17.57	19.65	1.25	22.14	17.67
C4	21.59	1.74	24.26	14.52	20.51	1.33	23.77	17.48	19.42	1.09	20.81	17.48	19.21	1.13	21.00	17.48
Cext	4.80	1.90			2.30	2.20			5.50	2.20			2.50	2.50		
D1	19.70	0.75	20.70	16.70	19.33	0.69	20.60	17.70	19.00	0.60	19.70	18.20	19.05	0.48	19.70	18.20
D2	17.42	1.96	20.80	12.80	16.07	1.88	19.30	11.70	13.86	1.12	15.30	11.40	13.16	1.13	14.80	11.10
D3	16.04	0.38	17.09	15.47	15.81	0.54	16.81	14.80	15.75	0.84	16.71	14.61	15.80	0.69	16.71	14.61
Dext	7.26	2.28	19.00	1.50	4.84	2.44	9.50	-0.50	6.58	1.75	8.50	1.50	4.91	2.53	7.50	0.00
E1	17.87	0.94	19.30	14.10	17.92	0.70	19.70	15.00	17.86	0.27	18.30	17.40	17.69	0.29	18.40	17.30
E3	18.26	0.53	19.09	15.38	18.03	0.48	19.28	15.57	18.21	0.12	18.43	18.05	18.19	0.16	18.52	17.86
Eext	7.03	2.96	14.50	0.50	3.00	1.66	8.50	0.00	2.63	0.67	3.50	0.50	2.42	0.53	3.50	1.00
F1	20.54	1.93	22.90	15.20	20.10	2.21	22.90	15.00	15.57	0.33	16.00	15.20	15.58	0.46	16.70	15.10

Table C.1: Measured temperature in winter (°C), continued.

	Weekday Occupied				Weekday Unoccupied				Weekend Occupied				Weekend Unoccupied			
	Mean	Stdev	Max	Min	Mean	Stdev	Max	Min	Mean	Stdev	Max	Min	Mean	Stdev	Max	Min
F2	20.69	1.49	22.80	17.30	20.28	1.59	22.70	16.80	17.06	0.06	17.10	16.90	17.15	0.21	17.90	16.90
F3	18.54	0.88	19.76	16.43	18.43	1.06	19.66	16.24	16.43	0.14	16.62	16.24	16.46	0.17	16.81	16.24
F4	19.61	1.38	21.09	14.71	18.60	1.81	21.09	13.75	14.22	0.17	14.52	13.94	14.22	0.33	15.09	13.85
Fext	9.57	0.69	11.00	7.50	8.57	0.75	10.00	6.50	7.22	1.86	9.50	3.50	5.84	2.66	9.00	0.50
G1	19.22	1.03	20.80	14.10	18.13	0.70	20.10	15.70	16.89	0.74	18.60	16.30	16.78	0.64	17.80	15.80
G2	18.51	0.74	19.80	14.80	18.21	0.53	19.10	16.70	18.04	0.60	19.00	17.60	18.03	0.60	18.90	17.10
G3	17.99	0.47	18.90	16.90	18.02	0.53	19.09	16.52	17.57	0.54	18.33	17.09	17.51	0.55	18.33	16.62
Gext	8.36	2.04	13.00	5.00	6.67	1.83	12.00	3.50	9.59	2.04	18.00	6.00	8.33	2.06	11.00	4.50
H1	18.24	1.51	21.00	15.40	17.78	1.76	20.30	14.90	17.56	1.62	19.60	15.10	17.45	1.75	19.60	15.10
H2	19.99	2.95	24.40	15.10	19.48	3.01	24.70	14.30	17.55	2.44	21.10	14.40	17.28	2.34	20.80	14.20
H3	19.66	4.89	30.86	13.85	19.18	3.99	30.86	13.65	15.63	0.96	16.81	14.13	15.65	1.13	17.28	13.94
H4	19.04	3.45	26.98	13.46	18.15	3.21	26.98	12.98	15.83	2.40	18.81	12.98	15.76	2.49	18.81	12.59
Hext	6.13	2.04	10.00	3.00	6.03	1.88	10.00	2.50	8.51	3.07	12.50	4.00	7.45	3.02	11.50	2.00
I1	18.05	3.31	22.80	10.60	17.44	4.12	22.80	9.40	12.42	1.03	13.70	10.90	12.16	0.85	13.70	10.90
I2	18.22	2.16	20.90	11.90	17.11	2.33	19.30	11.70	14.83	1.28	16.40	13.20	14.42	1.02	16.40	13.20
I3	16.55	2.49	19.76	10.94	15.63	2.70	18.52	9.97	12.10	0.59	13.17	10.75	11.41	0.71	12.88	10.16
I4	14.93	2.71	18.90	8.68	13.78	2.77	17.28	7.58	10.05	0.39	11.43	9.28	9.73	0.56	10.75	9.08
Iext	6.09	2.94	10.50	0.00	4.53	3.16	9.50	-3.00	2.33	3.89	7.50	-2.50	0.80	3.61	7.00	-3.00

Table C.2: Measured air temperature in summer (°C).

	Weekday Occupied				Weekday Unoccupied				Weekend Occupied				Weekend Unoccupied			
	Mean	Stdev	Max	Min	Mean	Stdev	Max	Min	Mean	Stdev	Max	Min	Mean	Stdev	Max	Min
C1	21.79	0.76	23.50	19.90	21.40	0.76	23.60	20.00	20.46	0.19	20.80	19.90	20.31	0.26	21.00	19.90
C2	21.11	1.07	23.70	19.30	20.62	0.77	24.30	19.30	19.29	0.15	19.70	19.10	19.43	0.31	19.80	18.90
C3	22.03	0.65	23.10	20.42	21.55	0.62	22.53	20.14	20.40	0.10	20.52	20.23	20.47	0.12	20.81	20.23
C4	21.73	0.58	23.00	19.95	21.41	0.61	22.72	20.23	20.08	0.13	20.42	19.85	20.27	0.29	20.71	19.76
Cext	18.94	2.20	23.00	14.00	16.14	3.21	24.00	10.50	19.88	1.41	22.50	17.00	15.30	3.93	23.50	9.00
D1	19.64	0.36	20.60	18.90	19.28	0.51	22.40	18.20	19.15	0.22	19.40	18.70	19.15	0.26	19.50	18.60
D2	21.08	0.85	22.70	16.60	20.35	1.70	26.70	18.20	20.86	0.31	21.30	20.10	20.66	0.97	24.90	19.70
D3	20.63	1.21	23.29	18.24	18.04	2.20	26.59	14.71	19.12	0.68	20.52	17.76	18.23	1.25	21.38	15.95
Dext	18.22	2.45	25.00	14.50	14.14	4.27	32.00	8.00	17.08	1.21	21.50	15.00	15.45	2.98	25.50	9.50
E1	20.47	1.48	22.80	17.30	20.60	1.18	22.80	18.00	19.34	0.35	19.80	18.60	19.21	0.35	19.80	18.50
E3	22.18	1.22	24.93	19.28	21.29	1.78	24.55	17.09	20.65	0.48	21.19	18.62	19.53	1.33	20.90	16.14

Table C.2: Measured temperature in summer (°C), continued.

	Weekday Occupied				Weekday Unoccupied				Weekend Occupied				Weekend Unoccupied			
	Mean	Stdev	Max	Min	Mean	Stdev	Max	Min	Mean	Stdev	Max	Min	Mean	Stdev	Max	Min
Eext	19.20	3.19	25.50	9.50	15.00	4.39	31.00	9.00	19.97	1.30	23.00	17.50	13.86	3.50	21.00	9.50
F1	23.03	1.01	25.80	21.50	22.71	1.78	25.70	18.70	22.55	0.57	23.60	21.50	22.42	1.16	23.80	20.10
F2	23.33	1.02	25.90	21.10	23.85	0.84	25.90	21.40	23.98	0.20	24.40	23.70	24.06	0.34	24.60	23.40
F3	22.59	1.42	26.78	19.38	23.29	0.89	26.10	21.38	22.95	0.37	23.68	22.43	23.23	0.51	24.16	22.43
F4	22.44	1.32	25.22	19.85	23.23	0.91	25.13	20.42	23.54	0.21	23.87	23.10	23.43	0.46	24.06	22.62
Fext	16.81	3.45	22.50	10.00	12.94	3.86	22.50	8.50	21.04	1.94	24.50	17.00	16.17	3.90	24.50	11.00
G1	18.70	0.63	20.00	17.20	18.45	0.73	20.10	17.00	17.22	0.09	17.30	17.00	17.24	0.17	17.50	16.90
G2	19.19	0.52	20.20	17.90	18.84	0.68	20.20	17.50	17.76	0.05	17.80	17.70	17.79	0.10	18.00	17.60
G3	20.31	1.54	27.37	18.14	20.36	1.96	25.32	17.67	21.03	2.65	24.64	18.14	21.16	2.81	25.42	18.05
Gext	17.40	2.40	22.00	12.50	13.95	3.13	26.50	10.00	16.58	2.45	21.00	13.00	14.50	2.40	21.00	11.50
H1	21.75	0.51	22.70	20.00	21.79	0.37	24.60	20.60	21.81	0.16	22.00	21.40	21.77	0.30	22.30	21.10
H2	23.43	0.59	24.50	21.60	22.84	0.48	24.40	21.70	23.15	0.27	23.60	22.40	22.75	0.65	23.70	21.60
H3	22.98	1.74	26.98	20.52	22.34	0.81	26.39	20.14	24.64	1.11	26.39	23.29	22.66	1.12	25.03	21.09
H4	25.68	1.38	28.56	22.24	23.29	1.28	28.06	21.38	26.76	1.78	29.75	24.45	23.70	1.71	27.76	21.38
Hext	18.43	2.64	25.00	14.00	15.68	3.38	34.50	12.00	16.64	1.99	21.50	14.00	15.75	4.51	31.50	11.00
I1	22.63	0.72	23.60	20.80	22.60	0.84	24.00	20.80	21.93	0.27	22.20	21.60	22.02	0.30	22.50	21.40
I2	22.23	1.08	23.70	18.70	21.87	1.83	25.30	17.30	20.90	0.69	22.20	19.30	20.68	1.23	22.90	18.40
I3	23.21	0.92	24.93	21.28	22.94	1.15	25.13	20.33	22.37	0.21	22.81	21.95	22.10	0.53	23.00	21.09
I4	22.33	1.17	24.64	19.09	22.06	1.75	26.98	18.24	20.70	0.40	21.28	19.85	20.75	0.79	23.10	19.38
Iext	19.38	2.23	24.00	14.00	17.09	3.77	33.50	11.00	18.89	1.84	22.00	14.50	16.31	3.11	27.00	11.50

C.2 Carbon Dioxide

Table C.3: Measured carbon dioxide in winter (ppm).

	Weekday Occupied				Weekday Unoccupied				Weekend Occupied				Weekend Unoccupied			
	Mean	Stdev	Max	Min	Mean	Stdev	Max	Min	Mean	Stdev	Max	Min	Mean	Stdev	Max	Min
C1	1824.54	847.33	4336	567	641.30	203.19	2008	503	524.00	47.61	586	475	518.83	37.56	585	473
C2	1700.64	565.39	3169	477	545.58	160.88	2154	443	493.79	65.67	593	421	493.89	61.01	597	422
D1	964.66	341.76	1826	434	434.47	122.79	1262	353	362.58	6.30	379	356	363.75	9.38	384	348
D2	1662.93	382.94	2626	923	947.14	324.00	2443	441	994.67	10.81	1033	970	993.24	17.51	1035	970
E1	1046.68	510.29	2540	469	537.66	164.50	1668	451	630.21	266.96	1457	452	497.42	78.81	831	451
F1	1130.16	428.63	2120	337	782.49	455.52	2284	331	336.65	4.40	346	329	340.40	12.63	379	328
F2	993.94	296.85	1936	458	627.77	288.06	1883	399	400.86	5.10	412	391	403.24	8.86	423	391
G1	1057.88	233.81	1623	504	500.31	111.27	1093	376	395.14	24.47	481	373	386.18	10.98	415	370
G2	1336.19	393.14	2152	425	577.41	212.75	1403	307	328.86	15.53	388	315	326.08	8.12	347	314
H1	1545.27	969.80	4010	427	646.09	377.71	3668	344	362.76	34.22	433	311	367.07	36.47	471	318
H2	1408.52	845.73	4323	475	746.65	495.67	4386	393	417.04	17.88	448	376	421.87	21.88	500	397
I1	1239.50	382.80	2472	585	543.24	137.86	1930	455	488.99	21.24	519	464	494.43	21.26	529	461
I2	1641.29	583.18	3210	496	480.04	141.47	1344	359	403.90	28.56	439	370	407.01	27.30	446	366

Table C.4: Measured carbon dioxide in summer (ppm).

	Weekday Occupied				Weekday Unoccupied				Weekend Occupied				Weekend Unoccupied			
	Mean	Stdev	Max	Min	Mean	Stdev	Max	Min	Mean	Stdev	Max	Min	Mean	Stdev	Max	Min
C1	858.10	412.02	3083	449	503.15	123.19	1856	433	432.98	7.24	454	424	437.36	12.11	469	423
C2	876.52	515.51	3383	444	473.53	101.09	1581	433	433.89	8.07	465	426	450.81	22.00	520	427
D1	587.71	129.30	1265	431	451.49	37.37	929	422	434.24	6.61	448	424	436.48	4.70	448	426
D2	588.10	146.36	1086	423	451.97	55.88	800	416	416.89	6.66	433	408	420.48	5.15	433	409
E1	798.96	423.36	2499	407	425.83	61.22	897	326	641.19	219.75	1225	359	455.31	91.30	796	351
F1	567.45	180.56	1444	455	503.97	54.56	763	427	492.24	28.82	568	458	503.73	51.52	631	445
F2	569.24	84.99	788	434	495.91	76.92	753	402	461.02	24.81	517	423	448.07	41.17	524	401
G1	678.77	157.92	1073	403	360.14	79.90	893	237	246.45	5.33	259	237	239.57	15.56	270	209
G2	659.02	164.88	1432	392	381.16	45.08	583	293	296.78	7.56	316	282	296.11	16.18	326	268
H1	680.09	196.43	1710	393	460.67	141.21	1790	366	372.40	10.13	394	355	379.98	24.07	423	343
H2	718.24	212.71	1471	312	455.34	74.78	1033	303	376.74	27.57	410	310	398.58	30.44	456	301
I1	644.66	186.69	1473	449	478.54	36.10	848	440	443.24	2.60	450	435	447.35	5.45	458	434
I2	634.01	141.66	1130	438	456.87	38.76	1099	433	441.94	2.14	446	437	447.99	3.81	455	438

C.3 Relative Humidity

Table C.5: Measured relative humidity in winter (%).

	Weekday Occupied				Weekday Unoccupied				Weekend Occupied				Weekend Unoccupied			
	Mean	Stdev	Max	Min	Mean	Stdev	Max	Min	Mean	Stdev	Max	Min	Mean	Stdev	Max	Min
C1	34.65	3.71	53.90	25.20	31.06	1.66	37.10	27.80	31.69	1.81	34.10	28.80	32.86	1.00	34.30	30.70
C2	40.81	4.07	55.00	29.80	34.91	2.68	46.80	27.40	35.18	2.09	37.80	31.90	35.59	2.10	38.70	31.60
D1	43.15	6.33	56.60	32.90	39.27	4.41	53.50	30.00	36.10	2.84	40.80	32.00	36.52	3.17	41.80	31.20
D2	50.17	6.52	65.90	39.80	46.03	4.62	58.60	35.10	47.56	2.57	54.80	45.00	50.47	2.71	56.50	45.50
E1	49.88	4.83	60.60	38.00	47.66	2.37	55.90	37.00	50.39	2.78	56.60	47.30	49.42	1.49	52.70	47.20
F1	52.47	4.47	58.50	37.30	52.36	2.98	62.60	42.60	45.46	2.74	48.90	42.40	45.84	2.51	49.80	42.20
F2	51.09	2.02	56.40	39.40	50.41	1.51	55.00	39.90	46.15	2.31	48.70	42.90	46.42	2.37	49.40	42.50
G1	55.12	3.68	62.00	41.20	53.53	2.63	60.10	42.30	55.90	0.61	58.00	55.30	56.78	0.72	58.10	55.60
G2	58.67	2.94	65.70	43.30	54.88	2.30	63.00	44.80	54.15	2.15	61.10	52.40	55.20	1.50	57.60	52.90
H1	47.06	5.23	57.80	35.20	45.62	3.30	57.10	36.30	45.46	0.80	46.90	43.60	45.41	0.56	46.60	44.30
H2	43.95	9.49	63.70	25.10	41.35	6.11	64.10	29.20	42.42	3.39	47.70	38.00	42.47	2.64	46.80	38.30
I1	49.16	9.69	68.00	33.50	43.65	8.97	64.70	30.20	40.95	2.01	43.50	38.40	41.58	3.29	49.10	37.00
I2	52.64	5.93	68.50	36.60	46.39	4.24	61.50	36.40	40.96	1.68	43.00	38.90	41.81	2.45	47.20	38.20

Table C.6: Measured relative humidity in summer (%).

	Weekday Occupied				Weekday Unoccupied				Weekend Occupied				Weekend Unoccupied			
	Mean	Stdev	Max	Min	Mean	Stdev	Max	Min	Mean	Stdev	Max	Min	Mean	Stdev	Max	Min
C1	55.14	5.46	67.90	46.60	52.51	5.61	68.30	46.10	50.78	1.43	52.90	48.40	50.42	1.38	52.90	47.80
C2	56.85	5.55	70.20	46.30	54.45	6.00	73.80	45.50	51.43	2.86	55.70	43.80	50.47	2.73	55.60	43.60
D1	54.39	1.92	58.90	49.60	52.13	3.97	65.90	38.40	62.17	5.70	71.10	54.20	63.08	9.61	73.80	44.20
D2	51.56	2.50	61.00	44.10	50.57	5.59	66.20	33.00	57.64	4.81	64.20	50.30	59.29	9.37	68.90	38.60
E1	48.78	5.48	60.80	37.10	52.12	3.57	59.40	38.50	50.17	3.07	56.20	41.80	51.33	1.41	54.80	47.90
F1	42.70	4.71	52.50	28.30	42.15	2.67	47.80	29.60	44.17	1.40	45.90	41.00	43.38	2.05	47.50	39.60
F2	44.05	4.18	52.40	33.80	42.13	3.34	51.60	34.80	44.68	0.96	46.40	43.10	44.66	1.60	47.50	41.80
G1	62.44	6.89	73.00	45.60	63.37	4.57	73.00	50.40	63.96	0.26	64.70	63.60	64.22	0.44	65.10	63.60
G2	60.04	5.63	69.40	45.80	61.23	4.37	69.40	44.40	61.73	0.20	62.20	61.40	62.16	0.33	63.10	61.40
H1	52.56	4.60	64.70	42.80	51.12	4.13	65.10	41.60	49.18	0.83	50.30	47.70	48.45	1.57	52.00	46.70
H2	46.41	4.92	64.10	36.30	45.66	4.46	63.40	34.60	43.22	0.78	44.70	41.80	43.14	1.76	46.90	41.20
I1	46.21	5.63	58.10	35.70	45.38	5.82	56.70	36.20	43.96	5.18	52.30	37.60	44.06	6.23	54.80	36.40
I2	46.77	4.30	53.90	38.80	46.40	5.45	59.70	38.50	45.83	6.27	58.20	37.50	46.03	8.57	60.70	35.80

Appendix D

Ventilation Rates

Table D.1: Estimated ventilation rate using the tracer gas decay method.

Room	Windcatcher Damper Position	Estimated Window Area A_5 (m^2)	Ventilation Rate $\dot{Q}$ (m^3/s)	Temperature Difference ΔT (°C)	Wind Speed u_w (m/s)	Wind Direction θ (°)
C1	Closed	0.00	0.0041 ± 0.0002	4.70	1.81	50
C1	Open	0.00	0.0198 ± 0.0009	5.42	1.76	140
C1	Open	0.00	0.0264 ± 0.0001	4.87	2.41	30
C1	Open	0.00	0.0466 ± 0.0030	14.18	2.94	305
C1	Open	0.00	0.0363 ± 0.0028	14.04	3.02	300
C1	Open	0.00	0.0321 ± 0.0007	13.99	3.02	300
C1	Open	0.00	0.0371 ± 0.0017	14.95	1.21	300
C1	Open	0.00	0.0441 ± 0.0035	14.74	1.81	310
C1	Open	0.87	0.2888 ± 0.0015	4.86	2.26	25
C1	Open	0.58	0.3642 ± 0.0030	5.11	2.35	140
C1	Closed	0.87	0.0630 ± 0.0021	5.04	2.11	20
C2	Closed	0.00	0.0048 ± 0.0007	3.47	1.66	195
C2	Open	0.00	0.1278 ± 0.0043	7.95	1.76	150
C2	Open	0.00	0.2161 ± 0.0016	14.14	2.11	310
C2	Open	0.00	0.2123 ± 0.0007	13.42	2.11	310
C2	Open	0.00	0.2251 ± 0.0009	12.97	2.41	310
C2	Open	0.00	0.2256 ± 0.0016	14.01	2.41	310

a = façade windows open; b = clerestory windows open; c = all windows open.

Table D.1: Estimated ventilation rate using the tracer gas decay method, continued.

Room	Windcatcher Damper Position	Estimated Window Area A_5 (m^2)	Ventilation Rate $\dot{Q}$ (m^3/s)	Temperature Difference ΔT (°C)	Wind Speed u_w (m/s)	Wind Direction θ (°)
C2	Open	0.00	0.2013 ± 0.0025	13.99	2.57	310
C2	Open	0.00	0.1016 ± 0.0016	3.40	1.66	35
C2	Open	0.00	0.2237 ± 0.0008	14.04	2.41	310
C2	Open	0.00	0.2204 ± 0.0011	13.22	2.41	310
C2	Open	0.00	0.1989 ± 0.0009	12.81	2.11	315
C2	Open	0.00	0.1898 ± 0.0033	15.27	1‘.81	310
C2	Open	0.00	0.1603 ± 0.0013	14.78	1.81	310
C2	Open	0.00	0.0992 ± 0.0007	14.48	2.41	290
C2	Open	0.00	0.0854 ± 0.0026	13.84	2.41	290
C2	Open	0.00	0.1297 ± 0.0019	10.84	2.41	290
C2	Open	0.00	0.0716 ± 0.0086	12.55	2.41	290
C2	Open	0.87	0.1617 ± 0.0013	3.03	1.81	40
C2	Open	0.73	0.3339 ± 0.0040	6.55	1.76	150
C2	Closed	0.87	0.0596 ± 0.0042	3.14	2.11	40
C3	Open	0.00	0.0119 ± 0.0018	6.55	2.35	95
C3	Open	0.00	0.0437 ± 0.0027	15.03	1.21	290
C3	Open	0.00	0.0420 ± 0.0012	14.69	1.21	300
C3	Open	0.87	0.3939 ± 0.0046	5.98	2.35	50
C4	Open	0.00	0.1550 ± 0.0052	5.73	1.76	50
C4	Open	0.00	0.1312 ± 0.0011	12.74	0.91	270
C4	Open	0.00	0.1054 ± 0.0010	14.12	1.21	290
C4	Open	0.00	0.0949 ± 0.0039	14.09	1.21	290
C4	Open	0.87	0.3797 ± 0.0007	14.04	2.72	310
C4	Open	0.44	0.2609 ± 0.0044	5.17	1.76	50
D1	Closed	0.00	0.0189 ± 0.0021	3.83	3.50	70
D1	Closed	0.00	0.0325 ± 0.0026	0.18	0.81	320
D1	Open	0.00	0.0469 ± 0.0422	3.04	3.50	70
D1	Open	0.00	0.0620 ± 0.0484	-4.58	1.08	110
D1	Open	0.31	0.1907 ± 0.0400	-4.35	0.94	170

a = façade windows open; b = clerestory windows open; c = all windows open.

Table D.1: Estimated ventilation rate using the tracer gas decay method, continued.

Room	Windcatcher Damper Position	Estimated Window Area A_5 (m^2)	Ventilation Rate $\dot{Q}$ (m^3/s)	Temperature Difference ΔT (°C)	Wind Speed u_w (m/s)	Wind Direction θ (°)
D1	Open	0.51	0.1725 ± 0.0621	-3.69	0.81	230
D1	Open	1.53	0.1097 ± 0.0296	-2.85	0.81	265
D1	Open	1.53	0.2973 ± 0.0773	-4.50	1.08	110
D1	Open	1.53	0.2966 ± 0.0386	1.59	3.50	80
D1	Closed	0.31	0.0900 ± 0.0234	-0.21	0.81	320
D1	Closed	0.51	0.1574 ± 0.0551	-0.32	0.81	300
D1	Closed	1.53	0.1112 ± 0.0645	-0.44	0.81	300
D1	Closed	1.53	0.2255 ± 0.0316	1.86	3.50	75
D2	Open	0.00	0.1687 ± 0.0186	-1.67	3.23	70
D2	Open	1.53	0.0810 ± 0.0704	1.35	3.23	70
D2	Open	1.53	0.1869 ± 0.0280	0.66	2.69	80
D3	Open	0.00	0.0923 ± 0.0388	-2.27	3.23	80
D3	Open	1.53	0.2542 ± 0.0305	-3.24	3.23	80
E1	Closed	0.00	0.0017 ± 0.0013	9.43	1.51	235
E1	Open	0.00	0.0245 ± 0.0028	8.79	2.12	240
E1	Open	0.49	0.3954 ± 0.0042	7.34	2.57	245
E1	Closed	0.49	0.0952 ± 0.0019	6.39	3.03	250
E2	Closed	0.00	0.0100 ± 0.0018	5.71	3.33	270
E2	Open	0.00	0.0192 ± 0.0021	9.62	2.88	280
E2	Open	0.49	0.3526 ± 0.0125	5.78	3.33	270
E2	Closed	0.49	0.1110 ± 0.0012	4.83	3.33	280
F1	Closed	0.00	0.0727 ± 0.0080	12.52	3.63	110
F1	Open	0.00	0.1850 ± 0.0111	12.44	3.96	120
F1	Open	0.00	0.2263 ± 0.0091	10.46	1.91	20
F1	Open	0.00	0.1732 ± 0.0052	10.92	1.58	40
F1	Open	0.00	0.1503 ± 0.0030	11.14	1.58	40
F2	Closed	0.00	0.0625 ± 0.0150	11.76	2.64	110
F2	Open	0.00	0.2271 ± 0.0250	11.38	3.14	110
F2	Open	0.00	0.0853 ± 0.0111	7.48	0.69	360

a = façade windows open; b = clerestory windows open; c = all windows open.

Table D.1: Estimated ventilation rate using the tracer gas decay method, continued.

Room	Windcatcher Damper Position	Estimated Window Area A_5 (m^2)	Ventilation Rate $\dot{Q}$ (m^3/s)	Temperature Difference ΔT (°C)	Wind Speed u_w (m/s)	Wind Direction θ (°)
F2	Open	0.00	0.1204 ± 0.0024	7.19	1.05	5
F2	Open	0.00	0.1097 ± 0.0011	8.07	1.41	10
F2	Open	0.00	0.1082 ± 0.0087	8.24	1.41	10
F2	Open	0.00	0.0991 ± 0.0059	8.31	1.97	30
F2	Open	0.00	0.0625 ± 0.0175	8.15	2.53	50
F2	Open	0.00	0.1097 ± 0.0022	8.40	2.53	50
F2	Open	0.00	0.1067 ± 0.0032	8.22	2.57	45
F2	Open	0.00	0.0960 ± 0.0038	8.27	2.60	40
F2	Open	0.00	0.0838 ± 0.0059	8.47	2.60	40
F2	Open	0.00	0.1052 ± 0.0042	8.52	2.25	30
F3	Closed	0.00	0.0736 ± 0.0029	11.52	3.96	120
F3	Open	0.00	0.1195 ± 0.0072	11.45	3.96	120
F4	Closed	0.00	0.0304 ± 0.0015	11.52	3.96	120
F4	Open	0.00	0.1798 ± 0.0090	10.75	3.96	120
G1	Closed	0.00	0.0141 ± 0.0024	0.87	3.17	250
G1	Open	0.00	0.0164 ± 0.0115	-0.22	3.17	250
G1	Open	1.84	0.5559 ± 0.0111	-1.09	3.33	250
G2	Open	0.00	0.0113 ± 0.0032	1.27	2.22	240
G2	Open	1.84	0.4329 ± 0.0130	0.74	2.22	240
G3	Closed	0.00	0.0175 ± 0.0075	-0.26	5.07	250
G3	Open	0.00	0.0164 ± 0.0100	0.12	4.91	250
G3	Closed	1.72	0.2514 ± 0.0050	-0.33	4.75	250
G3	Closed	1.72	0.1429 ± 0.0443	-0.82	4.75	250
G3	Closed	3.88	1.0371 ± 0.0622	-0.69	4.12	260
G3	Open	1.72	0.3672 ± 0.0073	-1.39	4.12	260
G3	Open	0.86	0.2056 ± 0.0103	-1.67	4.44	250
G3	Open	0.86	0.2282 ± 0.0183	-3.19	4.44	250
G3	Open	1.72	0.3209 ± 0.0321	-2.74	4.60	255
G3	Open	3.88	1.2456 ± 0.0623	-1.16	4.75	260

a = façade windows open; b = clerestory windows open; c = all windows open.

Table D.1: Estimated ventilation rate using the tracer gas decay method, continued.

Room	Windcatcher Damper Position	Estimated Window Area A_5 (m^2)	Ventilation Rate $\dot{Q}$ (m^3/s)	Temperature Difference ΔT (°C)	Wind Speed u_w (m/s)	Wind Direction θ (°)
H1	Closed	0.00	0.0096 ± 0.0010	7.40	2.18	260
H1	Open	0.00	0.0187 ± 0.0008	9.08	1.87	250
H1	Open	0.46	0.3351 ± 0.0037	8.48	1.87	250
H1	Closed	0.46	0.1132 ± 0.0050	9.77	1.87	250
H2	Closed	0.00	0.0109 ± 0.0002	9.30	1.87	250
H2	Open	0.00	0.0191 ± 0.0015	9.50	2.18	270
H2	Open	0.46	0.3068 ± 0.0025	7.30	2.18	270
H2	Closed	0.46	0.1027 ± 0.0019	7.39	2.18	260
H3	Closed	0.00	0.0104 ± 0.0015	8.35	2.18	260
H3	Open	0.00	0.0231 ± 0.0034	7.66	2.18	260
H3	Open	0.46	0.3316 ± 0.0049	7.40	2.18	260
H3	Closed	0.46	0.1123 ± 0.0036	9.08	2.02	265
H4	Closed	0.00	0.0100 ± 0.0003	8.78	2.18	270
H4	Open	0.00	0.0252 ± 0.0011	8.98	2.18	260
H4	Closed	0.46	0.0657 ± 0.0023	8.35	2.18	260
H4	Open	0.46	0.1501 ± 0.0024	7.66	1.87	250
I1	Closed	0.00	0.0156 ± 0.0024	10.17	3.36	40
I1	Closed	0.77	0.1376 ± 0.0022	7.90	3.36	40
I2	Closed	0.00	0.0212 ± 0.0050	6.18	2.75	240
I2	Open	0.00	0.0856 ± 0.0032	6.66	2.60	240
I2	Open	0.81[a]	0.4248 ± 0.0069	6.35	2.44	240
I2	Open	0.66[b]	0.3424 ± 0.0021	13.06	2.14	310
I2	Open	1.47[c]	0.4661 ± 0.0050	11.39	2.14	310
I2	Closed	0.81[a]	0.1431 ± 0.0039	11.60	2.44	310
I2	Closed	0.66[b]	0.1543 ± 0.0023	5.40	4.28	50
I2	Closed	1.47[c]	0.8797 ± 0.0055	4.73	3.67	40
I3	Closed	0.00	0.0170 ± 0.0009	8.24	3.67	40
I3	Closed	0.77	0.1461 ± 0.0034	8.36	3.06	40
I4	Closed	0.00	0.0437 ± 0.0012	5.61	3.97	50

a = façade windows open; b = clerestory windows open; c = all windows open.

Table D.1: Estimated ventilation rate using the tracer gas decay method, continued.

Room	Windcatcher Damper Position	Estimated Window Area A_5 (m^2)	Ventilation Rate $\dot{Q}$ (m^3/s)	Temperature Difference ΔT (°C)	Wind Speed u_w (m/s)	Wind Direction θ (°)
I4	Open	0.00	0.1212 ± 0.0025	12.43	2.44	305
I4	Open	0.81[a]	0.5042 ± 0.0076	12.34	2.44	300
I4	Open	0.66[b]	0.2480 ± 0.0068	11.55	2.14	295
I4	Open	1.47[c]	0.3355 ± 0.0153	11.27	1.83	290
I4	Closed	0.81[a]	0.2649 ± 0.0020	5.14	3.97	50
I4	Closed	0.66[b]	0.1093 ± 0.0019	5.27	3.97	50
I4	Closed	1.47[c]	0.6041 ± 0.0100	4.89	4.28	50

a = façade windows open; b = clerestory windows open; c = all windows open.

Appendix E

Sound Pressure Levels

Table E.1: Measured sound pressure level, $L_{Aeq,30m}$ (dBA).

School	Room	Duct Acoustic Lining (mm)	Specified Upper limit (dBA)	Measured sound pressure level (dBA)		
				Windcatcher Dampers closed	Windcatcher Dampers open	External
C	1	25	35.0	27.8	35.1	57.5
	2	25	35.0	27.3	31.1	57.5
	3	25	35.0	30.0	32.4	57.5
	4	25	35.0	28.0	34.0	57.5
D	1	0	35.0	33.5	43.9	44.4
	2	0	35.0		31.1	44.4
	3	0	35.0		29.0	44.4
E	1	25	35.0	24.3	26.1	38.4
	3	25	35.0			38.4
F	1	50	40.0	26.4	26.6	42.9
	2	50	40.0	25.3	32.4	42.9
	3	50	40.0	32.5	30.4	42.9
	4	50	40.0	26.6	25.9	42.9
G	1	0	35.0	34.7	32.3	50.9
	2	0	35.0	32.1	33.8	50.9
	3	0	35.0	34.8	34.7	50.9

Table E.1: Measured sound pressure level, $L_{Aeq,30m}$ (dBA), continued.

School	Room	Duct Acoustic Lining (mm)	Specified Upper limit (dBA)	Measured sound pressure level (dBA)		
				Windcatcher Dampers closed	Windcatcher Dampers open	External
H	1	0	35.0	36.8	33.5	53.5
	2	0	35.0	42.0	39.2	53.5
	3	0	35.0	33.9	33.8	53.5
	4	0	35.0	30.5	40.1	53.5
I	1	0	35.0	38.1		66.6
	2	0	35.0	44.3	38.9	66.6
	3	0	35.0	33.5		66.6
	4	0	35.0	42.4	42.4	66.6

Appendix F

Published Literature

Jones, BM, Kirby, R, Kolkotroni, M, & Payne, T. 2007. Air Quality Measured in a Classroom Serviced by Natural Ventilation Windcatchers. *In: 2nd PALENC and 28th AIVC Conference: Building Low Energy Cooling and Advanced Ventilation Technologies in the 21st Century.*

Jones, BM, Kirby, R, & Kolokotroni, M. 2008. Quantifying the Performance of a Top–Down Natural Ventilation Windcatcher. *In: The 29th AIVC Conference: Advanced Building Ventilation and Environmental Technology for Addressing Climate Change Issues.*

Jones, BM, Kirby, R, Kolkotroni, M, & Payne, T. 2008. Air Quality Measured in a Classroom Served by Roof Mounted Natural Ventilation Windcatchers. *In: Proceedings of the 2008 Brunel/Surrey University EngD Conference.*

Jones, BM, & Kirby, R. 2009. Quantifying the Performance of a Top–Down Natural Ventilation Windcatcher™. *Building and Environment*, 44(9), 1925–1934.

Jones, BM, & Kirby, R. 2010. The Performance of Natural Ventilation Windcatchers in Schools: A Comparison between Prediction and Measurement. *International Journal of Ventilation*, 9(3), 273–286.